Chemical Constituents from *Rhodomyrtus tomentosa* (Aiton) Hassk. and Antibacterial Activity

Asadhawut Hiranrat

A Thesis Submitted in Partial Fulfillment of the Requirements
for the Degree of Doctor of Philosophy in Organic Chemistry
Prince of Songkla University
2010

Thesis Title	Chemical Constituents from *Rhodomyrtus tomentosa* (Aiton) Hassk. and Antibacterial Activity
Author	Mr. Asadhawut Hiranrat
Major Program	Organic Chemistry

Major Advisor:

……...……

(Assoc. Prof. Dr. Wilawan Mahabusarakam)

Co-advisor:

……

(Assoc. Prof. Chanita Ponglimanont)

Examining Committee:

……..…Chairperson

(Assoc. Prof. Dr. Kan Chantrapromma)

……

(Assoc. Prof. Dr. Wilawan Mahabusarakam)

……

(Assoc. Prof. Chanita Ponglimanont)

……

(Assoc. Prof. Dr. Chatchanok Karalai)

The Graduate School, Prince of Songkla University, has approved this thesis as a partial fulfillment of the requirements for the Doctor of Philosophy degree in Organic Chemistry.

……..……..…..

(Prof. Dr. Amornrat Phongdara)

Dean of Graduate School

ชื่อวิทยานิพนธ์ องค์ประกอบทางเคมีจากโทะและฤทธิ์ต้านแบคทีเรีย
ผู้เขียน นายอัษฎาวุธ หิรัญรัตน์
สาขาวิชา เคมีอินทรีย์
ปีการศึกษา 2553

บทคัดย่อ

โทะ (*Rhodomyrtus tomentosa*) เป็นพืชในวงศ์ชมพู่ (Myrtaceae) ส่วนสกัดหยาบไดคลอโรมีเทนและอะซิโตนจากใบโทะมีฤทธิ์ในการยับยั้งการเจริญของแบคทีเรีย *Staphylococcus aureus* ATCC 25923 และ methicillin-resistant *S. aureus* (MRSA) NRPC R01 ด้วยค่าความเข้มข้นต่ำสุด (MIC) 31.25 และ 62.5 μg/mL ตามลำดับ การศึกษาองค์ประกอบทางเคมีของใบ ต้นและผลโทะเพื่อหาสารที่แสดงฤทธิ์ในการยับยั้งการเจริญของเชื้อแบคทีเรีย แยกสารองค์ประกอบได้ 41 สาร เป็นสารกลุ่มเอซิลฟลอโรกลูซินอล (acylphloroglucinols) จำนวน 11 สาร คือ rhodomyrtosone A (**ART2**), rhodomyrtosone H (**ART3**), rhodomyrtosone C (**ART4**), rhodomyrtone (**ART6**), endoperoxide G3 (**ART8**), rhodomyrtosone B (**ART9**), rhodomyrtosone D (**ART11**), rhodomyrtosone E (**ART18**), rhodomyrtosone G (**ART19**), rhodomyrtosone F (**ART20**) และ rhodomyrtosone I (**ART38**) สารกลุ่มฟลาโวนอยด์ (flavonoids) จำนวน 4 สาร คือ combretol (**ART7**), 3,4',5',7-tetra-*O*-methylmyricetin (**ART13**), 3,3',5',7-tetra-*O*-methylmyricetin (**ART16**) และ 3,3',4',5'-tetra-*O*-methylmyricetin (**ART17**) สารกลุ่มเทอพีนอยด์ (terpenoids) จำนวน 7 สาร คือ (6*R*,7*E*,9*S*)-9-hydroxy-4,7-megastigmadien-3-one (**ART12**), loliolide (**ART14**), 3β-*O*-*E*-coumaroylmaslinic acid (**ART22**), 3β-*O*-*Z*-coumaroylmaslinic acid (**ART23**), 3β-*O*-*E*-coumaroyl oleanolic acid (**ART32**), arjunolic acid (**ART34**) และ oleanolic acid (**ART39**) สารกลุ่มสเตียรอยด์ (steroids) จำนวน 3 สาร คือ β-sitosterol (**ART5**), β-sitosterol glucopyranoside (**ART24**) และ stigmast-4-en-3-one (**ART37**) อนุพันธ์ของกรดแอลลาจิก (ellagic acid derivatives) จำนวน 3 สาร คือ 3,3',4-tri-*O*-methylellagic acid (**ART10**), 4-*O*-[β-D-glucopyranosyl-

tetraacetate]-3,3',4'-tri-*O*-methylellagic acid (**ART28**) และ 3-*O*-methylellagic acid 4-*O*-α-rhamnopyranoside (**ART41**) อนุพันธ์ของกรดฟลาเวลลาจิก (flavellagic acid derivatives) จำนวน 2 สาร คือ 3',4'-dioxymethylene-3,4-di-*O*-methylflavellagic acid (**ART25**) และ 3,4,3',4'-tetra-*O*-methylflavellagic acid (**ART31**) สารกลุ่มอนุพันธ์เบนซีน (benzenoids) จำนวน 6 สาร คือ α-tocopherol (**ART1**), *trans*-triacontyl-4-hydroxy-3-methoxycinnamate (**AR21**), *trans*-triacontyl-4-hydroxycinnamate (**ART30**), 4-hydroxy-3-methoxybenzoic acid (**ART35**), gallic acid (**ART36**) และ methyl gallate (**ART40**) อนุพันธ์ลิกแนน (lignans) จำนวน 1 สาร คือ 9,9'-*O*-diferuloyl-(-)-secoisolariciresinol (**ART33**) อนุพันธ์ของบิวไทโรแลคโทน (butyrolactone derivatives) จำนวน 1 สาร คือ (3a*S**,6a*R**)-3a-(hydroxymethyl)-2,2-dimethyldihydro-furo[3,4-*d*][1,3]dioxol-4(3a*H*)-one (**ART15**) และน้ำตาล จำนวน 3 สาร คือ β-D-glucopyranoside penta-acetate (**ART26**), α-D-glucopyranoside penta-acetate (**ART27**) และ sucrose octa-acetate (**ART29**) สาร 11 สาร คือ **ART2**, **ART3**, **ART4**, **ART9**, **ART11**, **ART15**, **ART18**, **ART19**, **ART20**, **ART31** และ **ART38** เป็นสารที่ยังไม่มีรายงานการวิจัย โครงสร้างของสารประกอบเหล่านี้วิเคราะห์ด้วยข้อมูลทางสเปกโทรสโกปี UV IR NMR และ MS นอกจากนี้ยังได้เปรียบเทียบข้อมูลทางสเปกโทรสโกปีกับสารที่มีรายงานการวิจัยแล้ว

การทดสอบฤทธิ์ของสารกลุ่มเอซิลฟลอโรกลูซินอล (**ART2**, **ART4**, **ART6, ART9**, **ART11**, **ART18**, **ART19** และ **ART20**) ในการต้านเชื้อแบคทีเรีย *S. aureus*, MRSA และ *Streptococcus pyogenes* DMST 101 พบว่า rhodomyrtone (**ART6**) และ rhodomyrtosone B (**ART9**) สามารถยับยั้งการเจริญของเชื้อทั้งสามสายพันธุ์ ด้วยค่าความเข้มข้นต่ำสุด (MIC) 0.39, 6.25 μg/mL 0.39, 12.5 μg/mL และ 0.39, 3.125 μg/mL ตามลำดับ นอกจากนี้ยังพบว่า rhodomyrtosone G (**ART19**) ยับยั้งการเจริญของ *S. aureus* และ MRSA ด้วยค่าความเข้มข้นต่ำสุด (MIC) 1.56 μg/mL และ rhodomyrtosone D (**ART11**) ยับยั้งการเจริญของ *S. pyogenes* ด้วยค่าความเข้มข้นต่ำสุด (MIC) 12.5 μg/mL

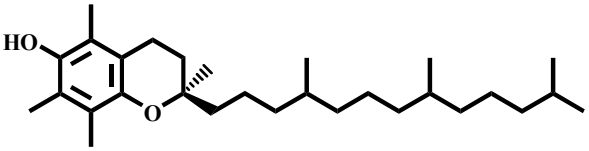

ART1

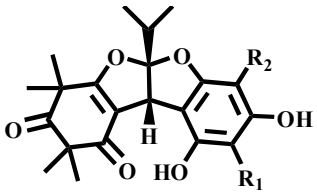

ART2 : R_1 = H, R_2 = isovaleryl

ART3 : R_1 = isovaleryl, R_2 = H

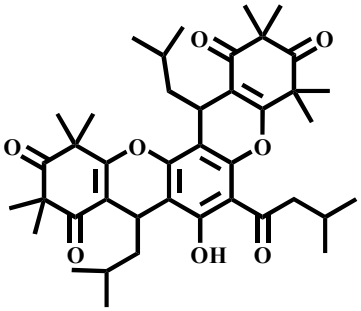

ART4

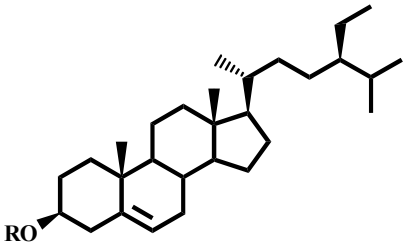

ART5 : R = H

ART24 : R = -β-D-glucose

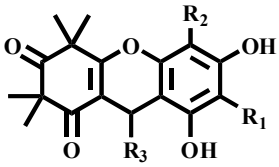

ART6 : R_1 = isovaleryl, R_2 = H, R_3 = isobutyl

ART9 : R_1 = H, R_2 = isovaleryl, R_3 = isobutyl

ART19 : R_1 = 2-methylbutyryl, R_2 = H, R_3 = isobutyl

ART38 : R_1 = isovaleryl, R_2 = H, R_3 = phenyl

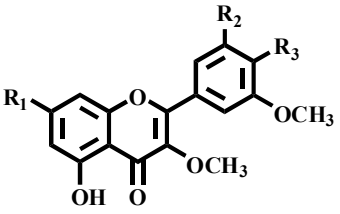

ART7 : R_1 = R_2 = R_3 = OCH_3

ART13 : R_1 = R_3 = OCH_3, R_2 = OH

ART16 : R_1 = R_2 = OCH_3, R_3 = OH

ART17 : R_1 = OH, R_2 = R_3 = OCH_3

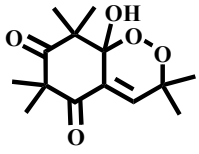

ART8

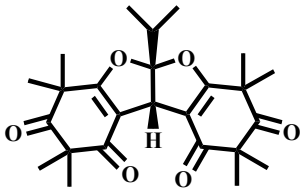

ART11

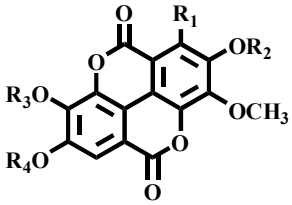

ART10 : R_1 = R_2 = H, R_3 = R_4 = CH_3

ART25 : R_1 = OH, R_2 = CH_3, R_3, R_4 = -CH_2-

ART28 : R_1 = H, R_2 = -β-D-glucose tetra-acetate, R_3 = R_4 = CH_3

ART31 : R_1 = OH, R_2 = R_3 = R_4 = CH_3

ART41 : R_1 = R_3 = R_4 = H, R_2 = -β-D-rhamnose

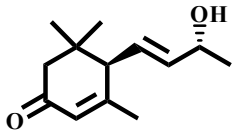

ART12

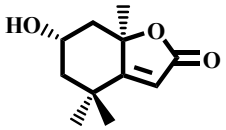

ART14

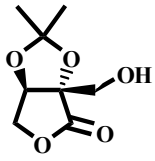

ART15

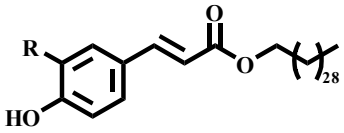

ART21 : R = OCH_3
ART30 : R = H

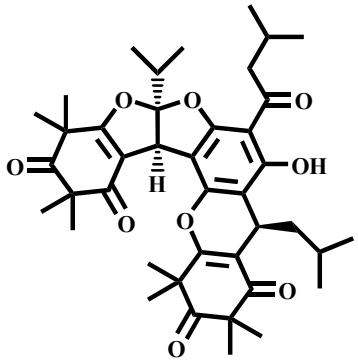

ART18

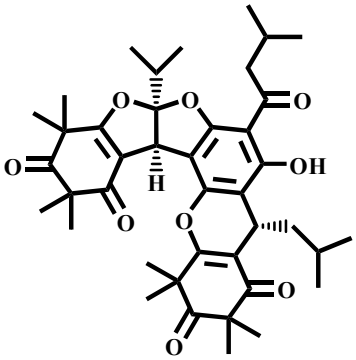

ART20

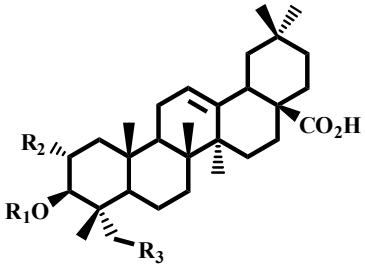

ART22 : R_1 = *trans*-coumaroyl, R_2 = OH, R_3 = H
ART23 : R_1 = *cis*-coumaroyl, R_2 = OH, R_3 = H
ART32 : R_1 = *trans*-coumaroyl, R_2 = R_3 = H
ART34 : R_1 = H, R_2 = R_3 = OH
ART39 : R_1 = R_2 = R_3 = H

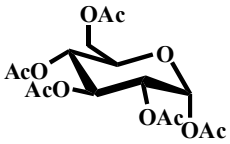

ART26

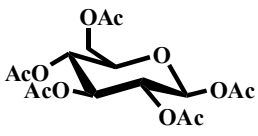

ART27

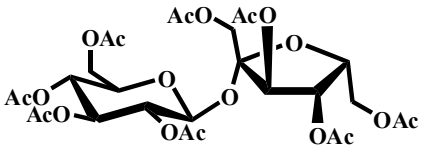

ART29

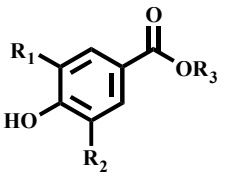

ART35 : $R_1 = OCH_3$, $R_2 = R_3 = H$

ART36 : $R_1 = R_2 = OH$, $R_3 = H$

ART40 : $R_1 = R_2 = OH$, $R_3 = CH_3$

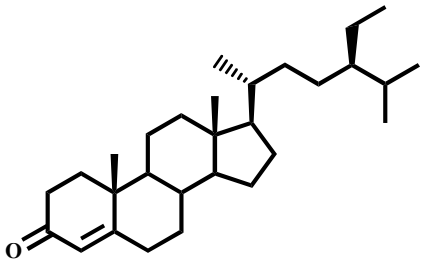

ART37

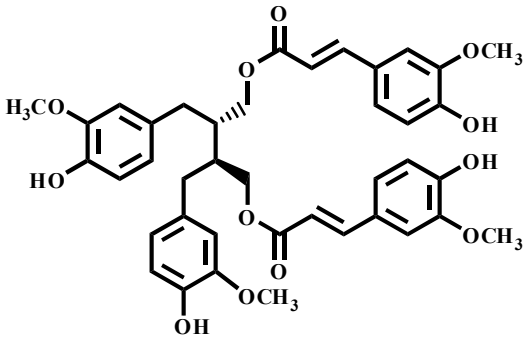

ART33

Thesis Title	Chemical Constituents from *Rhodomyrtus tomentosa* (Aiton) Hassk. and Antibacterial Activity
Author	Mr. Asadhawut Hiranrat
Major Program	Organic Chemistry
Academic Year	2010

ABSTRACT

Rhodomyrtus tomentosa (Aiton) Hassk. is a flowering plant belonging to the family Myrtaceae. The preliminary study has revealed that the crude CH_2Cl_2 and Me_2CO extracts from its leaves exhibited strong antibacterial activities against *Stephylococcus aureus* ATCC 25923 and methicillin-resistant *S. aureus* NRPC R01 (MRSA) with MIC values of 31.25 and 62.5 μg/mL, respectively. Investigation of the chemical constituents from the leaves, stems and fruits of *R. tomentosa* yielded forty one compounds. They were determined to be eleven acylphloroglucinols: rhodomyrtosone A (**ART2**), rhodomyrtosone H (**ART3**), rhodomyrtosone C (**ART4**), rhodomyrtone (**ART6**), endoperoxide G3 (**ART8**), rhodomyrtosone B (**ART9**), rhodomyrtosone D (**ART11**), rhodomyrtosone E (**ART18**), rhodomyrtosone G (**ART19**), rhodomyrtosone F (**ART20**) and rhodomyrtosone I (**ART38**), four flavonoids: combretol (**ART7**), 3,4',5',7-tetra-*O*-methylmyricetin (**ART13**), 3,3',5',7-tetra-*O*-methylmyricetin (**ART16**) and 3,3',4',5'-tetra-*O*-methylmyricetin (**ART1**7), seven terpenoids: (6*R*,7*E*,9*S*)-9-hydroxy-4,7-megastigmadien-3-one (**ART12**), loliolide (**ART14**), 3β-*O*-*E*-coumaroylmaslinic acid (**ART22**), 3β-*O*-*Z*-coumaroyl-maslinic acid (**ART23**), 3β-*O*-*E*-coumaroyloleanolic acid (**ART32**), arjunolic acid (**ART34**) and oleanolic acid (**ART39**), three steroids: β-sitosterol (**ART5**), β-sitosterol glucopyranoside (**ART24**) and stigmast-4-en-3-one (**ART37**), three ellagic acid derivatives: 3,3',4-tri-*O*-methylellagic acid (**ART10**), 4-*O*-[β-D-glucopyranosyl-tetraacetate]-3,3',4'-tri-*O*-methylellagic acid (**ART28**) and 3-*O*-methyl- ellagic acid 4-*O*-α-rhamnopyranoside (**ART41**), two flavellagic acid derivatives: 3',4'-dioxymethylene-

3,4-di-*O*-methyl-flavellagic acid (**ART25**) and 3,4,3',4'-tetra-*O*-methylflavellagic acid (**ART31**), six benzenoids: α-tocopherol (**ART1**), *trans*-triacontyl-4-hydroxy-3-methoxycinnamate (**AR21**), *trans*-triacontyl-4-hydroxy-cinnamate (**ART30**), 4-hydroxy-3-methoxy-benzoic acid (**ART35**), gallic acid (**ART36**) and methyl gallate (**ART40**), one lignan: 9,9'-*O*-diferuloyl-(-)-secoisolariciresinol (**ART33**), one butyrolactone derivative: (3a*S**,6a*R**)-3a-(hydroxymethyl)-2,2-dimethyldihydrofuro[3,4-*d*][1,3] dioxol-4(3a*H*)-one (**ART15**) and three sugars: β-D-glucopyranoside penta-acetate (**ART26**), α-D-glucopyranoside penta-acetate (**ART27**) and sucrose octa-acetate (**ART29**). Eleven compounds: **ART2**, **ART3**, **ART4**, **ART9**, **ART11**, **ART15**, **ART18**, **ART19**, **ART20**, **ART31** and **ART38** were newly found compounds. Their structures were elucidated on the basis of spectroscopic analyses including UV, IR, NMR, MS and by comparison of their spectroscopic data with those reported in the literature.

Some of the isolated acylphloroglucinol compounds (**ART2**, **ART4**, **ART6**, **ART9**, **ART11**, **ART18**, **ART19** and **ART20**) were also evaluated for their antibacterial activity against three types of Gram-positive bacteria, *S. aureus*, MRSA and *Streptococcus pyogenes* DMST 101. It was found that rhodomyrtone (**ART6**) and rhodomyrtosone B (**ART9**) showed good activity to inhibit the growth of *S. aureus*, MRSA and *S. pyogenes* with MIC values of 0.39, 6.25 μg/mL, 0.39, 12.5 μg/mL, and 0.39, 3.125 μg/mL, respectively. In addition, rhodomyrtosone G (**ART19**) inhibited the growth of both *S. aureus* and MRSA with the MIC value of 1.56 μg/mL while rhodomyrtosone D (**ART11**) further showed the inhibitory activity against *S. pyogenes* with the MIC value of 12.5 μg/mL. Interestingly, rhodomyrtone (**ART6**) exhibited the activity more than the standard, vancomycin (*S. aureus*: 0.60 μg/mL, MRSA: 1.25 μg/mL).

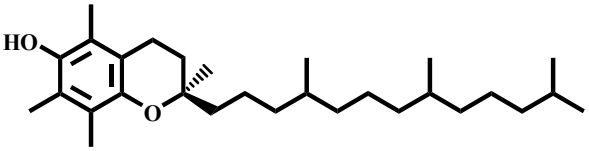

ART1

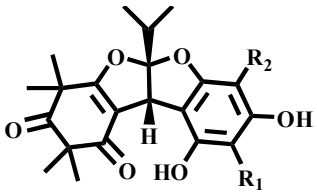

ART2 : R_1 = H, R_2 = isovaleryl

ART3 : R_1 = isovaleryl, R_2 = H

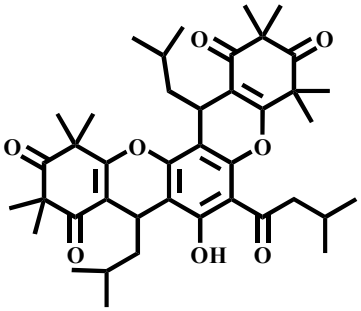

ART4

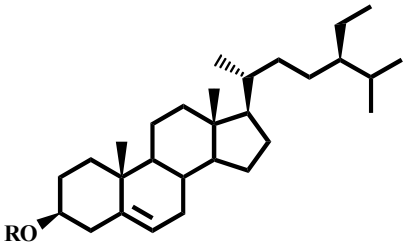

ART5 : R = H

ART24 : R = -β-D-glucose

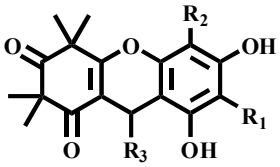

ART6 : R_1 = isovaleryl, R_2 = H, R_3 = isobutyl

ART9 : R_1 = H, R_2 = isovaleryl, R_3 = isobutyl

ART19 : R_1 = 2-methylbutyryl, R_2 = H, R_3 = isobutyl

ART38 : R_1 = isovaleryl, R_2 = H, R_3 = phenyl

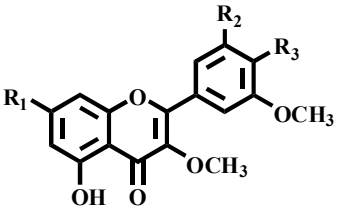

ART7 : R_1 = R_2 = R_3 = OCH_3

ART13 : R_1 = R_3 = OCH_3, R_2 = OH

ART16 : R_1 = R_2 = OCH_3, R_3 = OH

ART17 : R_1 = OH, R_2 = R_3 = OCH_3

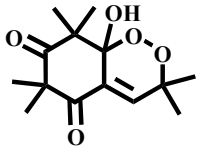

ART8

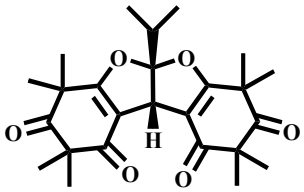

ART11

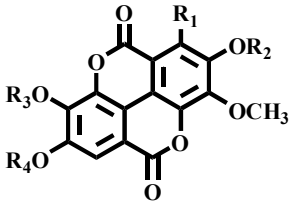

ART10 : R_1 = R_2 = H, R_3 = R_4 = CH_3

ART25 : R_1 = OH, R_2 = CH_3, R_3, R_4 = -CH_2-

ART28 : R_1 = H, R_2 = -β-D-glucose tetra-acetate, R_3 = R_4 = CH_3

ART31 : R_1 = OH, R_2 = R_3 = R_4 = CH_3

ART41 : R_1 = R_3 = R_4 = H, R_2 = -β-D-rhamnose

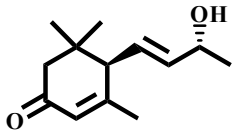

ART12

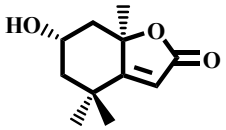

ART14

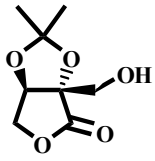

ART15

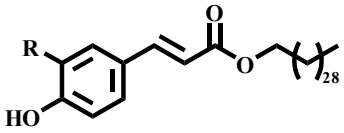

ART21 : R = OCH_3
ART30 : R = H

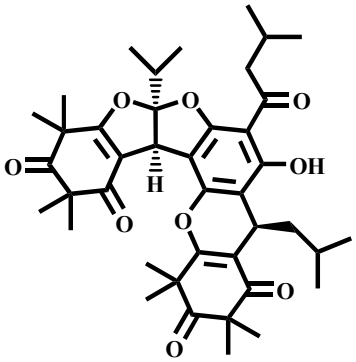

ART18

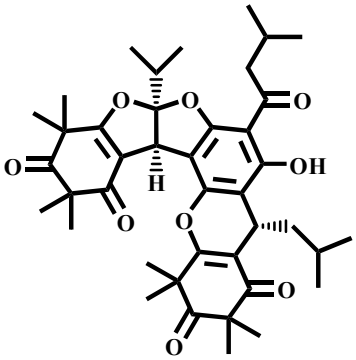

ART20

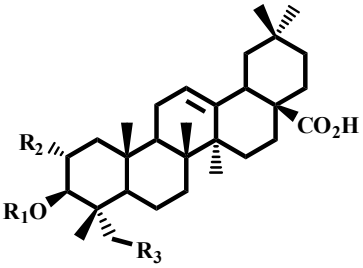

ART22 : R_1 = *trans*-coumaroyl, R_2 = OH, R_3 = H
ART23 : R_1 = *cis*-coumaroyl, R_2 = OH, R_3 = H
ART32 : R_1 = *trans*-coumaroyl, R_2 = R_3 = H
ART34 : R_1 = H, R_2 = R_3 = OH
ART39 : R_1 = R_2 = R_3 = H

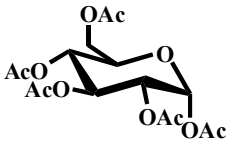

ART26

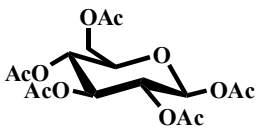

ART27

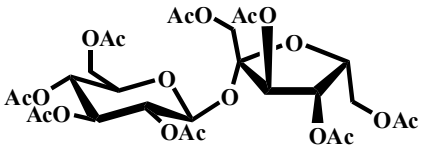

ART29

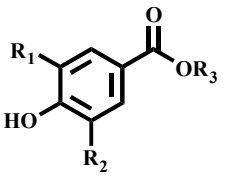

ART35 : $R_1 = OCH_3$, $R_2 = R_3 = H$

ART36 : $R_1 = R_2 = OH$, $R_3 = H$

ART40 : $R_1 = R_2 = OH$, $R_3 = CH_3$

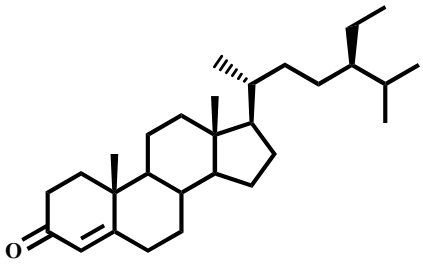

ART37

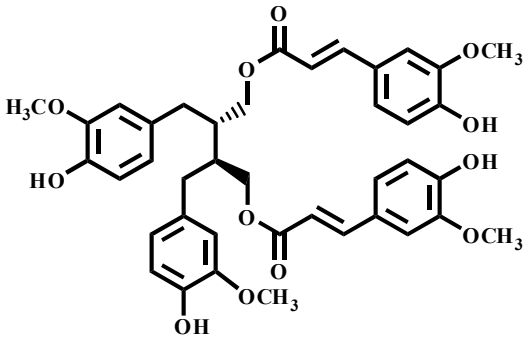

ART33

ACKNOWLEDGEMENTS

I wish to express my deepest and sincere gratitude to my supervisor, Associate Professor Dr. Wilawan Mahabusarakam, for her valuable instruction, expert guidance, excellent suggestion and kindness. I would also like to express my appreciation to Associate Professor Chanita Ponglimanont, my co-advisor, for correction of my thesis and her kindness. Without their help, my thesis work would not be successful.

My sincere thanks are expressed to Associate Professor Dr. Supayang Piyawan Voravuthikunchai and Mr. Surasak Limsuwan, Department of Microbiology, Faculty of Science, Prince of Songkla University for antibacterial activities testing and to Mr. J. Wai, Department of Biology, Faculty of Science, Prince of Songkla University for plant identification. I also would like to thank Assoc. Prof. Dr. Anthony R. Carroll, School of Environment, Griffith University, Queensland, Australia for his valuable instruction, expert guidance, excellent suggestion and kindness during my research visit with him at Griffith University.

I would like to acknowledge my sincere thanks to the Thailand Research Fund through the Royal Golden Jubilee Ph.D. program (Grant No. PHD/0206/2549) and the Center for Innovation in Chemistry (PERCH-CIC), Office of the Higher Education Commission, Ministry of Education for a scholarship and financial support. The CHE-RES-RG, Office of the Higher Education Commission, Ministry of Education and the Graduate School, Prince of Songkla University are gratefully acknowledged for the partly financial support.

I would like to thank Department of Chemistry, Faculty of Science, Prince of Songkla University for making available the facilities used in this research.

Finally, I am greatly indebted to my family especially my wife and my daughters for their encouragement, love, understanding and moral support.

Asadhawut Hiranrat

THE RELEVANCE OF THE RESEARCH WORK TO THAILAND

This work is a basic research on the evaluation for utilization of Thai medicinal plants as a source of the bioactive constituents. The aims of this research are to investigate the chemical constituents of *Rhodomyrtus tomentosa* and to evaluate the antibacterial activity. In this research, we have reported on the isolation and structural elucidation of forty one compounds of eleven new and thirty known compounds from the leaves, stems and fruits of *R. tomentosa*. The crude dichloromethane and acetone extracts showed strong antibacterial activity. The isolated compounds were also evaluated for their antibacterial activity. We found that a known acylphloroglucinol, rhodomyrtone (**ART6**) and the new one, rhodomyrtosone B (**ART9**) showed strong activity. Interestingly, rhodomyrtone (**ART6**) exhibited better activity than the standard, vancomycin. This research demonstrated that *R. tomentosa* can be utilized as a potential source of the bioactive compounds.

CONTENTS

	Page
ABTRACT (in Thai)	iii
ABTRACT (in English)	viii
ACKNOWLEDGEMENTS	xiii
THE RELEVANCE OF THE RESEARCH WORK TO THAILAND	xiv
CONTENTS	xv
LIST OF TABLES	xviii
LIST OF ILLUSTRATIONS	xxiii
ABBREVIATIONS AND SYMBOLS	xxiv
CHAPTER 1 INTRODUCTION	1
1.1 Introduction	1
1.2 The family Myrtaceae	2
1.2.1 Description of the Myrtaceous plants	2
1.2.2 Advantages and traditional uses of the Myrtaceous plants	2
1.2.3 Unique secondary metabolites of the family Myrtaceae	6
1.2.4 Biosynthetic proposal of some phloroglucinols	12
1.2.5 Biological activities of some phloroglucinols	16
1.3 The *Rhodomyrtus* genus	19
1.3.1 Chemical constituents of *Rhodomyrtus* genus	19
1.3.2 Biological activities of *Rhodomyrtus* plants	29
1.4 *Rhodomyrtus tomentosa* (Aiton) Hassk.	30
1.4.1 Description of *R. tomentosa*	30
1.4.2 Nomenclature, Synonyms and Common names	31
1.5 The objectives	33

CONTENTS (Continued)

	Page
CHAPTER 2 EXPERIMENTAL	34
2.1 General methods	34
2.2 Plant material	35
2.3 Chemical investigation of the leaves	35
2.3.1 Extraction and isolation	35
2.3.2 Purification of the Me_2CO extract from the leaves	36
2.3.2.1 Separation of fraction A	36
2.3.2.2 Separation of fraction C	43
2.3.3 Purification of the CH_2Cl_2 extract from the leaves	45
2.3.3.1 Separation of fraction E	45
2.3.3.2 Separation of fraction D	48
2.3.4 Purification of the MeOH extract from the leaves	50
2.3.5 Acetylation of the MeOH extract from the leaves	52
2.4 Chemical investigation of the stems	55
2.4.1 Extraction and isolation	55
2.4.2 Purification of the CH_2Cl_2 extract from the stems	56
2.4.3 Purification of the Me_2CO extract from the stems	58
2.5 Chemical investigation of the fruits	61
2.5.1 Extraction and isolation	61
2.5.2 Purification of the MeOH extract from the fruits	61
2.6 Antibacterial activity	65
CHAPTER 3 RESULTS AND DISCUSSION	66
3.1 Structure elucidation	66
3.1.1 Phloroglucinols	67
ART6, **ART2**, **ART3**, **ART4**, **ART8**, **ART9**, **ART11,** **ART18**, **ART19**, **ART20** and **ART38**	

CONTENTS (Continued)

	Page
3.1.2 Flavonoids	110
ART7, **ART13**, **ART16** and **ART17**	
3.1.3 Ellagic acid derivatives	121
ART10, **ART28** and **ART41**	
3.1.4 Flavellagic acid derivatives	131
ART31 and **ART25**	
3.1.5 Terpenoids	136
ART12, **ART14**, **ART22**, **ART23**, **ART32**, **ART34** and **ART39**	
3.1.6 Steroids	161
ART5, **ART24** and **ART37**	
3.1.7 Benzenoids	170
ART1, **ART21**, **ART30**, **ART35**, **ART36** and **ART40**	
3.1.8 Lignans	181
ART33	
3.1.9 Miscellaneous compounds	185
ART15, **ART26**, **ART27** and **ART29**	
3.2 Antibacterial activities of some of the isolated phloroglucinols	194
3.3 Biosynthetic proposal of some of the isolated phloroglucinols	196
REFERENCES	198
APPENDIX	211
The NMR spectral data of known compounds from the literatures	212
VITAE	229

LIST OF TABLES

Table		Page
1	Compounds isolated from the plants of the *Rhodomyrtus* genus	20
2	Physical appearance and weight of fractions obtained from QCC of fraction A	37
3	Physical appearance and weight of fractions obtained from QCC of fraction C	43
4	Physical appearance and weight of fractions obtained from CC of fraction E	46
5	Physical appearance and weight of fractions obtained from CC of fraction D	49
6	Physical appearance and weight of fractions from QCC of the MeOH extract	50
7	Physical appearance and weight of fractions obtained from CC of the crude AcF	53
8	Physical appearance and weight of fractions obtained from QCC of the CH_2Cl_2 extract	56
9	Physical appearance and weight of fractions obtained from CC of the acetoneMe_2CO extract of the stems	59
10	Physical appearance and weight of fractions obtained from CC of the MeOH extract	62
11	The NMR spectral data of **ART6**	69
12	The NMR spectral data of **ART2**	73
13	The NMR spectral data of **ART3**	77
14	The NMR spectral data of **ART4**	80
15	The NMR spectral data of **ART8**	84
16	The NMR spectral data of **ART9**	86
17	The NMR spectral data of **ART11**	91

LIST OF TABLES (Continued)

Table		**Page**
18	The NMR spectral data of **ART18**	96
19	The NMR spectral data of **ART19**	99
20	The NMR spectral data of **ART20**	104
21	The NMR spectral data of **ART38**	108
22	The NMR spectral data of **ART7**	111
23	The NMR spectral data of **ART13**	114
24	The NMR spectral data of **ART16**	117
25	The NMR spectral data of **ART17**	120
26	The NMR spectral data of **ART10**	123
27	The NMR spectral data of **ART28**	126
28	The NMR spectral data of **ART41**	130
29	The NMR spectral data of **ART31**	133
30	The NMR spectral data of **ART25**	135
31	The NMR spectral data of **ART12**	138
32	The NMR spectral data of **ART14**	141
33	The NMR spectral data of **ART22**	144
34	The NMR spectral data of **ART23**	148
35	The NMR spectral data of **ART32**	152
36	The NMR spectral data of **ART34**	156
37	The NMR spectral data of **ART39**	159
38	The NMR spectral data of **ART5**	162
39	The NMR spectral data of **ART24**	165
40	The NMR spectral data of **ART37**	168

LIST OF TABLES (Continued)

Table		**Page**
41	The NMR spectral data of **ART1**	171
42	The NMR spectral data of **ART21**	175
43	The NMR spectral data of **ART30**	177
44	The NMR spectral data of **ART35**	178
45	The NMR spectral data of **ART36**	179
46	The NMR spectral data of **ART40**	180
47	The NMR spectral data of **ART33**	183
48	The NMR spectral data of **ART15**	187
49	The NMR spectral data of **ART26**	189
50	The NMR spectral data of **ART27**	191
51	The NMR spectral data of **ART29**	193
52	Antibacterial activity of the extracts from *R. tomentosa*	195
53	Antibacterial activity of some of the isolated acylphloroglucinols from *R. tomentosa*	195
54	The NMR spectral data of **rhodomyrtone**	212
55	The NMR spectral data of **combretol**	213
56	The NMR spectral data of **3',5-dihydroxy-3,4',5',7-tetramethoxyflavone**	213
57	The NMR spectral data of **3,3',4-tri-*O*-methylellagic acid**	214
58	The NMR spectral data of **4-*O*-[*β*-D-glucopyranosyl-tetraacetate]-3,3',4'-tri-*O*-methylellagic acid**	214

LIST OF TABLES (Continued)

Table		**Page**
59	The ^{1}H NMR spectral data of **4-*O*-methylellagic acid 3'-α-rhamnoside** (A), **3-*O*-methylellagic acid 3'-*O*-α-rhamno-pyranoside** (B) and **3-*O*-methylellagic acid 4-*O*-α-rhamno-pyranoside** (C)	215
60	The ^{13}C NMR spectral data of **4-*O*-methylellagic acid 3'-α-rhamnoside** (A), **3-*O*-methylellagic acid 3'-*O*-α-rhamno-pyranoside** (B) and **3-*O*-methylellagic acid 4-*O*-α-rhamno-pyranoside** (C)	216
61	The NMR spectral data of **(6*R*,7*E*,9*R*)-9-hydroxy-4,7-megastigmadien-3-one** (A) and **(6*R*,7*E*,9*S*)-9-hydroxy-4,7-megastigmadien-3-one** (B)	217
62	The NMR spectral data of **loliolide** and **isololiolide**	218
63	The NMR spectral data of **3*β*-O-*E*-coumaroylmaslinic acid**	219
64	The NMR spectral data of **3*β*-O-*Z*-coumaroylmaslinic acid**	219
65	The NMR spectral data of **3*β*-*O*-*E*-coumaroyloleanolic acid**	220
66	The NMR spectral data of **arjunolic acid** and **hyptatic acid-A**	221
67	The NMR spectral data of **oleanolic acid**	223
68	The NMR spectral data of ***β*-sitosterol**	224
69	The NMR spectral data of ***β*-sitosterol glucopyranoside** (**daucosterol**)	225
70	The NMR spectral data of **stimast-4-en-3-one**	226
71	The NMR spectral data of ***trans*-triacontyl-4-hydroxy-3-methoxycinnamate**	227

LIST OF TABLES (Continued)

Table		**Page**
72	The NMR spectral data of ***trans*-triacontyl-4-hydroxy-cinnamate**	227
73	The NMR spectral data of **9,9′-*O*-diferuloyl-(-)-secoisolariciresinol**	228

LIST OF ILLUSTRATIONS

Scheme		Page
1	The extract preparations obtained from the leaves of *R. tomentosa*	35
2	Fractions obtained from the acetone extract utilizing its solubility	36
3	Separation and purification of **ART1-ART12**	37
4	Separation and purification of **ART6**, **ART7**, **ART10** and **ART12-ART17**	43
5	Separation and purification of **ART2**, **ART4**, **ART6** and **ART18-ART20**	45
6	Separation and purification of **ART6** and **ART21**	48
7	Separation and purification of **ART6**, **ART10** and **ART22-ART24**	51
8	Separation and purification of **ART25-ART29**	53
9	The extract preparations obtained from the stems	55
10	Separation and purification of **ART30-ART32**	56
11	Separation and purification of **ART33-ART36**	58
12	Separation and purification of **ART6**, **ART11** and **ART37-ART41**	61

Figure

1	*Rhodomyrtus tomentosa* (Aiton) Hassk.	32

LIST OF ABBREVIATIONS AND SYMBOLS

s	=	singlet
d	=	doublet
t	=	triplet
m	=	multiplet
q	=	quartet
quin	=	quintet
sext	=	sextet
hept	=	heptet
dd	=	doublet of doublet
dt	=	doublet of triplet
tt	=	triplet of triplet
td	=	triplet of doublet
ddd	=	doublet of doublet of doublet
br	=	broad
br s	=	broad singlet
μg	=	microgram
mg	=	milligram
g	=	gram
kg	=	kilogram
%	=	percentage
nm	=	nanometer
mp	=	melting point
cm^{-1}	=	reciprocal centimeter (wave number)
δ	=	chemical shift relative to TMS
J	=	coupling constant
λ_{max}	=	maximum wavelength
ν	=	absorption frequencies

LIST OF ABBREVIATIONS AND SYMBOLS (Continued)

ε	=	molar extinction coefficient
^{O}C	=	degree celceis
MHz	=	Megahertz
ppm	=	part per million
IR	=	Infrared
UV	=	Ultraviolet
EI-MS	=	Electron Impact Mass Spectroscopy
HREI-MS	=	High-Resolution Electron Impact Mass Spectroscopy
FAB-MS	=	Fast Atom Bombardment Mass Spectroscopy
HRFAB-MS	=	High-Resolution Fast Atom Bombardment Mass Spectroscopy
NMR	=	Nuclear Magnetic Resonance
2D NMR	=	Two Dimentional Nuclear Magnetic Resonance
COSY	=	Correlated Spectroscopy
DEPT	=	Distortionless Enhancement by Polarization Transfer
HMBC	=	Heteronuclear Multiple Bond Correlation
HMQC	=	Heteronuclear Multiple Quantum Coherence
NOE	=	Nuclear Overhouser Enhancement
NOESY	=	Nuclear Overhouser Enhancement Spectroscopy
ROESY	=	Rotating-frame Overhouser Enhancement Spectroscopy
TMS	=	tetramethylsilane
$CDCl_3$	=	deuterochloroform
CD_3OD	=	tetra-deuteromethanol
DMSO-d_6	=	hexa-deuterodimethylsulphoxide
CH_2Cl_2	=	dichloromethane
Me_2CO	=	acetone
MeOH	=	methanol

LIST OF ABBREVIATIONS AND SYMBOLS (Continued)

CC	=	column chromatography
QCC	=	quick column chromatography
TLC	=	thin-layer chromatography
MIC	=	minimum inhibition concentration

CHAPTER 1

INTRODUCTION

1.1 Introduction

In the present time, all people around the world have extensively concerned about their health which in turn occur from many causes such as air pollutions, water pollutions, and unhealthy food consumption. These are the causes of many types of diseases including cancer, diabetes, alzheimer, hypertension, rheumatoid arthritis, inflammatory bowel disease, immune system decline, brain dysfunctions, cataracts and malaria *etc*. Thus, the new drug discovery or the development in nutrient supplement has very high competition between the suppliers within country and also abroad. Herbal plants play important roles and are mainly sources of natural remedy which are neglected for a long time in many countries. People gained knowledge to utilize the leaves, stem, bark, fruits, bulbs and roots of the plants in the folk medicines from the ancestors for their basic health care needs including the treatments of infections. Furthermore some cosmetics have herbs and some parts of plants for their active ingredients. Unsurprisingly, the medicinal plants are interesting as a source of pharmacologically active substances.

Thailand is in the tropical country abundance with many kinds of herbal plants that can promise to cure many diseases such as *Andrographis paniculata* Wall. ex Nees (ฟ้าทะลายโจร) reliefs the symptom of cold, *Curcuma longa* Linn (ขมิ้นชัน) protects and heals ulcer and *Aloe barbadensis* Mill (ว่านหางจระเข้) uses as ingredients in cosmetics *etc*. Therefore Thai scientists have realized that it is necessary to conduct a research on active constituents from herbal plants which have pharmacological and biological activities.

1.2 The family Myrtaceae

1.2.1 Description of the Myrtaceous plants

The family Myrtaceae (Myrtle or guava family), which consists of evergreen trees or shrubs usually with essential oils-containing cavities in foliage, has at least 4,500 species, possibly more than 5,000 species, and is distributed in about 130 genera. This family is the eighth largest flowering plant family. They have a wide distribution in tropical and warm-temperate regions of the world such as Mediterranean, sub-Saharan Africa, Madagascar, tropical and temperate Asia, Australia, Pacific islands, tropical and South America (Jie and Craven, 2007). The Myrtaceous plants were conventionally classified in which the primary division into two subfamilies based on morphological of the fruits, capsular-fruited Leptospermoideae and fleshy-fruited Myrtoideae (Wilson *et al*., 2001). Capsular-fruited genera such as *Eucalyptus, Corymbia, Angophora, Leptospermum, Melaleuca, Metrosideros* are absent from the Americas except for the monotypic Chilean genus *Tepualia* (Lucas *et al*., 2005). Fleshy-fruited genera have their greatest concentrations in eastern Australia and the Neotropics. *Eucalyptus* is a dominant, nearly ubiquitous genus in Australia and extends north sporadically to the Philippines. *Eucalyptus regnans* or Mountain Ash is the tallest flowering plant in the world, reaching heights of more than 100 meters (State of Victoria, 2003).

1.2.2 Advantages and traditional uses of the Myrtaceous plants

Many Myrtaceae are cultivated as a popular ornamental plant in gardens, street trees or plantation trees in the tropical and subtropical areas, and some members grown for its abundant flowers and sweeten edible fruits (Jie and Craven, 2007). Furthermore, Myrtaceous plants are economically important in the spices, fruits, honeys, timbers and pharmacology industries with other economic potential beginning to be realized (bioactive compounds, vitamin-rich soft fruits *etc*.). *Eucalyptus* is one of the world's most important and most widely planted genera and is a large genus of aromatic trees comprising more than 900 species (Tian *et al*., 2009). It is widely cultivated to provide shade and for the timber and pulp industries (Menut *et al*., 1995;

Ghisalberti, 1996; Kim *et al*., 2001; Benyahia *et al*., 2005; Hasegawa *et al*., 2008; Singh *et al*., 2009; Tian *et al*., 2009). *Syzygium aromatica* (clove) (Charles *et al*., 1998; Jirovetz *et al*., 2006) and *Pimenta dioica* (allspice) (Kikuzaki *et al*., 2008; Nitta *et al*., 2009) are important in the spice industry. *Myrtus comminis* (Tuberoso *et al*., 2006), *Pimenta racemosa* (bay rum) (García *et al*., 2004), *Melaleuca* (cajeput), *Euginia uniflora* (Brazilian cherry tree) (Amorim *et al*., 2009) and *Eucalyptus* (Menut *et al*., 1995; Singh *et al*., 2009; Goodger *et al*., 2009) provide oils for the perfume industry, while antiseptic oils are extracted from *Eucalyptus* (Ghisalberti, 1996; Siddiqui *et al*., 2000; Benyahia *et al*., 2005; Hasegawa *et al*., 2008), *Melaleuca alternifolia* (tea tree) (Russell and Southwell, 2002), *Callistemon* and *Leptospermum* (Melching *et al*., 1997). Almost all fleshy-fruited Myrtaceae are edible; economically important fruits are *Psidium guajava* (guava) (Lapčík *et al*., 2005; Reynertson *et al*., 2008; Steinhaus *et al*., 2008), *Syzygium jambos* (rose apple), *Syzygium malaccensis* (Malay apple), *Syzygium samaramgense* (wax apple), *Syzygium aqueum* (water apple) (Nonaka *et al*., 1992) and *Feijoa sellowiana* (pineapple guava) (Ruberto and Tringali, 2004), with many lesser known species locally important for juice, sweets and jams, such as *Myrciaria cauliflora* (jaboticaba) (Reynertson *et al*., 2006), *Campomanesia lineatifolia* (Osorio *et al*., 2006), *Feijoa sellowiana* (Ruberto and Tringali, 2004; Rossi *et al*., 2007; Weston, 2010) and *Eugenia uniflora* (pitangueira).

Furthermore, several Myrtaceous plants have also been used in folk medicinal purposes. In Hong Kong, *Baeckea frutescens* is widely used in traditional medicine for treating rheumatism and snake bites (Tsui and Brown, 1996) and as an anti-febrile in Southeast Asia and China (Fujimoto *et al*., 1996). The leaves and stem bark of *Campomanesia xanthocarpa*, Brazilian species, are traditionally employed as a remedy for dysentery, stomach problems, fever and as anti-inflammatory agent (Markman *et al*., 2004). Some *Kunzea* species in New Zealand have been reported to utilize the essential oils, including *K. ambigua*, for the treatment of diarrhea, cold, inflammation, and wounds (Ito *et al*., 2004). The bark and leaves of *Melaleuca leucadendron* are used in folk medicine in Taiwan as tranquiling, sedating, evil-dispelling, and pain-relieving agents (Lee, 1998). In Brazil, an astringent decoction of the sun-dried skins of *Myrciaria cauliflora* (jaboticaba) has traditionally been used as

a treatment for hemoptysis, asthma, and diarrhea and gargled for chronic inflammation of the tonsils (Reynertson *et al*., 2006). *Plinia edulis* has commonly been employed in the treatment of stomach disorders, throat infections, diabetes and also as a tonic by traditional seaside settlers of the Brazilian southeastern coast (Ishikawa *et al*., 2008). *Rhodomyrtus tomentsa* has been used as traditional medicine for diarrhea and wound treatments in Vietnam (Tung *et al*., 2009).

Psidium guajava (guava) has been claimed to be useful in a traditional medicine for the treatment of various human ailments such as wounds, ulcers, bowels and cholera. The young leaves are used as a tonic in diseases of digestive function. The decoction of young leaves and shoots is prescribed as a febrifuge, diarrheic disease and spasmolytic effect (Begum *et al*., 2002; Oh *et al*., 2005). The bark is valued as an astringent and as an anti-diarrhoeatic in children whereas the flowers are used to cool the body and for the treatment of bronchitis and eye sores. Furthermore, the fruit has a tonic and laxative and is good for bleeding gums (Begum *et al*., 2002).

In New Zealand, *Leptospermum scoparium* have been employed for the treatment of fevers and pain by the Maori tribes. In addition, its honey has been reported to exhibit antimicrobial activity against *Staphylococcus aureus* and *Helicobacter pylori* (Jeong *et al*., 2009). Traditionally, *L. recurvum* has been used to stimulate appetite and relieve stomach disorders and menstrual discomfort in Malaysia (Mustafa *et al*., 2003).

Pimenta racemosa var. *ozua* is widely used in the folk medicine of the Caribbean basin for different afflictions; for example, in the Dominican Republic, the essential oil from leaves has commonly used for the local treatment of rheumatism or for toothache. The decoction of seed is not used only as a stimulant in Cuba but it is also employed for colds and influenza in Trinidad. In addition, the decoction of leaves has been used to treat abdominal pains in Haití (Fernández *et al*., 2001). *P. dioica* (allspice) has widely used in foods as spice such as its oil has been claimed to relieve neuralgia and rheumatism (Nitta *et al*., 2009) and acted as an antimicrobial and a digestive agent (Kikuzaki et al., 2008).

In the *Eucalyptus* genus, several species have been reported for utilization in traditional medicine such as essential oils from its leaves are acted as antiseptics for

the treatment of infection of upper respiratory tract, the common cold, influenza and sinus congestion (Siddiqui *et al*., 2000; Hasegawa *et al*., 2008) and for curing certain skin diseases while the gum is used in diarrhoea and as astringent in dentistry, cuts, *etc* (Siddiqui *et al*., 2000). The leaves extract has become a potential for larvicidal and repellent properties against mosquito vectors with very eco-friendly (Nathan, 2007). The essential oil further has a therapeutic application to treat pulmonary infections by inhalation (Hasegawa *et al*., 2008). Their barks and leaves have been believed to cure colds, influenza, toothaches, snakebites, fevers, diarrhea and other complaints (Kim *et al*., 2001). The leaves of *E. robusta* are also used for the treatment of dysentery, malaria, and other bacterial diseases (Xu *et al*., 1984). The essential oil from the leaves of *E. tereticornis* has long been recognized for its insecticidal properties, especially its mosquito repellent activity (Nathan, 2007).

The *Eugenia* genus has been reported to be used as several folk medicines. For examples, the infusions or decoctions of *E. uniflora* (Brazilian cherry) leaves have been used as a popular medicine for the treatment of inflammations, against rheumatic pains and fever, as hypoglycemiant, diuretic and to avoid stomach problems (Consolini and Sarubbio, 2002; Amorim *et al*., 2009) whereas its red fruits have been used in infusions as an antihypertensive agent as well as in the treatment of digestive disorders (Consolini *et al*., 1999). The infusions or decoction of the leaves of *E. punicifolia* have been used in the treatment of hyperglycaemic disturbs, such as diabetes mellitus (Grangeiro *et al*., 2006).

The *Syzygium* genus has further been reported for several different uses in medicine; for examples, *S. aromaticum* buds (clove) have folk medicinally been used as diuretic, odontalgic, stomachic, tonicardiac, aromatic condiment and condiment with carminative and stimulant properties (Nassar, 2006). Traditionally the bark of *S. jambos* (syn. *E. jambos*) has been used to treat pernicious attack, amenorrhea, abdominal pain and diarrhea (Djipa *et al*., 2000). Furthermore, in Venezuela, its leaves infusions have been used in traditional medicine as febrifuge and remedy for the relief of inflammatory pain, especially in sore throats (Ávila-Peña *et al*., 2007). In South Africa, the barks, leaves and roots of *S. cordatum* have been claimed to use for the treatment of ailments including tuberculosis, diarrhoea, stomach and respiratory

complaints (Musabayane *et al*., 2005). The barks of *S. guineense* which distributed in Subsaharan Africa (Uganda, Swaziland and Cameroon) have been traditionally used for the treatment of stomachache and diarrhea (Djoukeng *et al*., 2005). In Malaysia, the leaves of *S. aqueum* (watery rose apple or water apple) have been used to treat a cracked tongue whereas the root to relieve itching and to reduce swelling (Osman *et al*., 2009).

1.2.3 Unique secondary metabolites of the family Myrtaceae

Many plants in the family Myrtaceae have been phytochemically investigated and also have been reported on the isolation of the several constituents including phloroglucinols, flavonoids, anthocyanins, terpenoids, tannins, and stilbenoids. Among these the phloroglucinols, a rare natural product containing the unique structure, which mainly obtained from the plants of the family Myrtaceae, have been recently become the interesting compounds. Apart from the structural identity, they also exhibited significantly the wild ranges of biological activities.

Myrtaceous plants produced a range of phloroglucinols, a major class of secondary metabolites, with different levels of methylation of the nuclear carbons and oxygens. These compounds have been classified according to a number of phloroglucinol units into monomeric phloroglucinols, dimeric phloroglucinols, trimeric phloroglucinols, tetrameric and higher phloroglucinols, and phlorotannins (Singh and Bharate, 2006).

A large number of differently substituted and structurally diverse monomeric phloroglucinols have been reported to occur amongst plants as well as other natural sources, and have been shown to possess various biological activities. Monomeric phloroglucinols can be further divided into different subclasses such as acylphloroglucinols: BF-1, leptospermone and champanone A (Fujimoto *et al*., 1996; Bonilla *et al*., 2005) and phloroglucinol-terpene adducts: BF-2, eucalyptone and euglobal G8 (Fujimoto *et al*., 1996; Osawa *et al*., 1995; Umehara *et al*., 1998) *etc*.

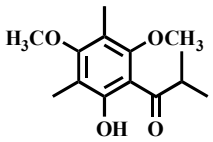

BF-1

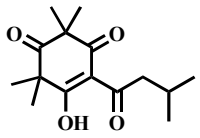

leptospermone

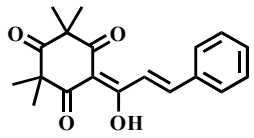

champanone A

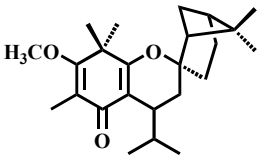

BF-2

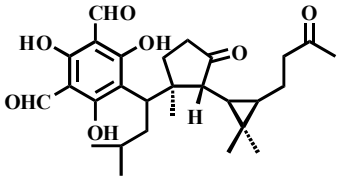

eucalyptone

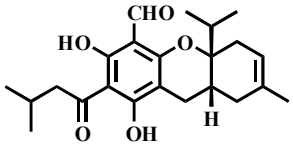

euglobal G8

Structures of some monomeric phloroglucinols

Dimeric phloroglucinols comprised of two units of phloroglucinol joined either through a carbon-carbon linkage or by the formation of a chroman ring and have been found in many genera including *Myrtus*, *Lophomyrtus*, *Rhodomyrtus*, *Eucalyptus*, *Kunzea*, and *Corymbia etc*. such as myrtucommulone B (Shaheen *et al*., 2006), semimyrtucommulone (Appendino *et al*., 2002), rhodomyrtone (Dachriyanus *et al*., 2002), dimer of jensenone (Mitaine-Offer *et al*., 2003), bullataketals A and B (Larsen *et al*., 2005), and corymbones A and B (Carroll *et al*., 2008b).

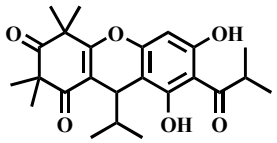

myrtucommulone B

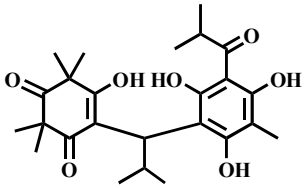

semimyrtucommulone

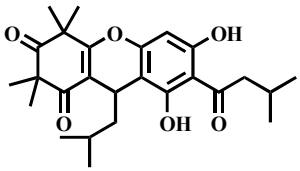

rhodomyrtone

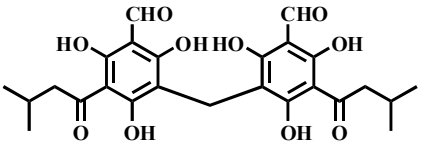

dimer of jensenone

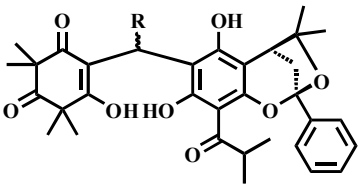

R = β-isopropyl: bullataketal A

R = α-isopropyl: bullataketal B

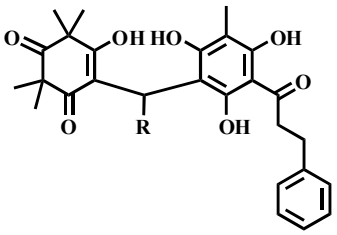

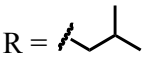

: corymbone A

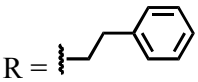

: corymbone B

Structures of some dimeric phloroglucinols

Many genera of the Myrtaceous plants such as *Callistemon*, *Corymbia*, *Eucalyptus*, and *Myrtus etc*. have been reported to produce the trimeric phloroglucinols. Examples of trimeric phloroglucinols were myrtucommulone A, myrtucommulones C-I (Kashman *et al*., 1974; Carroll *et al*, 2008a; Appendino *et al*., 2002) and eucalyptone G (Mohamed and Ibrahim, 2007).

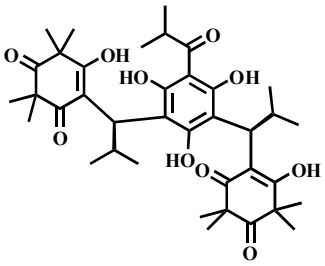

myrtucommulone A

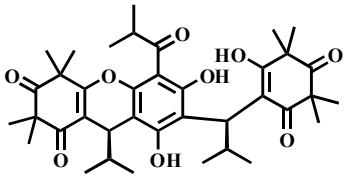

myrtucommulone C

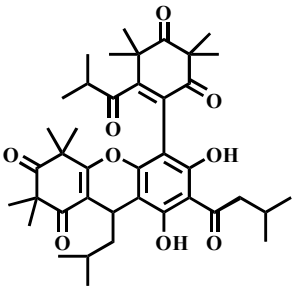

eucalyptone G

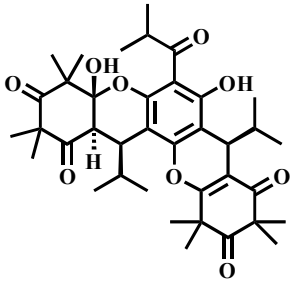

myrtucommulone D

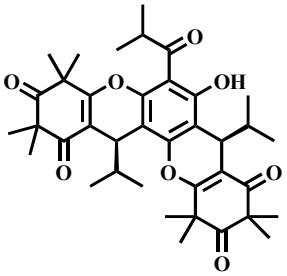

myrtucommulone E

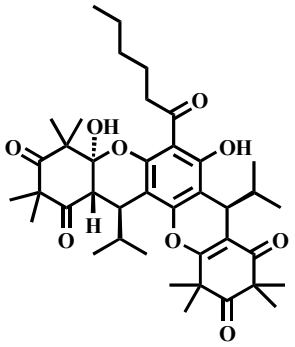

myrtucommulone G

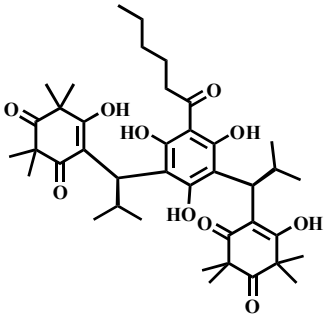

myrtucommulone F

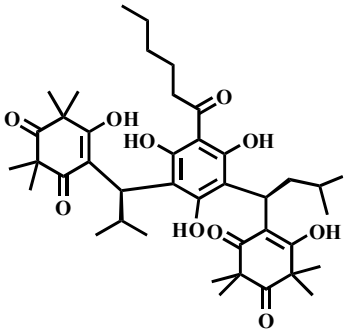

myrtucommulone H

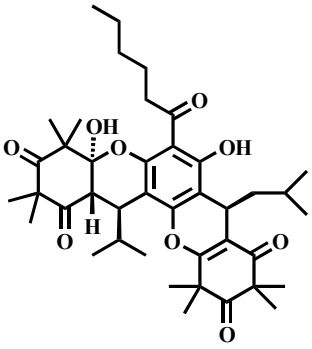

myrtucommulone I

Structures of some trimeric phloroglucinols

Tetrameric and higher phloroglucinol compounds covered the phloroglucinol derivatives bearing more than three phloroglucinol units. Based on the literature surveys, this group has not been found to isolate from the plants in the family Myrtaceae. They were reported on the isolation from the other sources such as tetra-albaspidin ABBA (dryocrassin) from ferns *Dryopteris crassirhizoma*. Tetra-albaspidin BBBB was independently isolated from the ferns *D. austriaca* and *D. aitoniana* whereas tetraflavaspidic acid BBBB, penta-albaspidin BBBBB, hexaflavaspidic acid and hexa-albaspidin BBBBBB have been reported on the isolation from *D. aitoniana* (Singh and Bharate, 2006).

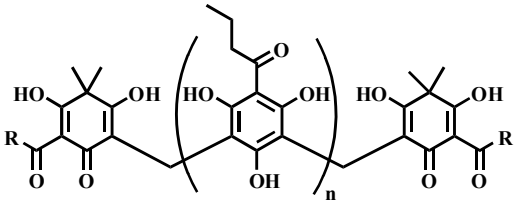

n = 2; R = CH_3 : tetra-albaspidin ABBA

n = 2; R = $CH_2CH_2CH_3$: tetra-albaspidin BBBB

n = 3; R = $CH_2CH_2CH_3$: penta-albaspidin BBBBB

n = 4; R = $CH_2CH_2CH_3$: hexa-albaspidin BBBBBB

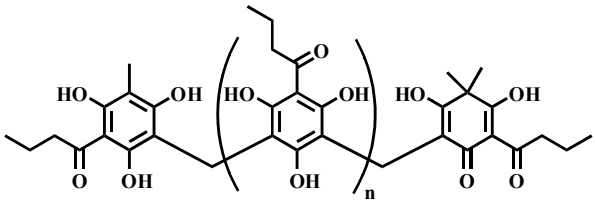

n = 2 : tetraflavaspidic acid BBBB

n = 4 : hexaflavaspidic acid

Structures of some tetrameric and higher phloroglucinols

Phlorotannins consist of phloroglucinol units linked to each other in various ways, and are of wide occurrence amongst marine organisms, especially brown and red algae. This group can be classified into four subclasses: phlorotannins with an ether linkage (fuhalols and phlorethols) such as hydroxyhexaphlorethol and

trihydroxyheptaphlorethol A, with a phenyl linkage (fucols) such as difucol-4,4'-di-*O*-sulfate and tetrafucol A, with an ether and a phenyl linkage (fucophlorethols) such as fucophlorethol A and bisfucotriphlorethol, and with a dibenzodioxin linkage (eckols and carmalols) such as 7-hydroxyeckol and 2-phloro-6,6'-bieckol (Singh and Bharate, 2006).

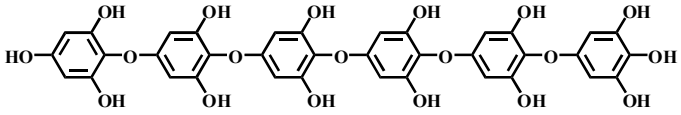

Hydroxyhexaphlorethol

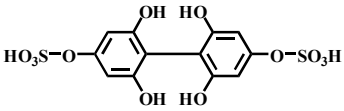

difucol-4,4'-di-*O*-sulfate

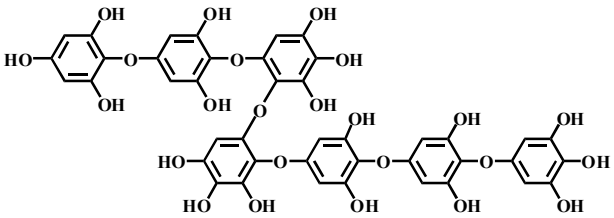

trihydroxyheptaphlorethol A

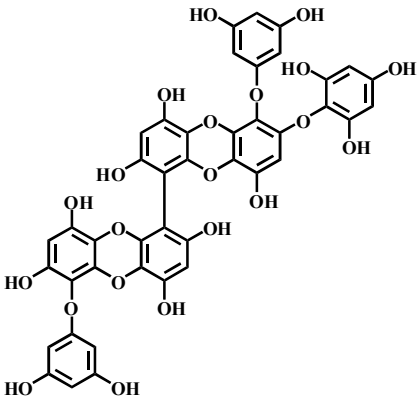

2-phloro-6,6'-bieckol

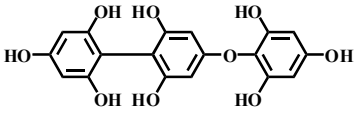

fucophlorethol A

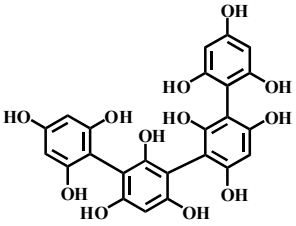

tetrafucol A

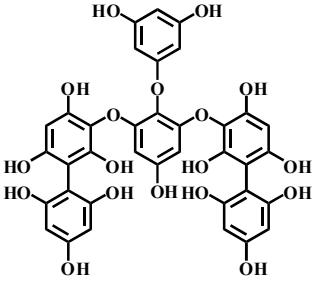

bisfucotriphlorethol

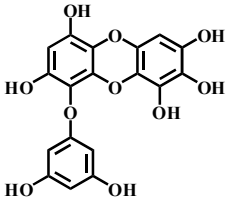

7-hydroxyeckol

Structures of some phlorotannins

1.2.4 Biosynthetic proposal of some phloroglucinols

The biosynthesis of naturally myrtucommulones from *Myrtus communis* has been proposed in 1974 by Kashman and co-workers. They could be derived from the similar pathway suggested for the fern acylphloroglucinols through cyclization of linear polyketomethylene intermediates (Kashman *et al*., 1974).

The phloroglucinol-monoterpene adducts named euglobals G6-G12 could be biogenetically formed between an appropriate monoterpene and an *O*-quinone methide derived from grandinol by Diels-Alder cycloaddition (Singh *et al*., 1998; Umehara *et al*., 1998).

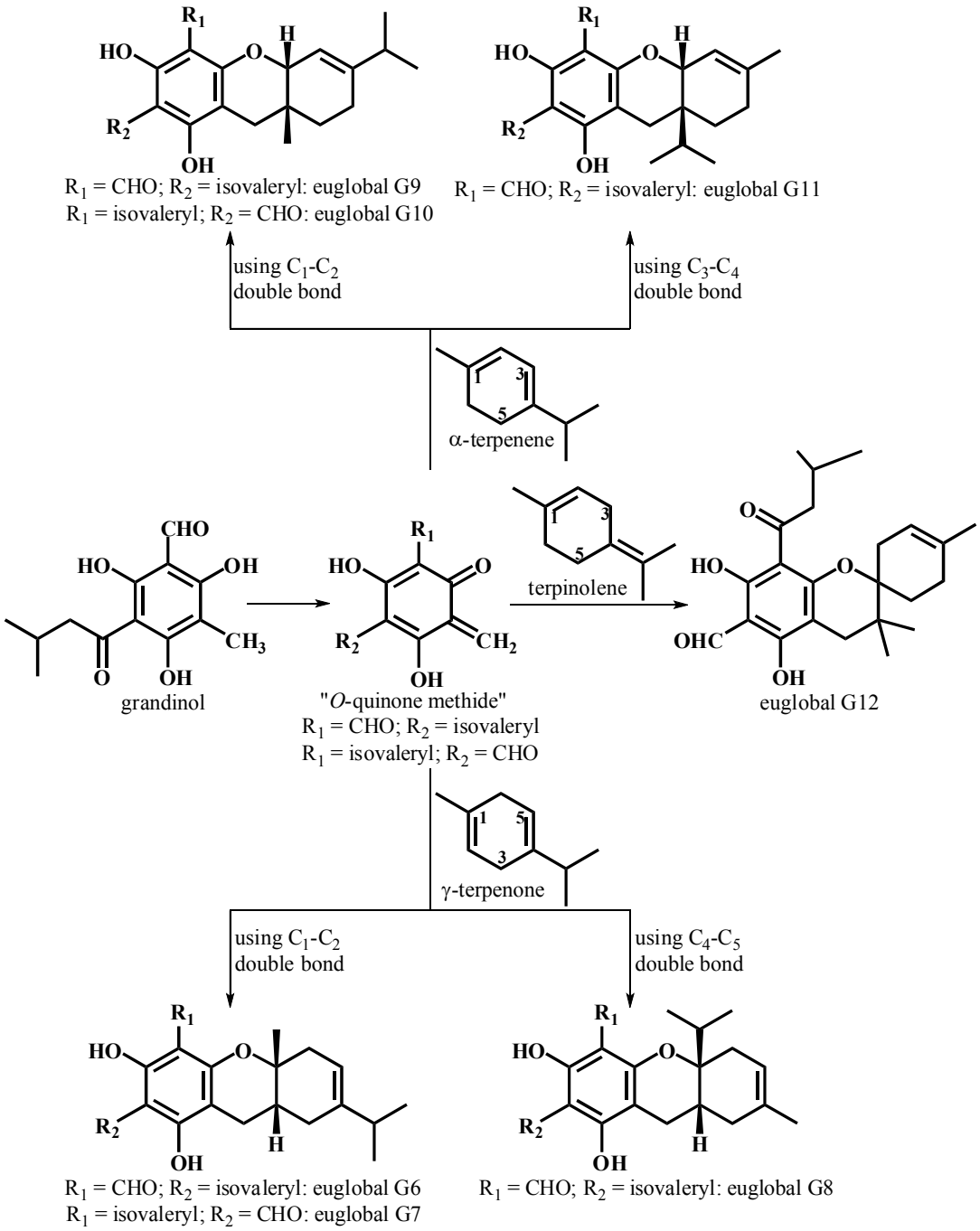

Proposed biosynthetic pathway for euglobals G6 - G12

Dachriyanus and co-workers have suggested that the biogenetically route for rhodomyrtone involved a condensation of leptospermone with the appropriate isovalerylphloroglucinol followed by hemiketal formation between phenolic hydroxyl group and a keto group with concomitant loss of water (Dachriyanus *et al*., 2002).

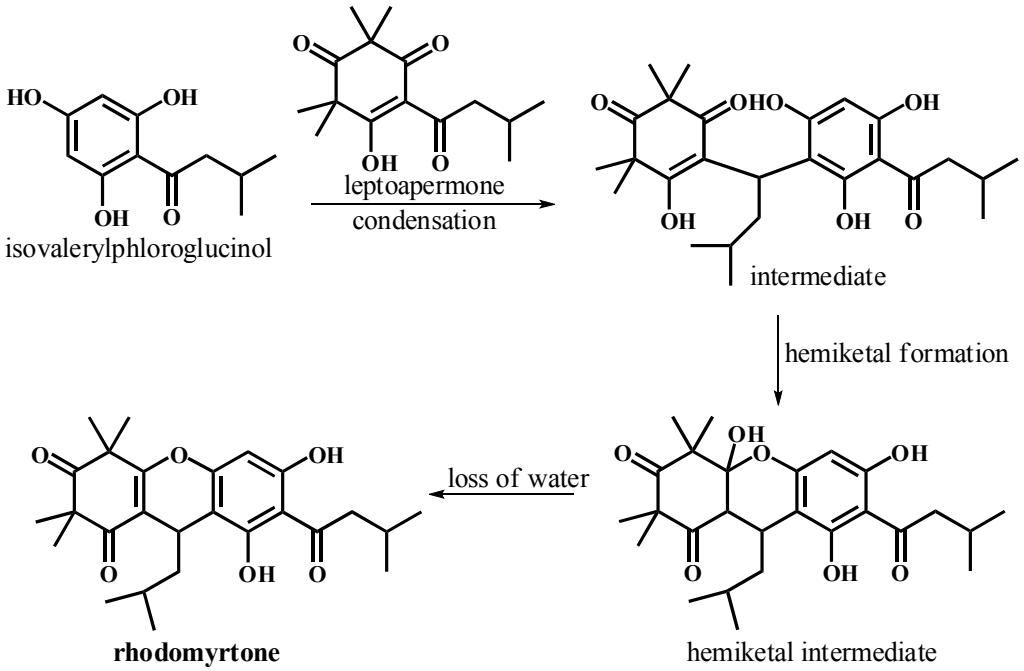

Proposed biosynthetic pathway of rhodomyrtone

Bullataketals A and B have been biosynthetically proposed by Larsen and co-workers in year 2005. This route involved an enzymatic process, polyketide synthase (PKS) inducing the combination between isobutyryl-CoA and three malonyl-CoA units to form an isobutyrylphloroglucinol. Methylation of this phloroglucinol with *S*-adenosyl methionine (SAM) could produce a *β*-triketone moiety. Aldol-like condensation of phloroglucinol and *β*-triketone units would give intermediate as a mixture of stereoisomers, followed by combination with bullatenone. Bullataketals A and B could finally be derived by acid-catalysed cyclisation (Larsen *et al*., 2005).

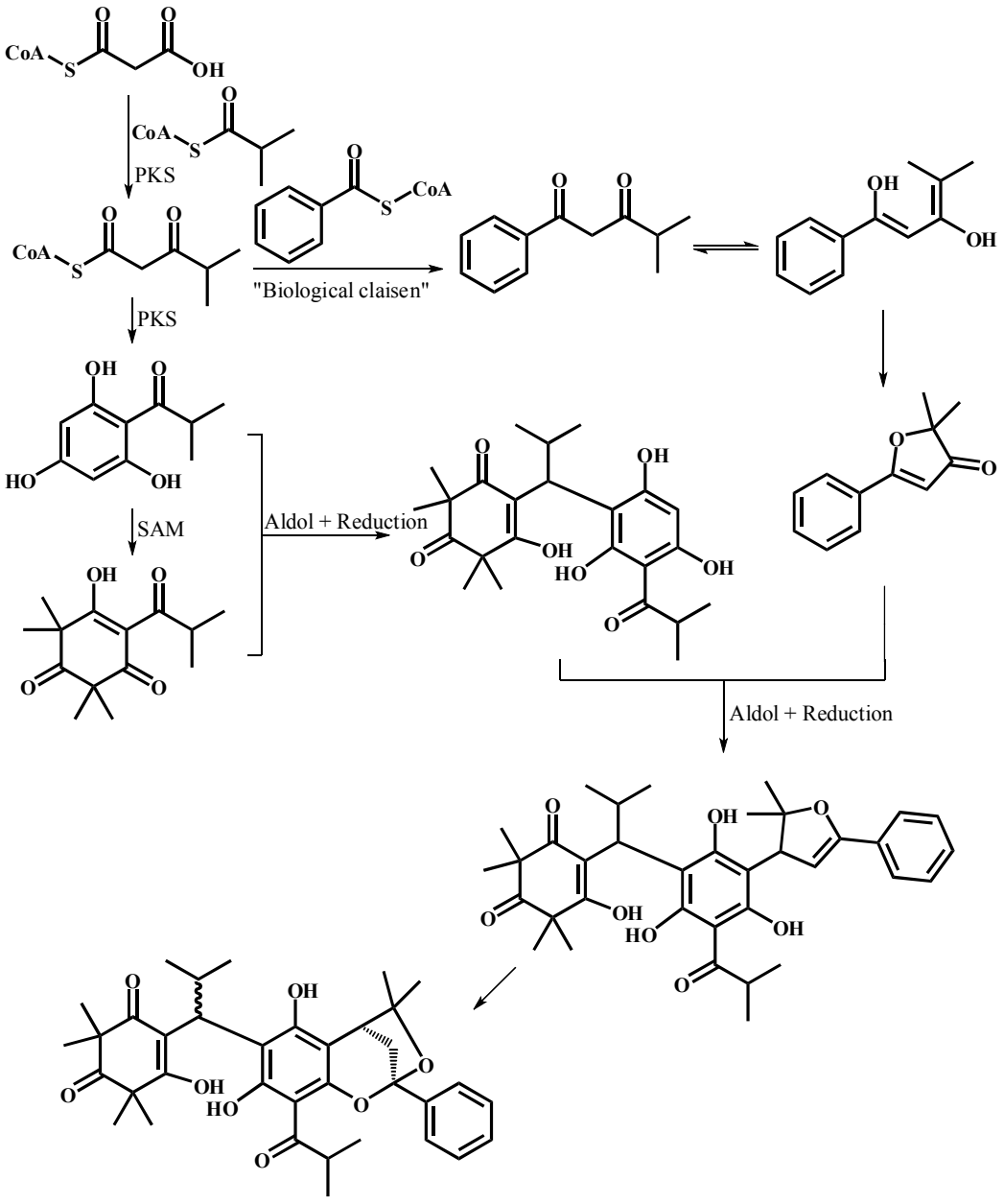

Proposed biosynthetic pathway of bullataketals A and B

The corymbone phloroglucinols could be biogenetically derived from the condensation of 2',4',6'-trihydroxy-3'-methyldihydrochalcone with the appropriate cyclohexatriones (Carroll *et al*., 2008a).

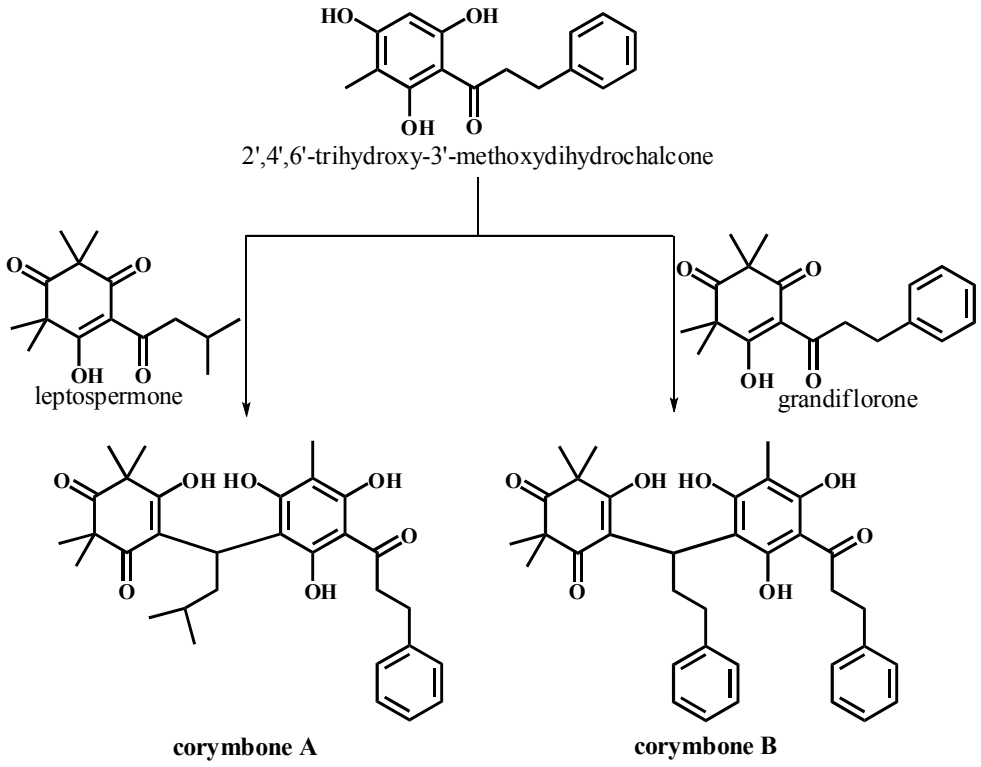

Proposed biosynthetic pathway of corymbones A and B

1.2.5 Biological activities of some phloroglucinols

Some of phloroglucinols from the family Myrtaceae exhibited interesting antibacterial activities. The constituent from the leaves of *Rhodomyrtus tomentosa*, rhodomyrtone, showed significant activity to inhibit *Escherichia coli* and *Staphylococcus aureus*, but without the value and details reported (Dachriyanus *et al*., 2002). Eucalyptone, obtained from the leaves of *Eucalyptus globulus*, has antibacterial activity against cariogenic bacteria including against *Streptococcus mutans* (MIC 6.25 μg/mL) and *Streptococcus sobrinus* (MIC 12.5 μg/mL). It also showed an inhibitory effect on adherent water-insoluble glucan synthesis by GTase

with 97.6 and 44.0% inhibition at concentration of 100 and 10 μg/mL, respectively, prepared from the supernatant of *S. sobrinus*. These data indicated that eucalyptone might be a promising natural substance for the development of a new cariostatic drug (Osawa *et al*., 1995). Eucalyptone G, isolated from the bark of small twigs of *Eucalyptus globulus* Labill, was found to be active against *Bacillus subtilis*, *Staphylococcus aureus*, and *Escherichia coli* (Mohamed and Ibrahim, 2007). Champanone A showed activity against *Micrococcus luteus*, *Staphylococcus aureus*, *Bacillus subtilis*, and *Pseudomonas aeruginosa* with the MIC value of 30 μg/mL and against *Streptococcus faecalis* with the MIC value of 15 μg/mL. Champanone B was active against *M. luteus* (MIC 30 μg/mL) and champanone C against both *B. subtilis* and *S. faecalis* (MIC 30 μg/mL). These data indicated that the three champanones displayed mild antimicrobial activity (Bonilla *et al*., 2005). Myrtucommulone A which was first isolated from *Myrtus communis* L. showed strong antibacterial activity against Gram-positive bacteria with the concentration of 1γ/mL (Kashman *et al*., 1974) whereas Appendino *et al* have also conducted from the leaves of *Myrtus communis* L. showing significant activity against multidrug-resistant (MRD) clinically relevant bacteria, *Staphylococcus aureus* (Appendino *et al*., 2002). Furthermore myrtucommulone A was also obtained from the leaves of *Callistemon lanceolatus* (Lounasmaa *et al*, 1977) and the seeds of *Corymbia scabrida* (Carroll *et al*, 2008b). Shaheen *et al* have reported that myrtucommulones D and E, isolated from the aerial parts of *Myrtus communis* L., exhibited significant antibacterial activity against *Staphylococcus aureus* (Shaheen *et al*, 2006). Myrtucommulone D was also isolated and identified from the seeds of *Corymbia scabrida* (Carroll *et al*, 2008b).

In 1992, Bloor have reported that 2,6-dihydroxy-4-methoxyisobutyrophenone and 4,6-dihydroxy-2-methoxyisobutyrophenone, the phloroglucinol constituents from the leaves and twigs of *Kunzea sinclairii*, showed antiviral activities against Herpes simplex Type I and Polio Type I viruses with the inhibition of cytopathic effect of either viruses of 5 μg/disk (Bloor, 1992). Phloroglucinols from the leaves of *Eucalyptus globulus* named euglobals G6 and G7 have been reported as inhibitors of Epstein Barr Virus (EBV) activation induced by 12-*O*-tetradecanoylphorbol-13-

acetate (TPA). Both compounds showed *ca* 80% inhibition at 1000 mol ratio/TPA, while maintaining 70% viability of Raji cells (Singh *et al*., 1998). In addition to euglobals G6 and G7, euglobals G8, G9 and G12 showed around 100% inhibition at 1000 mol ratio/TPA while maintaining 70% viability of the Raji cells (Umehara *et al*., 1998).

Some of them acted as insecticidal such as 4-[1-(5,7-Dihydroxy-6-methyl-4-oxo-2-phenyl-chroman-8-yl)-3-methyl-butyl]-5-hydroxy-2,2,6,6-tetramethyl-cyclohex-4-en-1,3-dione, which comprised a pair of epimers, each of which is a pair of conformers, from the hexane extract of the aerial parts of *Kunzea ambigua* and *K. baxterii*. It showed the LD_{50} by topical application to mustard beetles, *Phaedon cochleariae*, the aphid, *Aphis fabae* and the thrips, *Thrips tabaci* of 1.0, 3.9 and 15 μg/insect, respectively. A dose of 10 μg/insect caused 83% mortality of houseflies, *Musca domestica*. (Khambay *et al*., 2002). The constituents from the aerial parts of *Callistemon viminalis*, viminadione A, also exhibited insecticidal activity to houseflies, *Musca domestica*, the aphid, *Aphis fabae*, and the thrips, *Thrips tabaci* with the LD_{50} of 1.9, 5.9 and 4.2 μg/insect, respectively (Khambay *et al*., 1999).

Apart from myrtucommulones A and D, the seeds of *Corymbia scabrida* have been reported on the isolation of four further trimeric phloroglucinols named myrtucommulones F-I. Myrtucommulones A, D and F-I inhibited the specific binding of [^{3}H]3-methylhistidylTRH to HEK cell membranes expressing recombinant rat TRH receptor 2 with respectively IC_{50} values of 39, 11, 16, 24, 31, and 16 μM (Carroll *et al*., 2008a). In addition, corymbones A and B obtained from the flowers of *Corymbia peltata* also exhibited rat TRH receptor 2 binding affinity with IC_{50} values of 23 and 19 μM, respectively (Carroll *et al*., 2008b).

Phloroglucinols named myrtucommulones B-E were found to be more potent α-glucosidase inhibitors than the clinically used standard acarbose while myrtucommulone C exhibited the highest activity among all the phloroglucinols with the IC_{50} 35.4±1.15 μM (Shaheen *et al*., 2006).

Furthermore, some of them showed interesting cytotoxic activities such as BF-2 isolated from the dried leaves of *Baeckea frutescens*, against leukaemia cells (L 1210) in tissue culture with the IC_{50} 5.0 μg/mL (Fujimoto *et al*., 1996).

The phloroglucinols, nemed bullataketals A and B from the leaves and twigs of *Lophomyrtus bullata*, have cytotoxic activity against the P388 mouse leukaemia cell line with the IC_{50} 1 μg/mL (Larsen *et al*., 2005).

14 Genera with about 79 species of the family Myrtaceae were found in Thailand: *Acmena* (1 species), *Baeckia* (1 species), *Callistemon* (2 species), *Cleistocalyx* (2 species), *Decaspermum* (2 species), *Eucalyptus* (2 species), *Eugenia* (3 species), *Syzygium* (56 species), *Melaleuca* (1 species), *Myrtus* (1 species), *Psidium* (2 species), *Rhodamnia* (2 species), *Rhodomyrtus* (1 species) and *Tristania* (3 species) (Smitinand, 2001).

1.3 The *Rhodomyrtus* genus

1.3.1 Chemical constituents of the *Rhodomyrtus* genus

The genus *Rhodomyrtus* comprises of about 20 species which widely distributed in tropical Asia, Australia and Southwest Pacific islands (Jie and Craven, 2007). Based on SciFinder Scholar database, only 8 species from the *Rhodomyrtus* plants have been reported for phytochemically investigation including *R. effussa*, *R. macrocapa*, *R. pervagata*, *R. psidioides*, *R. sericea*, *R. tomentosa*, *R. trineura* subsp. *trineura*, and *R. trineura* subsp. *capensis*. The chemical studies on this genus have concentrated on essential oils, with little work having been published on non-volatiles from *R. macrocapa* and *R. tomentosa*. The chemical constituents isolated from the *Rhodomyrtus* genus were summarized in **Table 1**.

Table 1 Compounds isolated from the plants of the *Rhodomyrtus* genus

Compounds	Structure	References
R. effussa		
Essential oil from leaves		
Globulol	8e	Brophy *et. al.*, 1997
Viridiflorol	8f	
Spathulenol	8j	
R. macrocapa		
Fruit		
Rhodomyrtoxin	3a	Trippett, 1957
ψ-Rhodomyrtoxin	3b	Anderson *et. al.*, 1969
Rhodomyrtoxin B	3c	Igboechi *et al.*, 1984
Rhodomyrtoxin C	3d	
Essential oil from leaves		
β-Caryophyllene	8h	Brophy *et. al.*, 1997
Aromadendrene	8g	
Globulol	8e	
R. pervagata		
Essential oil from leaves		
α-Pinene	8b	Brophy *et. al.*, 1997
β-Pinene	8c	
R. psidioides		
Essential oil from leaves		
α-Pinene	8b	Brophy *et. al.*, 1997
Limonene	8d	

Table 1 (Continued)

Compounds	Structure	References
R. sericea		
Essential oil from leaves		
α-Pinene	8b	Brophy *et. al*., 1997
β-Pinene	8c	
β-Caryophyllene	8h	
R. tomentosa		
Leaves		
Lupeol	8k	Hui *et. al*., 1975
β-Amyrin	8p	
β-Amyrenonol	8q	
Betulin	8l	
21α*H*-Hop-22(29)-en-3β,30-diol	8n	Hui *et. al*., 1976
3β-Hydroxy-21αH-hop-22(29)-en-30-al	8o	
Tomentosin	7a	Lui *et. al.*, 1997
Peduculagin	7b	Lui *et. al.*, 1998
Casuariin	7c	
Castalagin	7d	
Myricetin 3-*O*-α-L-furanoarabinoside	4a	Hou *et. al.*, 1999
Myricetin 3-*O*-β-D-glucoside	4b	
Myricetin 3-*O* -α-L-rhamnoside	4c	
2,3-Hexahydroxydiphenyl-D-glucose	7e	
Rhodomyrtone	1	Dachriyanus *et. al.*, 2002
Piceatannol 4-*O*-β-D-glucoside	6	Nojima *et. al.*, 2007
Stems		
Friedelin	8t	Hui *et. al*., 1975
Lupeol	8k	
α-Amyrin	8s	

Table 1 (Continued)

Compounds	Structure	References
R. tomentosa		
Stems		
Taraxerol	8r	Hui *et. al*., 1975
Betulin	8m	
Betulin-3-acetate	8l	
3β-Acetoxy-11α,12α -epoxyoleanan-28,13β-olide	8w	Hui *et. al*., 1976
3β-Acetoxy-12α-hydroxyoleanan-28,13β-olide	8v	
3β-Acetoxy-12-oxo-oleanan-28,13β-olide	8u	
Flowers		
Malvidin-3-glucoside	2a	Lowry, 1976
Pelargonidin-3,5-biglucoside	2b	He *et. al.*, 1998
Cyanidin-3-galactoside	2c	
Delphinidin-3-galactoside	2d	
Barks and Twigs		
Combretol (3,3',4',5',7-penta-*O*-methylmyricetin)	4d	Dachriyanus *et. al.*, 2004
Aerial parts		
4,8,9,10-Tetrahydroxy-2,3,7-trimethoxy-anthracene-6-*O*-β-D-glucopyranoside	5a	Tung *et. al.*, 2009
2,4,7,8,9,10-Hexahydroxy-3-methoxy-anthracene-6-*O*-α-L-rhamnopyranoside	5b	
Quercetin	4f	
Myricitrin	4e	
(3*S*,5*R*,6*R*,7*E*,9*S*)-Megastiman-7-ene-3,5,6,9-tetrol	8a	

Table 1 (Continued)

Compounds	Structure	References
R. tomentosa		
Buds		
Kaempferol 3-*O*-*β*-sambubioside		Phan *et al*., 2007
Essential oil from leaves		
α-Pinene	8b	Brophy *et. al.*, 1997
β-Pinene	8c	
Aromadendrene	8g	
R. trineura* subsp. *trineura		
Essential oil from Leaves		
β-Caryophyllene	8h	Brophy *et. al.*, 1997
Caryophyllene oxide	8i	
Globulol	8e	
R. trineura* subsp. *capensis		
Essential oil from Leaves		
α-Pinene	8b	Brophy *et. al.*, 1997
Globulol	8e	
Viridiflorol	8f	
Spathulenol	8j	

The literature surveys demonstrated that the *Rhodomyrtus* genus has been investigated and resulted in the isolation of several components including acylphloroglucinols, anthocyanins, dibenzofurans, flavonoids, naphthalenoids, stilbenoids, tannins, and terpenoids. The structures of compounds isolated from the *Rhodomyrtus* genus were summarized as following.

Structures of the isolated compounds from the *Rhodomyrtus* genus

1. Acylphloroglucinols

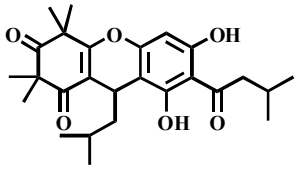

1a: rhodomyrtone

2. Anthocyanins

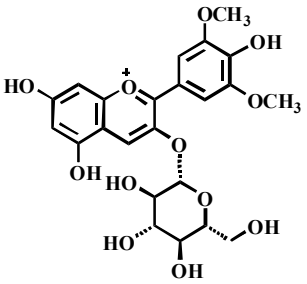

2a: malvidin-3-glucoside

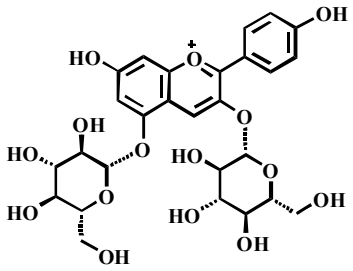

2b: pelargonidin-3,5-biglucoside

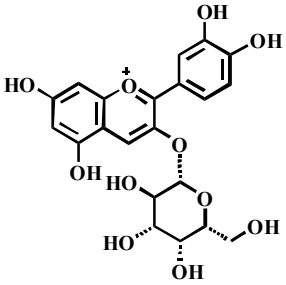

2c: cyanidin-3-galactoside

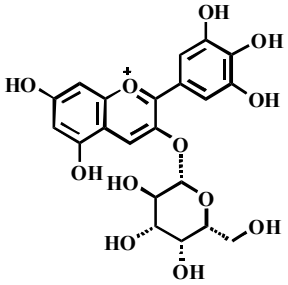

2d: delphinidin-3-galactoside

3. Dibenzofurans

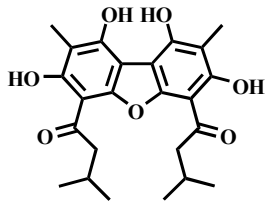

3a: rhodomyrtoxin

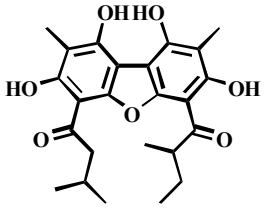

3b: ψ-rhodomyrtoxin

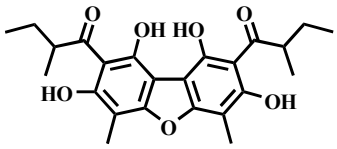

3c: rhodomyrtoxin B

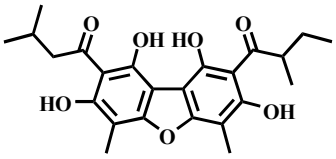

3d: rhodomyrtoxin C

4. Flavonoids

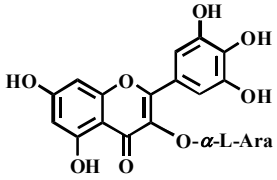

4a: myricetin 3-*O*-α-L-furanoarabinoside

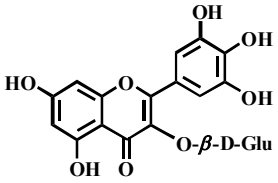

4b: myricetin 3-*O*-β-D-glucoside

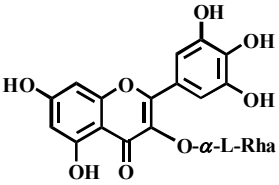

4c: myricetin 3-*O*-α-L-rhamnoside

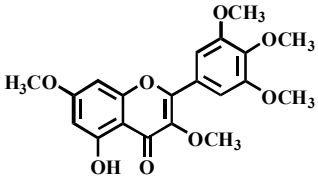

4d: combretol

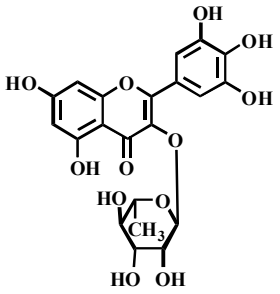

4e: myricitrin

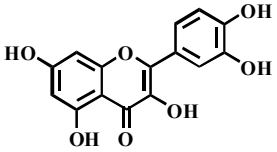

4f: quercetin

5. Naphthalenoids

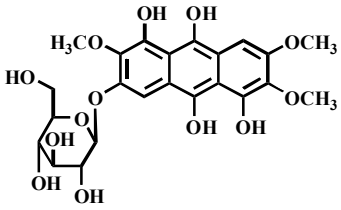

5a: 4,8,9,10-tetrahydroxy-2,3,7-trimethoxy-anthracene-6-*O*-β-D-glucopyranoside

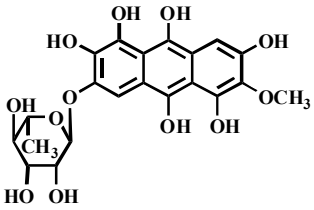

5b: 2,4,7,8,9,10-hexahydroxy-3-methoxyanthracene-6-*O*-α-L-rhamnopyranoside

6. Stilbenoids

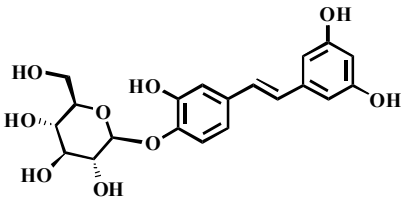

6: piceatannol 4-*O*-β-D-glucoside

7. Tannins

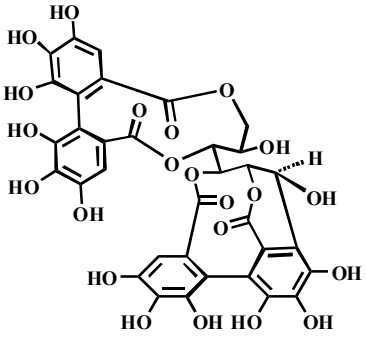

7a: tomentosin

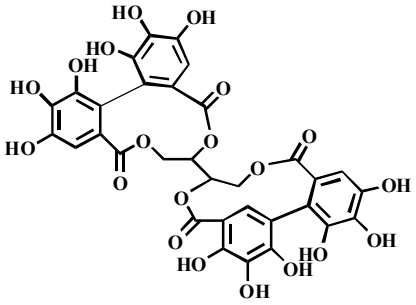

7b: peduculagin

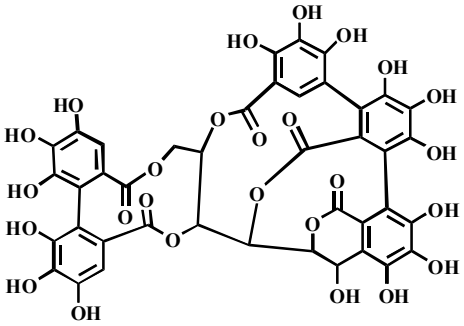

7c: casuariin

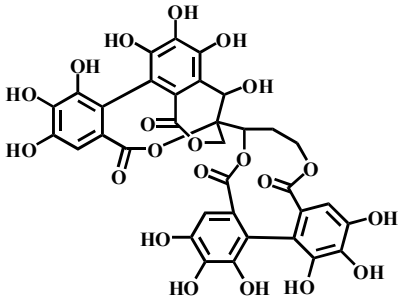

7d: castalagin

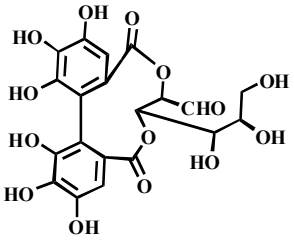

7e: 2,3-hexahydroxydiphenyl-D-glucose

8. Terpenoids

a) Nor-terpenes

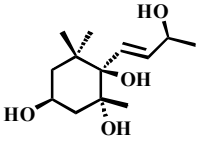

8a: (*3S,5R,6R,7E,9S*)-megastiman-7-ene-3,5,6,9-tetrol

b) Monoterpenes

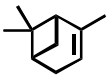

8b: α-pinene

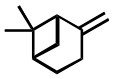

8c: β-pinene

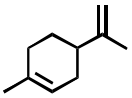

8d: limonene

c) Sesquiterpenes

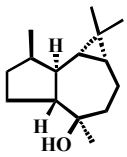

8e: globulol

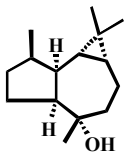

8f: viridiflorol

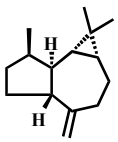

8g: aromadendrene

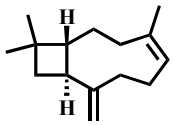

8h: β-caryophyllene

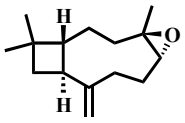

8i: caryophyllene oxide

d) Triterpenes

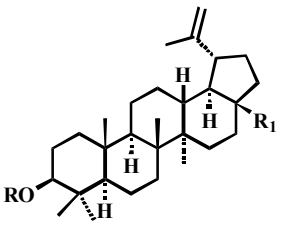

8k: R = H; $R_1 = CH_3$: lupeol

8l: R = H; $R_1 = CH_2OH$: betulin

8m: R = Ac; $R_1 = CH_2OH$: betulin-3-acetate

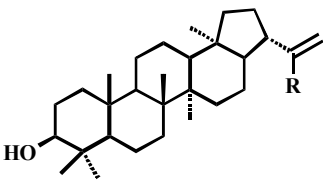

8n: R = CH_2OH : 21αH-hop-22(29)-en-3β,30-diol

8o: R = CHO : 3β-hydroxy-21αH-hop-22(29)-en-30-al

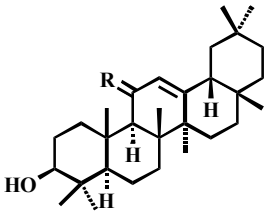

8p: R = H_2: β-amyrin

8q: R = O: β-amyrenonol

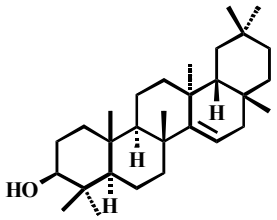

8r: taraxerol

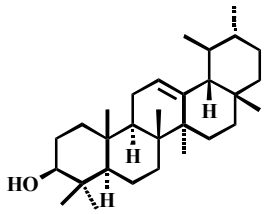

8s: α-amyrin

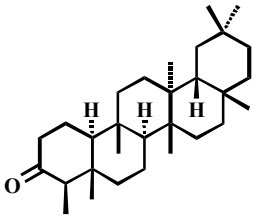

8t: friedelin

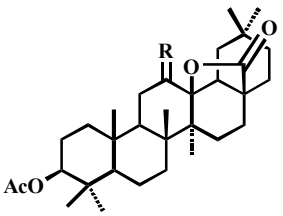

8u: R = O : 3β-acetoxy-12-oxo-oleanan-28,13β-olide

8v: R = α-OH, β-H : 3β-acetoxy-12α-hydroxy-oleanan-28,13β-olide

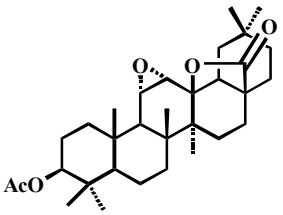

8w: 3β-acetoxy-11α,12α-epoxyoleanan-28,13β-olide

1.3.2 Biological activities of some *Rhodomyrtus* genus

Based on the SciFinder scholar database, only three reports have investigated and identified the active components from the *Rhodomyrtus* genus. The methanolic extract of *R. tomentosa* leaves showed significant antimicrobial activity to inhibit *Escherichia coli* and *Staphylococcus aureus*. Bioassay-guided chromatography of this fraction revealed the isolation of active compound, rhodomyrtone (Dachriyanus *et al*., 2002). Piceatannol 4'-*O*-β-D-glucopyranoside was purified from aq. ethanol extract of dried fruit of *R. tomentosa* showed superoxide-scavenging activity at IC_{50} of 81.7 μg/mL

and it also stimulated the proliferation of cultured human skin fibroblasts and normal human epidermal keratinocytes (Nojima *et al*., 2007). The anthracene glycosides named 4,8,9,10-tetrahydroxy-2,3,7-trimethoxyanthracene-6-*O*-*β*-D-gluco-pyranoside and 2,4,7,8,9,10-hexahydroxy-3-methoxyanthracene-6-*O*-*α*-L-rhamno-pyranoside, isolated from the aerial parts of *R. tomentosa* significantly increased the alkaline phosphatase activity, collagen synthesis, and mineralization of the nodules of MC3T3-E1 osteoblastic cells (Tung *et al*., 2009).

1.4 *Rhodomyrtus tomentosa* (Aiton) Hassk.

Rhodomyrtus tomentosa (Aiton) Hassk. is only one species of the genus *Rhodomyrtus* in Thailand, and locally named as "Toh (โทะ) or Pruad (พรวด)" (Smitinand, 2001). *R. tomentosa* has been used in the traditional medicine for a long time. The ripe fruits are eaten raw to treat diarrhea (Ong and Nordiana, 1999). The liquid that is present in this plant can be used to treat gynaecopathy including morbid leucorrhoea, menoxenia, dysmenorrhoea, endometritis, appendagitis, and pelvic inflammation (Wei, 2006). Recent studies demonstrated that its ethanolic extract showed good activity against several Gram-positive bacteria (Voravuthikunchai *et al*., 2007). *R. tomentsa* has also been used as traditional medicine for diarrhea and wound treatments in Vietnam (Tung *et al*., 2009).

1.4.1 Description of *R. tomentosa*

R. tomentosa (Aiton) Hassk. (**Figure 1**) is a flowering plant in the family Myrtaceae, native to southern and southeastern Asia, from India, east to southern China, Taiwan and the Philippines, and south to Malaysia and Sulawesi including Thailand. It is an evergreen shrub growing up to 2 meters in height. The leaves are opposite, leathery with the size of 5-7 cm long and 2-3.5 cm broad. It has three-veined from base with an oval and obtuse to sharp pointed at the tip. Its leaves also have glossy green above, densely grey or rarely yellowish-hairy beneath, with a wide petiole about 4-7 mm and an entire margin. The flowers are solitary or in clusters of two or three, 2-4 cm in diameter, with five petals which are tinged white outside with purplish-pink or all pink. The fruit is edible, round with 10-15 mm long and has a

purplish black when mature. It is contained three or four-celled, capped with persistent calyx lobes, soft. Its fruit has many seeds, around 40-45 seeds, in a double row in each cell. This plant has flowers around April-May and further can be propagated by seeds. The seed dispersal is spread by humans who use this plant in landscaping and by fruit eating birds and mammals (Jie and Craven, 2007).

R. tomentosa grows in coasts, natural forest, riparian zones, wetlands, moist and wet forests, bog margins, from sea level up to 2,400 meters elevation. It also grows in a wide range of soil types, including salty coastal soil, but is sensitive to heavy salt spray (APIRS, 2001). Furthermore *R. tomentosa* has become an invasive species in some countries, spreading to form large, monospecific thickets that displace native flora and fauna through overcrowding and competition. Areas especially affected include Florida, Hawaii and French Polynesia. It is able to invade a range of habitats, from pine flatwoods to mangrove marshes (Winotai *et al*., 2005).

1.4.2 Nomenclature, Synonyms and Common names

The Scientific name, *Rhodomyrtus tomentosa*, is derived from the Greek "*rhodon*" meaning red and "*myrtos*" meaning myrtle which referred to rose-colored flowers that are common in plants of this genus. It has several synonyms including *Myrtus tomentosa* Aiton, *Myrtus canescens* Loureiro, and *Rhodomyrtus parviflora* Alston. This plant has many common names such as downy rose myrtle (English-Florida), downy myrtle (English-Florida), rose myrtle (English-Florida), hill gooseberry (English), Ceylon hill berry (English), hill guava (English), feijoa (French), isenberg bush (English-Hawaii), myrte-groseille (French) (Wagner *et al*., 1999). In Thailand, it was commonly known as "Toh (โทะ)", "Pruad (พรวด)", and "Pruad Yai (พรวดใหญ่)" *etc* (Smitinand, 2001).

Figure 1 *Rhodomyrtus tomentosa* (Aiton) Hassk.

1.5 The objectives

The objectives of this research are to investigate the chemical constituents from the leaves, stems and fruits of *Rhodomyrtus tomentosa* and to evaluate the antibacterial activity of the crude extracts and the isolated compounds.

CHAPTER 2

EXPERIMENTAL

2.1 General methods

Melting points (^{O}C) were determined on a Fisher-Johns melting point apparatus and were uncorrected. Optical rotations were measured in chloroform solution on a JASCO P-1020 polarimeter. UV spectra were recorded by a SPECORD S100 spectrophotometer (Analytikjena). The IR spectra were measured with a FTS 165 FT-IR Perkins-Elmer spectrophotometer. The ^{1}H and ^{13}C NMR spectra were obtained from FT-NMR Bruker Avance Ultra Shield^{TM} 300 and 500 MHz spectrometers at the Department of Chemistry, Faculty of Science, Prince of Songkla University. The spectra were recorded as δ value in ppm downfield from TMS (internal standard δ 0.00). The EI-MS, HREI-MS, FAB-MS and HRFAB-MS mass spectra were obtained from a MAT 95 XL mass spectrometer (Thermofinigan) at the Scientific Equipment Center, Prince of Songkla University. Column chromatography (CC) was performed on silica gel 100 (70-230 Mesh, Merck) or Sephadex^{TM} LH-20 (GE Healthcare Bio-Sciences AB) while quick column chromatography (QCC) was performed on silica gel 60H (Merck). Thin-layer chromatography (TLC), aluminum sheets of silica gel 60 F_{254} (20x20 cm, layer thickness 0.2 mm, Merck), and preparative TLC (silica gel 60 F_{254}, 20x20 cm, layer thickness 0.25 mm, Merck) were used for analytical purposes. All solvents for extraction and chromatography were distilled at their boiling points prior to use.

2.2 Plant material

The leaves and stems of *Rhodomyrtus tomentosa* were collected in February 2007 from Singha Nakorn District, Songkhla Province. The fruits were collected in March 2008 from Khuan Khanun District, Phatthalung Province in the southern part of Thailand. The voucher specimen (A. Hiranrat 001) was identified by J. Wai and has been deposited in the herbarium of the Department of Biology, Faculty of Science, Prince of Songkla University, Thailand.

2.3 Chemical investigation of the leaves

2.3.1 Extraction and isolation

The dried ground leaves of *R. tomentosa* (2.1 kg) were successively extracted at room temperature with dichloromethane, acetone and methanol (twice for each extract time of 3 days) to give dark green gums of the dichloromethane (37.8 g), acetone (46.6 g) and methanol (111.5 g) extracts, respectively. The extract preparations were shown in **Scheme 1**.

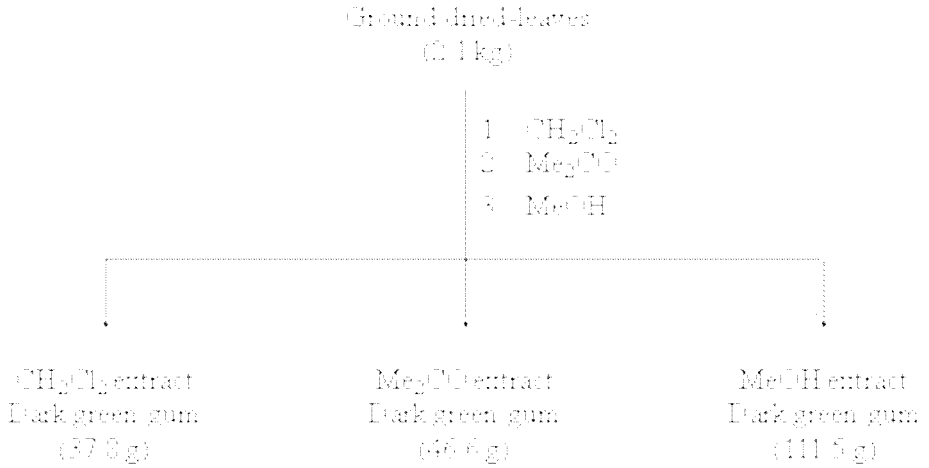

Scheme 1 The extract preparations from the leaves of *R. tomentosa*

2.3.2 Purification of the Me_2CO extract from the leaves

The Me_2CO extract (46.6 g) was fractionated by dissolving in hexane to give soluble- (fraction A; 21.4 g) and insoluble (25.2 g) fractions as a dark green gum and a dark green solid, respectively. The insoluble fraction was further dissolved in Me_2CO to afford the soluble fraction (fraction C; 12.8 g) as a dark green gum, and insoluble fraction (fraction B; 12.4 g) as a brownish solid (**Scheme 2)**.

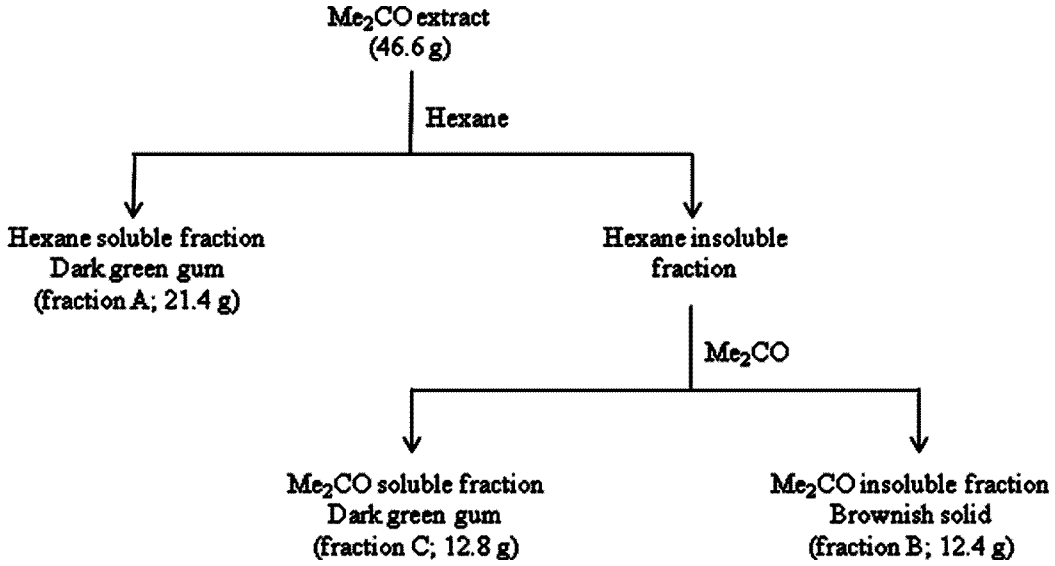

Scheme 2 Fractions obtained from the Me_2CO extract utilizing its solubility

2.3.2.1 Separation of fraction A

Fraction A (20.3 g) was subjected to QCC and eluted with a gradient of hexane-CH_2Cl_2, CH_2Cl_2, CH_2Cl_2-Me_2CO and Me_2CO. The eluted fractions were combined into fractions A1 to A17 on the basis of their TLC characteristics. Physical appearance and weight of each fraction are summarized in **Table 2**. After separation and purification, twelve compounds were obtained (**Scheme 3**).

Table 2 Physical appearance and weight of fractions obtained from QCC of fraction A

Fraction	Eluent	Weight (mg)	Physical Appearance
A1	10% CH_2Cl_2/hexane	49.3	white powder
A2	10% CH_2Cl_2/hexane	199.3	white powder
A3	10-15% CH_2Cl_2/hexane	73.7	yellow gum
A4	15-20% CH_2Cl_2/hexane	60.2	yellow gum
A5	20% CH_2Cl_2/hexane	272.7	yellow gum
A6	20-35% CH_2Cl_2/hexane	153.5	yellow gum
A7	35% CH_2Cl_2/hexane	43.3	orange gum
A8	35-50% CH_2Cl_2/hexane	165.4	orange-brown gum
A9	50% CH_2Cl_2/hexane	177.6	brown gum
A10	50-70% CH_2Cl_2/hexane	1.3 g	brown gum
A11	70-85% CH_2Cl_2/hexane	315.4	dark green gum
A12	85% CH_2Cl_2/hexane	198.5	dark green gum
A13	CH_2Cl_2	185.4	dark green gum
A14	CH_2Cl_2	606.0	dark green gum
A15	5% Me_2CO/CH_2Cl_2	2.9 g	dark green gum
A16	5-10% Me_2CO/CH_2Cl_2	1.6 g	dark green gum
A17	10% Me_2CO/CH_2Cl_2-Me_2CO	10.0 g	dark green gum

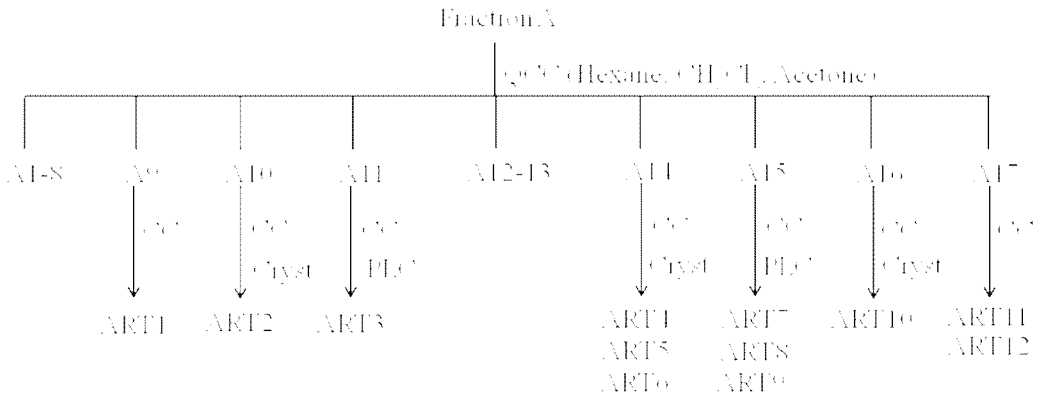

Scheme 3 Separation and purification of **ART1-ART12**

Isolation of ART1

Fraction A9 (177.6 mg) was subjected to CC and eluted with 15% CH_2Cl_2 in hexane to give three fractions (A9.1-A9.3). Fraction A9.2 (122.7 mg) was further purified by CC using 15% CH_2Cl_2 in hexane as an eluent to produce a yellow gum of **ART1** (73.5 mg).

ART1

UV ($CHCl_3$) λ_{max} nm (logε)	246 (4.31), 291 (4.16), 383 (3.23)
IR ($CHCl_3$) ν_{max} (cm^{-1})	3349, 2925, 2863, 1460, 1377, 1158, 1095
^1H (300 MHz) and ^{13}C NMR (75 MHz) ($CDCl_3$)	See **Table 41**

Isolation of ART2

Fraction A10 (1.3 g) was subjected to CC and eluted with a gradient of 10% CH_2Cl_2 in hexane to 5% Me_2CO in CH_2Cl_2 to give fractions A10.1-A10.8. Separation of fraction A10.6 (105.5 mg) on silica gel CC and eluted with 50% CH_2Cl_2 in hexane gave four fractions (A10.61-A10.64). Crystallization of fraction A10.64 (42.5 mg), upon standing at room temperature, gave the white needles of **ART2** (14.1 mg).

ART2

mp.	125-126 ^{O}C
$[\alpha]_D^{29}$	-1.1 (*c* 0.80, $CHCl_3$)
HREI-MS *m*/*z*	456.2133 (calcd for $C_{26}H_{32}O_7$ 456.2148)
EI-MS *m*/*z* (% rel. int.)	456 (M^+, 61), 441 (33), 414 (20), 399 (100), 372 (17), 247 (40)
UV ($CHCl_3$) λ_{max} nm (logε)	270 (4.39), 327 (3.42)
IR ($CHCl_3$) ν_{max} (cm^{-1})	3126, 2969, 2935, 2874, 1720, 1650, 1617, 1502, 1452, 1303, 1180, 1052
^1H (300 MHz) and ^{13}C NMR (75 MHz) ($CDCl_3$)	See **Table 12**

Isolation of ART3

Fraction A11 (315.4 mg) was subjected to CC and eluted with gradient solvents from 20% CH_2Cl_2 in hexane to 40% CH_2Cl_2 in hexane to give six fractions (A11.1-A11.6). Fraction A11.6 (166.9 mg) was further separated by silica gel CC and eluted with 3% Me_2CO in hexane affording nine fractions (A11.61-A11.69). Fraction A11.63 (46.7 mg) was subjected to CC on silica gel and eluted with 3% Me_2CO in hexane to give fractions A11.63A-A11.63E. Fraction A11.63D (3.2 mg) was then purified by preparative TLC using 1% Me_2CO in hexane as a mobile phase to produce a white powder of **ART3** (1.0 mg).

ART3

$[\alpha]_D^{29}$	-4.2 (*c* 0.05, $CHCl_3$)
HREI-MS *m*/*z*	456.2133 (calcd for $C_{26}H_{32}O_7$ 456.2148)
EI-MS *m*/*z* (% rel. int.)	456 (M^+, 50), 441 (32), 414 (20), 399 (100), 372 (15), 247 (36)
UV ($CHCl_3$) λ_{max} nm (logε)	244 (4.33), 271 (4.62), 325 (3.84)
IR ($CHCl_3$) ν_{max} (cm^{-1})	3316, 2963, 2930, 2891, 1720, 1636, 1627, 1594, 1471, 1438
^1H (500 MHz) and ^{13}C NMR (125 MHz) ($CDCl_3$)	See **Table 13**

Isolation of ART4, ART5 and ART6

Fraction A14 (606.0 mg) was subjected to CC and eluted with CH_2Cl_2 and CH_2Cl_2-MeOH gradient to give seven fractions (A14.1-A14.7). Fraction A14.2 (194.8 mg) was rechromatographed on CC using 3% Me_2CO in hexane as an eluent to produce **ART4** (103.9 mg). Fraction A14.3 (183.6 mg) was further fractionated by silica gel CC and eluted with CH_2Cl_2 to give fractions A14.31-A14.36. Compound **ART5** (34.0 mg) was crystallized from fraction A14.33 (138.1 mg) as white needles. The filtrate was further separated by CC eluting with 3% Me_2CO in hexane to give seven fractions (A14.33-61-A14.33-67). White needles of **ART6** (23.0 mg) were obtained from crystallization of fraction A14.33-66 (31.4 mg) in Me_2CO-hexane (1:5).

ART4

mp.	80-81 ^{O}C
$[\alpha]_D^{29}$	-23.5 (*c* 0.39, $CHCl_3$)
HREI-MS *m*/*z*	674.3853 (calcd for $C_{41}H_{54}O_8$ 674.3819)
EI-MS *m*/*z* (% rel. int.)	674 (M^+, 1), 617 (100), 547 (7), 419 (8)
UV ($CHCl_3$) λ_{max} nm (logε)	263 (4.15), 306 (4.19), 348 (3.60)
IR ($CHCl_3$) ν_{max} (cm^{-1})	3423, 2952, 2868, 1717, 1659, 1617, 1594, 1466, 1382, 1362, 1183, 1158, 1038
^{1}H (300 MHz) and ^{13}C NMR (75 MHz) ($CDCl_3$)	See **Table 14**

ART5

IR ($CHCl_3$) ν_{max} (cm^{-1})	3410, 2945, 2932, 1453, 1050
^{1}H (300 MHz) and ^{13}C NMR (75 MHz) ($CDCl_3$)	See **Table 38**

ART6

mp.	188-189 ^{O}C
$[\alpha]_D^{29}$	-9.4 (*c* 1.0, $CHCl_3$)
UV ($CHCl_3$) λ_{max} nm (logε)	244 (3.95), 262 (4.01), 302 (4.14)
IR ($CHCl_3$) ν_{max} (cm^{-1})	3244, 2959, 2935, 1720, 1630, 1594, 1385, 1167, 1092
^{1}H (300 MHz) and ^{13}C NMR (75 MHz) ($CDCl_3$)	See **Table 11**

Isolation of ART7, ART8 and ART9

Fraction A15 (2.9 g) was subjected to CC eluting with CH_2Cl_2-MeOH gradient systems to give fractions A15.1-A15.5. Fraction A15.3 (1.1 g) was fractionated by CC eluting with 10% Me_2CO in hexane to give fractions A15.3-51 to A15.3-59. Fraction A15.3-54 (66.2 mg) was subjected to CC and eluted with 5% Me_2CO in hexane to give five fractions (A15.3-541-A15.3-545). A yellow solid of **ART7** (4.2 mg) was obtained from crystallization of fraction A15.3-545 (36.9 mg) in hexane-Me_2CO (5:1). The filtrate was further purified by CC eluting with 5% Me_2CO in hexane to produce **ART8** (0.7 mg) and **ART9** (1.3 mg) as yellowish gum.

ART7

mp.	142-144 ^{O}C
UV (MeOH) λ_{max} nm (logε)	210 (4.15), 265 (4.19), 342 (3.60)
IR ($CHCl_3$) ν_{max} (cm^{-1})	3421, 1663, 1659, 1505, 1460, 1173, 1142
^{1}H (300 MHz) and ^{13}C NMR (75 MHz) ($CDCl_3$)	See **Table 22**

ART8

$[\alpha]_D^{29}$	0 (*c* 0.035, $CHCl_3$)
EI-MS *m*/*z* (% rel. int.)	268 (M^+, 15), 236 (86), 221 (32), 193 (16), 166 (100), 140 (30), 123 (55), 96 (25), 70 (47), 69 (42)
UV ($CHCl_3$) λ_{max} nm (logε)	243 (3.40), 294 (2.91)
IR ($CHCl_3$) ν_{max} (cm^{-1})	3479, 1714, 1693, 1639
^{1}H (500 MHz) and ^{13}C NMR (125 MHz) ($CDCl_3$)	See **Table 15**

ART9

$[\alpha]_D^{29}$	-182.0 (*c* 0.06, $CHCl_3$)
HREI-MS *m*/*z*	442.2352 (calcd for $C_{26}H_{34}O_6$ 442.2355)
EI-MS *m*/*z* (% rel. int.)	442 (M^+, 1), 428 (13), 413 (14), 386 (22), 385 (91), 330 (8), 315 (28), 236 (46), 221 (24), 167 (38), 166 (63), 149 (77), 123 (60), 97 (49), 70 (100), 69 (90)
UV ($CHCl_3$) λ_{max} nm (logε)	292 (3.82), 333 (3.20)
IR ($CHCl_3$) ν_{max} (cm^{-1})	3372, 2975, 2952, 2868, 1717, 1653, 1622, 1468, 1385, 1256, 1158, 1038
^{1}H (500 MHz) and ^{13}C NMR (125 MHz) ($CDCl_3$)	See **Table 16**

Isolation of ART10

Fraction A16 (1.6 g) was fractionated by CC eluting with hexane-Me_2CO gradient systems to give six fractions (A16.1-A16.6). Crystallization of fraction A16.5 (304.5 mg) in hexane-Me_2CO (5:1) gave a yellow solid of **ART10** (15.7 mg).

ART10

mp	298-300 ^{O}C
UV (EtOH) λ_{max} nm (logε)	247 (4.10), 372 (3.79)
IR ($CHCl_3$) ν_{max} (cm^{-1})	3410, 1656, 1641, 1026, 995
^{1}H (300 MHz) and ^{13}C NMR (125 MHz) ($CDCl_3$+DMSO-d_6)	See **Table 26**

Isolation of ART11 and ART12

Fraction A17 (10.0 g) was fractionated by CC and eluted with hexane-Me_2CO in a polarity gradient to give fractions A17.1 to A17.8. Fraction A17.4 (126.1 mg) was subjected to CC and eluted with 5% Me_2CO in hexane to produce **ART11** (9.9 mg) as a colorless crystal. Fraction A17.6 (210.6 mg) was subjected to CC and eluted with 10% Me_2CO in hexane to produce a yellowish gum of **ART12** (5.5 mg).

ART11

mp	160-162 ^{O}C
HREI-MS *m*/*z*	428.2214 (calcd for $C_{25}H_{32}O_6$ 428.2199)
EI-MS *m*/*z* (% rel. int.)	428 (M^+, 84), 413 (23), 385 (28), 358 (20), 330 (65), 315 (100), 288 (51), 287 (44), 273 (32), 260 (25), 245 (22), 232 (28), 217 (32), 189 (27), 96 (26), 91 (31), 69 (76)
UV ($CHCl_3$) λ_{max} nm (logε)	246 (4.08), 298 (3.24)
IR ($CHCl_3$) ν_{max} (cm^{-1})	2974, 2935, 2879, 1717, 1675, 1656, 1468, 1398, 1387
^{1}H (300 MHz) and ^{13}C NMR (75 MHz) ($CDCl_3$)	See **Table 17**

ART12

$[\alpha]_D^{29}$	+193.5 (*c* 0.60, $CHCl_3$)
UV ($CHCl_3$) λ_{max} nm (logε)	246 (4.13)
IR ($CHCl_3$) ν_{max} (cm^{-1})	3406, 2971, 2940, 2875, 1656, 1460, 1375, 1251
^{1}H (300 MHz) and ^{13}C NMR (75 MHz) ($CDCl_3$)	See **Table 31**

2.3.2.2 Separation of fraction C

Fraction C (11.5 g) was subjected to CC and eluted with gradient solvents from 5% Me_2CO in hexane to Me_2CO. The eluted fractions were combined into ten fractions (C1-C10) on the basis of their TLC characteristics. Physical appearance and weight of each fraction are summarized in **Table 3**. After separation and purification, nine compounds were obtained (**Scheme 4**).

Table 3 Physical appearance and weight of fractions obtained from QCC of fraction C

Fraction	Eluent	Weight (mg)	Physical Appearance
C1	5-7% Me_2CO/hexane	114.7	yellow gum
C2	7% Me_2CO/hexane	118.0	dark green gum
C3	7% Me_2CO/hexane	50.5	dark green gum
C4	7-12% Me_2CO/hexane	76.7	dark green gum
C5	12-17% Me_2CO/hexane	968.5	dark green gum
C6	17-25% Me_2CO/hexane	340.6	dark green gum
C7	25-30% Me_2CO/hexane	179.7	dark green gum
C8	30% Me_2CO/hexane	846.6	dark green gum
C9	50% Me_2CO/hexane	729.6	dark green gum
C10	Me_2CO	7.2 g	dark green gum

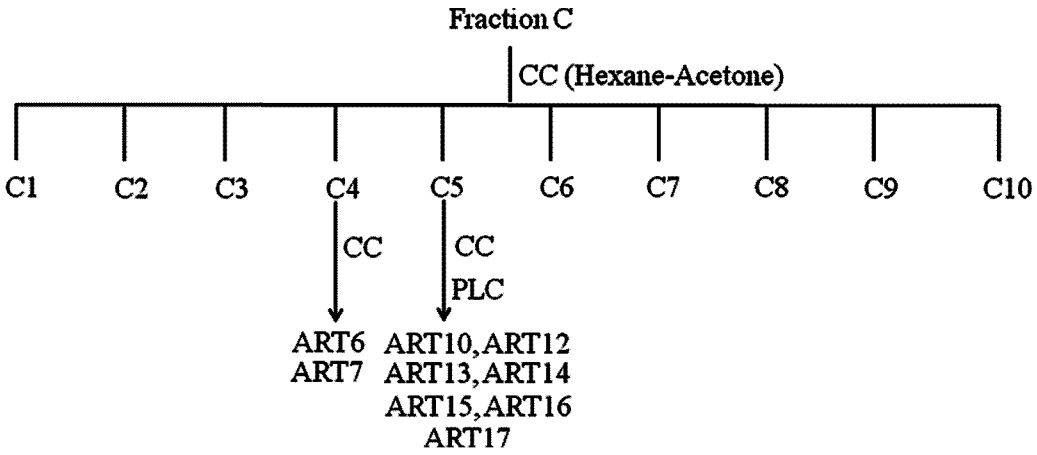

Scheme 4 Separation and purification of **ART6**, **ART7**, **ART10** and **ART12-ART17**

Isolation of ART6 and ART7

ART7 (15.1 mg) was obtained as a yellow solid from fraction C4 (76.7 mg) by crystallization in hexane-Me_2CO (5:1). The filtrate was further separated by CC eluting with 3% Me_2CO in hexane to give six fractions (C4.1-C4.6). Fraction C4.2 (33.9 mg) was further purified by CC using 3% Me_2CO in hexane as an eluent to yield yellow needles of **ART6** (18.3 mg).

Isolation of ART10, **ART12**, **ART13**, **ART14**, **ART15, ART16, and ART17**

Fraction C5 (968.5 mg) was chromatographed on CC and eluted with gradient solvents from 8% Me_2CO in hexane to Me_2CO to give eight fractions (C5.1-C5.8). Fraction C5.3 (89.3 mg) was further separated by CC eluting with 10% Me_2CO in hexane to give fractions C5.3.1-C5.3.7. Fraction C5.3.4 (34.6 mg) was then applied to TLC plate using 1% MeOH in CH_2Cl_2 as a mobile phase to yield a yellow gum of **ART13** (4.0 mg), a colorless gum of **ART14** (1.3 mg), a colorless gum of **ART15** (1.0 mg) and a yellowish gum of **ART12** (9.6 mg). Fraction C5.4 (25.0 mg) was also purified by TLC plate using 1% MeOH in CH_2Cl_2 as a mobile phase to give compounds **ART16** (1.6 mg), **ART10** (1.1 mg) and **ART17** (0.9 mg) as yellow gums.

ART13

UV (MeOH) λ_{max} nm (logε)	248*sh* (3.23), 270 (3.38), 305*sh* (3.26), 345 (3.32)
IR ($CHCl_3$) ν_{max} (cm^{-1})	3375, 2925, 2847, 1659, 1597, 1499, 1364, 1215, 1163, 1106
^1H (300 MHz) and ^{13}C NMR (75 MHz) ($CDCl_3$)	See **Table 23**

ART14

UV ($CHCl_3$) λ_{max} nm (logε)	247 (3.72), 255*sh* (3.67)
IR ($CHCl_3$) ν_{max} (cm^{-1})	3449, 2948, 2923, 1718, 1545
^1H (500 MHz) and ^{13}C NMR (125 MHz) ($CDCl_3$)	See **Table 32**

ART15

IR ($CHCl_3$) ν_{max} (cm^{-1}) 3340, 2976, 2935, 2894, 1750, 1037

^1H (500 MHz) and ^{13}C NMR (125 MHz) ($CDCl_3$) See **Table 48**

ART16

UV ($CHCl_3$) λ_{max} nm (logε) 252 (3.38), 266 (3.32), 302*sh* (3.12), 355 (3.43)

IR ($CHCl_3$) ν_{max} (cm^{-1}) 3375, 2920, 2847, 1656, 1597, 1496, 1460, 1217, 1119

^1H (500 MHz) and ^{13}C NMR (125 MHz) ($CDCl_3$) See **Table 24**

ART17

UV ($CHCl_3$) λ_{max} nm (logε) 252 (4.06), 268 (4.13), 308*sh* (4.05), 348 (4.11)

IR ($CHCl_3$) ν_{max} (cm^{-1}) 3255, 2920, 2852, 1656, 1638, 1579, 1460, 1160, 1126

^1H (500 MHz) and ^{13}C NMR (125 MHz) ($CDCl_3$) See **Table 25**

2.3.3 Purification of the CH_2Cl_2 extract from the leaves

The CH_2Cl_2 extract (37.8 g) was further fractionated by dissolving in MeOH to afford soluble- (fraction E; 27.9 g) and insoluble (fraction D; 9.9 g) fractions.

2.3.3.1 Separation of fraction E

Fraction E (20.8 g) was separated by CC and eluted with hexane-Me_2CO gradient solvent systems. The eluted fractions were combined into fifteen fractions (E1-E15) on the basis of their TLC characteristics. Physical appearance and weight of each fraction are summarized in **Table 4**. After separation and purification, three compounds were additionally isolated (**Scheme 5**).

Table 4 Physical appearance and weight of fractions obtained from CC of fraction E

Fraction	Eluent	Weight (mg)	Physical Appearance
E1	2-5% Me_2CO/hexane	1.85 g	orange gum
E2	5-10% Me_2CO/hexane	1.33 g	orange gum
E3	5-10% Me_2CO/hexane	382.1	yellow gum
E4	10% Me_2CO/hexane	739.3	dark green gum
E5	15% Me_2CO/hexane	348.0	dark green gum
E6	15-20% Me_2CO/hexane	322.7	dark green gum
E7	20% Me_2CO/hexane	1.42 g	dark green gum
E8	20% Me_2CO/hexane	4.31 g	dark green gum
E9	30% Me_2CO/hexane	858.9	dark green gum
E10	30-40% Me_2CO/hexane	447.0	dark green gum
E11	40% Me_2CO/hexane	349.1	dark green gum
E12	40-50% Me_2CO/hexane	783.5	dark green gum
E13	50-60% Me_2CO/hexane	163.4	dark green gum
E14	60-80% Me_2CO/hexane	1.83 g	dark green gum
E15	Me_2CO	1.40 g	dark green gum

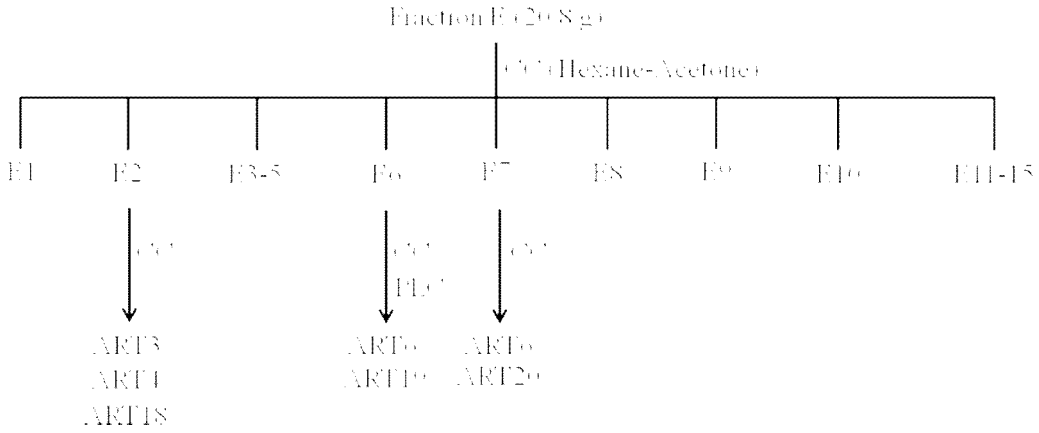

Scheme 5 Separation and purification of **ART2**, **ART4**, **ART6** and **ART18-ART20**

Isolation of ART3, ART4 and ART18

Fraction E2 (1.33 g) was subjected to CC eluting with 2% Me_2CO in hexane to give nine fractions (E2.1-E2.9). Fraction E2.5 (888.9 mg) was further rechromatographed on CC and eluted with 2% Me_2CO in hexane to afford a white solid of **ART3** (54.0 mg) and a yellowish solid of **ART4** (416.4 mg). Fraction E2.7 (60.7 mg) was further purified by CC using 2% Me_2CO in hexane as an eluent to produce a yellowish gum of **ART18** (22.2 mg).

ART18

$[\alpha]_D^{25}$	-9.3^O (*c* 0.92, $CHCl_3$)
HREI-MS *m*/*z*	688.3610 (calcd for $C_{41}H_{52}O_9$ 688.3611)
EI-MS *m*/*z* (% rel. int.)	688 (M^+, 2), 632 (51), 630 (100), 617 (14), 561 (5), 477 (5), 385 (3), 247 (7), 177 (4)
UV ($CHCl_3$) λ_{max} nm (logε)	246 (4.28), 260 (4.36), 304 (4.26), 347sh (3.68)
IR ($CHCl_3$) ν_{max} (cm^{-1})	3135, 2975, 2945, 1720, 1656, 1617, 1500, 1452, 1303, 1190

^1H (300 MHz) and ^{13}C NMR (75 MHz) ($CDCl_3$) See **Table 18**

Isolation of ART6 and ART19

Fraction E6 (322.7 mg) was separated by CC and eluted with gradient solvents of 5% Me_2CO in hexane to 10% Me_2CO in hexane to afford ten fractions (E6.1-E6.10). Fraction E6.7 (65.1 mg) was then subjected to CC using 60% CH_2Cl_2 in hexane to give fractions E6.71-E6.76. Fraction E6.71 (5.4 mg) was purified by TLC plate using 40% CH_2Cl_2 in hexane as an eluent to produce a yellowish gum of **ART19** (1.5 mg). Compound **ART6** (8.2 mg) was obtained from fraction E6.74 (19.5 mg) as a white solid.

ART19

$[\alpha]_D^{29}$	$+62.0^{O}$ (*c* 0.10, $CHCl_3$)
HRFAB-MS *m/z*	443.2429 (calcd for $C_{26}H_{35}O_6$ 443.2434)
FAB-MS *m/z* (% rel. int.)	443 ($[M+H]^+$, 28%), 385 (17), 185 (20), 133 (100), 93 (56)
EI-MS *m/z* (% rel. int.)	385 ($[M-C_4H_9]^+$, 100), 367 (5), 315 (8), 297 (7)
UV ($CHCl_3$) λ_{max} nm (logε)	245 (4.09), 262 (4.14), 300 (4.24)
IR ($CHCl_3$) ν_{max} (cm^{-1})	3365, 2970, 2955, 1717, 1655, 1622, 1465, 1382, 1249

^1H (500 MHz) and ^{13}C NMR (125 MHz) ($CDCl_3$) See **Table 19**

Isolation of ART6 and ART20

Fraction E7 (1.42 g) was subjected to CC and eluted with gradient solvents of 5% Me_2CO in hexane to 10% Me_2CO in hexane to give ten fractions (E7.1-E7.10). A yellowish solid of **ART20** (15.4 mg) was obtained from crystallization of fraction E7.2 (55.2 mg) in hexane:Me_2CO (5:1). Crystallization of fraction E7.5 (264.6 mg) from hexane:Me_2CO (5:1) gave a white solid of **ART6** (206.9 mg).

ART20

mp.	198-199 ^{O}C
$[\alpha]_D^{29}$	-10.7^{o} (*c* 0.68, $CHCl_3$)
HREI-MS *m/z*	688.3610 $[M]^+$ (calcd for $C_{41}H_{52}O_9$, 688.3611)
EI-MS *m/z* (% rel. int.)	688 $[M]^+$, 632, 630, 617, 561, 477, 385, 247, 177
UV ($CHCl_3$) λ_{max} nm (logε)	246 (4.23), 262 (4.28), 306 (4.21), 350sh (3.72)
IR ($CHCl_3$) ν_{max} (cm^{-1})	3128, 2969, 2935, 1718, 1650, 1617, 1502, 1452, 1303

^1H (300 MHz) and ^{13}C NMR (75 MHz) ($CDCl_3$) See **Table 20**

2.3.3.2 Separation of fraction D

Fraction D (9.0 g) was separated by CC and eluted with gradient solvents from 3% Me_2CO in hexane to Me_2CO. The eluted fractions were combined to give thirteen fractions (D1-D13) on the basis of their TLC characteristics. Physical appearance and

weight of each fraction are summarized in **Table 5**. After separation and purification, only two compounds were isolated (**Scheme 6**).

Table 5 Physical appearance and weight of fractions obtained from CC of fraction D

Fraction	Eluent	Weight (mg)	Physical Appearance
D1	3% Me_2CO/hexane	959.8	white amorphous solid
D2	3% Me_2CO/hexane	890.0	yellow amorphous solid
D3	3% Me_2CO/hexane	452.1	yellow powder
D4	3% Me_2CO/hexane	502.4	yellow powder
D5	3% Me_2CO/hexane	225.6	yellow gum
D6	5% Me_2CO/hexane	379.6	dark green gum
D7	5% Me_2CO/hexane	558.2	dark green gum
D8	10% Me_2CO/hexane	508.9	dark green powder
D9	10% Me_2CO/hexane	338.5	dark green powder
D10	20% Me_2CO/hexane	768.5	dark green powder
D11	20% Me_2CO/hexane	868.3	dark green powder
D12	20-50% Me_2CO/hexane	526.3	dark green powder
D13	50% Me_2CO/hexane-Me_2CO	710.0	dark green powder

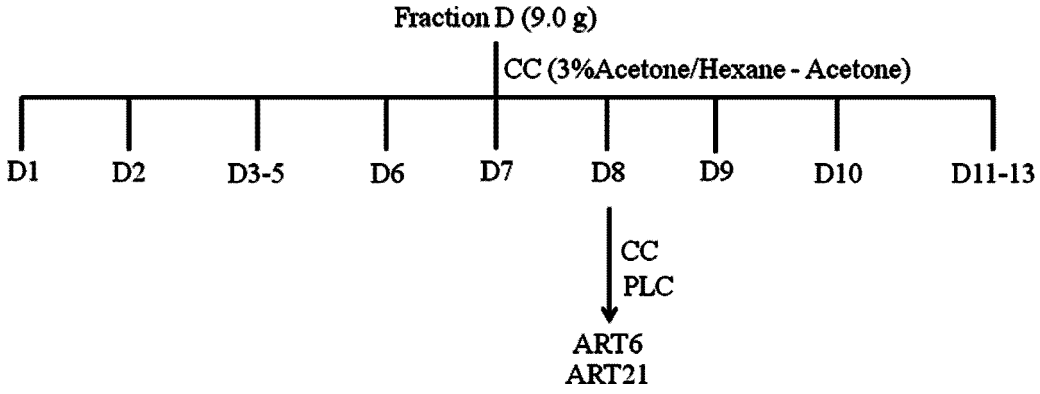

Scheme 6 Separation and purification of **ART6** and **ART21**

Isolation of ART6 and ART21

Fraction D8 (508.9 mg) was chromatographed on CC and eluted with 10% Me_2CO in hexane. The eluted fractions were combined into four fractions (D8.1-D8.4) based on their TLC characteristics. Fraction D8.2 (68.3 mg) was further rechromatographed on CC using 5% Me_2CO in hexane as an eluent to give six fractions (D8.21-D8.26). Fraction D8.21 (19.6 mg) was further purified by TLC plate using 5% Me_2CO in hexane as a mobile phase to produce a white solid of **ART6** (2.4 mg). Purification of fraction D8.22 (9.3 mg) by TLC plate using 5% Me_2CO in hexane as a mobile phase gave a white solid of **ART21** (3.2 mg).

ART21

mp	75-77 ^{O}C
EI-MS *m*/*z* (% rel. int.)	614 (M^+, 90), 194 (27), 120 (100), 43 (15)
UV (MeOH) λ_{max} nm (logε)	240 (3.80), 327 (3.59)
IR ($CHCl_3$) ν_{max} (cm^{-1})	3445, 1720, 1642, 1619, 1505, 1460, 1173
^{1}H (300 MHz) and ^{13}C NMR (75 MHz) ($CDCl_3$)	See **Table 42**

2.3.4 Purification of the MeOH extract from the leaves

The MeOH extract (54.0 g) was separated by QCC and eluted with the gradient solvents from CH_2Cl_2 to 50% MeOH in CH_2Cl_2. The eluted fractions were combined into ten fractions (F1-F10) on the basis of their TLC characteristics. Physical appearance and weight of each fraction are summarized in **Table 6**. After separation and purification, three compounds were additionally isolated (**Scheme 7**).

Table 6 Physical appearance and weight of fractions from QCC of the MeOH extract

Fraction	Eluent	Weight (g)	Physical Appearance
F1	CH_2Cl_2	0.22	dark brown gum
F2	CH_2Cl_2	0.61	dark brown gum
F3	CH_2Cl_2-2% MeOH/CH_2Cl_2	0.19	dark brown gum
F4	2-5% MeOH/CH_2Cl_2	2.11	dark brown gum
F5	5% MeOH/CH_2Cl_2	0.74	dark brown gum
F6	10% MeOH/CH_2Cl_2	0.81	dark brown gum
F7	10% MeOH/CH_2Cl_2	5.14	dark brown gum
F8	15-20% MeOH/CH_2Cl_2	6.34	dark brown gum
F9	20-30% MeOH/CH_2Cl_2	14.50	dark brown gum
F10	30-50% MeOH/CH_2Cl_2	12.43	dark brown gum

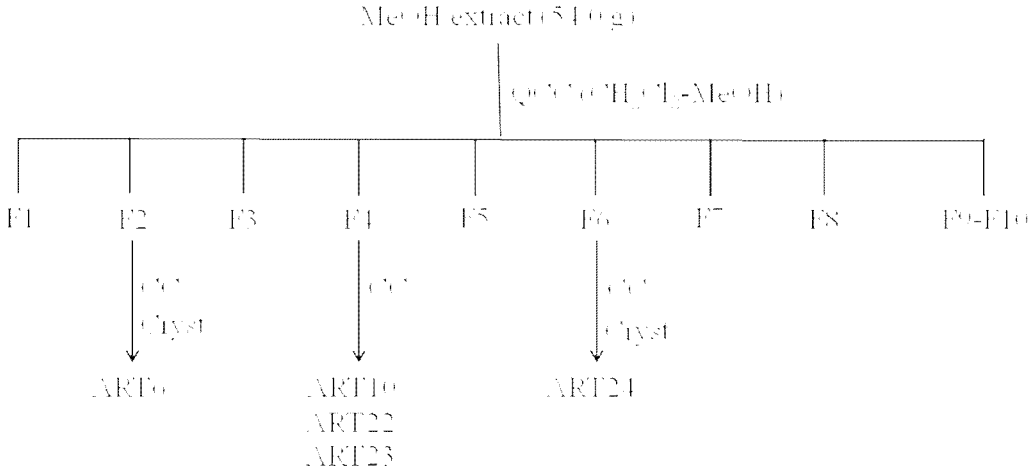

Scheme 7 Separation and purification of **ART6**, **ART10** and **ART22-ART24**

Isolation of ART6

Fraction F2 (610.5 mg) was separated by CC on silica gel and eluted with 80% CH_2Cl_2 in hexane. The eluted fractions were combined into eighteen fractions (F2.1-F2.18) based on their TLC characteristics. Crystallization of the combined fractions F2.10-F2.13 (175.7 mg) from a mixed solvent of hexane: Me_2CO (5:1) gave **ART6** (99.7 mg) as a white solid.

Isolation of ART10, ART22 and ART23

Fraction F4 (2.11 g) was subjected to CC and eluted with the gradient solvents of 10% Me_2CO in hexane to Me_2CO. The eluted fractions were combined into fractions F4.1-F4.9 based on their TLC characteristics. Fraction F4.8 (457.1 mg) was rechromatographed on CC eluting with 20% Me_2CO in hexane to afford ten fractions (F4.81-F4.810). Compound **ART10** (6.4 mg) was then crystallized from fraction F4.86 (14.0 mg) using hexane:Me_2CO (3:2) as a solvent. Crystallization of the combined fractions F4.87-F4.89 (212.2 mg) in a mixed solvent of hexane:Me_2CO (3:2) produced F4.87S (42.5 mg) as a yellow solid. The solid F4.87S was subjected to CC and eluted with gradient solvents of 2% MeOH in CH_2Cl_2 to 10% MeOH in CH_2Cl_2 to give fractions F4.87S1-F4.87S6. A yellow solid of **ART10** (4.3 mg) was obtained from fraction F4.87S1. Fractions 4.87S3 (4.9 mg) and F4.87S4 (15.6 mg) were combined and then purified by TLC plate using 3% MeOH in CH_2Cl_2 as an eluent to produce **ART22** (8.7 mg) and **ART23** (4.3 mg) as white solids.

ART22

mp 272-274 ^{O}C

UV (MeOH) λ_{max} nm (logε) 211 (2.40), 229 (2.16), 315 (3.96)

IR ($CHCl_3$) ν_{max} (cm^{-1}) 3359, 2929, 2858, 1696, 1610, 1455, 1169, 1021

^{1}H (300 MHz) and ^{13}C NMR (75 MHz) ($CDCl_3$+CD_3OD) See **Table 33**

ART23

mp 188-189 ^{O}C

UV (MeOH) λ_{max} nm (logε) 205 (4.29), 227 (2.09), 312 (3.08)

IR ($CHCl_3$) ν_{max} (cm^{-1}) 3340, 2923, 2852, 1697, 1604, 1458, 1169, 1020

^{1}H (300 MHz) and ^{13}C NMR (75 MHz) ($CDCl_3$+CD_3OD) See **Table 34**

Isolation of ART24

Fraction F6 (0.81 g) was separated by CC and eluted with gradient solvents from 2% MeOH in CH_2Cl_2 to 20% MeOH in CH_2Cl_2. The eluted fractions were combined into seven fractions (F6.1-F6.7) based on their TLC characteristics. Fraction F6.5 (64.7 mg) was crystallized from a solvent system of hexane:Me_2CO (3:2) to produce a white solid of **ART24** (25.3 mg).

ART24

IR ($CHCl_3$) ν_{max} (cm^{-1}) 3450, 1665, 1600, 1460, 1073

^1H (300 MHz) and ^{13}C NMR (75 MHz) ($CDCl_3$+CD_3OD) See **Table 39**

2.3.5 Acetylation of the MeOH extract from the leaves

The MeOH extract (14.0 g) was reacted with acetic anhydride in pyridine at room temperature overnight. The reaction mixture was worked up in usual manner, to give the crude product (AcF; 6.29 g) as a dark green gum. The crude AcF (6.00 g) was then subjected to CC and eluted with solvent systems from 15% Me_2CO in hexane and increasing a polarity with Me_2CO. The eluted fractions were combined into eighteen fractions (AcF1-AcF18) on the basis of their TLC characteristics. Physical appearance and weight of each fraction are summarized in **Table 7**. After separation and purification, five compounds were obtained (**Scheme 8**).

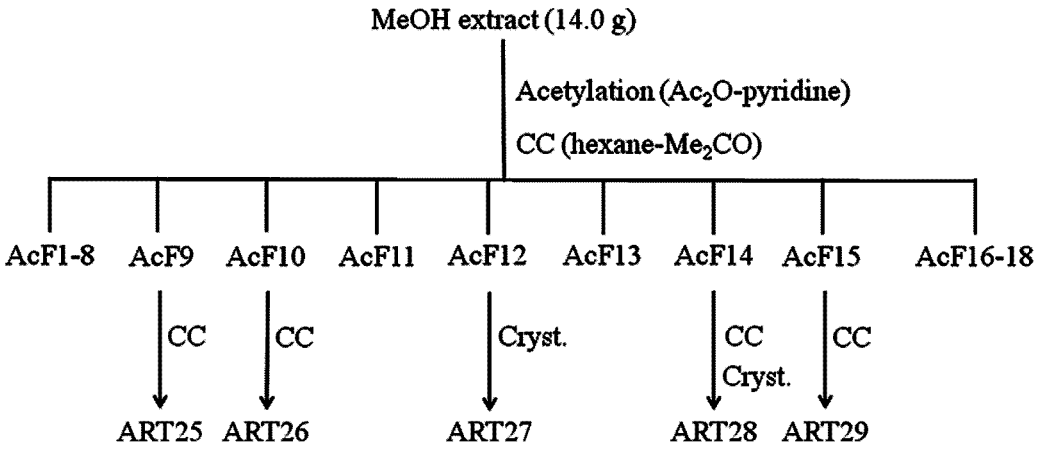

Scheme 8 Separation and purification of **ART25-ART29**

Table 7 Physical appearance and weight of fractions obtained from CC of the crude AcF

Fraction	Eluent	Weight (mg)	Physical Appearance
AcF1	15% Me_2CO/hexane	147.7	pale yellow gum
AcF2	15% Me_2CO/hexane	54.6	pale brown gum
AcF3	15% Me_2CO/hexane	61.7	green gum
AcF4	15% Me_2CO/hexane	62.9	green gum
AcF5	15% Me_2CO/hexane	20.2	green gum
AcF6	20% Me_2CO/hexane	54.8	green gum
AcF7	20% Me_2CO/hexane	31.0	green gum
AcF8	30% Me_2CO/hexane	44.9	green gum
AcF9	30% Me_2CO/hexane	87.6	green gum
AcF10	30% Me_2CO/hexane	110.0	pale yellow gum
AcF11	30% Me_2CO/hexane	233.0	pale yellow gum
AcF12	50% Me_2CO/hexane	529.5	pale yellow gum + solid
AcF13	50% Me_2CO/hexane	389.1	pale yellow gum
AcF14	50% Me_2CO/hexane	1.39g	pale yellow gum
AcF15	50% Me_2CO/hexane	390.0	pale yellow gum
AcF16	50-70% Me_2CO/hexane	345.3	brown gum
AcF17	70% Me_2CO/hexane	117.0	brown gum
AcF18	Me_2CO	79.6	brown gum

Isolation of ART25

Fraction AcF9 (87.6 mg) was further separated by CC eluting with 15% Me_2CO in hexane to produce a pale yellow solid of **ART25** (2.7 mg).

ART25

UV ($CHCl_3$) λ_{max} nm (logε) 248 (3.41), 307 (2.49), 320 (2.44), 365 (2.71), 380 (2.73)

IR ($CHCl_3$) ν_{max} (cm^{-1}) 3302, 2920, 2853, 1656, 1638, 1597, 1442, 1021

^1H (300 MHz) and ^{13}C NMR (75 MHz) ($CDCl_3$) See **Table 30**

Isolation of ART26

Fraction AcF10 (110.0 mg) was subjected to CC and eluted with 15% Me_2CO in hexane to yield a white solid of **ART26** (54.5 mg).

ART26

IR ($CHCl_3$) ν_{max} (cm^{-1}) 3027, 2965, 1750, 1373, 1224, 1046

^1H (300 MHz) and ^{13}C NMR (75 MHz) ($CDCl_3$) See **Table 49**

Isolation of ART27

Fraction AcF12 (529.5 mg) was crystallized in 15% Me_2CO in hexane at room temperature to give **ART27** (232.1 mg) as a white solid.

ART27

IR ($CHCl_3$) ν_{max} (cm^{-1}) 3025, 2964, 1759, 1369, 1221, 1078, 1038

^1H (300 MHz) and ^{13}C NMR (75 MHz) ($CDCl_3$) See **Table 50**

Isolation of ART28

Fraction AcF14 (1.39 g) was fractionated by CC and eluted with gradient solvent systems from 2% MeOH in CH_2Cl_2 to 25% MeOH in CH_2Cl_2 to give fractions AcF14.1-AcF14.8. Fraction AcF14.1 (95.5 mg) was recrystallized in 5% MeOH in CH_2Cl_2 to produce **ART28** (10.5 mg) as a white solid.

ART28

UV (EtOH) λ_{max} nm ($\log\varepsilon$) 248 (4.12), 371 (3.90)

IR ($CHCl_3$) ν_{max} (cm^{-1}) 1735, 1720, 1606, 1272, 1054

^1H (300 MHz) and ^{13}C NMR (75 MHz) ($CDCl_3$) See **Table 27**

Isolation of ART29

Fraction AcF15 (409.6 mg) was subjected to CC eluting with gradient manner by increasing a polarity from 2% MeOH in CH_2Cl_2 to 50% MeOH in CH_2Cl_2 to give eight fractions (AcF15.1-AcF15.8). Compound **ART29** (59.5 mg) was obtained as a white solid from fraction AcF15.5.

ART29

IR ($CHCl_3$) ν_{max} (cm^{-1}) 3026, 2965, 1757, 1747, 1372, 1235, 1041

^1H (300 MHz) and ^{13}C NMR (75 MHz) ($CDCl_3$) See **Table 51**

2.4 Chemical investigation of the stems

2.4.1 Extraction and isolation

The dried ground stems of *R. tomentosa* (2.1 kg) were successively extracted at room temperature with CH_2Cl_2, Me_2CO and MeOH to give the CH_2Cl_2, Me_2CO and MeOH extracts as a brown solid (20.6 g), a dark brown solid (73.4 g) and a dark brown solid (36.5 g), respectively. The extract preparations were shown in **Scheme 9**.

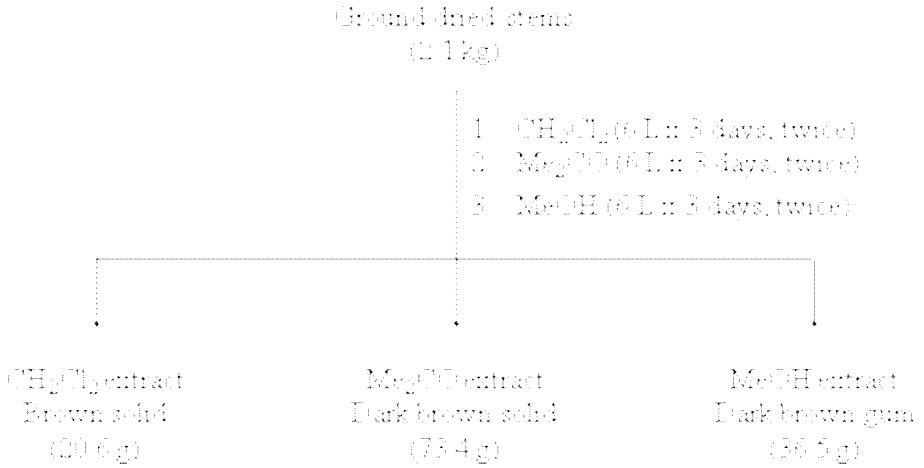

Scheme 9 The extract preparations from the stems

2.4.2 Purification of the CH_2Cl_2 extract from the stems

The CH_2Cl_2 extract (20.0 g) was separated by QCC and eluted with gradient solvents from CH_2Cl_2 to 30% MeOH in CH_2Cl_2. The eluted fractions were combined into eight fractions (M1-M8) on the basis of their TLC characteristics. Physical appearance and weight of each fraction are summarized in **Table 8**. After separation and purification, three compounds were isolated (**Scheme 10**).

Table 8 Physical appearance and weight of fractions obtained from QCC of the CH_2Cl_2 extract

Fraction	Eluent	Weight (g)	Physical Appearance
M1	CH_2Cl_2	0.25	yellow gum
M2	CH_2Cl_2	0.43	yellow gum
M3	CH_2Cl_2	3.46	yellow gum
M4	CH_2Cl_2-2% MeOH/CH_2Cl_2	0.50	dark yellow gum
M5	2% MeOH/CH_2Cl_2	6.61	dark yellow gum
M6	5% MeOH/CH_2Cl_2	1.42	dark yellow gum
M7	10-15% MeOH/CH_2Cl_2	3.58	dark yellow gum
M8	20-30% MeOH/CH_2Cl_2	4.64	dark yellow gum

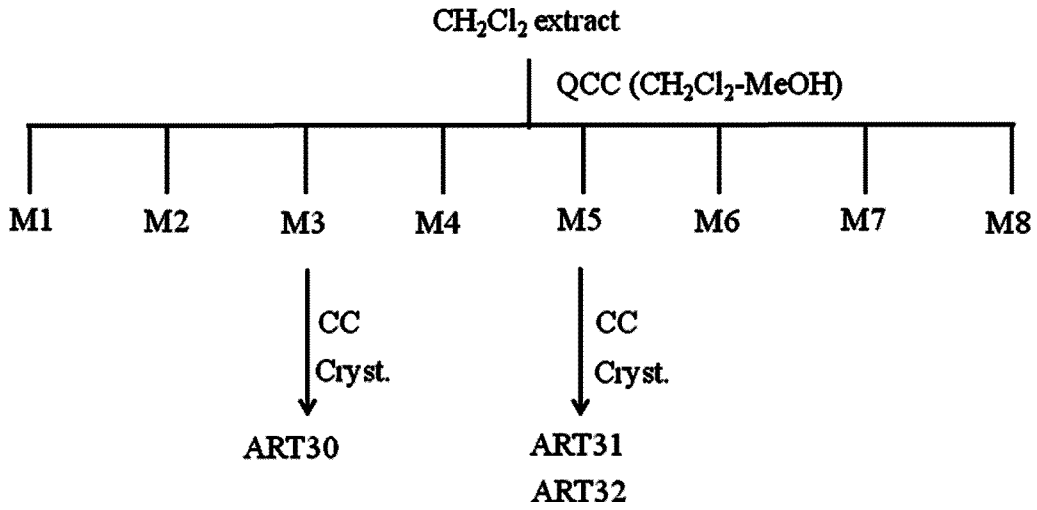

Scheme 10 Separation and purification of **ART30-ART32**

Isolation of ART30

Fraction M3 (3.46 g) was subjected to CC and eluted with 3% Me_2CO in hexane to afford twelve fractions (M3.1-M3.12) based on their TLC characteristics. Fraction M3.5 (89.5 mg) was further chromatographed on CC using 3% Me_2CO in hexane as an eluent to give fractions M3.51-M3.54. Upon standing at room temperature, a white solid of **ART30** (2.0 mg) was obtained from crystallization of fraction M3.53 (13.4 mg) in 3% Me_2CO in hexane.

ART30

mp	90-92 ^{O}C
EI-MS *m*/*z* (% rel. int.)	584 (M^+, 13), 556 (17), 528 (15), 248 (100), 203 (75), 166 (59), 164 (100), 147 (57)
UV (MeOH) λ_{max} nm (logε)	234 (4.15), 327 (4.06)
IR ($CHCl_3$) ν_{max} (cm^{-1})	3490, 1696, 1668, 1472, 1158
^{1}H (300 MHz) and ^{13}C NMR (75 MHz) ($CDCl_3$)	See **Table 43**

Isolation of ART31 and ART32

Fraction M5 (6.61 g) was subjected to CC and eluted with a polarity gradient from 5% Me_2CO in hexane to 40% Me_2CO in hexane to give sixteen fractions (M5.1-M5.16) based on their TLC characteristics. Fraction M5.7 (15.2 mg) was further purified by CC using 10% Me_2CO in hexane as an eluent to produce a pale yellow amorphous powder of compound **ART31** (2.0 mg). Fraction M5.12 (379.4 mg) was separated by CC eluting with 10% Me_2CO in hexane to afford fractions M5.121-M5.126. Compound **ART32** (15.0 mg) was crystallized from fraction M5.125 (64.0 mg) using 10% Me_2CO in hexane as a solvent.

ART31

HR EI-MS	374.0645 (calcd. for $C_{18}H_{14}O_9$, 374.0638)
EI-MS (% rel. int.)	374 (M^+, 100), 359 (54), 331 (28), 127 (35), 98 (31), 69 (76)
UV (EtOH) λ_{max} nm (logε)	248 (4.15), 376 (3.90), 410*sh* (3.57)
IR ($CHCl_3$) ν_{max} (cm^{-1})	3336, 1719, 1656, 1472, 1024
^{1}H (300 MHz) and ^{13}C NMR (75 MHz) ($CDCl_3$)	See **Table 29**

ART32

mp	240-242 ^{O}C
UV (MeOH) λ_{max} nm (logε)	230 (4.09), 315 (4.25)
IR (MeOH) ν_{max} (cm^{-1})	3345, 1700, 1608, 1508, 1452, 1170
^{1}H (300 MHz) and ^{13}C NMR (75 MHz) ($CDCl_3$+CD_3OD)	See **Table 35**

2.4.3 Purification of the Me_2CO extract from the stems

The Me_2CO extract (25.0 g) was separated by QCC and eluted with gradient solvents from CH_2Cl_2 to 80% MeOH in CH_2Cl_2. The eluted fractions were combined into thirteen fractions (N1-N13) on the basis of their TLC characteristics. Physical appearance and weight of each fraction are summarized in **Table 9**. After separation and purification, four compounds were obtained (**Scheme 11**).

Table 9 Physical appearance and weight of fractions obtained from CC of the Me_2CO extract of the stems

Fraction	Eluent	Weight (mg)	Physical Appearance
N1	CH_2Cl_2	108.9	yellow solid
N2	CH_2Cl_2	151.3	pale green solid
N3	CH_2Cl_2-1% MeOH/CH_2Cl_2	143.8	pale green solid
N4	1-2% MeOH/CH_2Cl_2	319.1	pale green solid
N5	2-5% MeOH/CH_2Cl_2	968.5	pale green solid
N6	10% MeOH/CH_2Cl_2	915.4	dark brown solid
N7	10% MeOH/CH_2Cl_2	79.7	brown solid
N8	10% MeOH/CH_2Cl_2	185.4	brown solid
N9	10% MeOH/CH_2Cl_2		dark brown solid
N10	10% MeOH/CH_2Cl_2	165.0	dark brown solid
N11	20% MeOH/CH_2Cl_2	619.7	dark brown solid
N12	20% MeOH/CH_2Cl_2	1.61g	dark brown solid
N13	40-80% MeOH/CH_2Cl_2		dark brown solid

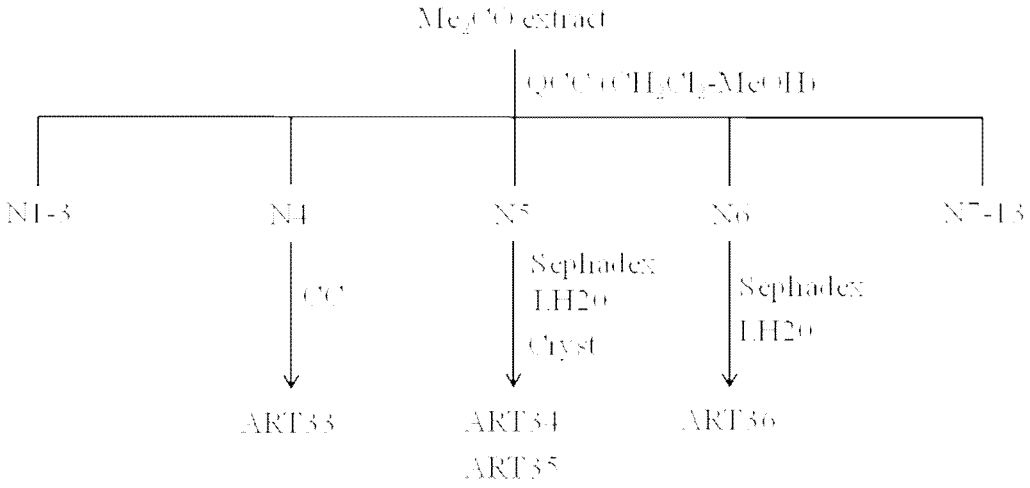

Scheme 11 Separation and purification of **ART33-ART36**

Isolation of ART33

Fraction N4 (319.1 mg) was further subjected to CC and eluted with gradient solvent systems from 1% MeOH in $CH_2Cl_2$to 25% MeOH in CH_2Cl_2 to produce a pale yellow solid of **ART33** (26.2 mg).

ART33

$[\alpha]_D^{29}$	-37.5 (*c* 0.40, MeOH)
UV (MeOH) λ_{max} nm (logε)	216 (4.10), 230 (4.13), 290 (4.07), 327 (4.11)
IR ($CHCl_3$) ν_{max} (cm^{-1})	3422, 2938, 2849, 1700, 1684, 1516, 1270
^1H (300 MHz) and ^{13}C NMR (75 MHz) ($CDCl_3$)	See **Table 47**

Isolation of ART34 and ART35

Fractions N5 (968.5 mg) was further separated by CC using gradient manner from 30% Me_2CO in hexane to Me_2CO to give sixteen fractions (N5.1-N5.13). Fraction N5.9 (96.8 mg) was further subjected to CC on Sephadex LH-20 eluting with 60% MeOH in CH_2Cl_2 to afford five fractions (N5.9A-N5.9E). Crystallization of fraction N5.10 (461.9 mg) using 50% Me_2CO in hexane produced compound **ART34** (30.5 mg) as a white solid. Fraction N5.11 (701.0 mg) was separated by CC on Sephadex LH-20 and eluted with gradient solvent systems from 2% MeOH in CH_2Cl_2

to 50% MeOH in CH_2Cl_2 affording sixteen fractions (N5.11A-N5.11P). Fraction N5.11L (67.6 mg) was then subjected to CC on Sephadex LH-20 eluting with 60% MeOH in CH_2Cl_2 to produce **ART35** (3.8 mg) as a pale yellow gum.

ART34

mp	300-302 ^{O}C
$[\alpha]_D^{25}$	+60.1 (c 1.0, EtOH)
IR ($CHCl_3$) ν_{max} (cm^{-1})	3422, 2929, 2868, 1765, 1684, 1051

^{1}H (300 MHz) and ^{13}C NMR (75 MHz) ($CDCl_3$+CD_3OD) See **Table 36**

ART35

UV (MeOH) λ_{max} nm (logε)	220 (3.30), 257 (3.23), 290 (2.96)
IR (MeOH) ν_{max} (cm^{-1})	3338, 2925, 2853, 1687, 1600, 1302, 1207

^{1}H (300 MHz) and ^{13}C NMR (75 MHz) ($CDCl_3$+CD_3OD) See **Table 44**

Isolation of ART36

Fraction N6 (915.4 mg) was further subjected to CC on Sephadex LH-20 and eluted with MeOH to yield compound **ART36** (40.6 mg) as a yellowish solid.

ART36

UV (MeOH) λ_{max} nm (logε)	216 (3.78), 272 (3.54), 355 (2.45)
IR (MeOH) ν_{max} (cm^{-1})	3345, 2920, 2852, 1690, 1556, 1039

^{1}H (300 MHz) and ^{13}C NMR (75 MHz) (DMSO-d_6) See **Table 45**

2.5 Chemical investigation from the fruits

2.5.1 Extraction and isolation

The dried green fruits of *R. tomentosa* (161.7 g) were chopped and were successively extracted at room temperature with MeOH for three times to give the MeOH extract as a dark brown gum (9.6 g).

2.5.2 Purification of the MeOH extract from the fruits

The MeOH extract (9.3 g) was separated by CC and eluted with gradient solvents from 1% MeOH in CH_2Cl_2 to 40% MeOH in CH_2Cl_2. The eluted fractions were combined into sixteen fractions (P1-P16) based on the TLC characteristics. Physical appearance and weight of each fraction are summarized in **Table 10**. After separation and purification, seven compounds were obtained (**Scheme 12**).

Table 10 Physical appearance and weight of fractions obtained from CC of the MeOH extract

Fraction	Eluent	Weight (mg)	Physical Appearance
P1	1% MeOH/CH_2Cl_2	284.2	yellow gum
P2	1% MeOH/CH_2Cl_2	95.9	yellow gum
P3	1% MeOH/CH_2Cl_2	35.5	yellow gum
P4	1% MeOH/CH_2Cl_2	45.3	yellow gum
P5	1-2% MeOH/CH_2Cl_2	170.2	yellow-green gum
P6	2% MeOH/CH_2Cl_2	24.8	yellow gum
P7	2% MeOH/CH_2Cl_2	30.9	yellow gum
P8	5% MeOH/CH_2Cl_2	48.0	yellow gum
P9	5% MeOH/CH_2Cl_2	317.3	dark green gum
P10	5% MeOH/CH_2Cl_2	325.3	dark green gum
P11	5-10% MeOH/CH_2Cl_2	113.7	dark green gum
P12	10% MeOH/CH_2Cl_2	116.2	dark green gum
P13	10-20% MeOH/CH_2Cl_2	163.5	dark green gum
P14	20% MeOH/CH_2Cl_2	291.0	dark green gum
P15	20% MeOH/CH_2Cl_2	263.9	dark green gum
P16	20-40% MeOH/CH_2Cl_2	569.1	dark green gum

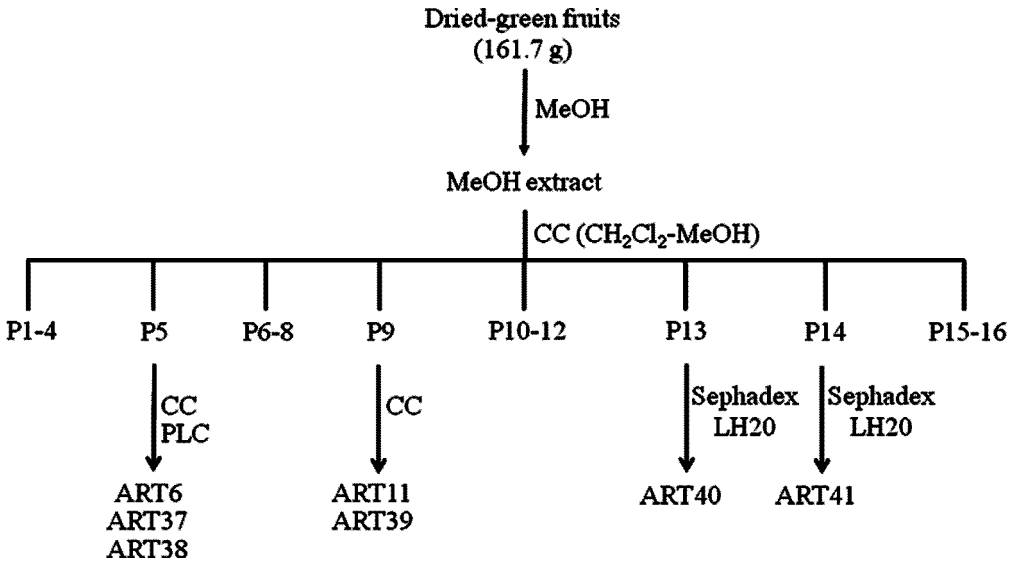

Scheme 12 Separation and purification of **ART6**, **ART11** and **ART37-ART41**

Isolation of ART6, ART37 and ART38

Fraction P5 (170.2 mg) was fractionated by CC and eluted with CH_2Cl_2 to give five fractions (P5.1-P5.5). Fraction P5.1 (16.6 mg) was purified by TLC plate using 5% Me_2CO in hexane as a mobile phase to produce **ART37** (1.1 mg), **ART6** (4.5 mg) and **ART38** (1.0 mg) as a pale yellow gum.

ART37

UV ($CHCl_3$) λ_{max} nm (logε) 246 (4.08)

IR ($CHCl_3$) ν_{max} (cm^{-1}) 2935, 2873, 1674, 1463, 1024

^1H (500 MHz) and ^{13}C NMR (125 MHz) ($CDCl_3$) See **Table 40**

ART38

HR EI-MS 462.2019 (calcd. for $C_{28}H_{30}O_6$, 462.2037)

EI-MS (% rel. int.) 462 (M^+, 70), 434 (57), 405 (26), 385 (100), 315 (301), 257 (18), 149 (17)

UV ($CHCl_3$) λ_{max} nm (logε) 246 (3.97), 267 (4.10), 304 (4.20)

IR ($CHCl_3$) ν_{max} (cm^{-1}) 3304, 2961, 2932, 1718, 1650, 1590, 1387, 1165, 1085

^1H (500 MHz) and ^{13}C NMR (125 MHz) ($CDCl_3$) See **Table 21**

Isolation of ART11 and ART39

Fraction P9 (317.3 mg) was subjected to CC and eluted with 30% Me_2CO in hexane affording fractions P9.1-P9.7. Fraction P9.2 (88.0 mg) was further purified by CC using 20% Me_2CO in hexane as an eluent to produce **ART11** (3.7 mg) and **ART39** (10.5 mg) as white solids.

ART39

mp	284-286 ^{O}C
IR (MeOH) ν_{max} (cm^{-1})	3406, 2925, 2858, 1685, 1654, 1458, 1274, 1029
^{1}H (300 MHz) and ^{13}C NMR (75 MHz) ($CDCl_3$+CD_3OD)	See **Table 37**

Isolation of ART40

Fraction P13 (163.5 mg) was subjected to CC on Sephadex LH-20 using MeOH as an eluent to give four fractions (P13.1-P13.4). Fraction P13.3 (39.0 mg) was further purified by CC on Sephadex LH-20 and eluted with MeOH to produce a yellow gum of **ART40** (7.0 mg).

ART40

UV (MeOH) λ_{max} nm (logε)	218 (3.98), 274 (3.66), 356 (2.66)
IR (MeOH) ν_{max} (cm^{-1})	3328, 2925, 2853, 1706, 1687, 1563, 1439, 1248, 1039
^{1}H (300 MHz) and ^{13}C NMR (75 MHz) ($CDCl_3$+CD_3OD)	See **Table 46**

Isolation of ART41

Fraction P14 (291.0 mg) was fractionated by CC on Sephadex LH-20 and eluted with MeOH to give four fractions (P14.1-P14.4). Crystallization of fraction P14.3 (39.1 mg) using 20% MeOH in CH_2Cl_2 as a solvent produced compound **ART41** (7.0 mg) as white solid.

ART41

$[\alpha]_D^{25}$	-33.0 (*c* 0.08, MeOH)
UV (MeOH) λ_{max} nm (logε)	207 (3.43), 253 (3.68), 274*sh* (3.53), 314 (3.12), 350 (3.18)
IR (MeOH) ν_{max} (cm^{-1})	3349, 2972, 2925, 1687, 1656, 1581, 1437, 1220, 1060

^1H (300 MHz) and ^{13}C NMR (75 MHz) ($CDCl_3$+CD_3OD) See **Table 28**

2.6 Antibacterial activity

Acylphloroglucinols: **ART2**, **ART4**, **ART6**, **ART9**, **ART11**, **ART18**, **ART19** and **ART20** were tested on antibacterial activity against three strain Gram-positive bacteria: *Stephylococcus aureus* ATCC 25923, methicillin-resistant *S. aureus* NRPC R01 (MRSA) and *Streptococcus pyogenes* DMST 101, and two strain Gram-negative bacteria: *Escherichia coli* ATCC 25922 and *E. coli* O157:H7 (RIMD 05091078).

The broth micro-dilution method was used to determine the minimal inhibitory concentration (MIC) (CLSI, 2006). The bacterial suspensions (10^5 cfu/mL) were added into Muller Hinton broth (MHB) supplemented with the plant extracts or pure compounds at concentrations that ranged from 0.049 to 100 μg/mL, incubated at 37^{o}C for 20 h (5% lysed blood was added to the MHB for *S. pyogenes*). All assays were carried out in triplicate. MIC values were recorded as the lowest concentration that produced a complete suppression of visible growth.

CHAPTER 3

RESULTS AND DISCUSSION

The preliminary study found that the crude extracts from its leaves exhibited strong antibacterial activity against *Stephylococcus aureus* and methicillin-resistant *S. aureus* (MRSA). The CH_2Cl_2 and Me_2CO extracts showed good activities with MIC values of 31.25 and 62.5 μg/mL, respectively, whereas the CH_2Cl_2 and Me_2CO extracts from its stems displayed no activities. The leaves, stems and fruits of *R. tomentosa* were investigated for chemical constituents and 41 compounds were obtained. The structures of all compounds were determined by analyses of spectral data in association with comparison with the literatures.

3.1 Structure elucidation

The dried ground leaves of *R. tomentosa* were successively extracted at room temperature with CH_2Cl_2, Me_2CO and MeOH. Separation of the Me_2CO extract yielded six new compounds: five acylphloroglucinols (**ART2-ART4**, **ART9** and **ART11**) and one butyrolactone derivative (**ART15**) together with eleven known compounds: **ART1**, **ART5-ART8**, **ART10**, **ART12-ART14**, **ART16** and **ART17**. Separation of the CH_2Cl_2 extract yielded additionally three new acylphloroglucinols: **ART18-ART20** along with one known: **ART21**. Separation of the MeOH extract yielded three known compounds: **ART22-ART24**. Addition to the above methods, the MeOH extract was further subjected to acetic anhydride acetylation in the presence of pyridine. After workup and purification, five known compounds, **ART25-ART29**, were also obtained.

The dried ground stems were successively extracted at room temperature with CH_2Cl_2, Me_2CO and MeOH to give the CH_2Cl_2, Me_2CO and MeOH extracts. Separation of the CH_2Cl_2 extract yielded one new flavellagic acid derivative: **ART31** along with two known compounds: **ART30** and **ART32**. Separation of the Me_2CO extract gave four known compounds: **ART33-ART36**.

The dried green fruits were extracted at room temperature with MeOH to give the MeOH extract. Separation of this extract gave two new acylphloroglucinols: **ART11** and **ART38** together with four known compounds: **ART37**, **ART39-ART41**.

3.1.1 Phloroglucinols

ART6: Rhodomyrtone

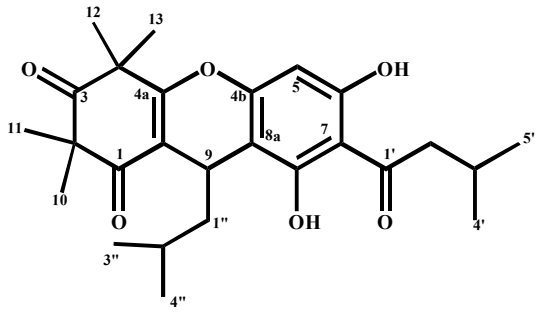

ART6 was obtained as a white solid, mp 188-189 ^{O}C with $[\alpha]_D^{25}$ -9.4^{O} (c = 1.0, $CHCl_3$). The UV spectrum exhibited absorption maxima at 244, 262, and 302 nm. The IR spectrum showed absorption bands for hydroxyl, saturated carbonyl and conjugated carbonyl groups at 3244, 1720 and 1630 cm^{-1}, respectively. The ^{1}H NMR spectrum (**Table 11**) showed the presence of a chelated hydroxyl group (δ_H 13.47, 8-OH), a free hydroxyl group (δ_H 8.22, 6-OH), an aromatic proton (δ_H 6.21, H-5), an isopentyl group (δ_H 4.31, *t*, H-9; 1.48, *obscure*, H_2-1" and H-2"; 0.88, *d*, H_3-3" and 0.85, *d*, H_3-4"), an isovaleryl group (δ_H 3.07 and 2.97, H_2-2'; 2.29, H-3' and 0.99, H_3-4' and H_3-5') and four singlet methyl groups of a β-triketone moiety (δ_H 1.57, H_3-12; 1.46, H_3-11; 1.44, H_3-13 and 1.40, H_3-10). The signals of H_3-12 and H_3-13 showed HMBC correlations (**Table 11**) to the carbonyl carbon C-3 (δ_C 212.17) and vinylic oxycarbon C-4a (δ_C 167.65) whereas H_3-10 and H_3-11 showed correlations to carbonyl carbons C-1 (δ_C 198.53) and C-3 (δ_C 212.17) supporting the presence of a β-triketone moiety. The methine proton H-9 and the chelated hydroxyl 8-OH exhibited the correlations with C-8 (δ_C 162.86) and C-8a (δ_C 106.41) in the HMBC experiment

indicating the location of the chelated hydroxyl at C-8. These data indicated that the isovaleryl side chain was consequently placed at C-7 (δ_C 107.76). The ^{13}C NMR and DEPT spectra (**Table 11**) displayed twenty five signals for twenty six carbon atoms; three carbonyl carbons (δ_C 212.17, 206.77, 198.53), nine quaternary carbons (δ_C 167.65, 162.86, 158.76, 155.70, 114.35, 107.76, 106.41, 56.08 and 47.29), four methine carbons [δ_C 94.81, 25.27 (2xC) and 25.17], two methylene carbons (δ_C 53.21 and 45.85) and eight methyl carbons (δ_C 24.78, 24.65, 26.64, 24.23, 23.57, 23.23, 22.84 and 22.78). The structure of **ART6** was then assigned as a known dimeric acylphloroglucinol named rhodomyrtone (**Table 54**), which was previously isolated from the leaves of this plant (Dachriyanus *et al*., 2002). The assignment was fully confirmed by the HMBC experiment.

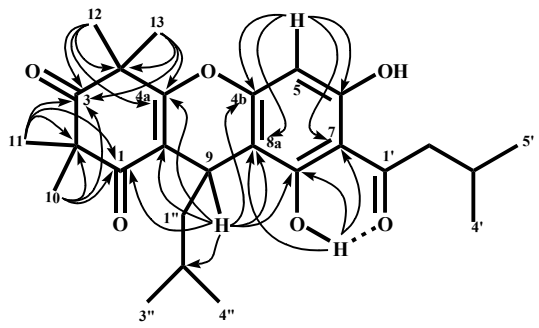

Selected HMBC correlations of **ART6**

Table 11 The NMR spectral data of **ART6**

Position	**δ_C (Type)**	**δ_H (*mult.*; J_{Hz})**	**HMBC correlations**
1	198.53 (C=O)		
2	56.08 (C)		
3	212.17 (C=O)		
4	47.29 (C)		
4a	167.65 (C)		
4b	155.70 (C)		
5	94.81 (CH)	6.21 (*s*)	C-4b, C-6, C-7, C-8a, C-9, C-1'
6	158.76 (C)		
7	107.76 (C)		
8	162.86 (C)		
8a	106.41(C)		
9	25.27 (CH)	4.31 (*t*; 5.7)	C-1, C-4a, C-4b, C-8, C-8a, C-9a, C-1", C-2"
9a	114.35 (C)		
10	24.23 (CH_3)	1.40 (*s*)	C-1, C-2, C-3, C-12
11	24.64 (CH_3)	1.46 (*s*)	C-1, C-2, C-3, C-11
12	24.65 (CH_3)	1.57 (*s*)	C-3, C-4, C-4a, C-14
13	24.78 (CH_3)	1.44 (*s*)	C-3, C-4, C-4a, C-13
1'	206.77 (C=O)		
2'	53.21 (CH_2)	3.07 (*dd*; 15.6, 6.6)	C-1', C-3', C-4', C-5'
		2.97 (*dd*; 15.6, 6.6)	
3'	25.17 (CH)	2.29 (*m*; 6.6)	C-1', C-2', C-4', C-5'
4'	22.84 (CH_3)	0.99 (*d*; 6.6)	C-2', C-3', C-5'
5'	22.78 (CH_3)	0.99 (*d*; 6.6)	C-2', C-3', C-4'

Table 11 (Continued)

Position	**δ_C (Type)**	**δ_H (*mult.*; J_{Hz})**	**HMBC correlations**
1"	45.85 (CH_2)	1.48 (*m*)	
2"	25.27 (CH)	1.48 (*m*)	
3"	23.57 (CH_3)	0.88 (*d*; 6.6)	C-1", C-2"
4"	23.23 (CH_3)	0.85 (*d*; 6.6)	C-1", C-2"
6-OH		8.22 (*br s*; OH)	
8-OH		13.47 (*br s*; OH)	C-7, C-8, C-8a

ART2: Rhodomyrtosone A

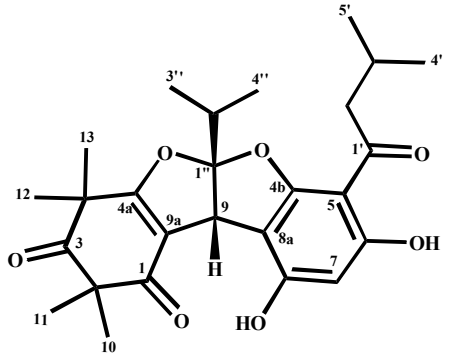

ART2 was obtained as a white solid, mp 125-126 ^{O}C. The IR spectrum displayed absorption bands of a hydroxyl (3126 cm^{-1}), a non-conjugated carbonyl (1720 cm^{-1}) and a conjugated carbonyl (1650 cm^{-1}) groups. The UV spectrum exhibited absorption maxima at 270 and 327 nm. The HREI-MS spectrum showed a molecular ion peak at *m/z* 456.2133 corresponding to a molecular formula of $C_{26}H_{32}O_7$ with eleven degrees of unsaturation. The ^{13}C NMR and DEPT spectra (**Table 12**) showed three carbonyl, ten quaternary, four methine, one methylene and eight methyl carbons. The ^{1}H NMR spectrum (**Table 12**) showed the resonances of four methyl groups at δ_H 1.52 (H_3-10), 1.42 (H_3-11), 1.41 (H_3-13) and 1.34 (H_3-12). The signals of H_3-12 and H_3-13 showed HMBC correlations (**Table 12**) to the carbonyl carbon C-3 (δ_C 211.14) and vinylic oxycarbon C-4a (δ_C 179.68) whereas H_3-10 and H_3-11 showed correlations to carbonyl carbons C-1 (δ_C 198.32) and C-3 (δ_C 211.14) indicating the presence of a β-triketone moiety similar to rhodomyrtone (Dachriyanus *et al*., 2002). The low field chemical shift of C-4a (δ_C 179.68) indicated that the β-triketone moiety was connected to the oxygen of a furan ring (Fukuyama *et al*., 1998; Shaheen *et al*., 2006). The signals of the two hydroxyl groups (δ_H 13.27, *s*, 6-OH and 9.78, *s*, 8-OH), an aromatic proton (δ_H 6.11, *s*, H-7) and signals corresponding to an isovaleryl group (δ_H 2.96 and 2.76, *dd* each, H_2-2'; 2.17, *m*, H-3'; 1.01, *d*, H_3-4' and 0.99, *d*, H_3-5') were derived from a di-*C*-substituted phloroglucinol moiety with

an isovaleryl group (Bloor, 1992). The spectrum further showed signals of a methine proton (δ_H 4.50, *s*, H-9) and an isopropyl group (δ_H 2.40, *hept*, H-2"; 1.11, *d*, H_3-3" and 1.09, *d*, H_3-4"). The loss of a 43 *m/z* (C_3H_7) and 85 *m/z* (C_4H_9CO) from a molecular ion, confirmed the presence of isopropyl and isovaleryl groups. The HMBC correlations of the methine proton H-9 to C-4a, C-4b, C-8, C-8a, C-9a and C-2" as well as of the methyl protons of an isopropyl group to C-1" (δ_C 129.36) provided evidence that the *β*-triketone was combined to a phloroglucinol moiety via a bisfuran fused-ring bearing the isopropyl group. The ^3J HMBC correlations of 6-OH and 8-OH to an aromatic methine carbon C-7 and of 6-OH to C-5 indicated that the aromatic proton was in between two hydroxyl groups (C-7), consequently the isovaleryl group was then placed at C-5 rather than C-7. The correlations of the methine proton (H-9) to the isopropyl protons in the NOESY experiment provided the assignment of a *cis* relative stereochemistry. **ART2**, a novel dimeric acylphloroglucinol named as rhodomyrtosone A, was thus identified as 8,10-dihydroxy-5a-isopropyl-2,2,4,4-tetramethyl-7-(3-methyl-butyryl)-5a,10b-dihydro-4*H*-benzo[*b*]benzo[4,5] furo[3,2-*d*]furan-1,3-dione.

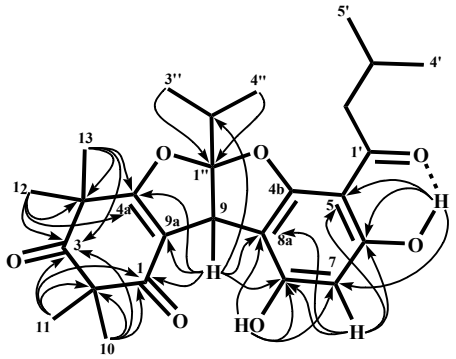

Selected HMBC correlations of **ART2**

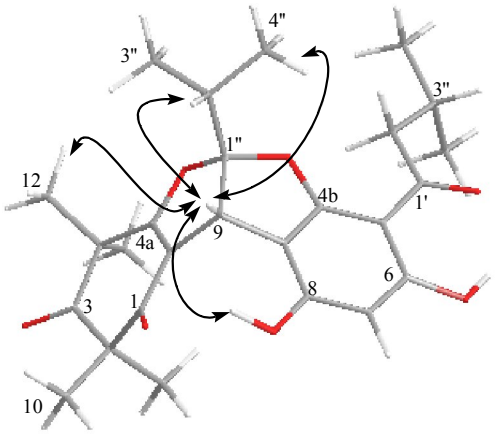

Energy-minimized (MM2) structure of **ART2**
showing selected NOESY experiments

Table 12 The NMR spectral data of **ART2**

Position	**δ_C (Type)**	**δ_H (*mult.*; J_{Hz})**	**HMBC correlations**
1	198.32 (C=O)		
2	55.12 (C)		
3	211.14 (C=O)		
4	45.62 (C)		
4a	179.68 (C)		
4b	159.76 (C)		
5	101.71 (C)		
6	166.70 (C)		
7	99.56 (CH)	6.11 (*s*)	C-5, C-6, C-8, C-8a
8	159.64 (C)		
8a	104.21 (C)		
9	44.97 (CH)	4.50 (*s*)	C-4a, C-8, C-8a, C-9a, C-2"
9a	113.20 (C)		

Table 12 (Continued)

Position	δ_C (Type)	δ_H (*mult.*; J_{Hz})	HMBC correlations
10	24.35 (CH_3)	1.52 (*s*)	C-1, C-2, C-3, C-11
11	24.11 (CH_3)	1.42 (*s*)	C-1, C-2, C-3, C-10
12	23.13 (CH_3)	1.34 (*s*)	C-3, C-4, C-5, C-13
13	25.90 (CH_3)	1.41 (*s*)	C-3, C-4, C-5, C-12
1'	203.68 (C=O)		
2'	51.51 (CH_2)	2.96 (*dd*; 14.7, 6.6)	C-1', C-3', C-4', C-5'
		2.76 (*dd*; 14.7, 6.6)	
3'	25.79 (CH)	2.17 (*m*; 6.6)	C-2', C-4', C-5'
4'	22.75 (CH_3)	1.01 (*d*; 6.6)	C-2', C-3', C-5'
5'	22.71 (CH_3)	0.99 (*d*; 6.6)	C-2', C-3', C-4'
1"	129.36 (C)		
2"	35.35 (CH)	2.40 (*hept*; 6.9)	C-1", C-3", C-4"
3"	15.71 (CH_3)	1.11 (*d*; 6.9)	C-1", C-2", C-4"
4"	15.65 (CH_3)	1.09 (*d*; 6.9)	C-1", C-2", C-3"
6-OH		13.27 (*s*)	C-5, C-6
8-OH		9.78 (*s*)	C-7, C-8

ART3: Rhodomyrtosone H

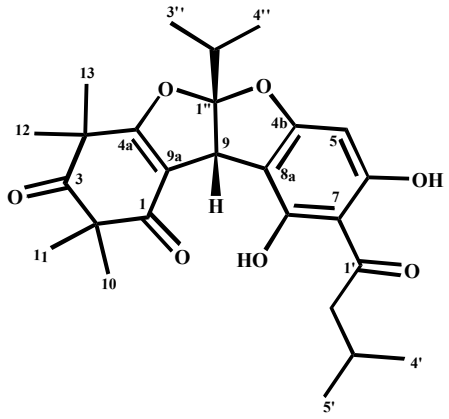

ART3 was obtained as a white solid. The IR spectrum displayed absorption bands of a hydroxyl (3316 cm^{-1}), a non-conjugated carbonyl (1720 cm^{-1}) and a conjugated carbonyl (1636 cm^{-1}) group whereas the UV spectrum exhibited the absorption bands at 244, 271 and 325 nm. A molecular formula of $C_{26}H_{32}O_7$ was established from a molecular ion peak at *m/z* 456.2133 in the HREI-MS spectrum. The ^{13}C NMR and DEPT spectra (**Table 13**) showed three carbonyl, ten quaternary, four methine, one methylene and eight methyl carbons. The ^{1}H NMR spectrum (**Table 13**) showed similar signals as those found in **ART2** including the presence of *β*-triketone moiety [δ_H 1.42 (H_3-10), 1.36 (H_3-11), 1.43 (H_3-13) and 1.51 (H_3-12)], two hydroxyl groups (δ_H 14.21, *s*, 6-OH and 10.20, *s*, 8-OH), an aromatic proton (δ_H 6.08, *s*, H-5) and signals corresponding to an isovaleryl group (δ_H 3.10 and 2.97, *dd* each, H_2-2'; 2.26, *m*, H-3'; 1.00, *d*, H_3-4' and 0.98, *d*, H_3-5'). The spectrum further showed signals of a methine proton (δ_H 4.48, *s*, H-9) and an isopropyl group (δ_H 2.39, *hept*, H-2''; 1.06, *d*, H_3-3'' and 1.04, *d*, H_3-4''). The above evidences indicated that **ART3** was a structural isomer of **ART2** (rhodomyrtosone A) which was each differed in only the acyl side chain position. The evidences from the HMBC correlations (**Table 13**) of two hydroxyl groups with C-7 indicated that the isovaleryl group was then placed at C-7. The higher field hydroxyl group (δ_H 10.20) at C-8 was confirmed

by the HMBC correlations of both this hydroxyl group and H-9 to C-8 and C-8a. Consequently, the lower field hydroxyl group (δ_H 14.21) was then located at C-6.

The correlations of the methine proton (H-9) to the isopropyl protons in the NOESY experiment provided the assignment of a *cis* relative stereochemistry. **ART3**, a novel dimeric acylphloroglucinol named as rhodomyrtosone H, was thus identified as 7,9-dihydroxy-1a-isopropyl-3,3,5,5-tetramethyl-8-(3-methylbutanoyl)-5,6b-dihydrobenzo[*b*]benzofuro[3,2-*d*]furan-4,6(1a*H*,3*H*)-dione.

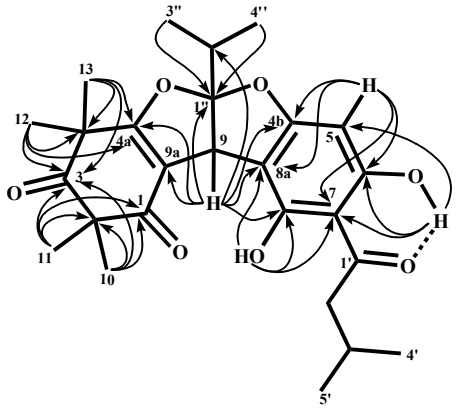

Selected HMBC correlations of **ART3**

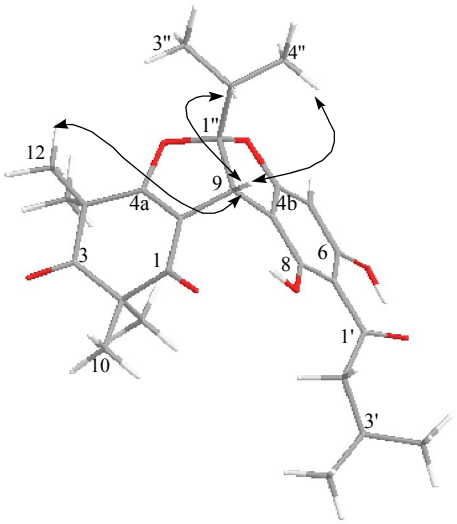

Energy-minimized (MM2) structure of **ART3**
showing selected NOESY experiments

Table 13 The NMR spectral data of **ART3**

Position	**δ_C (Type)**	**δ_H (*mult.*; J_{Hz})**	**HMBC correlations**
1	198.45 (C=O)		
2	55.98 (C)		
3	211.08 (C=O)		
4	45.69 (C)		
4a	179.80 (C)		
4b	163.07 (C)		
5	91.80 (CH)	6.08 (*s*)	C-4b, C-6, C-7, C-8a
6	168.51 (C)		
7	107.12 (C)		
8	156.54 (C)		
8a	103.79 (C)		
9	45.02 (CH)	4.48 (*s*)	C-4a, C-4b, C-8, C-8a, C-9a, C-1", C-2"
9a	113.15 (C)		

Table 13 (Continued)

Position	δ_C (Type)	δ_H (*mult.*; J_{Hz})	HMBC correlations
10	24.27 (CH_3)	1.42 (*s*)	C-1, C-2, C-3, C-11
11	23.29 (CH_3)	1.36 (*s*)	C-1, C-2, C-3, C-10
12	24.27 (CH_3)	1.51 (*s*)	C-3, C-4, C-4a, C-13
13	25.82 (CH_3)	1.43 (*s*)	C-3, C-4, C-4a, C-12
1'	206.32 (C=O)		
2'	51.94 (CH_2)	3.10 (*dd*; 16.0, 6.5)	C-1', C-3', C-4', C-5'
		2.97 (*dd*; 16.0, 6.5)	
3'	25.12 (CH)	2.26 (*m*; 6.5)	C-1', C-2', C-4', C-5'
4'	22.91 (CH_3)	1.00 (*d*; 6.5)	C-2', C-3', C-5'
5'	22.73 (CH_3)	0.98 (*d*; 6.5)	C-2', C-3', C-4'
1"	129.33 (C)		
2"	35.23 (CH)	2.39 (*hept*; 6.5)	C-9, C-1", C-3", C-4"
3"	15.58 (CH_3)	1.06 (*d*; 6.5)	C-1", C-2", C-4"
4"	15.53 (CH_3)	1.04 (*d*; 6.5)	C-1", C-2", C-3"
6-OH		14.21 (*s*)	C-5, C-6, C-7
8-OH		10.20 (*s*)	C-7, C-8, C8a

ART4: Rhodomyrtosone C

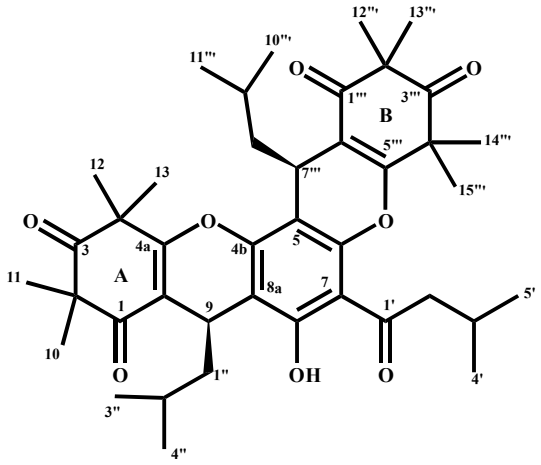

ART4 was obtained as a yellowish solid. The IR spectrum displayed absorptions of a hydroxyl (3423 cm^{-1}), non-conjugated carbonyl (1717 cm^{-1}) and conjugated carbonyl groups (1659 cm^{-1}) whereas the UV spectrum exhibited maximum absorptions at 263, 306 and 348 nm. Its molecular formula of $C_{41}H_{54}O_8$ was established on the basis of a molecular ion peak at m/z 674.3853 in its HREI-MS spectrum. The ^{1}H and ^{13}C NMR spectra (**Table 14**) showed the singlet signals that corresponded to two β-triketone moieties [ring A: δ_H 1.64 (H_3-12), 1.48 (H_3-13), 1.40 (H_3-10) and 1.37 (H_3-11); ring B: δ_H 1.66 (H_3-14'''), 1.52 (H_3-15'''), 1.44 (H_3-12''') and 1.42 (H_3-13''')]. Furthermore, two sets of resonances at δ_H 4.35 (*t*, H-9), 1.50 (obscure, H_2-1'' and H-2''), 0.90 (*d*, H_3-4'') and 0.83 (*d*, H_3-3'') and at δ_H 4.39 (*t*, H-7'''), 1.50 (obscure, H_2-8''' and H-9'''), 0.98 (*d*, H_3-11''') and 0.84 (*d*, H_3-10''') were in agreement with the resonances of two isopentyl groups. The remaining resonances were those of an isovaleryl group (δ_H 3.23 and 3.02, *dd* each, H_2-2'; 2.40, *m*, H-3'; 1.05, *d*, H_3-4' and 1.04, *d*, H_3-5') with their carbonyl function forming a hydrogen bonding to the hydroxyl group (δ_H 13.50, 8-OH). **ART4** was therefore identified as 7-hydroxy-8,14-diisobutyl-2,2,4,4,10,10,12,12-octamethyl-6-(3-methyl-butyryl)-4,8,12,14-tetrahydro-5,13-dioxapentaphene-1,3,9,11-tetraone and it was named as rhodomyrtosone C. The HMBC correlations confirmed the assigned structure (**Table 14**).

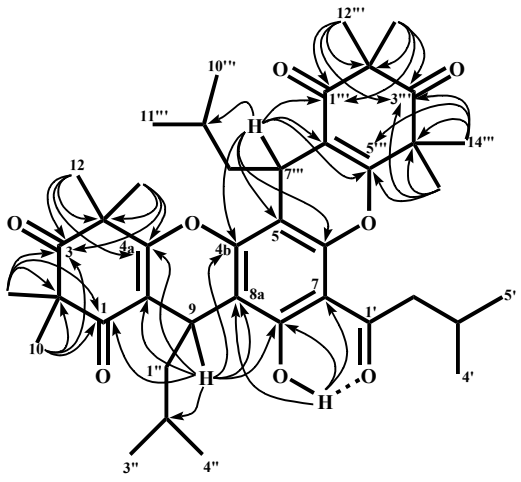

Selected HMBC correlations of **ART4**

Table 14 The NMR spectral data of **ART4**

Position	**δ_C (Type)**	**δ_H (*mult.*; J_{Hz})**	**HMBC correlations**
1	197.38 (C=O)		
2	56.01 (C)		
3	211.62 (C=O)		
4	47.25 (C)		
4[a]	166.69 (C)		
4b	152.37 (C)		
5	105.68 (C)		
6	150.50 (C)		
7	107.61 (C)		
8	160.61 (C)		
8a	107.76 (C)		
9	25.60 (CH)	4.35 (*t*; 5.7)	C-1, C-4a, C-4b, C-8, C-8a, C-9a, C-1", C-2"
9a	114.28 (C)		

Table 14 (Continued)

Position	δ_C (Type)	δ_H (*mult.*; J_{Hz})	HMBC correlations
10	24.87 (CH_3)	1.40 (*s*)	C-1, C-2, C-3, C-11
11	24.36 (CH_3)	1.37 (*s*)	C-1, C-2, C-3, C-10
12	24.69 (CH_3)	1.64 (*s*)	C-3, C-4, C-4a, C-13
13	25.03 (CH_3)	1.48 (*s*)	C-3, C-4, C-4a, C-12
1'	204.59 (C=O)		
2'	53.89 (CH_2)	3.23 (*dd*; 17.4, 6.6)	C-1', C-3', C-4', C-5'
		3.02 (*dd*; 17.4, 6.6)	
3'	24.53 (CH)	2.40 (*m*; 6.6)	C-1', C-2', C-4', C-5'
4'	22.64 (CH_3)	1.05 (*d*; 6.6)	C-2', C-3', C-5'
5'	22.80 (CH_3)	1.04 (*d*; 6.6)	C-2', C-3', C-4'
1"	45.44 (CH_2)	1.50 (obscure)	
2"	25.30 (CH)	1.50 (obscure)	
3"	23.32 (CH_3)	0.83 (*d*; 6.0)	C-1", C-2"
4"	23.28 (CH_3)	0.90 (*d*; 6.0)	C-1", C-2"
1"'	197.45 (C=O)		
2"'	56.20 (C)		
3"'	211.39 (C=O)		
4"'	47.28 (C)		
5"'	166.76 (C)		
6"'	113.53 (C)		
7"'	25.20 (CH)	4.39 (*t*; 5.4)	C-4b, C-5, C-6, C-1"', C-5"', C-6"', C-8"', C-9"'
8"'	46.78 (CH_2)	1.50 (obscure)	
9"'	25.03 (CH)	1.50 (obscure)	
10"'	23.36 (CH_3)	0.84 (*d*; 6.0)	C-8"', C-9"'
11"'	23.78 (CH_3)	0.98 (*d*; 6.0)	C-8"', C-10"'

Table 14 (Continued)

Position	**δ_C (Type)**	**δ_H (*mult.*; J_{Hz})**	**HMBC correlations**
12'''	24.17 (CH_3)	1.44 (*s*)	C-1''', C-2''', C-3'''
13'''	23.81 (CH_3)	1.42 (*s*)	C-1''', C-2''', C-3'''
14'''	25.34 (CH_3)	1.66 (*s*)	C-3''', C-4''', C-5'''
15'''	24.93 (CH_3)	1.52 (*s*)	C-3''', C-4''', C-5'''
6-OH		13.50 (*s*)	C-7, C-8, C-8a

ART8: Endoperoxide G3

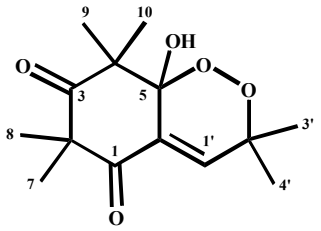

ART8 was obtained as a yellowish gum. The IR spectrum displayed absorption bands of a hydroxyl (3479 cm^{-1}), a non-conjugated carbonyl (1714 cm^{-1}) and a conjugated carbonyl (1693 cm^{-1}) group whereas the UV spectrum displayed absorption bands at 243 and 294 nm. The EI-MS spectrum showed a molecular ion peak at *m/z* 268. The ^{1}H NMR spectral data (**Table 15**) showed the resonances of four methyl groups at δ_H 1.39 (H_3-8), 1.37 (H_3-7), 1.34 (H_3-9) and 1.06 (H_3-10). The evidences that H_3-9 and H_3-10 showed ^{3}J HMBC correlations (**Table 15**) to carbonyl carbons C-3 (δ_C 210.51) whereas H_3-7 and H_3-8 showed ^{3}J HMBC correlations to the carbonyl carbons C-3 (δ_C 210.51) and C-1 (δ_C 198.23) indicated the presence of a β-triketone moiety. A peroxide moiety with an olefinic proton (δ_H 7.16, H-1'), two methyl groups (δ_H 1.51, H_3-3' and 1.39, H_3-4') and a hydroxyl group (δ_H 3.62, 5-OH) were proposed. The low field chemical shift of H-1' (δ_H 7.16) suggested that it was at a *peri* position to carbonyl group whereas the low field chemical shift of C-5 (δ_C 97.46) revealed that the hydroxyl group and a peroxide were located at C-5. Finally, the HMBC correlation of H-1' to C-1 (δ_C 198.23), C-5 (δ_C 97.46), C-6 (δ_C 131.74), C-3' (δ_C 23.71) and C-4' (δ_C 23.88) and the analysis of mass spectrum also confirmed this assignment. Thus **ART8** was elucidated to be endoperoxide G3 (Crow *et al*., 1971).

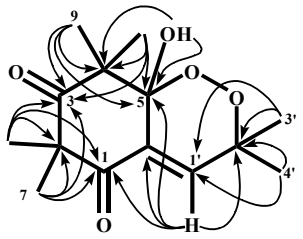

Selected HMBC correlations of **ART8**

Table 15 The NMR spectral data of **ART8**

Position	**δ_C (Type)**	**δ_H (*mult.*; J_{Hz})**	**HMBC correlations**
1	198.23 (C=O)		
2	55.01 (C)		
3	210.51 (C=O)		
4	51.63 (C)		
5	97.46 (C)		
6	131.74 (C)		
7	24.05 (CH_3)	1.37 (*s*)	C-1, C-2, C-3, C-8
8	26.59 (CH_3)	1.39 (*s*)	C-1, C-2, C-3, C-7
9	15.17 (CH_3)	1.34 (*s*)	C-3, C-4, C-5, C-10
10	20.94 (CH_3)	1.06 (*s*)	C-3, C-4, C-5, C-9
1'	142.92 (CH)	7.16 (*s*)	C-1, C-5, C-6, C-2'
2'	79.41 (C)		
3'	23.71 (CH_3)	1.51 (*s*)	C-1', C-2', C-4'
4'	23.88 (CH_3)	1.39 (*s*)	C-1', C-2', C-3'
5-OH		3.62 (*s*)	C-4, C-5

ART9: Rhodomyrtosone B

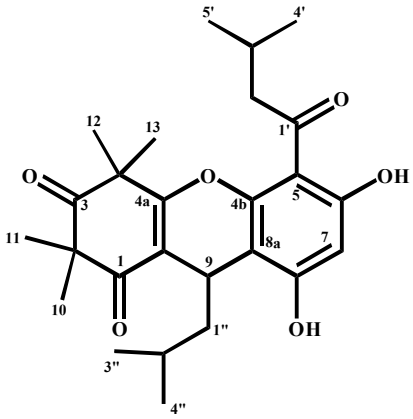

ART9 was a yellowish gum. The IR spectrum displayed absorption bands of a hydroxyl (3372 cm^{-1}), a non-conjugated carbonyl (1717 cm^{-1}) and a conjugated carbonyl (1653 cm^{-1}) group. The UV spectrum exhibited absorption bands at 292 and 333 nm. Its molecular ion peak at *m/z* 442.2352 in the HREI-MS spectrum corresponded to a molecular formula of $C_{26}H_{34}O_6$ with ten degrees of unsaturation. The appearance of the proton resonances (**Table 16**) of a chelated hydroxyl group (δ_H 13.43, 6-OH), a free hydroxyl group (δ_H 6.40, 8-OH), an aromatic proton (δ_H 6.23, H-7), an isopentyl group (δ_H 4.25, *t*, H-9; 1.38, obscure, H_2-1" and H-2"; 0.89, *d*, H_3-3" and 0.87, *d*, H_3-4"), an isovaleryl group (δ_H 3.18 and 2.96, H_2-2'; 2.37, H-3'; 1.04, H_3-4' and 1.01, H_3-5') and four singlet methyl groups of a β-triketone moiety (δ_H 1.63, H_3-12; 1.47, H_3-13; 1.42, H_3-11 and 1.39, H_3-10) as well as its molecular ion of 442.2352 indicated that **ART9** was a structural isomer of **ART6** (rhodomyrtone). There were slight differences observed for the chemical shifts of the chelated hydroxyl group (δ_H 13.43) and non-equivalent methylene protons of the isovaleryl group (δ_H 3.18 and 2.96), consequently the isovaleryl group was placed at C-5 rather than C-7. The assignment was fully confirmed by the HMBC experiment (**Table 16**). **ART9**, named rhodomyrtosone B, was therefore identified as 6,8-dihydroxy-9-isobutyl-2,2,4,4-tetramethyl-5-(3-methylbutyryl)-4,9-dihydro-xanthene-1,3-dione, a new naturally occurrence acylphloroglucinol. It was a

6-demethylated isomer of a synthetic 1,3-dioxo-4,9-dihydro-8-hydroxy-6-methoxy-2,2,4,4-tetramethyl-5-(3-methyl-1-oxobutyl)-9-(2-methylpropyl)-1*H*-xanthene (Bloor, 1992).

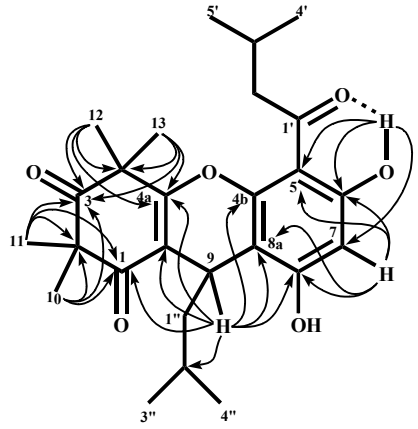

Selected HMBC correlations of **ART9**

Table 16 The NMR spectral data of **ART9**

Position	**δ_C (Type)**	**δ_H (*mult.*; J_{Hz})**	**HMBC correlations**
1	197.60 (C=O)		
2	56.13 (C)		
3	211.68 (C=O)		
4	47.21 (C)		
4a	166.89 (C)		
4b	153.27 (C)		
5	105.91 (C)		
6	164.32 (C)		
7	100.32 (CH)	6.23 (*s*)	C-5, C-6, C-8, C-9
8	159.02 (C)		

Table 16 (Continued)

Position	δ_C (Type)	δ_H (*mult.*; J_{Hz})	HMBC correlations
8a	105.91 (C)		
9	25.08 (CH)	4.25 (*t*; 5.7)	C-1, C-4a, C-4b, C-8, C-8a, C-9a, C-1", C-2"
9a	114.54 (C)		
10	24.29 (CH_3)	1.39 (*s*)	C-1, C-2, C-3, C-11
11	24.35 (CH_3)	1.42 (*s*)	C-1, C-2, C-3, C-10
12	24.77 (CH_3)	1.63 (*s*)	C-3, C-4, C-4a, C-13
13	25.36 (CH_3)	1.47 (*s*)	C-3, C-4, C-4a, C-12
1'	203.96 (C=O)		
2'	53.56 (CH_2)	3.18 (*dd*; 15.6, 6.5)	C-1', C-3', C-4', C-5'
		2.96 (*dd*; 15.6, 6.5)	
3'	24.48 (CH)	2.37 (*m*; 6.5)	C-1', C-2', C-4', C-5'
4'	22.89 (CH_3)	1.04 (*d*; 6.5)	C-2', C-3', C-5'
5'	22.65 (CH_3)	1.01 (*d*; 6.5)	C-2', C-3', C-4'
1"	46.90 (CH_2)	1.38 (obscure)	
2"	24.87 (CH)	1.38 (obscure)	
3"	23.41 (CH_3)	0.89 (*d*; 6.5)	C-1", C-2", C-4"
4"	23.10 (CH_3)	0.87 (*d*; 6.5)	C-1", C-2", C-3"
6-OH		13.43 (*s*)	C-5, C-6, C-7
8-OH		6.40 (*br s*)	

ART11: Rhodomyrtosone D

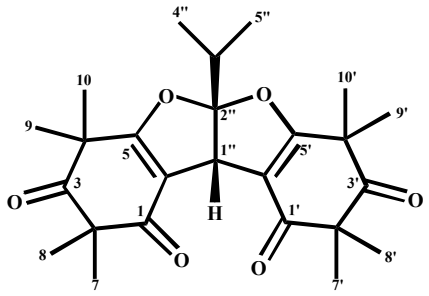

ART11 was a yellowish solid, mp 160-162 ^{O}C. The IR spectrum displayed absorption bands of a non-conjugated (1717 cm^{-1}) and a conjugated (1675 cm^{-1}) carbonyl functionalities. The HREI-MS spectrum showed a molecular ion peak at *m/z* 428.2214 corresponding to a molecular formula of $C_{25}H_{32}O_6$. The ^{13}C NMR and DEPT techniques (**Table 17**) showed signals for four carbonyl, nine quaternary, two methine and ten methyl carbons. The ^{1}H NMR spectrum (**Table 17**) revealed three singlet signals of methyl groups at δ_H1.27 (H_3-7 and H_3-7'), 1.34 (H_3-8 and H_3-8') and 1.44 (H_3-9, H_3-10, H_3-9' and H_3-10'). In the HMBC experiment (**Table 17**), these methyl groups correlated to the carbonyl carbons [δ_C 212.10 (2xC=O) and 192.35 (2xC=O)] thus indicating the presence of two moieties of a symmetrical β-triketone. The resonances of a methine proton (δ_H 4.69, *s*, H-1") and an isopropyl group (δ_H 2.37, *hept*, H-3" and 1.02, *d*, H_3-4", H_3-5"), similar to those in **ART2** (rhodomyrtosone A), were also observed. Compound **ART11** was therefore 5a-isopropyl-2,2,4,4,7,7,9,9-octamethyl-7,10b-dihydro-4*H*,5a*H*-benzo[*b*]benzo [4,5] furo [3,2-*d*]furan-1,3,8,10-tetraone. The HMBC correlations of the methine proton H-1" to the C-5(5'), C-6(6') of a β-triketone and to C-2", C-3" of the isopropyl group along with the downfield shift of C-2" (δ_C 128.19) confirmed the assigned structure. In addition, it was in good agreement with a molecular formula of $C_{25}H_{32}O_6$ and the ion peaks at *m/z* 385, 358, 315 and 288. In the NOEDIFF spectrum, irradiation at the resonance of the methine proton H-1" resulted in enhancement of the isopropyl

protons, indicating its *cis* stereochemistry. Thus **ART11** was a novel acylphloroglucinol named as rhodomyrtosone D.

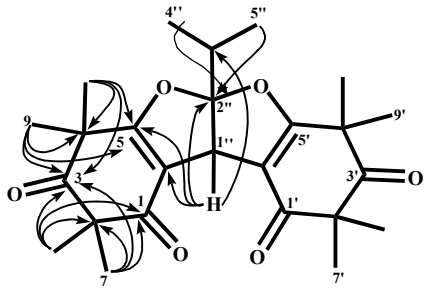

Selected HMBC correlations of **ART11**

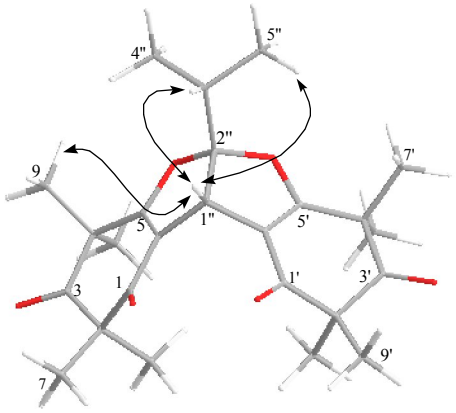

Energy-minimized (MM2) structure of **ART11**
showing selected NOEDIFF experiments

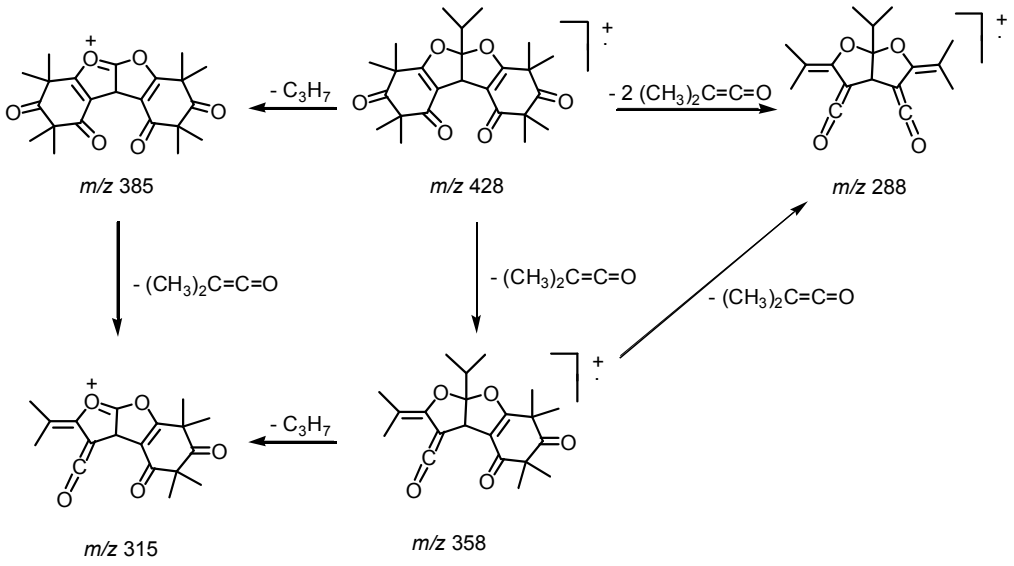

Major mass fragmentation patterns of **ART11**

Table 17 The NMR spectral data of **ART11**

Position	**δ_C (Type)**	**δ_H (*mult.*; J_{Hz})**	**HMBC correlations**
1 (1')	192.35 (C=O)		
2 (2')	56.48 (C)		
3 (3')	212.10 (C=O)		
4 (4')	45.18 (C)		
5 (5')	175.65 (C)		
6 (6')	113.07 (C)		
7 (7')	25.73 (CH_3)	1.27 (*s*)	C-1 (1'), C-2 (2'), C-3 (3'), C-8 (8')
8 (8')	22.31 (CH_3)	1.34 (*s*)	C-1 (1'), C-2 (2'), C-3 (3'), C-7 (7')
9 (9')	24.36 (CH_3)	1.44 (*s*)	C-3 (3'), C-4 (4'), C-5 (5')
10 (10')	23.91 (CH_3)	1.44 (*s*)	C-3 (3'), C-4 (4'), C-5 (5')
1"	46.47 (CH)	4.69 (*s*)	C-5 (5'), C-6 (6'), C-2", C-3"
2"	128.19 (C)		
3"	34.41 (CH)	2.37 (*hept*; 6.9)	C-2", C-4", C-5"
4",5"	15.46 (CH_3)	1.02 (*d*; 6.9)	C-2", C-3"

ART18: Rhodomyrtosone E

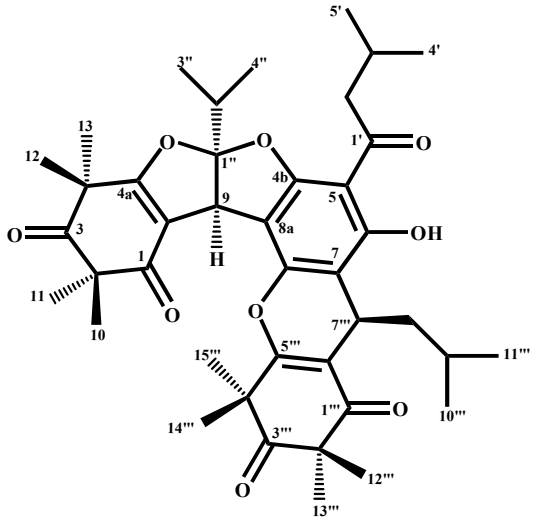

ART18 was obtained as a yellowish gum with $[\alpha]_D^{25}$ -9.3^O (*c* = 0.92, $CHCl_3$). The UV spectrum exhibited maximum absorption bands at 246, 260, 304 and 347 nm. The IR spectrum showed the absorption of a hydroxyl (3135 cm^{-1}), a conjugated carbonyl (1656 cm^{-1}) and a non-conjugated carbonyl (1720 cm^{-1}) groups. A molecular ion peak at *m*/*z* 688.3610 in the HREI-MS spectrum corresponded to the molecular formula of $C_{41}H_{52}O_9$. The ^{1}H NMR spectrum (**Table 18**) showed the resonances of four methyl groups of a *β*-triketone moiety at δ_H 1.47 (H_3-13), 1.43 (H_3-11), 1.36 (H_3-12), and 1.24 (H_3-10). The presence of an acylphloroglucinol moiety with an isovaleryl group was assigned from the resonances of a hydrogen bonded hydroxyl proton at δ_H 13.62 (6-OH), non equivalent methylene protons at δ_H 2.99 and 2.89 (H_2-2'), a methine proton at δ_H 2.23 (H-3'), and methyl protons at δ_H 1.03 (H_3-4') and 1.01 (H_3-5'). The spectrum further showed signals of a methine proton at δ_H 4.74 (*s*, H-9) and the protons of an isopropyl group at δ_H 2.37 (*hept*, H-2"), 1.11 (*d*, H_3-3") and 1.09 (*d*, H_3-4"). The HMBC correlations (**Table 18**) of the methine proton H-9 to C-4a, C-4b, C-8, C-8a, C-9a and C-2" as well as that of the methyl protons of the isopropyl group to C-1" (δ_C 128.84) indicated that the *β*-triketone was combined to a phloroglucinol moiety via a bisfuran fused-ring

bearing the isopropyl group as for **ART2** (rhodomyrtosone A). The resonance of additional *β*-triketone moiety with an isopentyl group was detected at δ_H 4.28 (*t*, H-7'''), 1.40 (obscure, H_2-8''' and H-9'''), 0.75 (*d*, H_3-10'''), 0.83 (*d*, H_3-11'''), 1.42 (*s*, H_3-12'''), 1.36 (*s*, H_3-13'''), 1.74 (*s*, H_3-14'''), and 1.67 (*s*, H_3-15'''). The ^3J HMBC correlations of the methine proton H-7''' to C-6 (δ_C 162.53), C-8 (δ_C 152.88), C-1''' (δ_C 197.51) and C-5''' (δ_C 167.70) indicated that the isopentyl *β*-triketone was linked to the acylphloroglucinol unit by C-7. The resonances of five carbonyl carbons, fifteen quaternary carbons, five methine carbons, two methylene carbons and fourteen methyl carbons that were deduced from the ^{13}C NMR and DEPT techniques (**Table 18**) were in agreement with the assigned structure.

The relative stereochemistry at C-9, C- 1'' and C-7''' was further studied. The methyl groups H_3-14''' (δ 1.74) and H_3-15''' (δ 1.67) on *β*-triketone moiety were found to resonate at the lower field than the others (δ 1.24-1.47). It was indicated that both methyl groups were lined on the deshielding zone of the carbonyl group at C-1 position (**b**). In addition, on the ROESY experiment (**a**), the methine proton H-9 showed strong correlation to methyl group H_3-15''' and weak correlation to methyl group H_3-14'''. The methyl group H_3-12''' exhibited the correlations to both methyl groups H_3-11'' and H_3-14'''. Furthermore the methyl groups H_3-10''' and H_3-11''' of the isobutyl moiety at C-7''' correlated to the methyl group H_3-10. These information suggested that the isopropyl group, methine proton H-9 and isobutyl group at C-7''' must be arranged in *cis-trans* configuration. The energy-minimized 3D structures generated by the MM2 force field as implemented in Chem3D® (CambridgeSoft) of **ART18** also confirmed the proposed stereochemistry. Furthermore the 3D structure showed that the non-equivalent methylene protons (H_2-2') of the isovaleryl group arranged in the similar region of environments (**b**), which was in agreement with the chemical shift at δ_H 2.99 and 2.89.

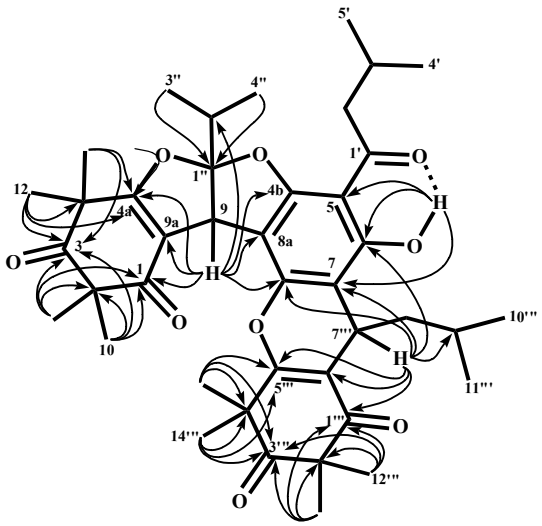

Selected HMBC correlations of **ART18**

(a)

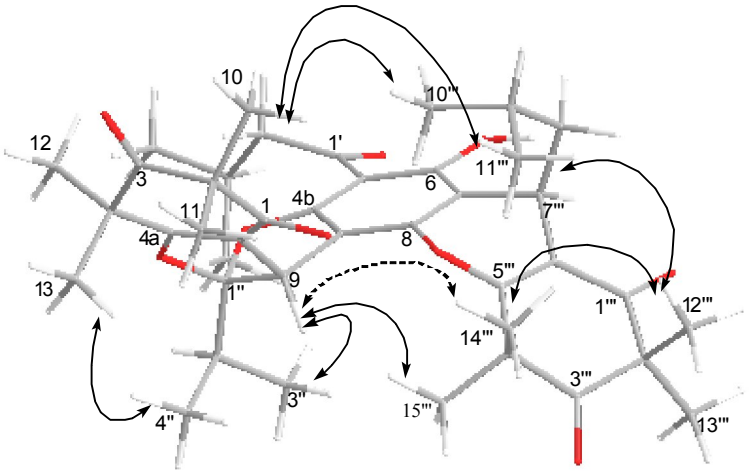

(b)

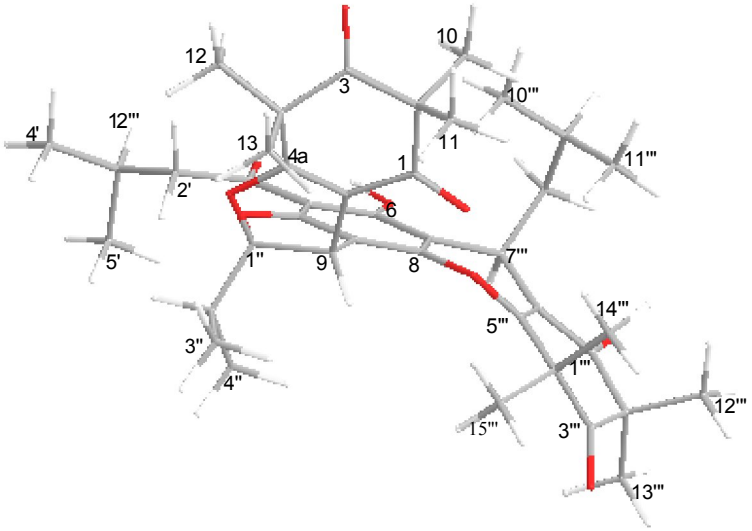

Energy-minimized (MM2) structure of **ART18** showing

(a) selected ROESY experiment

(b) interaction of C=O/Me-14''', Me-15''' and position of CH_2 of the isovaleryl group

Table 18 The NMR spectral data of **ART18**

Position	**δ_C (Type)**	**δ_H (*mult.*; J_{Hz})**	**HMBC correlations**
1	192.03 (C=O)		
2	56.09 (C)		
3	212.07 (C=O)		
4	45.46 (C)		
4a	175.99 (C)		
4b	158.37 (C)		
5	103.97 (C)		
6	162.53 (C)		
7	108.73 (C)		
8	152.24 (C)		
8a	104.88 (C)		
9	45.94 (CH)	4.74 (*s*)	C-1, C-4a, C-4b, C-8, C-8a, C-9a, C-1", C-2"
9a	113.01 (C)		
10	25.82 (CH_3)	1.24 (*s*)	C-1, C-2, C-3, C-11
11	23.84 (CH_3)	1.43 (*s*)	C-1, C-2, C-3, C-10
12	23.84 (CH_3)	1.36 (*s*)	C-3, C-4, C-4a, C-13
13	24.49 (CH_3)	1.47 (*s*)	C-3, C-4, C-4a, C-12
1'	204.64 (C=O)		
2'	51.94 (CH_2)	2.99 (*dd*; 15.0, 6.9)	C-1', C-3', C-4', C-5'
		2.89 (*dd*; 15.0, 6.9)	
3'	25.62 (CH)	2.23 (*m*; 6.9)	C-1', C-2', C-4', C-5'
4'	22.75 (CH_3)	1.03 (*d*; 6.9)	C-2', C-3', C-5'
5'	22.66 (CH_3)	1.01 (*d*; 6.9)	C-2', C-3', C-4'

Table 18 (Continued)

Position	δ_C (Type)	δ_H (*mult.*; J_{Hz})	HMBC correlations
1"	128.84 (C)		
2"	34.87 (CH)	2.37 (*hept*; 6.9)	C-9, C-1", C-3", C-4"
3"	15.84 (CH_3)	1.11 (*d*; 6.9)	C-1", C-2", C-4"
4"	15.84 (CH_3)	1.09 (*d*; 6.9)	C-1", C-2", C-3"
1"'	197.51 (C=O)		
2"'	56.27 (C)		
3"'	212.48 (C=O)		
4"'	47.55 (C)		
5"'	167.70 (C)		
6"'	113.86 (C)		
7"'	25.26 (CH)	4.28 (*t*; 5.4)	C-6, C-7, C-8, C-1"', C-5"', C-6"', C-8"', C-9"'
8"'	45.40 (CH_2)	1.40 (obscure)	
9"'	25.12 (CH)	1.40 (obscure)	
10"'	23.24 (CH_3)	0.83 (*d*; 6.6)	C-8"', C-9"', C-11"'
11"'	23.55 (CH_3)	0.75 (*d*; 6.6)	C-8"', C-9"', C-10"'
12"'	24.70 (CH_3)	1.42 (*s*)	C-1"', C-2"', C-3"'
13"'	22.04 (CH_3)	1.36 (*s*)	C-1"', C-2"', C-3"'
14"'	23.15 (CH_3)	1.74 (*s*)	C-3"', C-4"', C-5"', C-15"'
15"'	25.26 (CH_3)	1.67 (*s*)	C-3"', C-4"', C-5"', C-14"'
6-OH		13.62 (*s*)	C-5, C-6, C-7

ART19: Rhodomyrtosone G

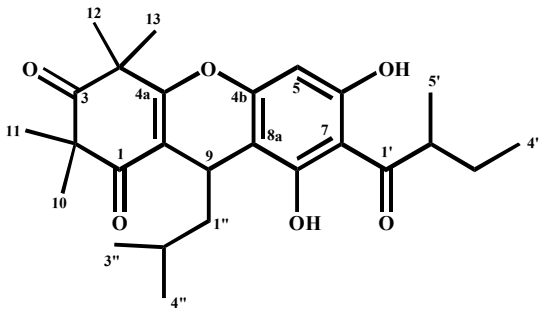

ART19 was obtained as a yellowish gum with $[\alpha]_D^{25}$ +62.0^O (*c* = 0.10, $CHCl_3$). The UV spectrum displayed absorption maxima at 245, 262 and 300 nm. The IR spectrum showed absorption bands of O-H stretching at 3365 cm^{-1} and C=O stretching at 1717 and 1655 cm^{-1}. Its $[M+H]^+$ peak at *m/z* 443.2429 in the HR-FAB-MS spectrum corresponded to a molecular formula of $C_{26}H_{34}O_6$. The ^1H NMR spectrum (**Table 19**) showed the resonances of four methyl groups (δ_H 1.55, H_3-13; 1.43, H_3-12; 1.40, H_3-11 and 1.36, H_3-10), an isopentyl group (δ_H 4.25, H-9; 1.45, H_2-1" and H-2"; 0.88, H_3-3" and 0.84, H_3-4"), a phloroglucinol moiety with two hydroxyl groups (δ_H 13.00, 8-OH and 7.18, 6-OH) and an aromatic proton (δ_H 6.07, H-5), as those of **ART6** (rhodomyrtone). The side chain at C-7 was suggested to be 2-methylbutyryl group from the resonances of two methyl groups (1.19, *d*, H_3-5' and 0.92, *t*, H_3-4'), a methine proton (δ_H 3.75, *sext*, H-2') and methylene protons (1.84 and 1.45, *m* each, H_2-3') as well as the resonance of a carbonyl carbon at δ_C 210.82 (C-1'). The assigned structure was then confirmed by the HMBC experiment recorded in $CDCl_3$ (**Table 19**). The correlations of H-9 (δ_H 4.25) to C-8, and that of the lower field hydroxyl group (δ_H 13.00) to C-7, C-8 and C-8a were expected to confirm the position of the acyl side chain at C-7. Unfortunately, the latter correlations were not observed due to the weak signal of the hydroxyl proton. The HMBC experiment was then rerecorded in acetone-d_6. The expected results were obtained. Therefore, 6,8-dihydroxy-9-isobutyl-2,2,4,4-tetramethyl-7-(2-methylbutanoyl)-4,9-dihydro-1*H*-

xanthene-1,3(2*H*)-dione was assigned for **ART19**. It was a new dimeric acylphloroglucinol named as rhodomyrtosone G.

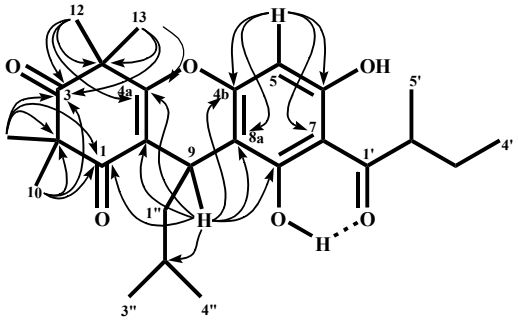

Selected HMBC correlations of **ART19**

Table 19 The NMR spectral data of **ART19**

Position	**δ_C (Type)**	**δ_H (*mult.*; J_{Hz})**	**HMBC correlations**
1	197.48 (C=O)		
2	56.09 (C)		
3	212.11 (C=O)		
4	47.14 (C)		
4a	166.81 (C)		
4b	155.58 (C)		
5	94.94 (CH)	6.07 (*s*)	C-4b, C-6, C-7, C-8a, C-1'
6	158.02 (C)		
7	107.14 (C)		
8	162.80 (C)		
8a	106.92 (C)		
9	25.23 (CH)	4.25 (*t*; 6.0)	C-1, C-4a, C-4b, C-8, C-8a, C-9a, C-1", C-2"
9a	114.25 (C)		

Table 19 (Continued)

Position	δ_C (Type)	δ_H (*mult.*; J_{Hz})	HMBC correlations
10	24.15 (CH_3)	1.36 (*s*)	C-1, C-2, C-3, C-11
11	24.54 (CH_3)	1.40 (*s*)	C-1, C-2, C-3, C-10
12	24.59 (CH_3)	1.43 (*s*)	C-3, C-4, C-4a, C-13
13	24.73 (CH_3)	1.55 (*s*)	C-3, C-4, C-4a, C-12
1'	210.82 (C=O)		
2'	46.39 (CH)	3.75 (*sext*; 6.5)	C-1', C-3', C-4', C-5'
3'	26.95 (CH_2)	1.84 (*m*)	C-1', C-2', C-4', C-5'
		1.45 (*m*)	
4'	11.89 (CH_3)	0.92 (*t*; 7.0)	C-2', C-3'
5'	16.40 (CH_3)	1.19 (*d*; 6.5)	C-1', C-2', C-3'
1"	45.89 (CH_2)	1.45 (*m*)	
2"	25.15 (CH)	1.45 (*m*)	
3"	23.46 (CH_3)	0.88 (*d*; 6.0)	C-1", C-2", C-4"
4"	23.16 (CH_3)	0.84 (*d*; 6.0)	C-1", C-2", C-3"
6-OH		7.18 (*br s*)	
8-OH		13.00 (*br s*)	

ART20: Rhodomyrtosone F

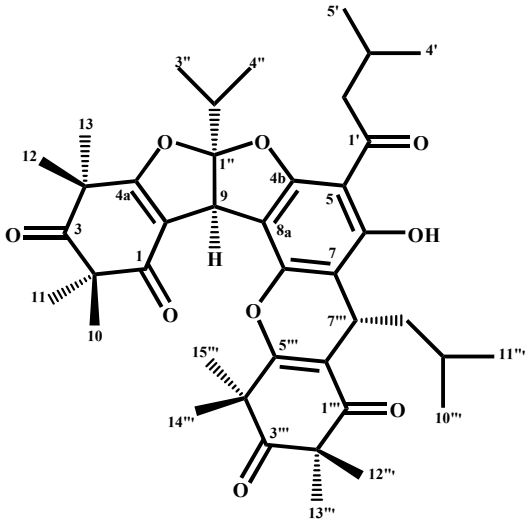

ART20 was obtained as a pale yellow solid with mp 198-199 ^{O}C and $[\alpha]_D^{25}$ -10.7^{O} (c = 0.68, $CHCl_3$). Its molecular formula of $C_{41}H_{52}O_9$ (M^+ 688.3610), its spectral data of UV, IR, MS, ^{1}H NMR (**Table 20**), ^{13}C NMR (**Table 20**) were very similar to those of **ART18** with the difference of methlyl proton signals (H_3-14'''/ H_3-15''', δ_H 1.42/1.81 for **ART20**; δ_H 1.74/1.67 for **ART18**) and non-equivalent methylene protons (H_2-2', δ_H 3.12/2.73 for **ART20**; δ_H 2.99/2.89 for **ART18**). It also showed the HMBC correlation in the same manner as **ART18** (**Table 20**). Consequently, **ART20** was suggested to be a diastereomer of **ART18**.

The relative stereochemistry at C-9, C- 1'' and C-7''' was further studied. The methyl group H_3-15''' (δ_H 1.81) on β-triketone moiety was found to resonate at the lower field than the others (δ_H 1.24-1.49). Thus indicating that this methyl group was lined in the deshielding zone of the carbonyl group at C-1 position (**a**). In addition, in the ROESY experiment (**a**), the methyl protons H_3-15''' showed correlations to a methine proton H-9 and a methyl group H_3-13''' indicating that all protons H-9, H_3-13''' and H_3-15''' were *cis*. Furthermore the methyl group H_3-13''' exhibited the correlation to a methyl group H_3-11'' of the isobutyl side chain. These information suggested that the isopropyl group, a methine proton H-9 and an isobutyl group at

C-7''' must be arranged in *cis*-*cis* configuration. The energy-minimized 3D structures generated by the MM2 force field as implemented in Chem3D® (CambridgeSoft) of **ART20** also confirmed the proposed stereochemistry. Furthermore the 3D structure showed that the non-equivalent methylene protons (H_2-2') of the isovaleryl group were arranged in the different environments (**b**), which was in agreement with the chemical shift at δ_H 3.12 and 2.73.

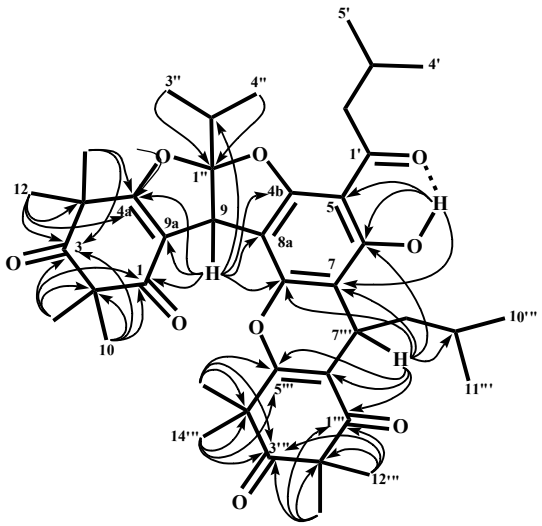

Selected HMBC correlations of **ART20**

(a)

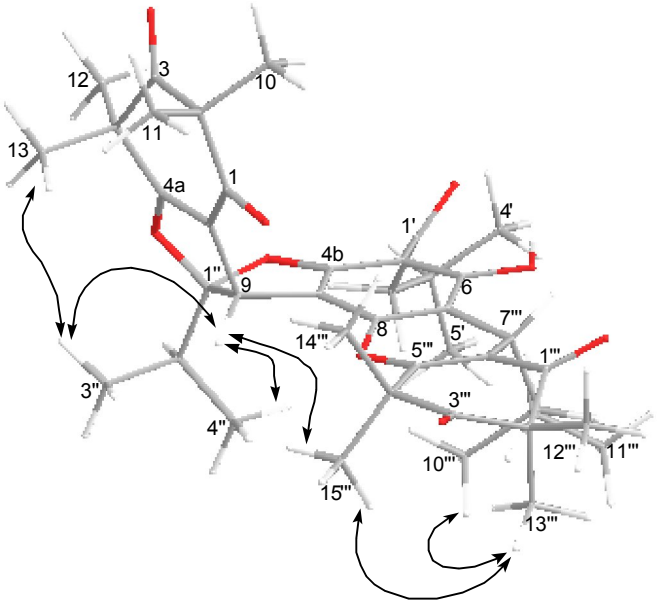

(b)

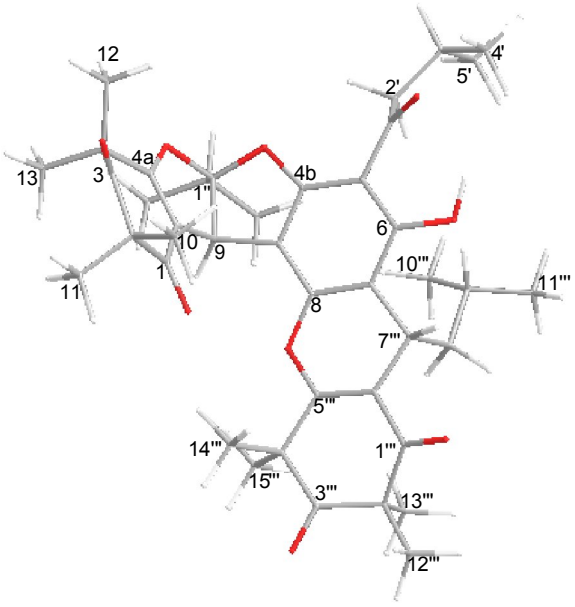

Energy-minimized (MM2) structure of **ART20** showing

(a) selected ROESY experiment and

interaction of C=O/Me-14''', Me-15'''

(b) position of CH_2 of the isovaleryl group

Table 20 The NMR spectral data of **ART20**

Position	**δ_C (Type)**	**δ_H (*mult.*; J_{Hz})**	**HMBC correlations**
1	192.11 (C=O)		
2	55.74 (C)		
3	211.99 (C=O)		
4	45.42 (C)		
4a	176.89 (C)		
4b	158.71 (C)		
5	103.92 (C)		
6	162.80 (C)		
7	107.90 (C)		
8	152.10 (C)		
8a	103.75 (C)		
9	46.32 (CH)	4.81 (*s*)	C-1, C-4a, C-4b, C-8, C-8a, C-9a, C-1", C-2"
9a	113.16 (C)		
10	24.10 (CH_3)	1.24 (*s*)	C-1, C-2, C-3, C-11
11	24.82 (CH_3)	1.36 (*s*)	C-1, C-2, C-3, C-10
12	23.98 (CH_3)	1.41 (*s*)	C-3, C-4, C-4a, C-13
13	24.22 (CH_3)	1.49 (*s*)	C-3, C-4, C-4a, C-12
1'	204.68 (C=O)		
2'	52.04 (CH_2)	3.12 (*dd*; 14.7, 6.6)	C-1', C-3', C-4', C-5'
		2.73 (*dd*; 14.7, 6.6)	
3'	25.95 (CH)	2.18 (*m*; 6.6)	C-1', C-2', C-4', C-5'
4'	22.52 (CH_3)	0.99 (*d*; 6.6)	C-2', C-3', C-5'
5'	22.86 (CH_3)	1.03 (*d*; 6.6)	C-2', C-3', C-4'

Table 20 (Continued)

Position	δ_C (Type)	δ_H (*mult.*; J_{Hz})	HMBC correlations
1"	128.86 (C)		
2"	34.86 (CH)	2.35 (*hept*; 6.9)	C-9, C-1", C-3", C-4"
3"	15.74 (CH_3)	1.11 (*d*; 6.9)	C-1", C-2", C-4"
4"	15.76 (CH_3)	1.08 (*d*; 6.9)	C-1", C-2", C-3"
1'"	198.32 (C=O)		
2'"	55.31 (C)		
3'"	212.57 (C=O)		
4'"	47.86 (C)		
5'"	165.93 (C)		
6'"	113.63 (C)		
7'"	25.44 (CH)	4.32 (*dd*; 5.7, 4.2)	C-6, C-7, C-8, C-1'", C-5'", C-6'", C-8'", C-9'"
8'"	45.27 (CH_2)	1.51 (*m*)	C-7, C-6'"
9'"	25.08 (CH)	1.40 (obscure)	
10'"	23.28 (CH_3)	0.85 (*d*; 6.3)	C-8'", C-9'", C-11'"
11'"	23.40 (CH_3)	0.69 (*d*; 6.3)	C-8'", C-9'", C-10'"
12'"	24.22 (CH_3)	1.39 (*s*)	C-1'", C-2'", C-3'"
13'"	24.33 (CH_3)	1.37 (*s*)	C-1'", C-2'", C-3'"
14'"	21.93 (CH_3)	1.42 (*s*)	C-3'", C-4'", C-5'", C-15'"
15'"	25.83 (CH_3)	1.81 (*s*)	C-3'", C-4'", C-5'", C-14'"
6-OH		13.64 (*s*)	C-5, C-6, C-7

ART38: Rhodomyrtosone I

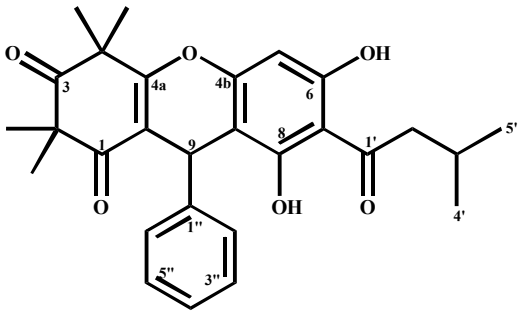

ART38 was obtained as a pale yellow gum. The UV spectrum exhibited absorption bands at 246, 261, and 304 nm. The IR spectrum showed absorption bands for hydroxyl, saturated carbonyl and conjugated carbonyl groups at 3304, 1718 and 1650 cm^{-1}, respectively. Its molecular formula of $C_{28}H_{30}O_6$ with 14 degrees of unsaturation was established from a molecular ion at *m/z* 462.2017 in the HR EI-MS spectrum. The ^{13}C NMR and DEPT spectra (**Table 21**) showed three carbonyl, ten quaternary, eight methine, one methylene and six methyl carbons. The ^{1}H NMR spectrum (**Table 21**) showed resonances of four methyl groups at δ_H 1.09 (H_3-11), 1.33 (H_3-10), 1.50 (H_3-12) and 1.59 (H_3-13). The signals of H_3-12 and H_3-13 showed HMBC correlations (**Table 21**) to the carbonyl carbon C-3 (δ_C 211.43) and vinylic oxycarbon C-4a (δ_C 164.58) whereas H_3-10 and H_3-11 showed correlations to the carbonyl carbons C-1 (δ_C 198.85) and C-3 (δ_C 211.43) indicating the presence of a β-triketone (Dachriyanus *et al*., 2002). The signals of the two hydroxyl groups (δ_H 13.47, *br s*, 8-OH and 8.22, *br s*, 6-OH), an aromatic proton (δ_H 6.17, *s*, H-5) and signals corresponding to an isovaleryl group (δ_H 2.92 and 2.87, *dd* each, H_2-2'; 2.21, *m*, H-3' and 0.93, *d*, H_3-4' and H_3-5') revealed a di-*C*-substituted phloroglucinol moiety with an isovaleryl group (Bloor, 1992). The spectrum further showed signals of a methine proton (δ_H 5.19, *s*, H-9) and four aromatic protons of mono-substituted benzene ring (δ_H 7.31, H-2"and H-6"; 7.24, H-3" and H-5" and 7.16, H-4"). The appearance of ion peak at *m/z* 385 in EI-MS which corresponded to the loss of a 77 *m/z* (C_6H_5) from a molecular ion confirmed the presence of the phenyl group.

The HMBC correlations of the methine proton H-9 to C-1 (δ_C 198.85), C-9a (δ_C 112.67) and C-4a (δ_C 164.58) of β-triketone, to C-8 (δ_C 162.01), C-8a (δ_C 105.13) and C-4b (δ_C 154.09) of phloroglucinol moiety, and to C-1" (δ_C 143.44), C-2"/C-6" (δ_C 128.52) of a benzene ring suggested that these three moieties were combined via C-9. The ^3J HMBC correlations of an aromatic H-5 to C-6 (δ_C 159.39) and C-4b (δ_C 154.09) confirmed the location of the aromatic proton at C-5, consequently the isovaleryl group was then placed at C-7. Therefore **ART38**, named rhodomyrtosone I, was assigned as 6,8-dihydroxy-2,2,4,4-tetramethyl-7-(2-methylbutanoyl)-9-phenyl-4,9-dihydro-1H-xanthene-1,3(2H)-dione.

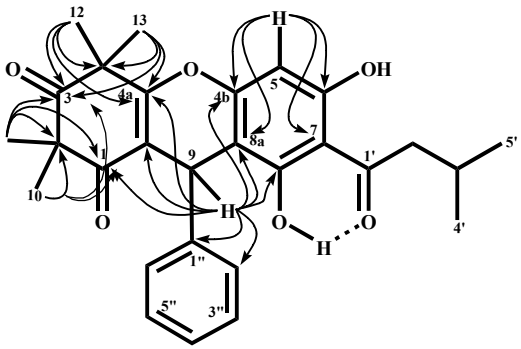

Selected HMBC correlations of **ART38**

Table 21 The NMR spectral data of **ART38**

Position	**δ_C (Type)**	**δ_H (*mult.*; J_{Hz})**	**HMBC correlations**
1	198.85 (C=O)		
2	56.24 (C)		
3	211.43 (C=O)		
4	46.95 (C)		
4a	164.58 (C)		
4b	154.09 (C)		
5	95.21 (CH)	6.17 (*s*)	C-4b, C-6, C-7, C-8a
6	159.39 (C)		
7	107.75 (C)		
8	162.01 (C)		
8a	105.13 (C)		
9	33.42 (CH)	5.19 (*s*)	C-1, C-4a, C-4b, C-8, C-8a, C-9a, C-1", C-2"
9a	112.67 (C)		
10	22.89 (CH_3)	1.33 (*s*)	C-1, C-2, C-3, C-11
11	24.55 (CH_3)	1.09 (*s*)	C-1, C-2, C-3, C-10
12	24.61 (CH_3)	1.50 (*s*)	C-3, C-4, C-4a, C-13
13	24.71 (CH_3)	1.59 (*s*)	C-3, C-4, C-4a, C-12
1'	205.92 (C=O)		
2'	53.10 (CH_2)	2.92 (*dd*; 16.0, 6.5)	C-1', C-3', C-4', C-5'
		2.87 (*dd*; 16.0, 6.5)	
3'	24.88 (CH)	2.21 (*m*; 6.5)	C-1', C-2', C-4', C-5'
4', 5'	22.73 (CH_3)	0.93 (*d*; 6.5)	C-2', C-3'

Table 21 (Continued)

Position	**δ_C (Type)**	**δ_H (*mult.*; J_{Hz})**	**HMBC correlations**
1"	143.44(C)		
2", 6"	128.52 (CH)	7.31 (*dd*; 7.5, 1.5)	C-9, C-3", C-4"
3", 5"	128.18 (CH)	7.24*	C-1", C-2"
4"	126.93 (CH)	7.16 (*tt*; 7.5, 1.5)	C-2", C-3"
6-OH		8.22 (*br*)	
8-OH		13.47 (*br*)	

*overlapped with solvent signal

3.1.2 Flavonoids

ART7: Combretol (3,3',4',5',7-Penta-*O*-methylmyricetin)

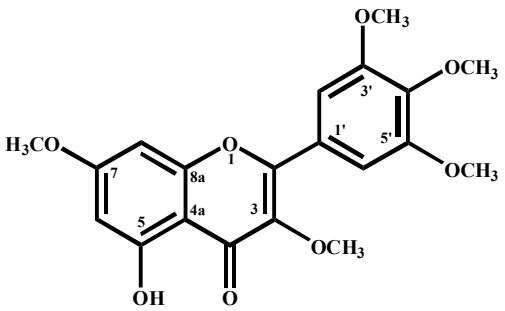

ART7 was obtained as a yellowish solid, mp 142-144 ^{O}C. The IR spectrum displayed absorption bands for a hydroxyl group at 3421 cm^{-1} and conjugated carbonyl group at 1663 cm^{-1}. The UV spectrum exhibited the maximum absorptions at 210, 265 and 342 nm. The ^{1}H NMR spectrum (**Table 22**) showed the resonances of a chelated hydroxyl group (δ_H 12.58, *s*, 5-OH), a vinylic methoxy group (δ_H 3.88, *s*, 3-OCH$_3$), and four methoxyl groups (δ_H 3.95, *s*, 3'-, 4'- and 5'-OCH$_3$; δ_H 3.89, *s*, 7-OCH$_3$). The presence of *meta* aromatic protons H-2' and H-6' was indicated from a broad singlet at δ_H 7.37 (2H) whereas those of H-8 and H-6 was suggested from *doublet* with J = 2.1 Hz at δ_H 6.45 and 6.37, respectively. The HMBC correlations (**Table 22**) of H-6, H-8 and 7-OCH$_3$ (δ_H 3.89) to C-7 (δ_C 165.58) and those of H-2' (H-6') and 3'-OCH$_3$ (5'-OCH$_3$) to C-3' (C-5') confirmed the assignment of the methoxyl groups. The assignment of **ART7** was also in agreement with that of 3,3',4',5',7-penta-*O*-methylmyricetin or combretol (**Table 55**) which was previously obtained from the seeds and wings of *Combretum quadrangular* (Mongkolsuk *et al*., 1966) and from the bark and twigs of *R. tomentosa* (Dachriyanus *et al*., 2004).

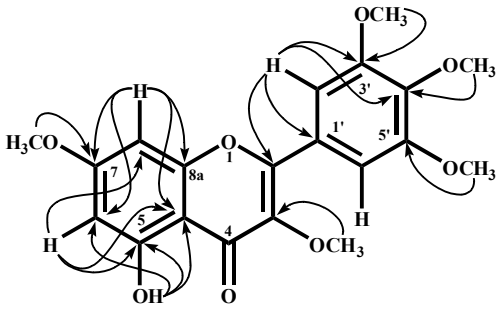

Selected HMBC correlations of **ART7**

Table 22 The NMR spectral data of **ART7**

Position	**δ_C (Type)**	**δ_H (*mult.*; J_{Hz})**	**HMBC correlations**
2	155.59 (C)		
3	139.41 (C)		
4	178.77 (C=O)		
4a	106.07 (C)		
5	162.06 (C)		
6	97.93 (CH)	6.37 (*d*; 2.1)	C-4a, C-5, C-8
7	165.58 (C)		
8	92.26 (CH)	6.45 (*d*; 2.1)	C-4a, C-6, C-7, C-8a
8a	156.72 (C)		
1'	125.46 (C)		
2', 6'	106.10 (CH)	7.37 (*s*)	C-2, C-1', C-3' (5'), C-4'
3', 5'	153.13 (C)		
4'	140.64 (C)		
3-OCH_3	60.34 (CH_3)	3.88 (*s*)	C-3
7-OCH_3	56.84 (CH_3)	3.89 (*s*)	C-7
3', 5'-OCH_3	56.35 (CH_3)	3.95 (*s*)	C-3', C-5'
4'-OCH_3	61.00 (CH_3)	3.95 (*s*)	C-4'
5-OH		12.58 (*s*)	C-4a, C-5, C-6

[a]300 MHz for ^{1}H and 75 MHz for ^{13}C

ART13: 3',5-Dihydroxy-3,4',5',7-tetramethoxyflavone
(3,4',5',7-Tetra-*O*-methylmyricetin)

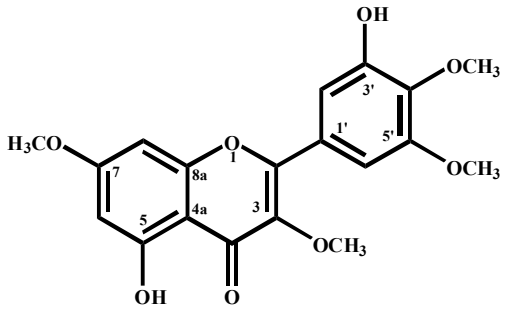

ART13 was obtained as a yellowish solid. The IR spectrum displayed absorption bands for a hydroxyl group at 3375 cm^{-1} and conjugated carbonyl group at 1659 cm^{-1} whereas the UV spectrum exhibited maximum absorptions at 248, 270, 305*sh* and 345 nm. The ^{1}H NMR spectrum (**Table 23**) which showed the resonances of two hydroxyl group (δ_H 12.58, 5-OH; 5.95, 3'-OH), four methoxyl groups (δ_H 4.01, 4'-OCH_3; 3.95, 5'-OCH_3; 3.89, 3- and 7-OCH_3), and *meta* aromatic protons (δ_H 7.36, H-2'; 7.34, H-6'; 6.46, H-8 and 6.37, H-6) indicated that it was an isomer of **ART16** and **ART17**. The NOE experiment by irradiation at the frequency of H-6 and H-8 affected the resonances of 7-OCH_3, whereas irradiation at the frequency of H-2' and H-6' enhanced the methoxyl signals at C-3 and C-5'. The assigned structure was in agreement with 3',5-dihydroxy-3,4',5',7-tetramethoxyflavone or 3,4',5',7-tetra-*O*-methylmyricetin (**Table 56**) (Martos *et al*., 1997; Datta *et al*., 2000). The HMBC correlations (**Table 23**) fully supported the assigned structure.

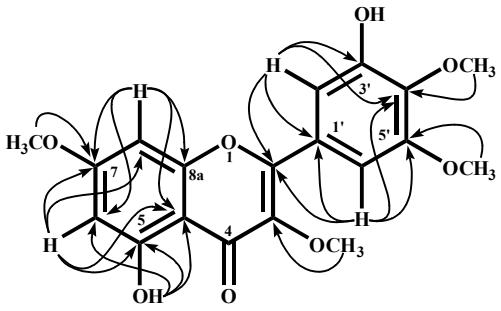

Selected HMBC correlations of **ART13**

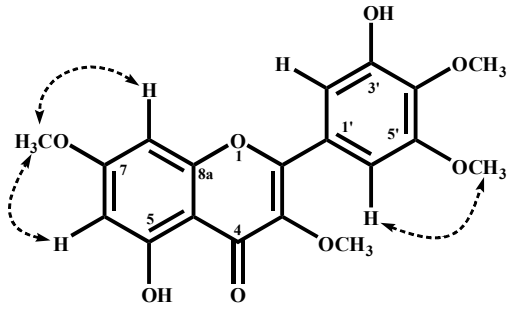

NOE correlations of **ART13**

Table 23 The NMR spectral data of **ART13**

Position	**δ_C (Type)**	**δ_H (*mult.*; J_{Hz})**	**HMBC correlations**
2	155.35 (C)		
3	139.52 (C)		
4	178.84 (C=O)		
4a	106.11 (C)		
5	162.02 (C)		
6	97.96 (CH)	6.37 (*d*; 2.4)	C-4a, C-5, C-7, C-8
7	165.60 (C)		
8	92.19 (CH)	6.46 (*d*; 2.4)	C-4a, C-6, C-7, C-8a
8a	156.76 (C)		
1'	125.96 (C)		
2'	108.59 (CH)	7.36 (*d*; 2.1)	C-2, C-1', C-3', C-4', C-6'
3'	149.21 (C)		
4'	137.81 (C)		
5'	152.06 (C)		
6'	105.06 (CH)	7.34 (*d*; 2.1)	C-2, C-1', C-2', C-4', C-5'
3-OCH_3	60.32 (CH_3)	3.89 (*s*)	C-3
7-OCH_3	55.82 (CH_3)	3.89 (*s*)	C-7
4'-OCH_3	61.10 (CH_3)	4.01 (*s*)	C-4'
5'-OCH_3	56.09 (CH_3)	3.95 (*s*)	C-5'
5-OH		12.58 (*s*)	C-4a, C-5, C-6
3'-OH		5.95 (*br s*)	

ART16: 3,3',5',7-Tetra-*O*-methylmyricetin

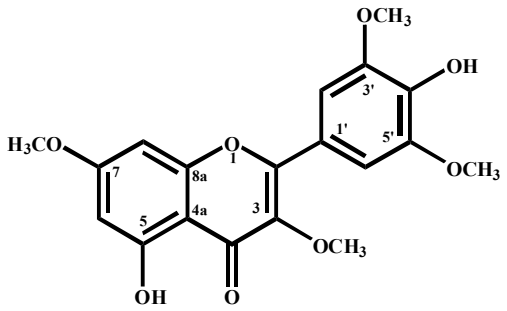

ART16 was obtained as a yellowish solid. The IR spectrum displayed absorption bands for a hydroxyl and conjugated carbonyl groups at 3375 and 1656 cm^{-1}, respectively. The UV spectrum exhibited absorption bands maxima at 252, 266, 302*sh* and 355 nm. It is an isomer of **ART13** and **ART17**. The ^{1}H NMR spectrum (**Table 24**) showed the resonances corresponding to a chelated hydroxyl group (δ_H 12.64, 5-OH), a hydroxyl group (δ_H 5.91, 4'-OH), four methoxyl groups (δ_H 3.99, 3'- and 5'-OCH_3; 3.89, 7-OCH_3 and 3.86, 3-OCH_3), meta aromatic protons (δ_H 7.42, H-2' and H-6'; 6.46, H-8 and 6.37, H-6). The NOE experiment by irradiation at the frequency of H-6 and H-8 affected the resonances of 7-OCH_3, whereas irradiation at the frequency of H-2' and H-6' enhanced the signals of the 3-, 3'- and 5'-OCH_3 groups. Therefore the structure of **ART16** was identified as 3,3',5',7-tetra-*O*-methylmyricetin (Kumari *et al*., 1985). The assigned structure was in good agreement with the HMBC correlations (**Table 24**).

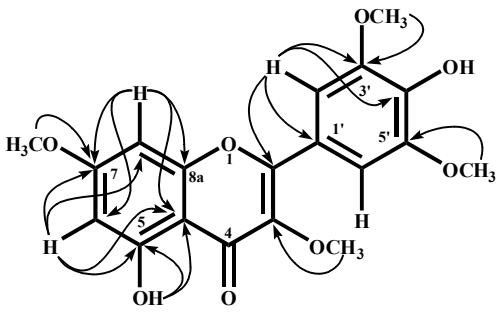

Selected HMBC correlations of **ART16**

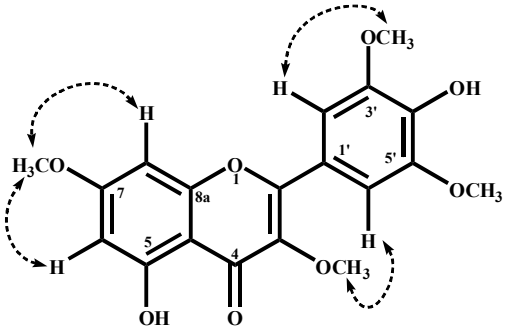

NOE correlations of **ART16**

Table 24 The NMR spectral data of **ART16**

Position	δ_C **(Type)**	δ_H (***mult.***; J_{Hz})	**HMBC correlations**
2	155.93 (C)		
3	139.11 (C)		
4	178.71 (C=O)		
4a	105.90 (C)		
5	162.12 (C)		
6	97.86 (CH)	6.37 (*d*; 1.5)	C-4a, C-5, C-7, C-8
7	165.53 (C)		
8	92.26 (CH)	6.46 (*d*; 1.5)	C-4, C-4a, C-6, C-7, C-8a
8a	156.70 (C)		
1'	121.44 (C)		
2', 6'	105.90 (CH)	7.42 (*s*)	C-2, C-1', C-3' (5'), C-4'
3', 5'	146.98 (C)		
4'	137.74 (C)		
3-OCH_3	60.18 (CH_3)	3.86 (*s*)	C-3
7-OCH_3	55.93 (CH_3)	3.89 (*s*)	C-7
3', 5'-OCH_3	56.56 (CH_3)	3.99 (*s*)	C-3', C-5'
5-OH		12.64 (*s*)	C-4a, C-5, C-6
4'-OH		5.91 (*s*)	

ART17: 3,3',4',5'-Tetra-*O*-methylmyricetin

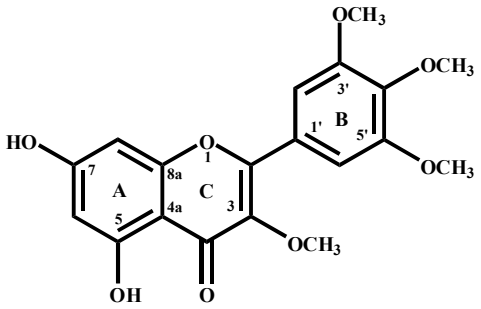

ART17 was obtained as a yellowish solid. The IR spectrum exhibited absorption bands for a hydroxyl group at 3255 cm^{-1} and a conjugated carbonyl group at 1656 cm^{-1}. The UV spectrum displayed maximum absorptions at 252, 268, 308*sh* and 348 nm. The ^{1}H NMR spectrum (**Table 25**) showed the resonances of chelated hydroxyl group at δ_H 12.62 (*s*, 5-OH), a hydroxyl group at δ_H 8.67 (*br s*, 7-OH), *meta* aromatic protons at δ_H 6.47 (*d*, H-8) and 6.35 (*d*, H-6), and at δ_H 7.36 (*s*, H-2' and H-6'). This compound was also an isomer of **ART13** and **ART16**. The NOE experiments by irradiation at the frequency of H-2' (H-6') affected the resonances of 3'-OCH_3 (5'-OCH_3), whereas irradiation at the frequency of H-6 and H-8 did not affect any methoxyl groups indicating that the methoxyl groups were substituted at ring C not in ring A. **ART17** was therefore identified as 3,3',4',5'-tetra-*O*-methylmyricetin (Lenherr *et al*., 1986). The assigned structure was completely confirmed by the HMBC correlations (**Table 25**).

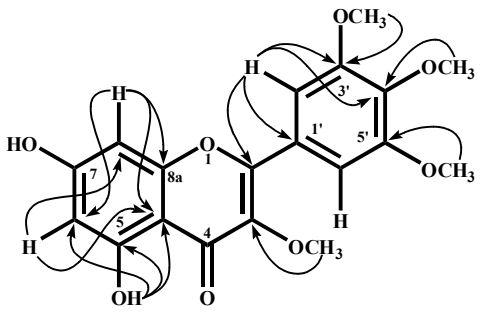

Selected HMBC correlations of **ART17**

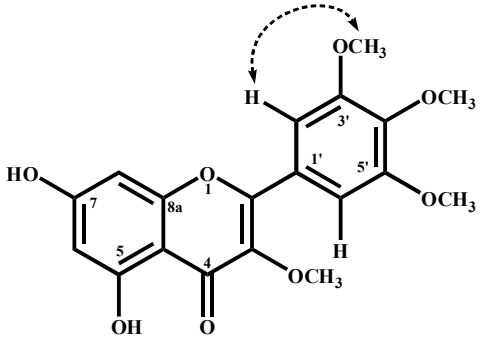

NOE correlations of **ART17**

Table 25 The NMR spectral data of **ART17**

Position	**δ_C (Type)**	**δ_H (*mult.*; J_{Hz})**	**HMBC correlations**
2	155.34 (C)		
3	139.12 (C)		
4	178.70 (C=O)		
4a	106.23 (C)		
5	162.23 (C)		
6	99.19 (CH)	6.35 (*d*; 1.2)	C-4a, C-5, C-8
7	163.35 (C)		
8	93.95 (CH)	6.47 (*d*; 1.2)	C-4a, C-6, C-7, C-8a
8a	156.91 (C)		
1'	125.54 (C)		
2', 6'	106.23 (CH)	7.36 (*s*)	C-2, C-1', C-3' (5'), C-4'
3', 5'	153.09 (C)		
4'	140.23 (C)		
3-OCH_3	60.30 (CH_3)	3.87 (*s*)	C-3
3', 5'-OCH_3	56.33 (CH_3)	3.94 (*s*)	C-3', C-5'
4'-OCH_3	60.94 (CH_3)	3.94 (*s*)	C-4'
5-OH		12.62 (*s*)	C-4a, C-5, C-6
7-OH		8.67 (*br s*)	

3.1.3 Ellagic acid derivatives

ART10: 3,3',4-Tri-*O*-methylellagic acid

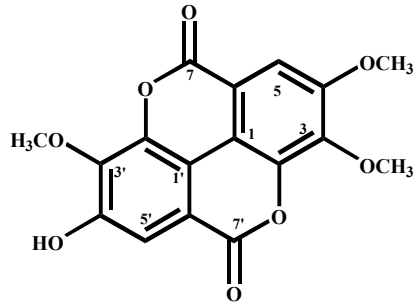

ART10 was obtained as a yellow solid, mp 298-300 ^{O}C. The UV spectrum revealed maximum absorption bands at 247 and 372 nm. The IR spectrum displayed absorption bands for a hydroxyl group (3410 cm^{-1}) and conjugated carbonyl group (1656 cm^{-1}), suggesting the presence of lactone functionallity. It was supported from the lactone carbonyls at δ_C 159.06 and 158.74 in the ^{13}C NMR spectrum (**Table 26**). The ^{13}C NMR and DEPT techniques showed 17 carbon signals including two carbonyl carbons (δ_C 159.06 and 158.74), ten quaternary carbons (δ_C 154.04, 152.77, 141.81, 141.38, 141.03, 140.74, 114.03, 112.70, 112.01 and 111.68), two methine carbons (δ_C 112.77 and 107.72) and three methyl carbons (δ_C 61.76, 61.54 and 56.77). The ^{1}H NMR spectrum (**Table 26**) showed the resonances of two isolated aromatic protons at δ_H 7.68 (*s*, H-5') and 7.64 (*s*, H-5), and three methoxyl groups at δ_H 4.19 (3'-OCH_3), 4.17 (3-OCH_3) and 4.04 (4-OCH_3). According to the low field chemical shift of H-5 and H-5', both aromatic protons were then located at the *peri* position to the carbonyl groups. The ^{3}J HMBC correlations (**Table 26**) of H-5 and 3-OCH_3 (δ_H 4.17) to oxygen-bearing carbon C-3 (δ_C 141.81) and the cross peak of aromatic proton H-5 to the 4-OCH_3 (δ_H 4.04) in the NOESY experiment confirmed the presence of the methoxyl groups at C-3 and C-4. In addition the ^{3}J HMBC correlations of H-5' and 3'-OCH_3 (δ_H 4.19) to an oxygen-bearing carbon C-3' (δ_C 140.74) suggested the

presence of the methoxyl groups at C-3' rather than C-4'. The assigned structure of **ART10** was identical to a known 3,3',4-tri-*O*-methylellagic acid (**Table 57**) (Khac *et al*., 1990).

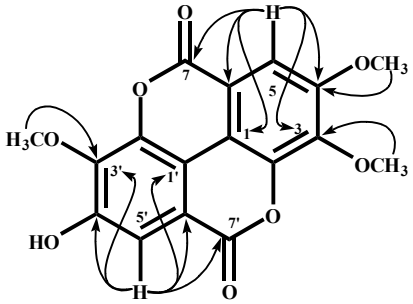

Selected HMBC correlations of **ART10**

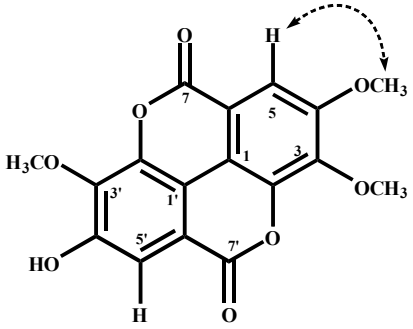

NOESY correlations of **ART10**

Table 26 The NMR spectral data of **ART10**

Position	**δ_C (Type)**	**δ_H (*mult.*)**	**HMBC correlations**
1	112.01 (C)		
2	141.38 (C)		
3	141.81 (C)		
4	154.04 (C)		
5	107.72 (CH)	7.64 (*s*)	C-1, C-3, C-4, C-6, C-7
6	114.03 (C)		
7	159.06 (C=O)		
1'	111.68 (C)		
2'	141.03 (C)		
3'	140.74 (C)		
4'	152.77 (C)		
5'	112.77 (CH)	7.68 (*s*)	C-1', C-3', C-4', C-6', C-7'
6'	112.70 (C)		
7'	158.74 (C=O)		
3-OCH_3	61.76 (CH_3)	4.17 (*s*)	C-3
4-OCH_3	56.77 (CH_3)	4.04 (*s*)	C-4
3'-OCH_3	61.54 (CH_3)	4.19 (*s*)	C-3'

ART28: 4-*O*-[*β*-D-Glucopyranosyl-tetraacetate]-3,3',4'-tri-*O*-methyl-ellagic acid

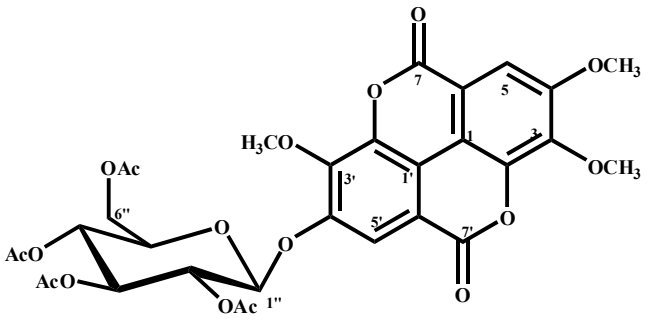

ART28 was obtained as a white powder. The IR spectrum exhibited absorption bands for a carbonyl stretching at 1735 and 1720 cm^{-1}. Its ^{1}H NMR spectrum (**Table 27**) revealed that **ART28** was tri-*O*-methylellagic acid glycoside. The presence of tri-*O*-methylellagic acid moiety was evidenced from the signals of two aromatic protons at δ_H 7.92 (H-5) and 7.71 (H-5'), and three methoxyl groups at δ_H 4.22 (3'-OCH_3), 4.14 (3-OCH_3) and 4.05 (4'-OCH_3), as shown for **ART10**. While the presence of a glucopyranoside tetra-acetate moiety was indicated from the signals of an anomeric proton at δ_H 5.17 (H-1"), methylene protons at δ_H 4.26 (H_2-6"), four methine protons at δ_H 5.41 (H-2") 5.34 (H-3"), 5.16 (H-4") and 4.01 (H-5"), and four acetyl groups at δ_H 2.19 (6"-OAc), 2.11 (4"-OAc), 2.08 (3"-OAc) and 2.06 (2"-OAc). The large coupling constant of the anomeric proton H-1" (J = 7.5 Hz) indicated an axial orientation. Accordingly, the sugar moiety was a *β*-D-glucopyranosyl tetra-acetate. The ^{3}J HMBC correlations (**Table 27**) of the anomeric proton H-1" to oxygen-bearing carbon C-4' (δ_C 155.18) suggested the connection of the sugar moiety at C-4'. This suggestion was confirmed by the NOESY experiment that the anomeric proton H-1" correlated to H-5' (δ_H 7.71) and 3'-OCH_3 (δ_H 4.22). The ^{13}C NMR and DEPT techniques (**Table 27**) showed 29 carbon signals for 31 carbon atoms: six carbonyl carbons (δ_C 171.14, 170.34, 169.69, 169.51, 158.82 and 158.61), ten quaternary carbons (δ_C 155.18, 151.72, 143.42, 141.65, 141.38, 141.03, 115.17,

113.23, 112.95 and 112.76), seven methine carbons (δ_C 113.97, 108.26, 100.33, 72.96, 72.60, 71.11 and 68.50), one methylene carbon (δ_C 62.28) and seven methyl carbons [δ_C 62.48, 62.20, 57.10, 20.91, and 20.83 (3xC)]. The structure of **ART28** was determined as a known 4-*O*-[*β*-D-glucopyranosyl-tetraacetate]-3,3',4'-tri-*O*-methylellagic acid (**Table 58**) (Khac *et al*., 1990).

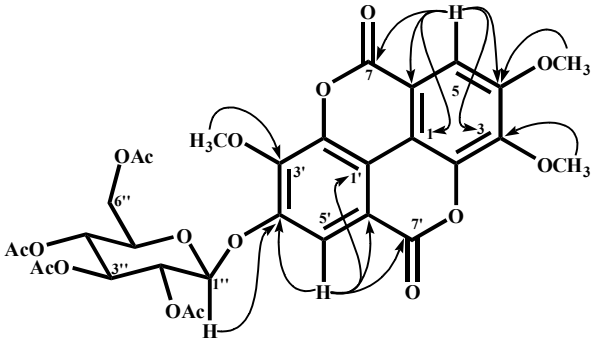

Selected HMBC correlations of **ART28**

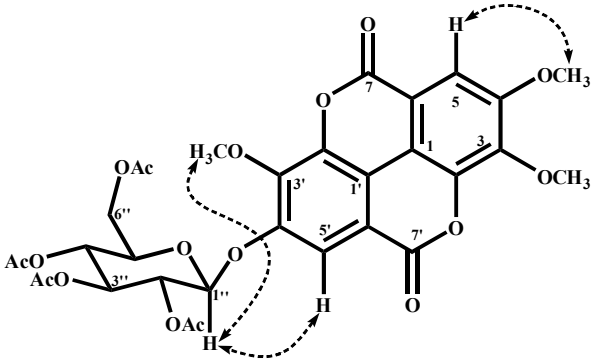

NOESY correlations of **ART28**

Table 27 The NMR spectral data of **ART28**

Position	**δ_C (Type)**	**δ_H (*mult.*; J_{Hz})**	**HMBC correlations**
1	115.17 (C)		
2	141.38 (C)		
3	143.42 (C)		
4	151.72 (C)		
5	113.97 (CH)	7.92 (*s*)	C-1, C-3, C-4, C-6, C-7, C-1'
6	112.76 (C)		
7	158.61 (C=O)		
1'	113.23 (C)		
2'	141.03 (C)		
3'	141.65 (C)		
4'	155.18 (C)		
5'	108.26 (CH)	7.71 (*s*)	C-1, C-1', C-3', C-4', C-6', C-7'
6'	112.95 (C)		
7'	158.82 (C=O)		
3-OCH_3	62.48 (CH_3)	4.14 (*s*)	C-3
3'-OCH_3	62.20 (CH_3)	4.22 (*s*)	C-3'
4'-OCH_3	57.10 (CH_3)	4.05 (*s*)	C-4'
1"	100.33 (CH)	5.17 (*d*, 7.5)	C-4, C-2", C-3", C-5"
2"	71.11 (CH)	5.41 (*dd*, 9.3, 7.5)	
3"	72.60 (CH)	5.34 (*t*, 9.3)	
4"	68.50 (CH)	5.16 (*t*, 9.3)	
5"	72.96 (CH)	4.01 (*m*)	
6"	62.28 (CH_2)	4.26 (*m*)	

Table 27 (Continued)

Position	**δ_C (Type)**	**δ_H (*mult.*; J_{Hz})**	**HMBC correlations**
2"-OAc	170.34 (C=O)		
	20.83 (CH_3)	2.06 (*s*)	2"-C=O
3"-OAc	169.69 (C=O)		
	20.83 (CH_3)	2.08 (*s*)	3"-C=O
4"-OAc	169.51 (C=O)		
	20.83 (CH_3)	2.11 (*s*)	4"-C=O
6"-OAc	171.14 (C=O)		
	20.91 (CH_3)	2.19 (*s*)	6"-C=O

ART41: 3-*O*-Methylellagic acid 4-*O*-α-rhamnopyranoside

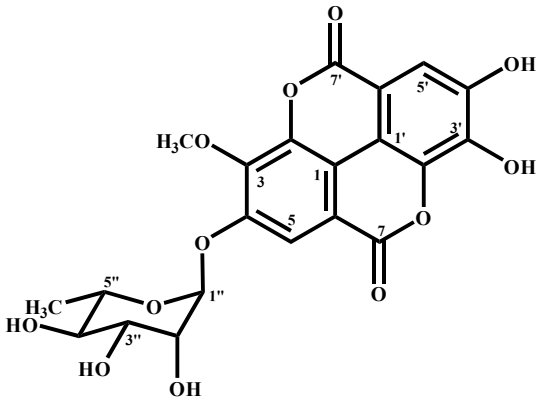

ART41 was a white powder. The IR spectrum showed a stretching of hydroxyl and carbonyl groups at 3349 and 1687 cm^{-1}, respectively. The UV spectrum exhibited absorption bands maxima at 207, 253, 274*sh*, 314 and 350 nm. The ^{1}H NMR spectral data (**Table 28**) showed the characteristic signals of ellagic acid derivative, with the resonances of two singlet aromatic protons at δ_H 7.85 (H-5') and 7.62 (H-5) and a methoxyl group at δ_H 4.14 (3-OCH_3). The presence of rhamnopyranosyl moiety was suggested from the resonances of an anomeric proton at δ_H 5.55, four methine protons at δ_H 4.14, 4.01, 3.61 and 3.47, and a methyl group at δ_H 1.23 as doublet with the coupling constant of 5.4 Hz. The NOESY experiment exhibited the correlations of the anomeric proton H-1" to both of H-5 and 3-OCH_3 indicating that the rhamnose moiety was linked at C-4. The ^{13}C NMR and DEPT techniques (**Table 28**) showed 21 carbon signals for 22 carbon atoms including two carbonyl carbons [δ_C 159.02 (2xC)], ten quaternary carbons (δ_C 152.95, 146.79, 141.95, 141.84, 140.57, 136.38, 114.64, 113.22, 112.14 and 107.45), seven methine carbons (δ_C 112.21, 112.14, 100.18, 72.41, 70.79, 70.20 and 70.04), one methylene carbon (δ_C 62.28) and two methyl carbons (δ_C 61.26 and 17.93). The structure of **ART41** could be assigned for three possible known ellagic acid derivatives, 4-*O*-methylellagic acid 3'-α-rhamnoside, 3-*O*-methylellagic acid 3'-*O*-α-rhamnopyranoside and 3-*O*-methylellagic acid 4-*O*-α-rhamnopyranoside. Further elucidation was made by comparison to the spectral data of those three related ellagic

acid derivatives (**Tables 59** and **60**) (Elkhateeb *et al*., 2005; Kim *et al*., 2001; El-Toumy and Rauwald, 2003). It was found to be closed to that of 3-*O*-methylellagic acid 4-*O*-α-rhamnopyranoside (El-Toumy and Rauwald, 2003). The HMBC experiment (**Table 28**) and the NOESY experiment completely supported the assigned structure.

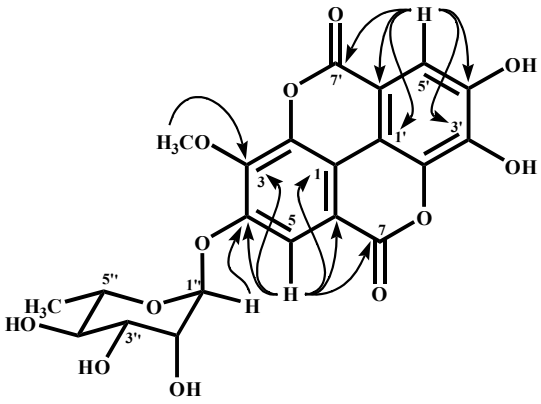

Selected HMBC correlations of **ART41**

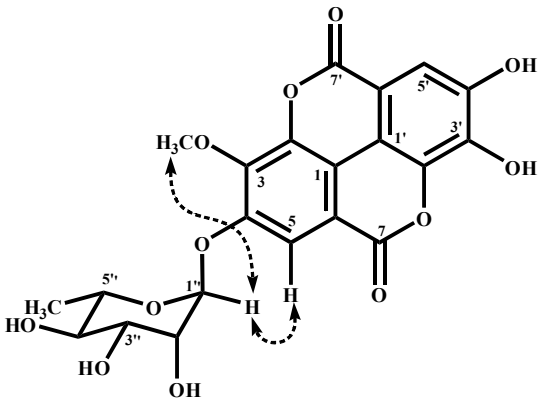

NOESY correlations of **ART41**

Table 28 The NMR spectral data of **ART41**

Position	**δ_C (Type)**	**δ_H (*mult.*; J_{Hz})**	**HMBC correlations**
1	114.64 (C)		
2	141.95 (C)		
3	140.57 (C)		
4	152.95 (C)		
5	112.21 (CH)	7.62 (*s*)	C-1, C-3, C-4, C-6, C-7
6	113.22 (C)		
7	159.02 (C=O)		
1'	112.14 (C)		
2'	136.38 (C)		
3'	141.84 (C)		
4'	146.79 (C)		
5'	112.14 (CH)	7.85 (*s*)	C-1', C-3', C-4', C-6', C-7'
6'	107.45 (C)		
7'	159.02 (C=O)		
1"	100.18 (CH)	5.55 (*br s*)	C-4, C-2", C-3", C-5"
2"	70.20 (CH)	4.14*	C-1", C-4"
3"	70.79 (CH)	4.01 (*d*, 7.8)	C-1", C-2", C-5"
4"	72.41 (CH)	3.47*	C-2", C-3", C-5", C-6"
5"	70.04 (CH)	3.67 (*m*)	C-1", C-3", C-4", C-6"
6"	17.93 (CH_3)	1.23 (*d*, 5.4)	C-4", C-6"
OCH_3	61.26 (CH_3)	4.14 (*s*)	C-3'

*overlapped signals

3.1.4 Flavellagic acid derivatives

ART31: 3,4,3',4'-Tetra-*O*-methylflavellagic acid

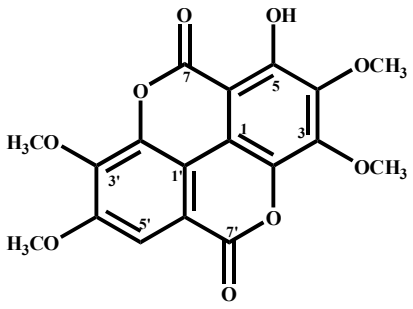

ART31 was obtained as a light yellow amorphous powder. Its molecular formula of $C_{18}H_{14}O_9$ was established from the HR EI-MS spectrum. The UV spectrum showed the maximum absorption bands at 248, 376, and 410*sh* nm. The IR spectrum displayed absorption bands of a hydroxyl group at 3336 cm^{-1} and conjugated carbonyl group at 1719 cm^{-1}. The carbonyl carbon signals at δ_C 163.14 (C-7) and 159.05 (C-7') in the ^{13}C NMR spectrum (**Table 29**) suggested the existence of lactone functionalities. The ^{1}H NMR spectrum (**Table 29**) exhibited the resonances of a phenolic hydroxyl proton at δ_H 10.36, an aromatic proton at δ_H 7.72, and four methoxyl groups at δ_H 4.30, 4.21, 4.05 and 4.02. The aromatic proton was located at C-5', a *peri*-position to carbonyl group due to its low field chemical shift value (δ_H 7.72) together with the HMBC correlations (**Table 29**) of it to C-1' (δ_C 113.47), C-3' (δ_C 141.94), C-4' (δ_C 154.91), C-6' (δ_C 108.21) and C-7' (δ_C 159.05). The correlations of the methoxyl groups at δ_H 4.21 to C-3' and at δ_H 4.05 to C-4' together with the enhancement of the methoxyl group at δ_H 4.05 by irradiation at the resonance of H-5' in the NOE experiment indicated that the methoxyl groups at δ_H 4.21 and 4.05 were then placed at the C-3' and C-4', respectively. The evidences that the hydroxyl proton (δ_H 10.36) showed the HMBC correlations to C-4 (δ_C 141.38), C-5 (δ_C 153.14) and C-6 (δ_C 96.88) as well as the methoxyl group which resonated at δ_H 4.02 showed correlation to C-4 (δ_C 141.38) suggesting that the hydroxyl group was at a *peri*

position to C=O (C-5), and the methoxy group was at C-4. The remaining methoxy group (δ_H 4.30) was consequently attributed to the position C-3. The ^{13}C NMR resonances were in good / positive agreement with the assigned structure, 3,4,3',4'-tetra-*O*-methylflavellagic acid. It was a new flavellagic acid derivative.

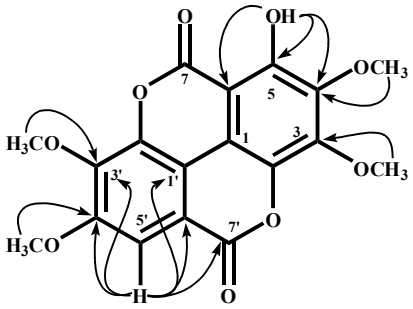

Selected HMBC correlations of **ART31**

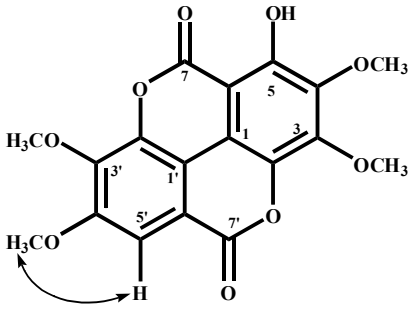

NOE correlations of **ART31**

Table 29 The NMR spectral data of **ART31**

Position	δ_C **(Type)**	δ_H (***mult.***)	**HMBC correlations**
1	112.42 (C)		
2	140.67 (C)		
3	148.40 (C)		
4	141.38 (C)		
5	153.14 (C)		
6	96.88 (C)		
7	163.14 (C=O)		
1'	113.47 (C)		
2'	140.67 (C)		
3'	141.94 (C)		
4'	154.91 (C)		
5'	108.21 (CH)	7.72 (*s*)	C-1', C-3', C-4', C-6', C-7'
6'	113.54 (C)		
7'	159.05 (C=O)		
5-OH		10.36 (*s*)	C-4, C-5, C-6
3-OCH_3	62.12 (CH_3)	4.30 (*s*)	C-3
4-OCH_3	61.63 (CH_3)	4.02 (*s*)	C-4
3'-OCH_3	62.02 (CH_3)	4.21 (*s*)	C-3'
4'-OCH_3	56.87 (CH_3)	4.05 (*s*)	C-4'

[a]recorded in $CDCl_3$; 300 MHz for ^1H and 125 MHz for ^{13}C

ART25: 3',4'-Dioxymethylene-3,4-di-*O*-methylflavellagic acid

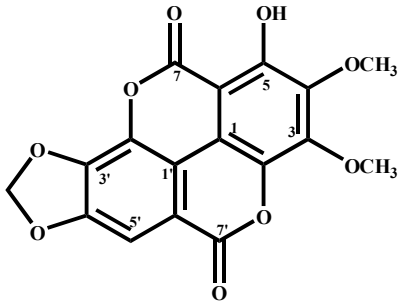

ART25 was obtained as a pale yellow amorphous powder. The IR spectrum exhibited absorptions for a hydroxyl group at 3302 cm^{-1} and conjugated carbonyl group at 1656 cm^{-1} whereas the UV spectrum displayed maximum absorptions at 248, 307, 320, 365 and 380 nm. Its ^{1}H NMR spectrum (**Table 30**) showed the resonances of a chelated hydroxyl proton (δ_H 10.39, 5-OH), an aromatic proton (δ_H 7.64, H-5'), two methoxyl groups (δ_H 4.29, 3-OCH_3 and 4.02, 4-OCH_3) and a dioxymethylene protons (δ_H 6.30). The ^{13}C NMR and HMBC data (**Table 30**) revealed that **ART25** was an ellagic acid which comprised of 5-OH, 3-OCH_3, 4-OCH_3 and H-5' as for **ART31**. Furthermore the HMBC experiment demonstrated that the aromatic proton H-5' (δ_H 7.64) and the dioxymethylene protons (δ_H 6.30) both exhibited the correlations to the carbons which resonated at δ_C 151.38 (C-4') and 138.60 (C-3') indicating that the dioxymethylene group connected with C-3' and C-4'. The ^{13}C NMR resonances were in good agreement with the assigned structure. **ART25** was a known flavellagic acid derivative, 3',4'-dioxymethylene-3,4-di-*O*-methylflavellagic acid.

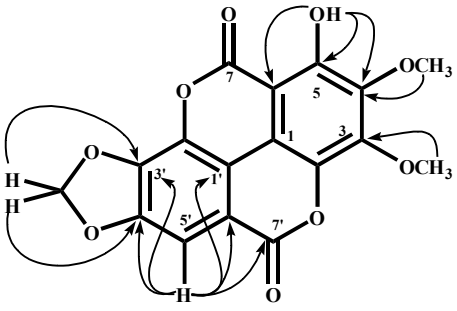

Selected HMBC correlations of **ART25**

Table 30 The NMR spectral data of **ART25**

Position	**δ_C (Type)**	**δ_H (*mult.*)**	**HMBC correlations**
1	113.79 (C)		
2	*		
3	148.50 (C)		
4	141.75 (C)		
5	153.35 (C)		
6	96.65 (C)		
7	162.30 (C=O)		
1'	116.35 (C)		
2'	*		
3'	138.60 (C)		
4'	151.38 (C)		
5'	104.01 (CH)	7.64 (*s*)	C-1', C-3', C-4', C-6', C-7'
6'	116.35 (C)		
7'	158.80 (C=O)		
5-OH		10.39 (*s*)	C-4, C-5, C-6
3-OCH_3	62.08 (CH_3)	4.29 (*s*)	C-3
4-OCH_3	61.60 (CH_3)	4.03 (*s*)	C-4
-OCH_2O-	104.01 (CH_2)	6.30 (*s*)	C-3', C-4'

*not observed

3.1.5 Terpenoids

ART12: (6*R*,7*E*,9*S*)-9-Hydroxy-4,7-megastigmadien-3-one

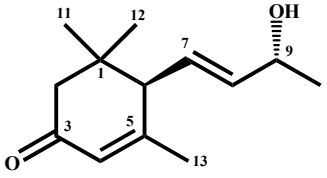

ART12 was a yellowish gum. The IR spectrum exhibited absorptions for a hydroxyl and conjugated carbonyl groups at 3406 and 1656 cm^{-1}, respectively, whereas the UV spectrum displayed maximum absorption at 246 nm. The ^{1}H NMR spectrum (**Table 31**) showed resonances of geminal methyl groups H_3-11 and H_3-12 at δ_H 1.04 (*s*) and 0.98 (*s*), non-equivalent methylene protons H_2-2 at δ_H 2.34 and 2.08 (each *d*, *J* = 16.5 Hz), an olefinic proton H-4 at δ_H 5.90 (*s*) and a vinylic methyl protons H_3-13 at δ_H 1.90 (*d*, *J* = 1.2 Hz,). The ^{3}J HMBC correlations (**Table 31**) of H_3-11 and H_3-12 to C-2 (δ_C 47.41) and C-6 (δ_C 55.37), and of H_3-13 to C-4 (δ_C 125.86) and C-6 (δ_C 55.37) suggested that the geminal methyl groups H_3-11 and H_3-12 were connected to C-1 (δ_C 36.10) whereas a vinylic methyl group H_3-13 was connected to C-5 (δ_C 161.78). The presence of hydroxybutenyl side chain was deduced from the ^{1}H-^{1}H COSY experiment. The result indicated the resonances at δ_H 5.68 (*dd*, *J* = 15.3 and 6.3 Hz) and 5.55 (*dd*, *J* = 15.3 and 8.7 Hz), 4.35 (*quin*, *J* = 6.3 Hz) and 1.29 (*d*, *J* = 6.3 Hz,), corresponded to *trans* olefinic protons H-8 and H-7, methine proton H-9 and methyl group H_3-10, respectively. The ^{3}J HMBC correlation of H-7 to C-1 and C-5 indicated that the side chain was connected to C-2.

By comparison of the ^{1}H and ^{13}C NMR spectroscopic data with the related compounds in the literatures (**Table 61**) (D' Abrosca *et al*., 2004; Cutillo *et al*., 2005), compound **ART12** was identical to a C-13 nor-terpene, (6*R*,7*E*,9*S*)-9-hydroxy-4,7-megastigmadien-3-one (Cutillo *et al*., 2005).

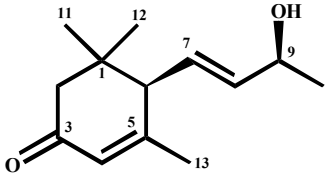

(6*R*,7*E*,9*R*)-9-hydroxy-4,7-megastigmadien-3-one

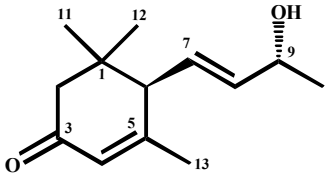

(6*R*,7*E*,9*S*)-9-hydroxy-4,7-megastigmadien-3-one

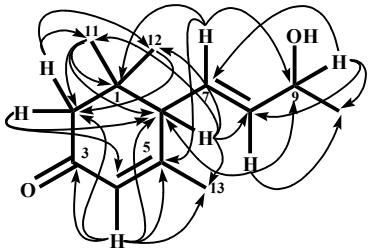

Selected HMBC correlations of **ART12**

Table 31 The NMR spectral data of **ART12**

Position	**δ_C (Type)**	**δ_H (*mult.*; J_{Hz})**	**HMBC correlations**
1	36.10 (C)		
2	47.41 (CH_2)	2.34 (*d*; 16.5)	C-4, C-6, C-11, C-12
		2.08 (*d*; 16.5)	
3	199.14 (C=O)		
4	125.86 (CH)	5.90 (*s*)	C-2, C-3, C-5, C-6, C-13
5	161.78 (C)		
6	55.37 (CH)	2.53 (*d*; 8.7)	C-1, C-2, C-4, C-5, C-7,
			C-8, C-11, C-12, C-13
7	126.59 (CH)	5.55 (*dd*; 15.3, 8.7)	C-1, C-6, C-8, C-9
8	138.43 (CH)	5.68 (*dd*; 15.3, 6.3)	C-6, C-7, C-9, C-10
9	68.32 (CH)	4.35 (*quin*; 6.3)	C-7, C-8, C-10
10	23.61 (CH_3)	1.29 (*d*; 6.3)	C-8, C-9
11	27.85 (CH_3)	1.04 (*s*)	C-2, C-6, C-12
12	27.11 (CH_3)	0.98 (*s*)	C-2, C-6, C-11
13	23.45 (CH_3)	1.90 (*d*; 1.2)	C-4, C-5, C-6

ART14: Loliolide

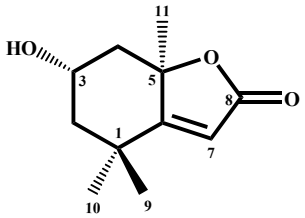

ART14 was obtained as a yellow gum. The IR spectrum showed absorptions at 3449 cm^{-1} for a hydroxyl group and 1718 cm^{-1} for a carbonyl group. The UV spectrum exhibited maximum absorptions at 247 and 255*sh* nm. The ^1H NMR spectrum (**Table 32**) displayed the signals of three methyl groups at δ_H 1.78, 1.47 and 1.28, and an olefinic proton at δ_H 5.70, which were assigned for H_3-11, H_3-9, H_3-10 and H-7, respectively. The spectrum further showed a multiplet of an oxygenated methine proton H-3 (δ_H 4.34), a doublet of doublet and doublet of triplet of non-equivalent methylene protons H_2-2 (δ_H 1.98 and 1.53) and a doublet of doublet and doublet of triplet of non-equivalent methylene protons H_2-4 (δ_H 2.46 and 1.79) indicating the presence of $-CH_2CH(OH)CH_2-$ unit as evidenced from the ^1H-^1H COSY data (**Table 32**). The HMBC correlations (**Table 32**) of H_3-9 and H_3-10 to C-1, C-2 and C-6 and of H_3-11 to C-4, C-5 and C-6 established the six membered-ring subunit. The HMBC correlations of H-7 to C-1, C-5, C-6 and C-8 supported that the olefinic proton was at C-7. Consequently, the possible structure could be loliolide or isololiolide, two known diastereomers. In comparison, the spectral data of **ART14** was close to those of loliolide rather than isololiolide (Kimura and Maki, 2002; Hattab *et al*., 2008). **ART14** was therefore elucidated to be loliolide (**Table 62**) (Kimura and Maki, 2002; Hattab *et al*., 2008).

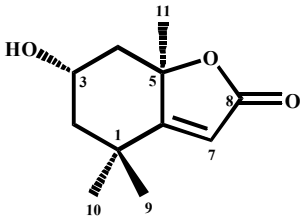

loliolide

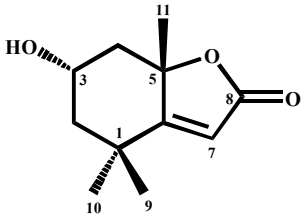

isololiolide

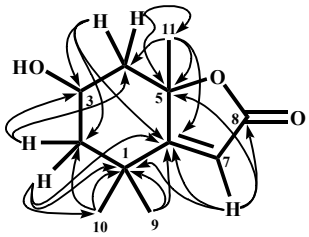

Selected HMBC correlations of **ART14**

Table 32 The NMR spectral data of **ART14**

Position	**δ_C (Type)**	**δ_H (*mult.*; J_{Hz})**	**COSY**	**HMBC correlations**
1	36.00 (C)			
2	47.35 (CH_2)	α: 1.98 (*td*; 15.0, 2.5) β: 1.53 (*dd*; 15.0, 3.5)	H-2β, H-3	C-1, C-3, C-4, C-6
3	66.87 (CH)	4.34 (*quin*; 3.0)	H-2α, H-2β, H-4α, H-4β	C-1, C-3, C-4, C-6, C-10
4	45.66 (CH_2)	2.46 (*td*; 14.0, 2.5) 1.79 (*dd*; 14.0, 4.0)	H-4β, H-3 H-4α, H-3	C-2, C-3, C-5, C-6 C-3, C-11
5	86.55 (C)			
6	182.45 (C)			
7	112.97 (CH)	5.70 (*s*)		C-1, C-5, C-6, C-8
8	172.01 (C=O)			
9	26.05 (CH_3)	1.47 (*s*)		C-1, C-2, C-6, C-10
10	30.64 (CH_3)	1.28 (*s*)		C-1, C-2, C-6, C-9
11	27.02 (CH_3)	1.78 (*s*)		C-4, C-5, C-6

ART22: 2α-Hydroxy-3β-*E*-coumaroyloxy-olean-12-en-28-oic acid
(3β-*O*-*E*-coumaroylmaslinic acid)

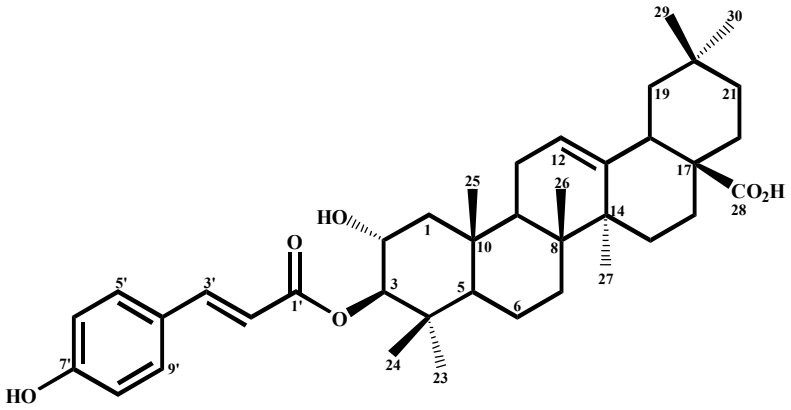

ART22 was obtained as a white solid. The IR spectrum showed absorption bands for a hydroxyl group at 3359 cm^{-1} and for a carbonyl group at 1696 cm^{-1}. The UV spectrum displayed maximum absorptions at 211, 229 and 315 nm. The ^{1}H NMR spectral data (**Table 33**) exhibited the presence of a *p*-coumaroyl moiety from the signals at δ_H 7.65 (*d*, *J* = 15.9 Hz, H-3'), 7.41 (*d*, *J* = 8.1 Hz, H-5' and H-8'), 6.82 (*d*, *J* = 8.1 Hz, H-6' and H-9') and 6.33 (*d*, *J* = 15.9 Hz, H-2'). The large coupling constant of 15.9 Hz indicated *E*-configuration of H-2' and H-3'. The spectrum further showed the signals due to one olefinic proton (δ_H 5.29, H-12), three methine protons (δ_H 4.62, H-3; 3.86, H-2 and 2.84, H-18) and seven quaternary methyl groups (δ_H 1.15, H_3-27; 1.02, H_3-25; 0.94, H_3-23 and H_3-30; 0.93, H_3-24; 0.92, H_3-29 and 0.78, H_3-26) as well as the presence of the carboxyl carbon at δ_C 180.66 in the ^{13}C NMR spectrum (**Table 33**) which were typical resonances of maslinic acid derivative. The doublet signal of an oxymethine proton H-3 (δ_H 4.62) with the coupling constant of 9.9 Hz indicated the α-axial orientation. Consequently, the oxymethine proton H-2 (*dt*, *J* = 9.9 and 5.1 Hz) was located at the β-axial position. The *p*-coumaroyl moiety at the C-3 β-equatorial position was implied from the down

field shift of the oxygenated methine proton H-3 (δ_H 4.62). This conclusion was supported by the ^3J HMBC correlation (**Table 33**) of the H-3 to the carbonyl ester C-1' (δ_C 168.85). The ^{13}C NMR spectrum revealed the resonance signals of two carbonyl carbons (δ_C 180.66 and 168.85), nine quaternary carbons (δ_C 159.18, 143.88, 126.17, 46.35, 41.75, 39.53, 39.30, 38.14 and 30.64), twelve methine carbons [δ_C 145.42, 130.01 (2xC), 122.05, 115.83 (2xC), 114.65, 84.82, 67.36, 55.11, 47.53 and 41.17], nine methylene carbons [δ_C 47.45, 45.90, 33.85, 32.49 (2xC), 27.62, 23.43, 22.98 and 18.30] and seven methyl carbons (δ_C 33.01, 28.52, 25.83, 23.51, 17.71, 16.84 and 16.42). The spectral data and comparison to the previous report (**Table 63**) (Yagi *et al*., 1978) indicated that **ART22** was a known 2α-hydroxy-3β-*E*-coumaroyloxyolean-12-en-28-oic acid or 3β-*O*-*E*-coumaroylmaslinic acid. The assigned structure was fully confirmed by the HMBC correlations.

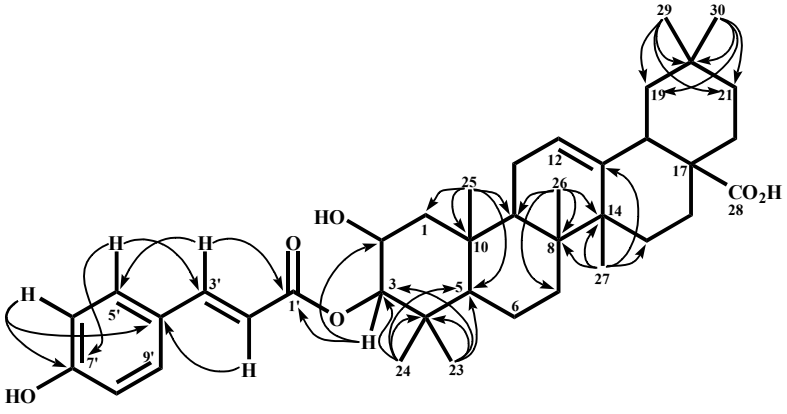

Selected HMBC correlations of **ART22**

Table 33 The NMR spectral data of **ART22**

Position	δ_C (Type)	δ_H (*mult.*; J_{Hz})	HMBC correlations
1	47.45 (CH_2)	2.08 (*m*), 1.05 (*m*)	
2	67.36 (CH)	3.86 (*dt*; 9.9, 5.1)	
3	84.82 (CH)	4.62 (*d*; 9.9)	C-2, C-1'
4	39.53 (C)		
5	55.11 (CH)	0.89 (*m*)	
6	18.30 (CH_2)	2.17 (*m*), 1.58 (*m*)	
7	32.49 (CH_2)	1.58 (*m*)	
8	39.30 (C)		
9	47.53 (CH)	1.60 (*m*)	
10	38.14 (C)		
11	22.98 (CH_2)	1.98 (*m*)	
12	122.05 (CH)	5.29 (*br s*)	
13	143.88 (C)		
14	41.75 (C)		
15	27.62 (CH_2)	1.26 (*m*), 1.08 (*m*)	
16	23.43 (CH_2)	1.90 (*m*), 1.65 (*m*)	
17	46.35 (C)		
18	41.17 (CH)	2.84 (*br d*; 12.6)	
19	45.90 (CH_2)	1.64 (*m*)	
20	30.64 (C)		
21	33.85 (CH_2)	1.80 (*m*), 1.58 (*m*)	
22	32.49 (CH_2)	2.18 (*m*)	
23	28.52 (CH_3)	0.94 (*s*)	C-3, C-4, C-5, C-24
24	17.71 (CH_3)	0.93 (*s*)	C-3, C-4, C-5, C-23
25	16.42 (CH_3)	1.02 (*s*)	C-1, C-5, C-9, C-10
26	16.84 (CH_3)	0.78 (*s*)	C-7, C-8, C-9, C-14
27	25.83 (CH_3)	1.15 (*s*)	C-8, C-13, C-14, C-15

Table 33 (Continued)

Position	**δ_C (Type)**	**δ_H (*mult.*; J_{Hz})**	**HMBC correlations**
28	180.66 (C=O)		
29	33.01 (CH_3)	0.92 (*s*)	C-19, C-20, C-21, C-30
30	23.51 (CH_3)	0.94 (*s*)	C-19, C-20, C-21, C-29
1'	168.85 (C=O)		
2'	114.65 (CH)	6.33 (*d*; 15.9)	C-4'
3'	145.42 (CH)	7.65 (*d*; 15.9)	C-1', C-5'
4'	126.17 (C)		
5', 9'	130.01 (CH)	7.41 (*d*; 8.1)	C-3', C-7'
6', 8'	115.83 (CH)	6.82 (*d*; 8.1)	C-4', C-7'
7'	159.18 (C)		

ART23: 2α-Hydroxy-3β-*Z*-coumaroyloxy-olean-12-en-28-oic acid
(3β-*O*-*Z*-coumaroylmaslinic acid)

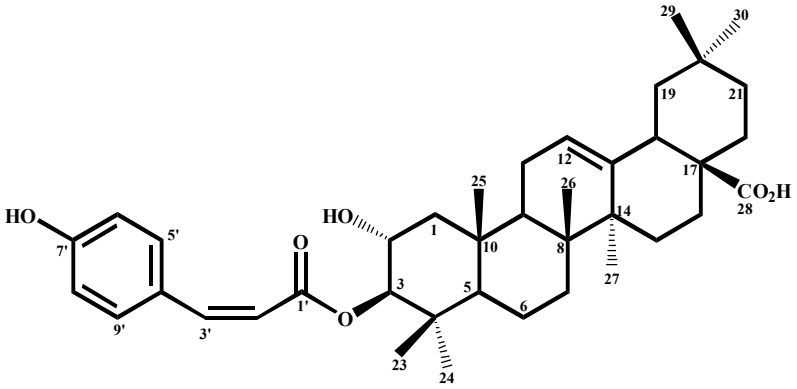

ART23 was obtained as a white solid. The IR spectrum exhibited absorptions at 3340 and 1697 cm^{-1} for hydroxyl and carbonyl groups, respectively. The UV spectrum displayed absorption bands maxima at 205, 227 and 312 nm. The ^{1}H NMR spectrum (**Table 34**) showed the signals corresponding to a *p*-coumaroyl moiety (δ_H 6.90, *d*, *J* = 12.0 Hz, H-3'; 7.65, *d*, *J* = 8.0 Hz, H-5' and H-8'; 6.80, *d*, *J* = 8.0 Hz, H-6' and H-9'; 5.91, *d*, *J* = 12.0 Hz, H-2'), an olefinic proton (δ_H 5.32, H-12). Three methine protons (δ_H 4.58, H-3; 3.67, H-2 and 2.84, H-18) and seven quaternary methyl groups (δ_H 1.15, H_3-27; 0.94, H_3-23 and H_3-30; 0.93, H_3-24; 0.92, H_3-29; 0.81, H_3-25; and 0.78, H_3-26) which belonged to a maslinic acid derivative were observed. These signals were similar to those of **ART22**. The slightly difference of the high-field chemical shift and the small coupling constant of olefinic protons H-2'/H-3' (δ_H 6.90 and 5.91, *J* = 12.0 Hz) indicated the *Z*-conformation of the double bond. The ^{13}C NMR spectrum (**Table 34**) revealed the presence of forty carbons including two carbonyl carbons (δ_C 180.94 and 167.65), nine quaternary carbons (δ_C 156.87, 142.66, 129.12, 46.35, 40.72, 40.15, 38.39, 38.14 and 30.64), twelve methine carbons (δ_C 143.23, 131.49, 121.46, 114.96, 114.00, 83.85, 66.71, 54.22,

47.53 and 40.15), nine methylene carbons (δ_C 47.45, 45.90, 33.85, 32.49, 26.67, 23.43, 22.98 and 18.30) and seven methyl carbons (δ_C 33.01, 29.74, 24.96, 23.51, 17.36, 16.84 and 16.42). The spectral data and comparison with the previous report (**Table 64**) (Yagi *et al*., 1978) indicated that compound **ART23** was a known 2α-hydroxy-3β-*Z*-coumaroyloxy-olean-12-en-28-oic acid or 3β-*O*-*Z*-coumaroyl-maslinic acid. The assigned structure was fully confirmed by the HMBC correlations (**Table 34**).

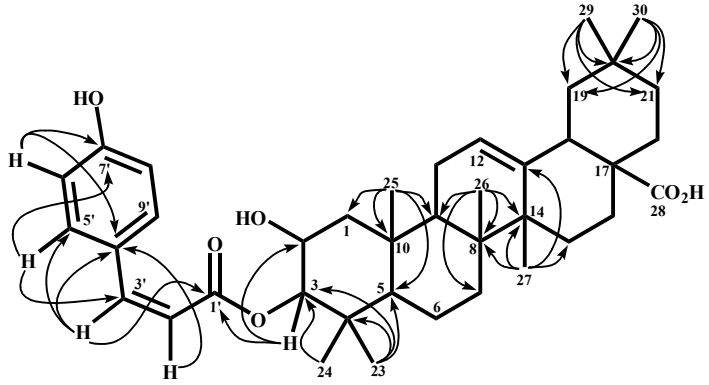

Selected HMBC correlations of **ART23**

Table 34 The NMR spectral data of **ART23**

Position	**δ_C (Type)**	**δ_H (*mult.*; J_{Hz})**	**HMBC correlations**
1	46.65 (CH_2)	2.06 (*m*), 1.01 (*m*)	
2	66.71 (CH)	3.85 (*m*)	
3	83.85 (CH)	4.58 (*d*; 9.6)	C-2, C-4, C-23, C-24, C-1'
4	40.15 (C)		
5	54.22 (CH)	0.90 (*m*)	
6	16.84 (CH_2)	2.17 (*m*), 1.56 (*m*)	
7	31.52 (CH_2)	1.58 (*m*)	
8	38.39 (C)		
9	46.65 (CH)	1.60 (*m*)	
10	37.24 (C)		
11	22.52 (CH_2)	1.94 (*m*)	
12	121.46 (CH)	5.32 (*br s*)	
13	142.66 (C)		
14	40.72 (C)		
15	26.67 (CH_2)	1.26 (*m*), 1.08 (*m*)	
16	27.63 (CH_2)	1.91 (*m*), 1.60 (*m*)	
17	45.51 (C)		
18	40.15 (CH)	2.83 (*br d*; 12.0)	
19	44.85 (CH_2)	1.64 (*m*)	
20	30.98 (C)		
21	32.11 (CH_2)	1.83 (*m*), 1.55 (*m*)	
22	31.52 (CH_2)	2.18 (*m*)	
23	17.36 (CH_3)	0.97 (*s*)	C-3, C-4,C-5
24	29.74 (CH_3)	0.94 (*s*)	C-3, C-4,C-5
25	16.64 (CH_3)	0.81 (*s*)	C-1, C-5, C-9, C-10
26	15.63 (CH_3)	0.78 (*s*)	C-7, C-8, C-9, C-14
27	24.96 (CH_3)	1.15 (*s*)	C-8, C-13, C-14, C-15

[a]recorded in $CDCl_3$+CD_3OD (1 drop)

Table 34 (Continued)

Position	δ_C (Type)	δ_H (*mult.*; J_{Hz})	HMBC correlations
28	180.94 (C=O)		
29	32.84 (CH_3)	0.91 (*s*)	C-19, C-20, C-21
30	22.62 (CH_3)	0.93 (*s*)	C-19, C-20, C-21
1'	167.65 (C=O)		
2'	114.96 (CH)	5.91 (*d*; 12.0)	C-1', C-3', C-4'
3'	143.23 (CH)	6.90 (*d*; 12.0)	C-1', C-2', C-4', C-5' (C-9')
4'	129.12 (C)		
5', 9'	131.49 (CH)	7.65 (*d*; 8.0)	C-3', C-4', C-6' (C-8'), C-7'
6', 8'	114.00 (CH)	6.80 (*d*; 8.0)	C-4', C-5' (C-9'), C-7', C-4'
7'	156.87 (C)		

[a]recorded in $CDCl_3$+CD_3OD (1 drop)

ART32: 3β-*O*-*E*-Coumaroyloleanolic acid

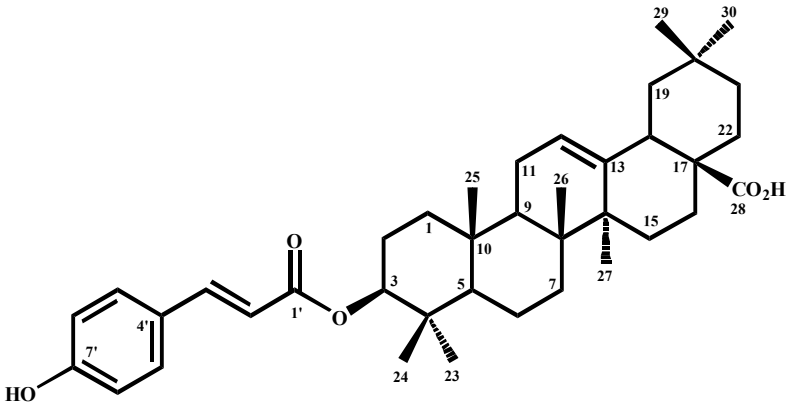

ART32 was obtained as a white solid, mp 240-242 ^{O}C. The IR spectrum exhibited absorptions at 3345 cm^{-1} for a hydroxyl group and at 1700 cm^{-1} for a carbonyl group. The UV spectrum displayed absorption bands maxima at 230 and 315 nm. The ^{1}H NMR spectral data (**Table 35**) showed the presence of a *p*-coumaroyl moiety from the resonances at δ_H 7.60 (*d*, *J* = 15.9 Hz, H-3'), 7.42 (*d*, *J* = 8.7 Hz, H-5' and H-8'), 6.81 (*d*, *J* = 8.7 Hz, H-6' and H-9') and 6.28 (*d*, *J* = 15.9 Hz, H-2'). The *E* geometry of *p*-coumaroyl moiety was assigned from the large coupling constant of olefinic protons H-2' and H-3' (*J* = 15.9 Hz). The spectrum further displayed the signals due to one olefinic proton (δ_H 5.28, H-12), one methine proton (δ_H 2.85, H-18) and seven quaternary methyl groups (δ_H 1.16, H_3-27; 0.97, H_3-25; 0.94, H_3-24 and H_3-30; 0.91, H_3-23 and H_3-29 and 0.80, H_3-26) which were typical resonances of oleanolic acid. The oxygenated methine proton at δ_H 4.61 was assigned to be the H-3 position. The splitting pattern and coupling constant value of H-3 (*dd*, *J* = 10.7 and 5.3 Hz) indicated that this proton was located at the α-axial orientation. The location of *p*-coumaroyl moiety at the C-3 β-equatorial position of oleanolic acid implied from the down field shift of the oxygenated methine proton H-3. This conclusion was supported by the ^{3}J HMBC correlation (**Table 35**) of the H-3 with the carbonyl ester

C-1' (δ_C 171.79) of the *p*-coumaroyl moiety. The ^{13}C NMR spectrum (**Table 35**) revealed the signals of ester and carboxylic carbonyl functionalities at δ_C 171.79 and 184.94, respectively. The remaining resonances were existence of nine quaternary carbons [δ_C 163.13, 147.76, 130.01, 50.31, 45.62, 43.16 (2xC), 40.83 and 34.53), eleven methine carbons (δ_C 148.63, 133.81, 126.12, 119.69, 119.03, 84.94, 59.24, 51.44 and 45.12), ten methylene carbons (δ_C 49.84, 41.82, 37.74, 36.54, 36.44, 31.54, 27.51, 27.37, 26.91 and 22.10) and seven methyl carbons [δ_C 36.89, 31.93, 29.70, 27.37, 20.69 (2xC) and 19.20]. The structure of **ART32** was identified as 3*β*-*O*-*E*-coumaroyloleanolic acid (**Table 65**) (Takahashi *et al*., 1999). The HMBC experiment fully confirmed the assigned structure. Therefore **ART32** was the 3*β*-*O*-*E*-coumaroylate of **ART39** or oleanolic acid.

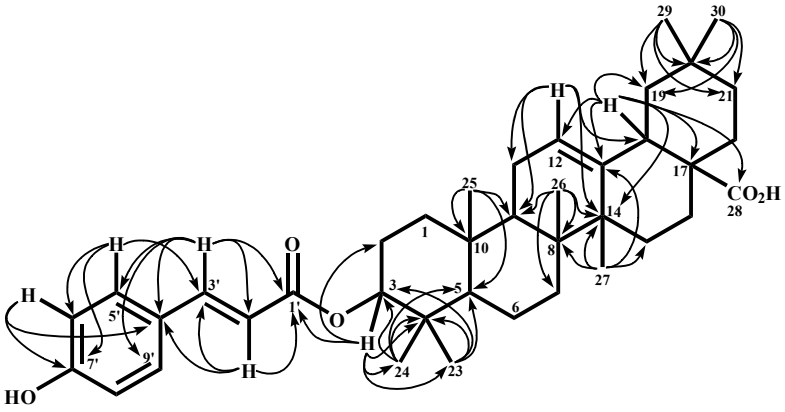

Selected HMBC correlations of **ART32**

Table 35 The NMR spectral data of **ART32**

Position	δ_C (Type)	δ_H (*mult.*; J_{Hz})	HMBC correlations
1	37.74 (CH_2)	1.34 (*m*), 1.19 (*m*)	
2	27.51 (CH_2)	1.69 (*m*)	
3	84.94 (CH)	4.61 (*dd*; 10.7, 5.3)	C-2, C-4, C-23, C-24, C-1'
4	43.16 (C)		
5	59.24 (CH)	0.89 (*m*)	
6	22.10 (CH_2)	1.85 (*m*), 1.40 (*m*)	
7	36.44 (CH_2)	1.77 (*m*)	
8	43.16 (C)		
9	51.44 (CH)	1.60 (*m*)	
10	40.83 (C)		
11	26.91 (CH_2)	1.96 (*m*), 1.60 (*m*)	
12	126.12 (CH)	5.28 (*t*; 3.1)	C-9, C-11, C-14, C-18
13	147.76 (C)		
14	45.62 (C)		
15	31.54 (CH_2)	1.73 (*m*)	
16	27.37 (CH_2)	1.89 (*m*), 1.69 (*m*)	
17	50.31 (C)		
18	45.12 (CH)	2.85 (*dd*; 13.8, 3.9)	C-12, C-13, C-14, C-17, C-19, C-28
19	49.84 (CH_2)	1.65 (*m*), 1.15 (*m*)	
20	34.53 (C)		
21	41.82 (CH_2)	1.68 (*m*)	
22	36.54 (CH_2)	1.55 (*m*), 1.31 (*m*)	
23	31.93 (CH_3)	0.91 (*s*)	C-3, C-5, C-24
24	20.69 (CH_3)	0.94 (*s*)	C-3, C-5, C-23
25	19.20 (CH_3)	0.97 (*s*)	C-5, C-9, C-10

[a]recorded in $CDCl_3$+CD_3OD (1 drop)

Table 35 (Continued)

Position	δ_C (Type)	δ_H (*mult.*; J_{Hz})	HMBC correlations
26	20.69 (CH_3)	0.80 (*s*)	C-7, C-8, C-9, C-14
27	29.70 (CH_3)	1.16 (*s*)	C-8, C-13, C-14, C-15
28	184.94 (C=O)		
29	36.89 (CH_3)	0.91 (*s*)	C-19, C-20, C-21, C-30
30	27.37 (CH_3)	0.94 (*s*)	C-19, C-20, C-21, C-29
1'	171.79 (C=O)		
2'	119.03 (CH)	6.28 (*d*; 15.9)	C-1', C-3', C-4'
3'	148.63 (CH)	7.60 (*d*; 15.9)	C-1', C-2', C-4', C-5', C-9'
4'	130.01 (C)		
5', 8'	133.81 (CH)	7.42 (*d*; 8.7)	C-3', C-6', C-7', C-8'
6', 9'	119.69 (CH)	6.81 (*d*; 8.7)	C-4', C-7'
7'	163.13 (C)		

[a]recorded in $CDCl_3$+CD_3OD (1 drop)

ART34: 2α,3β,23-Trihydroxyolean-12-en-28-oic acid
(Arjunolic acid)

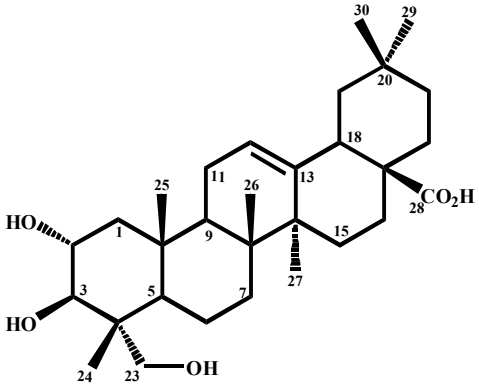

ART34 was obtained as a white solid. The IR spectrum showed the presence of a hydroxyl and carboxyl group at 3422 and 1765 cm^{-1}, respectively. The ^{13}C NMR spectrum (**Table 36**) confirmed the presence of a carbonyl carbon by the resonance at δ_C 181.08. The ^{1}H NMR spectrum (**Table 36**) revealed the resonances of six tertiary methyl groups (δ_H 1.24, 1.17, 1.00, 0.95, 0.91 and 0.82), an olefinic proton (δ_H 5.20, H-12), four carbinolic protons (δ_H 3.64, H-2; 3.46 and 3.26, H_2-23 and 3.27, H-3) and a methine proton (δ_H 2.76, H-18). These data indicated that **ART34** was also a maslinic acid derivative. The large coupling constant (J = 9.3 Hz) between H-2 and H-3 indicated the axial-axial coupling, so both hydroxyl groups were equatorially oriented. The presence of a hydroxymethyl group attached to C-4 was evidenced from the HMBC correlations (**Table 36**) of H_2-23 to C-3, C-4 and C-24. These data corresponded to two possible isomers, hyptatic acid-A or arjunolic acid. The difference between both structures was the orientation of the hydroxymethyl group. In comparison with the literatures of both compounds (Lee *et al*., 2008; Tripathi *et al*., 1992; Shao *et al*., 1995), especially the carbon resonances for C-3, C-23 and C-24 (arjunolic acid: 78.1, 66.3, 14.2; hyptatic acid-A: 84.5, 27.4, 64.7, respectively) (**Table 66**) and the optical rotation, the spectroscopic data and physical

properties of **ART34** was closer to that of arjunolic acid rather than hyptatic acid-A. Therefore **ART34** was identified to be 2α,3β,23-trihydroxyolean-12-en-28-oic acid or arjunolic acid (Tripathi *et al*., 1992; Shao *et al*., 1995).

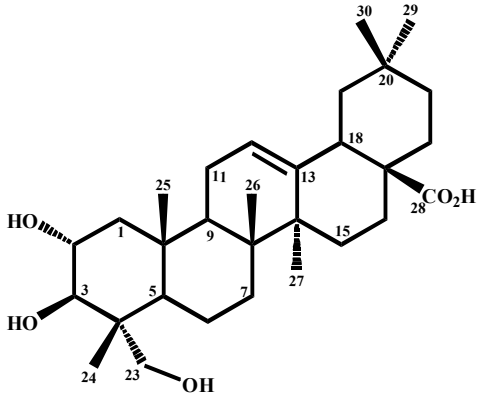

arjunolic acid

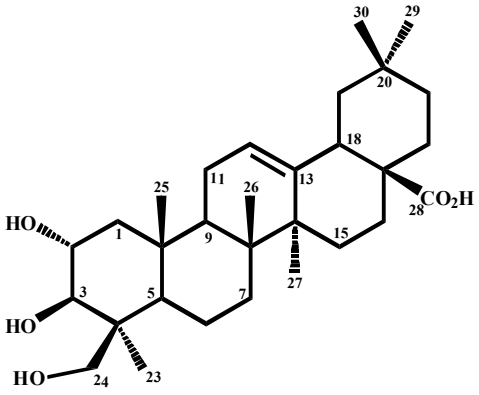

hyptatic acid-A

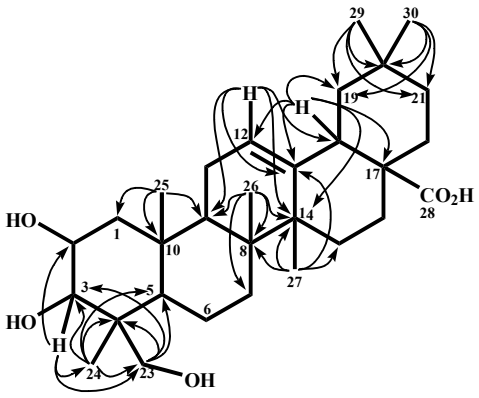

Selected HMBC correlations of **ART34**

Table 36 The NMR spectral data of **ART34**

Position	**δ_C (Type)**	**δ_H (*mult.*; J_{Hz})**	**HMBC correlations**
1	45.88 (CH_2)	1.88 (*dd*; 12.6, 3.9), 0.81 (*m*)	
2	68.35 (CH)	3.64 (obscure)	
3	78.86 (CH)	3.27 (*d*; 9.3)	C-2, C-4, C-23, C-24
4	42.55 (C)		
5	48.07 (CH)	1.55 (*m*)	
6	18.09 (CH_2)	1.31 (*m*)	
7	32.13 (CH_2)	1.47 (*m*), 1.19 (*m*)	
8	39.18 (C)		
9	47.44 (CH)	1.03 (*m*)	
10	37.94 (C)		
11	23.67 (CH_2)	1.86 (*m*)	
12	122.01 (CH)	5.20 (*br s*)	C-9, C-11, C-13, C-14, C-18
13	143.86 (C)		
14	41.70 (C)		
15	27.55 (CH_2)	1.64 (*m*)	
16	22.91 (CH_2)	1.53 (*m*)	
17	46.31 (C)		
18	41.11 (CH)	2.76 (*dd*; 13.8, 4.5)	C-12, C-13, C-14, C-17, C-19
19	45.88 (CH_2)	1.56 (*m*), 1.06 (*m*)	
20	30.58 (C)		
21	33.78 (CH_2)	1.27 (*m*), 1.11 (*m*)	
22	32.49 (CH_2)	1.68 (*m*)	

[a]recorded in $CDCl_3$+CD_3OD (1 drop)

Table 36 (Continued)

Position	**δ_C (Type)**	**δ_H (*mult.*; J_{Hz})**	**HMBC correlations**
23	67.98 (CH_2)	a: 3.46 (*d*; 10.8)	C-3, C-4, C-24
		b: 3.26 (*d*; 10.8)	
24	12.75 (CH_3)	0.70 (*s*)	C-3, C-4, C-5, C-23
25	16.81 (CH_3)	0.93 (*s*)	C-2, C-9, C-10
26	16.89 (CH_3)	0.70 (*s*)	C-7, C-8, C-9, C-14
27	25.77 (CH_3)	1.06 (*s*)	C-8, C-13, C-14, C-15
28	181.08 (C=O)		
29	32.95 (CH_3)	0.85 (*s*)	C-19, C-20, C-21, C-30
30	23.45 (CH_3)	0.83 (*s*)	C-19, C-20, C-21, C-29

[a]recorded in $CDCl_3$+CD_3OD (1 drop)

ART39: Oleanolic acid

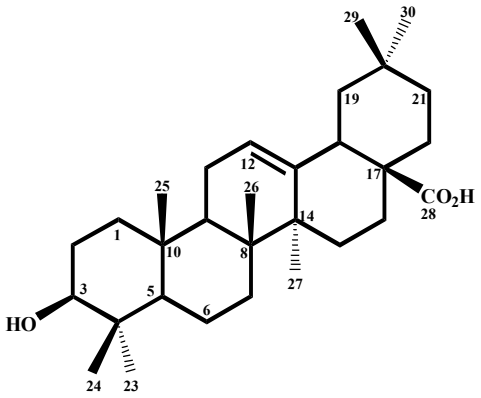

ART39 was obtained as a white solid. The IR spectrum exhibited absorptions for a hydroxyl group at 3406 cm^{-1} and for a carboxyl group at 1685 cm^{-1}.The ^{1}H NMR spectral data (**Table 37**) showed the presence of an olefinic proton (δ_H 5.27, H-12), an oxygenated methine proton (δ_H 3.21, H-3), a methine proton (δ_H 2.82, H-18) and seven quaternary methyl groups (δ_H 1.13, H_3-27; 0.98, H_3-23; 0.92, H_3-30; 0.90, H_3-29; 0.89, H_3-25 and 0.77, H_3-24 and H_3-26) which were typical resonances of the pentacyclic triterpenoic acid. The oxygenated methine proton at δ_H 3.21 was assigned to be the α-axail position according to the large coupling constant value of 9.9 Hz. The ^{13}C NMR spectrum (**Table 37**) revealed the signals of a carbonyl carbon (δ_C 181.52), seven quaternary carbons (δ_C 143.77, 46.42, 41.67, 38.71, 38.60, 37.02 and 30.66), five methine carbons (δ_C 125.61, 78.98, 55.20, 47.61 and 41.11), ten methylene carbons (δ_C 45.93, 38.41, 33.84, 32.66, 32.47, 27.67, 27.01, 23.38, 22.99 and 18.30) and seven methyl carbons (δ_C 33.06, 25.87, 28.05, 23.55, 16.92, 15.54 and 15.29). The structure of **ART39** was therefore determined to be oleanolic acid (**Table 67**) (Yang *et al*., 2009). The HMBC experiment (**Table 37**) completely confirmed the assigned structure.

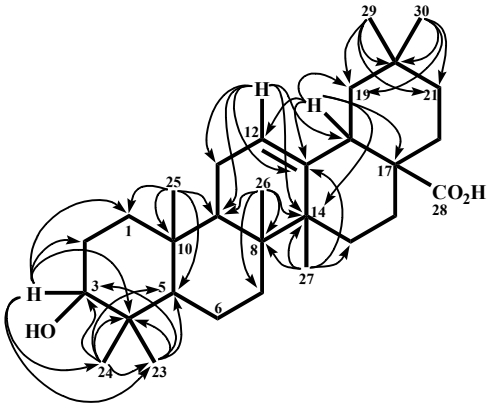

Selected HMBC correlations of **ART39**

Table 37 The NMR spectral data of **ART39**

Position	**δ_C (Type)**	**δ_H (*mult.*; J_{Hz})**	**HMBC correlations**
1	38.41 (CH_2)	1.58 (*m*), 0.97 (*m*)	
2	27.01 (CH_2)	1.59 (*m*)	
3	78.98 (CH)	3.21 (*dd*; 9.9, 5.1)	C-1, C-2, C-4, C-23, C-24
4	38.60 (C)[c]		
5	55.20 (CH)	0.72 (*br d*; 11.1)	
6	18.30 (CH_2)	1.35 (*m*)	
7	32.66 (CH_2)	1.41 (*m*)	
8	38.71 (C)[c]		
9	47.61 (CH)	1.52 (*m*)	
10	37.02 (C)		
11	22.99 (CH_2)	1.91 (*m*)	
12	125.61 (CH)	5.27 (*t*; 3.6)	C-9, C-11, C-14, C-18
13	143.77 (C)		
14	41.67 (C)[d]		

[a]recored in $CDCl_3$+CD_3OD (1 drop); [b,c,d]may be interchangeable

Table 37 (Continued)

Position	δ_C (Type)	δ_H (*mult.*; J_{Hz})	HMBC correlations
15	27.67 (CH_2)	1.71 (*m*), 1.59 (*m*)	
16	23.38 (CH_2)	1.91 (*m*), 1.62 (*m*)	
17	46.42 (C)[d]		
18	41.11 (CH)	2.82 (*dd*; 14.4, 4.5)	C-12, C-13, C-14, C-17, C-19
19	45.93 (CH_2)	1.64 (*m*), 1.13 (*m*)	
20	30.66 (C)		
21	33.84 (CH_2)	2.28 (*m*), 1.18 (*m*)	
22	32.47 (CH_2)	1.78 (*m*)	
23	28.05 (CH_3)	0.98 (*s*)	C-3, C-4, C-5, C-24
24	15.54 (CH_3)	0.77 (*s*)	C-3, C-4, C-5, C-23
25	15.29 (CH_3)	0.89 (*s*)[b]	C-1, C-5, C-9, C-10
26	16.92 (CH_3)	0.77 (*s*)	C-7, C-8, C-9, C-14
27	25.87 (CH_3)	1.13 (*s*)	C-8, C-13, C-14, C-15
28	181.52 (C=O)		
29	33.06 (CH_3)	0.90 (*s*)[b]	C-19, C-20, C-21, C-30
30	23.55 (CH_3)	0.92 (*s*)	C-19, C-20, C-21, C-29

[a]recorded in $CDCl_3$+CD_3OD (1 drop); [b,c,d]may be interchangeable

3.1.6 Steroids

ART5: β-Sitosterol

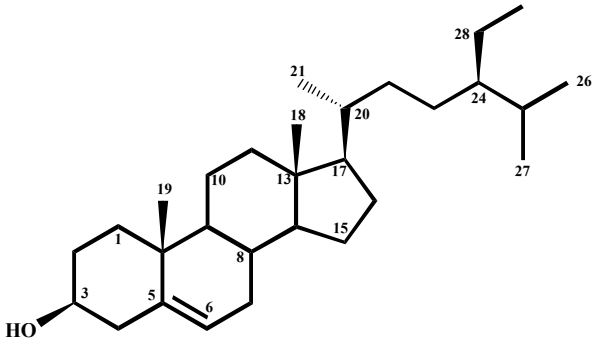

ART5 was obtained as a white solid. The IR spectrum displayed an absorption band at 3410 cm^{-1} for OH stretching. The ^{1}H NMR spectrum (**Table 38**) showed the resonances of a vinylic proton (δ_H 5.27), an oxymethine proton (δ_H 3.42) and six methyl groups of two singlet methyl groups (δ_H 0.93 and 0.61), three doublet methyl groups (δ_H 0.85, 0.76 and 0.73) and one triplet methyl group (δ_H 0.77). The ^{13}C NMR spectrum associated with DEPT experiments (**Table 38**) revealed the resonances of 29 carbon atoms consisting of three quaternary carbons (δ_C 139.84, 41.34 and 35.52), nine methine carbons (δ_C 120.64, 70.55, 55.79, 55.10, 49.18, 44.86, 35.16, 30.92 and 28.19), eleven methylene carbons (δ_C 41.07, 38.81, 36.28, 32.97, 30.40, 28.72, 27.26, 25.13, 23.31, 22.09 and 20.10) and six methyl carbons (δ_C 18.81, 18.38, 18.04, 17.79, 10.97 and 10.86).

By comparison of the ^{1}H and ^{13}C NMR spectral data with the previous report (**Table 68**), **ART5** was assigned as β-sitosterol (Kim *et al*., 2006).

Table 38 The NMR spectral data of **ART5**

Position	δ_C **(Type)**	δ_H (***mult.***; J_{Hz})
1	36.28 (CH_2)	1.77 (*m*), 1.08 (*m*)
2	28.72 (CH_2)	1.93 (*m*), 1.63 (*m*)
3	70.55 (CH)	3.42 (*m*)
4	41.07 (CH_2)	2.19 (*m*)
5	139.84 (C)	
6	120.64 (CH)	5.27 (*d*, 4.5)
7	30.40 (CH_2)	1.74 (*m*), 1.43 (*m*)
8	30.92 (CH)	1.95 (*m*)
9	49.18 (CH)	0.93 (*m*)
10	35.52 (C)	
11	20.10 (CH_2)	1.54 (*m*), 1.48 (*m*)
12	38.81 (CH_2)	1.76 (*m*), 1.18 (*m*)
13	41.34 (C)	
14	55.79 (CH)	1.03 (*m*)
15	23.31 (CH_2)	1.56 (*m*)
16	27.26 (CH_2)	1.31 (*m*)
17	55.10 (CH)	1.11 (*m*)
18	10.97 (CH_3)	0.61 (*s*)
19	18.81 (CH_3)	0.93 (*s*)
20	35.16 (CH)	1.38 (*m*)
21	17.79 (CH_3)	0.85 (*d*; 6.6)
22	32.97 (CH_2)	1.31 (*m*), 1.08 (*m*)

[a]recorded in $CDCl_3$+CD_3OD (1 drop)

Table 38 (Continued)

Position	**δ_C (Type)**	**δ_H (*mult.*; J_{Hz})**
23	25.13 (CH_2)	1.16 (*m*)
24	44.86 (CH)	0.93 (*m*)
25	28.19 (CH)	1.26 (*m*)
26	18.38 (CH_3)	0.76 (*d*; 6.6)
27	18.04 (CH_3)	0.73 (*d*; 6.6)
28	22.09 (CH_2)	1.25 (*m*)
29	10.86 (CH_3)	0.77 (*t*; 7.2)

[a]recorded in $CDCl_3$+CD_3OD (1 drop)

ART24: β-Sitosterol glucopyranoside

(Daucosterol)

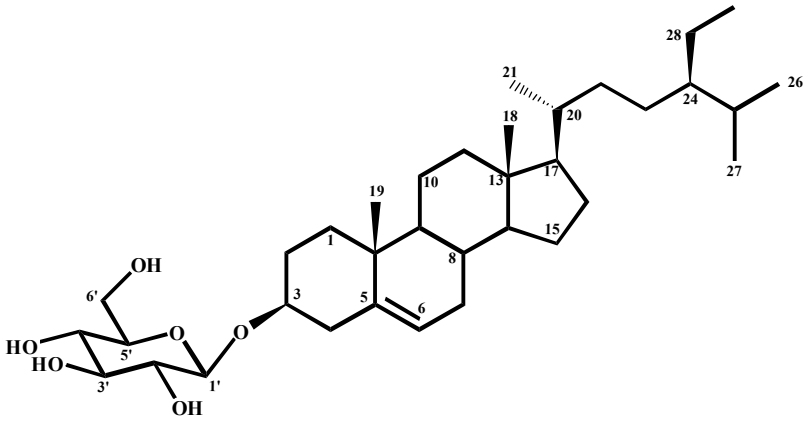

ART24 was obtained as a white solid with mp 276-278 ^{O}C. The IR spectrum displayed absorption for hydroxyl group at 3450 cm^{-1}. The ^{1}H NMR spectrum (**Table 39**) showed a characteristic signal of sitosterol glycoside. The sitosterol moiety was deduced from the resonances of one olefinic proton (δ_H 5.37, H-6), one oxymethine proton (δ_H 3.60, H-3) and six methyl groups of two singlet signals (δ_H 1.01, H_3-19 and 0.69, H_3-18), three doublet signals (δ_H 0.93, H_3-21, 0.84, H_3-26 and 0.82, H_3-27) and one triplet signal (δ_H 0.85, H_3-29). The sugar unit was assigned to a glucopyranose, which in the ^{1}H NMR spectrum, the resonance of an anomeric proton H-1′ was at δ_H 4.41, four methine protons were at δ_H 3.44 (H-4′); 3.41 (H-3′); 3.30 (H-5′); 3.24 (H-1′) and the oxygenated methylene protons were at δ_H 3.84 and 3.75 (H_2-6′, J = 12.0 Hz). The ^{13}C NMR spectrum associated with DEPT experiments (**Table 39**) showed the resonances of three quaternary carbons (δ_C 140.39, 42.44 and 36.83), fourteen methine carbons (δ_C 122.30, 101.21, 79.31, 76.50, 75.83, 73.66, 70.28, 56.87, 56.18, 50.30, 45.98, 36.26, 32.00 and 29.27), twelve methylene carbons

(δ_C 62.02, 39.87, 38.83, 37.37, 34.06, 32.04, 29.80, 28.35, 26.19, 24.39, 23.18 and 21.17) and six methyl carbons (δ_C 19.87, 19.40, 19.09, 18.85, 12.03 and 11.93).

By comparison of the ^{1}H and ^{13}C NMR spectral data with the previous report (**Table 69**), **ART24** was assigned to be β-sitosterol glucopyranoside or daucosterol (Lendl *et al*., 2005).

Table 39 The NMR spectral data of **ART24**

Position	**δ_C (Type)**	**δ_H (*mult.*; J_{Hz})**
1	37.37 (CH_2)	α: 1.08 (*m*)
		β: 1.87 (*m*)
2	29.80 (CH_2)	a: 1.63 (*m*)
		b: 1.91 (*m*)
3	79.31 (CH)	3.60 (*m*)
4	38.83 (CH_2)	a: 2.27 (*m*)
		b: 2.41 (*m*)
5	140.39 (C)	
6	122.30 (CH)	5.37 (*br d*, 5.1)
7	32.04 (CH_2)	a: 1.43 (*m*)
		b: 1.68 (*m*)
8	32.00 (CH)	1.45 (*m*)
9	50.30 (CH)	0.93 (*m*)
10	36.83 (C)	
11	21.17 (CH_2)	1.54 (*m*), 1.48 (*m*)
12	39.87 (CH_2)	α: 1.18 (*m*)
		β: 2.03 (*m*)
13	42.44 (C)	
14	56.87 (CH)	1.03 (*m*)
15	24.39 (CH_2)	a: 1.07 (*m*)
		b: 1.60 (*m*)

Table 39 (Continued)

Position	**δ_C (Type)**	**δ_H (*mult.*; J_{Hz})**
16	28.35 (CH_2)	a: 1.26 (*m*)
		b: 1.89 (*m*)
17	56.18 (CH)	1.11 (*m*)
18	11.93 (CH_3)	0.69 (*s*)
19	19.40 (CH_3)	1.01 (*s*)
20	36.26 (CH)	1.38 (*m*)
21	18.85 (CH_3)	0.93 (*d*; 6.3)
22	34.06 (CH_2)	a: 1.08 (*m*)
		b: 1.31 (*m*)
23	26.18 (CH_2)	1.16 (*m*)
24	45.98 (CH)	0.93 (*m*)
25	29.27 (CH)	1.68 (*m*)
26	19.87 (CH_3)	0.84 (*d*; 6.6)
27	19.09 (CH_3)	0.82 (*d*; 6.6)
28	23.18 (CH_2)	1.25 (*m*)
29	12.03 (CH_3)	0.85 (*t*; 6.6)
1′	101.21 (CH)	4.41 (*d*; 7.5)
2′	73.66 (CH)	3.24 (*m*)
3′	76.50 (CH)	3.41 (*m*)
4′	70.28 (CH)	3.44 (*m*)
5′	75.83 (CH)	3.30 (*m*)
6′	62.02 (CH_2)	a: 3.75 (*dd*; 12.0, 4.5)
		b: 3.84 (*dd*; 12.0, 3.0)

ART37: Stigmast-4-en-3-one

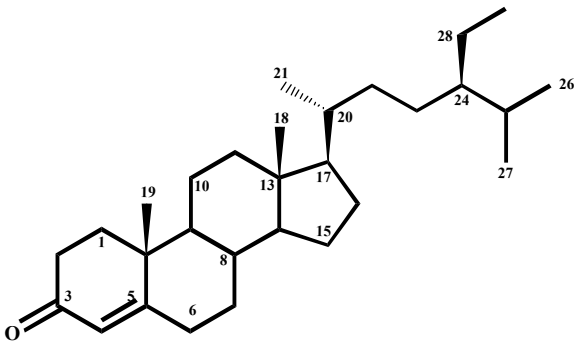

ART37 was obtained as a white solid. The IR spectrum showed a stretching of a conjugated carbonyl group at 1674 cm^{-1} whereas the UV spectrum exhibited absorption band maxima at 246 nm. The ^{13}C NMR spectrum (**Table 40**) displayed the signals for 29 carbons consisting of one carbonyl carbon (δ_C 199.61), three quaternary carbons (δ_C 171.64, 42.42 and 38.61), eight methine carbons (δ_C 123.75, 56.06, 55.91, 53.85, 45.88, 36.12, 35.66 and 29.21), eleven methylene carbons (δ_C 39.66, 35.71, 33.98, 33.92, 32.95, 32.07, 28.18, 26.16, 24.19, 23.10 and 21.05) and six methyl carbons [δ_C 19.79, 19.04, 18.70, 17.40 and 11.95 (2xC)]. The ^1H NMR spectrum (**Table 40**) showed the same characteristic signals of β-sitosterol except for the downfield shift of olefinic proton (δ_H 5.73, H-4) and the absence of oxygenated methine proton at C-3. Two sp^2 carbons at δ_C 123.75 (C-4) and 171.64 (C-5) and the down field chemical shift of C-5 associated with the presence of a carbonyl carbon at δ_C 199.61 indicating the existence of the conjugated carbonyl functionality at C-3. In the HMBC spectrum (**Table 40**), the olefinic proton H-4 exhibited the correlations with C-2 (δ_C 33.92), C-3 (δ_C 199.61), C-5 (δ_C 171.64), C-6 (δ_C 32.95) and C-10 (δ_C 38.61) suggesting the presence of a double bond at C-4 and C-5. On the basis of its spectral data as well as comparison with the literature (**Table 70**), compound **ART37** was therefore determined to be stigmast-4-en-3-one.

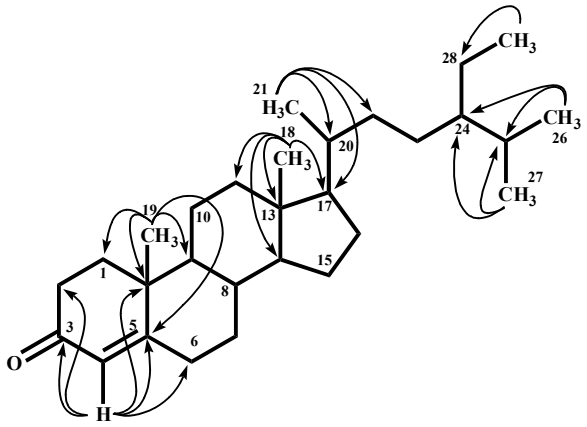

Selected HMBC correlations of **ART37**

Table 40 The NMR spectral data of **ART37**

Position	**δ_C (Type)**	**δ_H (*mult.*; J_{Hz})**	**HMBC correlations**
1	35.71 (CH_2)	1.67 (*m*), 1.54 (*m*)	
2	33.92 (CH_2)	2.50 (*m*), 2.28 (*m*)	
3	199.61 (C=O)		
4	123.75 (CH)	5.73 (*s*)	C-2, C-3, C-5, C-6, C-10
5	171.64 (C)		
6	32.95 (CH_2)	2.40 (*m*), 2.25 (*m*)	
7	32.07 (CH_2)	1.85 (*m*), 1.01 (*m*)	
8	35.66 (CH)	1.71 (*m*)	
9	53.85 (CH)	0.92 (*m*)	
10	38.61 (C)		
11	21.05 (CH_2)	1.50 (*m*), 1.40 (*m*)	
12	39.66 (CH_2)	2.04 (*m*), 1.15 (*m*)	
13	42.42 (C)		
14	55.91 (CH)	1.00 (*m*)	
15	24.19 (CH_2)	1.29 (*m*), 1.23 (*m*)	
16	28.18 (CH_2)	1.32 (*m*), 1.27 (*m*)	

Table 40 (Continued)

Position	**δ_C (Type)**	**δ_H (*mult.*; J_{Hz})**	**HMBC correlations**
17	56.06 (CH)	1.11 (*m*)	
18	11.95 (CH_3)	0.71 (*s*)	C-12, C-13, C-14, C-17
19	17.40 (CH_3)	1.18 (*s*)	C-1, C-5, C-9, C-10
20	36.12 (CH)	2.01 (*m*)	
21	18.70 (CH_3)	0.92 (*d*; 6.3)	C-17, C-20, C-22
22	33.98 (CH_2)	2.39 (*m*)	
23	26.16 (CH_2)	1.17 (*m*)	
24	45.88 (CH)	0.93 (*m*)	
25	29.21 (CH)	1.26 (*m*)	
26	19.79 (CH_3)	0.85 (*d*; 6.9)	C-24, C-25, C-27
27	19.04 (CH_3)	0.84 (*d*; 6.6)	C-24, C-25, C-26
28	23.10 (CH_2)	1.29 (*m*)	
29	11.95 (CH_3)	0.83 (*d*; 6.6)	C-24, C-28

3.1.7 Benzenoids

ART1: α-Tocopherol

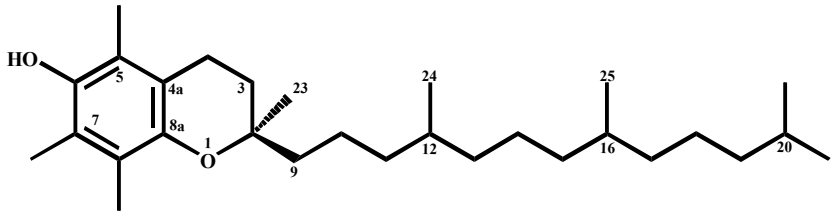

ART1 was obtained as a yellow gum. The UV spectrum displayed absorption maxima at 246, 291 and 383 nm. The IR spectrum showed absorption bands of O-H stretching at 3349 cm^{-1}. The ^{1}H and ^{13}C NMR spectral data (**Table 41**) displayed the resonances corresponding to three aryl methyl groups [δ_H 2.16 and 2.11 (2xCH_3); δ_C12.23, 11.79 and 11.30], four secondary methyl groups [δ_H 0.86 (2xCH_3), 0.85 and 0.84; δ_C 22.75, 22.65, 19.77 and 19.68] and a tertiary methyl group (δ_H 1.23; δ_C 23.82). The protons resonated at δ_H 2.60 (*t*) and 1.78 (*m*) which coupled to each other were assigned for methylene protons H_2-4 and H_2-3, respectively. The proton resonances at δ_H 1.02-1.60 and carbon resonances at δ_C 39.84, 39.39, 37.47 (2xC), 37.44, 37.41, 24.83, 24.47, and 21.06 corresponded to nine methylene groups. The ^{13}C NMR spectrum (**Table 41**) further showed the resonances of oxygenated aromatic carbon at δ_C 145.57 and 144.55 together with oxygenated quaternary carbon at δ_C 74.53. **ART1** was thus determined as α-tocopherol. The HMBC experiment (**Table 41**) was in agreement with the assigned structure.

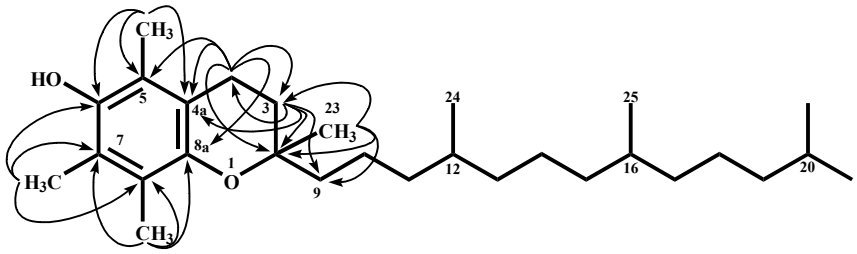

Selected HMBC correlations of **ART1**

Table 41 The NMR spectral data of **ART1**

Position	**δ_C (Type)**	**δ_H (*mult.*; J_{Hz})**	**HMBC correlations**
2	74.53 (C)		
3	31.58 (CH_2)	1.78 (*m*, 6.9)	C-2, C-4, C-4a, C-9
4	20.78 (CH_2)	2.60 (*t*, 6.9)	C-2, C-3, C-4a, C-5, C-8a
4a	117.36 (C)		
5	118.49 (C)		
6	144.55 (C)		
7	122.62 (C)		
8	121.04 (C)		
8a	145.57 (C)		
9	39.84 (CH_2)	1.47-1.60 (*m*)	C-2
10	21.06 (CH_2)	1.02-1.48 (*m*)	
11	37.47 (CH_2)[a]	1.02-1.48 (*m*)	
12	32.82 (CH)[b]	1.02-1.48 (*m*)	
13	37.47 (CH_2)[a]	1.02-1.48 (*m*)	
14	24.47 (CH_2)[c]	1.02-1.48 (*m*)	
15	37.44 (CH_2)[a]	1.02-1.48 (*m*)	
16	32.72 (CH)[b]	1.02-1.48 (*m*)	
17	37.41 (CH_2)[a]	1.02-1.48 (*m*)	
18	24.83 (CH_2)[c]	1.02-1.48 (*m*)	

[a,b,c,d,e]may be interchangeable in the same sign

Table 41 (Continued)

Position	**δ_C (Type)**	**δ_H (*mult.*; J_{Hz})**	**HMBC correlations**
19	39.39 (CH_2)	1.02-1.48 (*m*)	
20	28.00 (CH)	1.47-1.60 (*m*)	
21	22.75 (CH_3)[d]	0.86 (*d*; 6.6)	C-19, C-20
22	22.65 (CH_3)[d]	0.86 (*d*; 6.6)	C-19, C-20
23	23.82 (CH_3)	1.23 (*s*)	C-2, C-3, C-9
24	19.77 (CH_3)[e]	0.85 (*d*; 6.6)	C-11, C-12, C-13
25	19.68 (CH_3)[e]	0.84 (*d*; 6.6)	C-15, C-16, C-17
5-CH_3	11.30 (CH_3)	2.11 (*s*)	C-4a, C-5, C-6
7-CH_3	12.23 (CH_3)	2.16 (*s*)	C-6, C-7, C-8
8-CH_3	11.79 (CH_3)	2.11 (*s*)	C-7, C-8, C-8a

[a,b,c,d,e]may be interchangeable in the same sign

ART21: *trans*-Triacontyl-4-hydroxy-3-methoxycinnamate

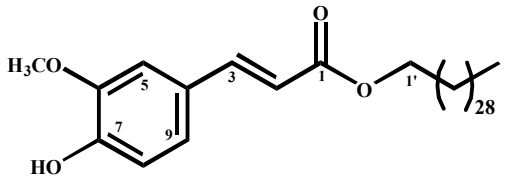

ART21 was obtained as a white powder. The IR spectrum displayed absorption bands for a hydroxyl and a carbonyl groups at 3445 and 1720 cm^{-1}, respectively. The UV spectrum exhibited absorptions maxima at 240 and 327 nm. The EI-MS spectrum displayed a molecular ion peak at *m*/*z* 614 which was 30 mass units higher than **ART30**. The ^{1}H NMR spectrum (**Table 42**) exhibited the resonances of aromatic protons at δ_H 7.04 (*d*; *J* = 1.8 Hz), 6.92 (*d*; *J* = 8.4 Hz) and 6.84 (*dd*; *J* = 8.4 and 1.8 Hz) corresponding to H-5, H-8 and H-9, respectively, which indicated the presence of 1,2,4-trisubstituted benzene ring. A hydroxyl proton resonated at δ_H 5.86 and a methoxyl group resonated at δ_H 3.93 (*s*) were proposed to be substituted at *ortho* position. The NOESY experiment exhibited the cross peak between the methoxyl group and the aromatic proton at δ_H 7.04 (H-5) indicating that the methoxyl substituent was then positioned at the C-6. The spectrum further showed the two *trans*-olefinic protons at δ_H 7.61 (*d*, *J* = 15.9 Hz) and 6.29 (*d*, *J* = 15.9 Hz) together with the 30 carbons side chain signals seen as signals of oxygenated methylene protons at δ_H 4.18 (*t*, *J* = 6.9 Hz, H_2-1'), metheylene protons at δ_H 1.69 (*m*, *J* = 6.9 Hz, H_2-2') and 1.25 (*br s*, H_2-3' - H_2-29') and one methyl group at δ_H 0.88 (*t*, *J* = 6.9 Hz, H_3-30'). These data corresponded to the feruloyl moiety with long chain hydrocarbons of 30 carbons. The connectivity of the 30 carbons side chain to an ester group was evidenced from the ^{3}J HMBC correlation (**Table 42**) of H_2-2' (δ_H 4.19) to the ester carbonyl carbon (δ_H 167.35). **ART21** was thus designated as *trans*-triacontyl-4-

hydroxy-3-methoxy-cinnamate (**Table 71**) (Boonyaratavej *et al*., 1992). The HMBC correlations completely confirmed the assigned structure.

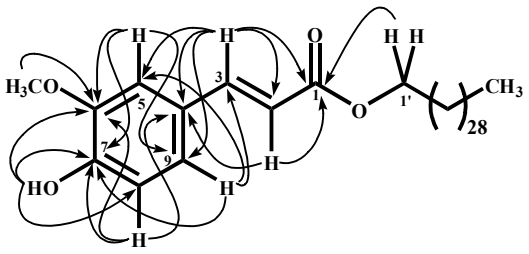

Selected HMBC correlations of **ART21**

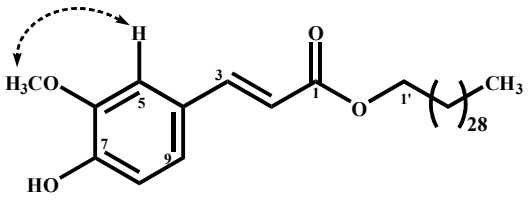

NOESY correlations of **ART21**

Table 42 The NMR spectral data of **ART21**

Position	**δ_C (Type)**	**δ_H (*mult.*; J_{Hz})**	**HMBC correlations**
1	167.35 (C=O)		
2	115.74 (CH)	6.29 (*d*; 15.9)	C-1, C-4
3	144.59 (CH)	7.61 (*d*; 15.9)	C-1, C-2, C-4, C-5, C-9
4	127.10 (C)		
5	109.33 (CH)	7.04 (*d*; 1.8)	C-3, C-6, C-7, C-9
6	147.90 (C)		
7	146.76 (C)		
8	114.70 (CH)	6.92 (*d*; 8.4)	C-4, C-6, C-7
9	123.02 (CH)	6.84 (*dd*; 8.4, 1.8)	C-3, C-5, C-7
1'	64.61 (CH_2)	4.19 (*t*; 6.6)	C-1, C-2', C-3'
2'	28.78 (CH_2)	1.69 (*m*)	
3'-29'	31.92, 29.54, 29.34, 29.30, 26.00, 22.68 (CH_2)	1.27 (*br s*)	
30'	14.09 (CH_3)	0.88 (*t*; 6.3)	C-28', C-29'
7-OH		5.86 (*s*)	C-6, C-7, C-8
6-OCH_3	55.95 (CH_3)	3.93 (*s*)	C-6

ART30: *trans*-Triacontyl-4-hydroxycinnamate

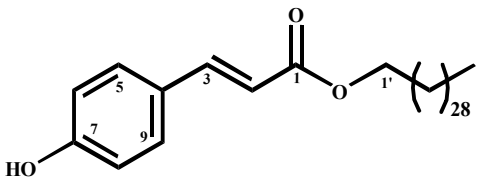

ART30 was obtained as white powder, mp 90-92 ^{O}C. The IR spectrum displayed absorptions for a hydroxyl and carbonyl groups at 3490 and 1696 cm^{-1}, respectively, whereas the UV spectrum showed maximum absorption bands at 234 and 327 nm. The EI-MS spectrum exhibited the molecular ion peak at *m*/*z* 584 which was 30 mass units less than **ART21**. The ^{1}H NMR spectral data (**Table 43**) showed the resonance of aromatic proton as AA'BB' of H-5/H-8 at δ_H 7.43 (*d*, *J* = 8.7 Hz) and H-6/H-9 at δ_H 6.84 (*d*, *J* = 8.7 Hz), and two doublets of *trans* olefinic protons H-3 and H-2 at δ_H 7.62 and 6.30 (*J* = 15.9 Hz), respectively, which corresponded to a *p*-coumaroyl moiety. The presence of long chain hydrocarbons was implied from the mass and signals of a triplet of oxygenated methylene proton H_2-1' at δ_H 4.18 (*J* = 6.9 Hz), multiplet of metheylene protons H_2-2' at δ_H 1.69 (*J* = 6.9 Hz) and H_2-3' - H_2-29' at δ_H 1.25 (*br s*) as well as a triplet of methyl protons H_3-30' at δ_H 0.88 (*J* = 6.9 Hz). The ester linkage was confirmed by the HMBC correlations (**Table 43**) of H_2-1' and H-3 to the ester carbonyl carbon (δ_H 167.41). The ion peak at *m*/*z* 421, which was in agreement with $C_{30}H_{61}$, suggested that the long chain hydrocarbon contained thirty carbons. **ART30** was then identified as *trans*-triacontyl-4-hydroxycinnamate (**Table 72**) (Wandji *et al*., 1990).

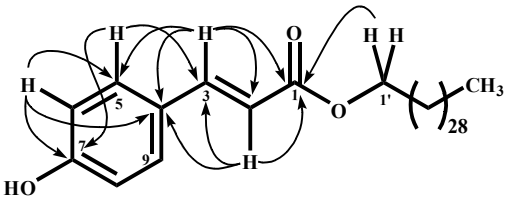

Selected HMBC correlations of **ART30**

Table 43 The NMR spectral data of **ART30**

Position	**δ_C (Type)**	**δ_H (*mult.*; J_{Hz})**	**HMBC correlations**
1	167.41 (C=O)		
2	115.96 (CH)	6.30 (*d*; 15.9)	C-1, C-3, C-4
3	144.09 (CH)	7.62 (*d*; 15.9)	C-1, C-2, C-4, C-5, C-9
4	127.50 (C)		
5, 9	129.89 (CH)	7.43 (*d*; 8.7)	C-3, C-7
6, 8	115.84 (CH)	6.84 (*d*; 8.7)	C-4, C-5, C-9, C-7
7	157.49 (C)		
1'	64.61 (CH_2)	4.18 (*t*; 6.9)	C-1, C-2', C-3'
2'	28.77 (CH_2)	1.69 (*m*; 6.9)	C-1', C-3', C-4'
3'-29'	31.91, 29.58, 29.53, 29.34, 29.29, 25.99, 22.67 (CH_2)	1.25 (*br s*)	
30'	14.07 (CH_3)	0.88 (*t*; 6.9)	C-28', C-29'

ART35: 4-Hydroxy-3-methoxybenzoic acid

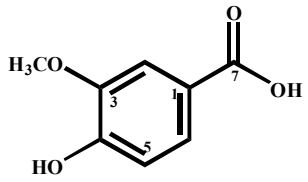

ART35 was obtained as a pale yellow solid. The IR spectrum showed the stretching of a hydroxyl and carbonyl groups at 3338 and 1687 cm^{-1}, respectively. The UV spectrum displayed absorption bands maxima at 220, 257 and 290 nm. The ^{1}H NMR spectrum (**Table 44**) exhibited signals of a methoxyl group at δ_H 3.93 and ABX signals of 1,2,4-trisubstituted benzene at δ_H 7.61 (*dd*; *J* = 8.1 and 1.8 Hz, H-6), 7.56 (*d*; *J* = 1.8 Hz, H-2) and 6.89 (*d*; *J* = 8.1 Hz, H-5). The downfield shifts of the aromatic protons H-2 and H-6 suggested that both protons were adjacent to the electron withdrawing group which was suggested as carboxyl group due to the carbon signal at δ_C 168.81 (**Table 44**). The methoxyl group was placed at C-3 which was *ortho* position to C-2 by irradiation at the resonance of this methoxyl group resulted in enhancement of the signal of H-2. It was thus concluded that **ART35** was 4-hydroxy-3-methoxybenzoic acid.

Table 44 The NMR spectral data of **ART35**

Position	**δ_C (Type)**	**δ_H (*mult*., J_{Hz})**	**HMBC correlations**
1	121.78 (C)		
2	112.43 (CH)	7.56 (*d*; 1.8)	C-1, C-3, C-4, C-6, C-7
3	146.65 (C)		
4	150.48 (C)		
5	114.43 (CH)	6.89 (*d*; 8.1)	C-1, C-3, C-4
6	124.25 (CH)	7.61 (*dd*; 8.1, 1.8)	C-2, C-4, C-7

7	168.81 (C=O)		
3-OCH_3		3.93 (*s*)	

[a]recorded in $CDCl_3$+CD_3OD (1 drop)

ART36: Gallic acid

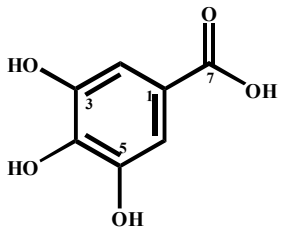

ART36 was obtained as a pale yellow solid. The IR spectrum exhibited absorptions for a hydroxyl stretching at 3345 cm^{-1} and for a carbonyl stretching at 1690 cm^{-1}whereas the UV spectrum displayed maximum absorption bands at 216, 272 and 355 nm. The ^{1}H NMR spectrum (**Table 45**) showed only the singlet resonance of the aromatic proton at δ_H 6.90. The ^{13}C NMR spectrum (**Table 45**) exhibited five signals for seven carbon atoms: one carbonyl (δ_C 167.96), four quaternary [δ_C 145.84 (2xC), 138.43 and 120.89] and two methine [δ_C 109.16 (2xC)] carbons. The above data suggested that **ART36** was gallic acid.

Table 45 The NMR spectral data of **ART36**

Position	**δ_C (Type)**	**δ_H (*mult.*)**	**HMBC correlations**
1	109.16 (C)		
2	145.84 (C)		
3	138.43 (C)		
4	145.84 (C)		
5	109.16 (CH)	6.90 (*s*)	C-1, C-3, C-4, C-6, C-7
6	120.89 (C)		
7	167.96 (C=O)		

ART40: Methyl gallate

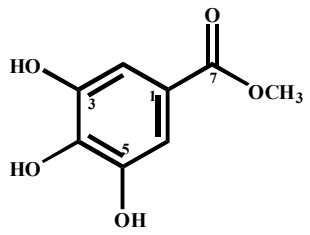

ART40 was obtained as a yellow gum. The IR spectrum showed a stretching of a hydroxyl group at 3328 cm-1 and a carbonyl group at 1706 cm^{-1} whereas the UV spectrum displayed maximum absorptions at 218, 274 and 356 nm. The ^{1}H NMR spectrum (**Table 46**) showed two singlet signals of an aromatic proton at δ_H 7.19 and methoxyl group at δ_H 3.88. The methoxyl protons exhibited the correlation to the carbonyl carbon (δ_C 167.11) in the HMBC experiment (**Table 46**) indicating the presence of a methyl ester, therefore **ART40** was determined as methyl gallate. The carbon signals of one carbonyl (δ_C 167.11), four quaternary [δ_C 144.85 (2xC), 137.43 and 121.00], two methine [δ_C 109.41 (2xC)] and one methyl (δ_C 51.67) carbons (**Table 46**) were in agreement with the assigned structure.

Table 46 The NMR spectral data of **ART40**

Position	**δ_C (Type)**	**δ_H (*mult.*)**	**HMBC correlations**
1	121.00 (C)		
2,6	109.41 (CH)	7.19 (*s*)	C-1, C-3(C-5), C-4, C-7
3,5	144.85 (C)		
4	137.34 (C)		
7	167.11 (C=O)		

OCH_3	51.67 (CH_3)	3.88 (*s*)	C-7

3.1.8 Lignans

ART33: 9,9′-*O*-Diferuloyl-(-)-secoisolariciresinol

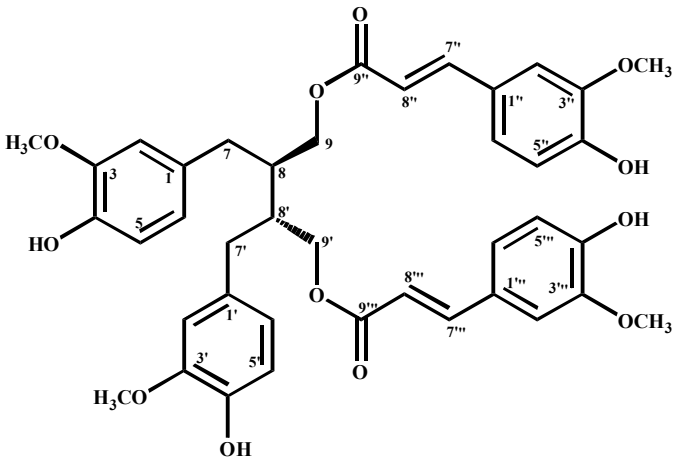

ART33 was obtained as a white solid with mp 276-278 ^{O}C. The IR spectrum showed the stretching of a hydroxyl group (3409 cm^{-1}), carbonyl ester (1702 cm^{-1}), double bond (1637 cm^{-1}), and aromatic ring (1602, 1513 cm^{-1}). The UV spectrum exhibited maximum absorptions at 216, 230, 290 and 327 nm. The ^{1}H NMR spectrum (**Table 47**) indicated the presence of a phenolic hydroxyl proton at δ_H 5.89 (*s*); two olefinic protons at δ_H 7.59 (*d*, *J* = 15.9 Hz) and 6.29 (*d*, *J* = 15.9 Hz) with *trans*- onfiguration; aromatic protons at δ_H 7.07 (*dd*, *J* = 8.1 and 1.5 Hz), 6.91 (*d*, *J* = 8.1 Hz) and 7.02 (*d*, *J* = 1.5 Hz) and methoxyl protons at δ_H 3.93 (*s*). The above data in association with the HMBC experiment (**Table 47**) indicated that the partial substructure was a feruloyl group. The remaining part of the spectrum showed a hydroxyl proton signal [δ_H 5.48 (*s*)]; an aromatic ABX proton signals [δ_H 6.62 (*dd*, *J* = 8.1 and 1.5 Hz), 6.81 (*d*, *J* = 8.1 Hz) and 6.53 (*d*, *J* = 1.5 Hz)] and a methoxyl group signal [δ_H 3.78 (*s*)], suggesting the presence of a 4-hydroxy-3-methoxyphenyl

group. In addition, the spectrum also showed the resonance signals for two sets of methylene protons [δ_H 4.40 (*dd*, *J* = 11.4 and 5.7 Hz) and 4.22 (*dd*, *J* = 11.4 and 5.7 Hz); and δ_H 2.70 (*dd*, *J* = 15.0, 7.0 Hz) and 2.76 (*dd*, *J* = 15.0, 7.0 Hz)] and one methine proton [δ_H 2.22 (*m*)]. The ^1H–^1H COSY, HMQC and HMBC correlations suggested that -$CH_2CH(CH_2O$-)- moiety was an additional partial substructure. The connectivity between the feruloyl, the 4-hydroxy-3-methoxyphenyl, and the -$CH_2CH(CH_2O$-)- moieties was established from the HMBC correlations (**Table 47**). The correlations of the oxygenated methylene protons H-9 (δ_H 4.40 and 4.22) with the carbonyl ester C-9" at δ_C 167.20 confirmed the connection of the feruloyl to -$CH_2CH(CH_2O$-)- moiety via ester linkage. The ^3J HMBC correlations of the methylene protons H_2-7 (δ_H 2.70 and 2.76) to C-2 (δ_C 111.31) and C-6 (δ_C 121.74) and of the aromatic protons H-2 (δ_H 6.53) and H-6 (δ_H 6.62) to C-7 (δ_C 35.31) indicated that 4-hydroxy-3-methoxyphenyl group was directly connected to -$CH_2CH(CH_2O$-)- moiety. The chemical shifts of H-8 (δ_H 2.22) and C-8 (δ_C 35.31) implied that of **ART33** could be a symmetrical dimeric compound.

Upon comparison of the spectral data and an optical rotation to the reported data, **ART33** was as a known lignan named 9,9′-*O*-diferuloyl-(-)-secoisolariciresinol (**Table 73**) (Fuchino *et al*., 1995).

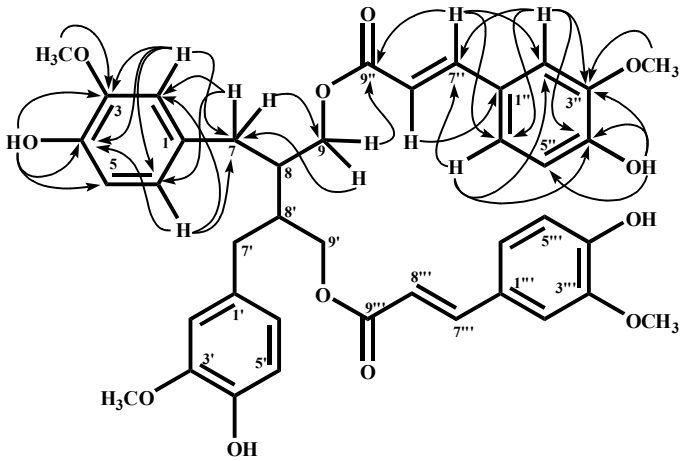

Selected HMBC correlations of **ART33**

Table 47 The NMR spectral data of **ART33**

Position	**δ_C (Type)**	**δ_H (*mult.*; J_{Hz})**	**HMBC correlations**
1,1'	131.71 (C)		
2,2'	111.31 (CH)	6.53 (*d*, 1.5)	C-1(C-1'), C-3(C-3'), C-4(C-4'), C-6(C-6'), C-7(C-7')
3,3'	146.47 (C)		
4,4'	143.96 (C)		
5,5'	114.15 (CH)	6.81 (*d*, 8.1)	C-1(C-1'), C-3(C-3'), C-4(C-4'), C-6(C-6')
6,6'	121.74 (CH)	6.62 (*dd*, 8.1, 1.5)	C-1(C-1'), C-4(C-4'), C-7(C-7')
7,7'	35.31 (CH_2)	2.76 (*dd*, 15.0, 7.0) 2.70 (*dd*, 15.0, 7.0)	C-1(C-1'), C-2(C-2'), C-6(C-6'), C-8(C-8'), C-9(C-9')
8,8'	40.21 (CH)	2.22 (*m*)	C-1(C-1'), C-7(C-7'), C-9(C-9')
9,9'	64.47 (CH_2)	4.40 (*dd*, 11.4, 5.7) 4.22 (*dd*, 11.4, 5.7)	C-7(C-7'), C-8(C-8'), C-9"(C-9"')
3,3'-OCH_3	55.77 (CH_3)	3.78 (*s*)	C-3(C-3')
4,4'-OH		5.48 (*s*)	C-3(C-3'), C-4(C-4'), C-5(C-5')
1",1"'	126.87 (C)		
2",2"'	109.51 (CH)	7.02 (*d*, 1.5)	C-1"(C-1"'), C-3"(C-3"'), C-4"(C-4"'), C-6"(C-6"'), C-7"(C-7"')
3",3"'	146.79 (C)		
4",4"'	148.09 (C)		

5",5‴	114.74 (CH)	6.91 (*d*, 8.1)	C-1"(C-1‴), C-3"(C-3‴), C-4"(C-4‴)

Table 47 (Continued)

Position	**δ_C (Type)**	**δ_H (*mult.*; J_{Hz})**	**HMBC correlations**
6",6‴	123.06 (CH)	7.07 (*dd*, 8.1, 1.5)	C-2"(C-2‴), C-4"(C-4‴), C-7"(C-7‴)
7",7‴	145.11 (CH)	7.59 (*d*, 15.9)	C-1", C-2", C-6", C-8", C-9"
8",8‴	115.25 (CH)	6.29 (*d*, 15.9)	C-1"(C-1‴), C-9"(C-9‴)
9",9‴	167.20 (C=O)		
3",3‴-OCH_3	55.98 (CH_3)	3.93 (*s*)	C-3"(C-3‴)
4",4‴-OH		5.89 (*s*)	C-3"(C-3‴), C-4"(C-4‴), C-5"(C-5‴)

3.1.9 Miscellaneous compounds

ART15: (3a*S**,6a*R**)-3a-(hydroxymethyl)-2,2-dimethyldihydrofuro [3,4-*d*][1,3]dioxol-4(3a*H*)-one

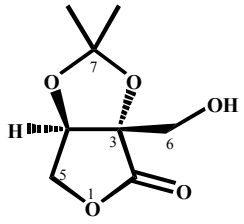

ART15 was obtained as colorless oil. The IR spectrum displayed absorption bands for a hydroxyl group at 3340 cm^{-1} and for a carbonyl group at 1750 cm^{-1}. The ^{1}H NMR spectrum (**Table 48**) showed the resonances of an oxymethine proton at δ_H 4.83 attributed to H-4, two non-equivalent oxymethylene protons at δ_H 4.45 and 4.39 attributed to H-5 and at δ_H 3.96 and 3.93 attributed to H-6. The spectrum further exhibited the signals of two singlet methyl groups at δ_H 1.49 and 1.43, assigned for H_3-8 and H_3-9, respectively. The five membered-ring lactone was evidenced from the ^{3}J HMBC correlations (**Table 48**) of H-4 and H_2-5 to the carbonyl functionality C-2 (δ_C 175.60). The hydroxymethyl group was then placed at C-3 (δ_C 85.53) due to the ^{3}J correlations of H-4 to C-6 (δ_C 61.41) and that of H-6 to C-2 (δ_C 175.60). The two methyl groups were assigned to be connected with the deoxygenated quaternary carbon C-7 (δ_C 113.51) according to its HMBC correlations (**Table 48**). The relative stereochemistry was deduced from the cross peaks in the NOESY experiment between H-4 and H_2-5α and H_3-8, but not to H_2-5β, H_2-6 and H_3-9. These data indicated that the H-4 and the hydroxymethyl group was a *trans*

stereorelatives. The ^{13}C NMR spectral data associated with DEPT experiments (**Table 48**) revealed the resonances of eight carbons: a carbonyl carbon (δ_C 175.60), two quaternary carbons (δ_C 113.51 and 85.53), a methine carbon (δ_C 78.09), two methylene carbons (δ_C 70.23 and 61.41) and two methyl carbons (δ_C 26.99 and 26.33). The above conclusion confirmed the assigned structure of **ART15** as a new butyrolactone derivative, (3a*S**,6a*R**)-3a-(hydroxymethyl)-2,2-dimethyldihydro-furo[3,4-*d*][1,3]dioxol-4(3a*H*)-one.

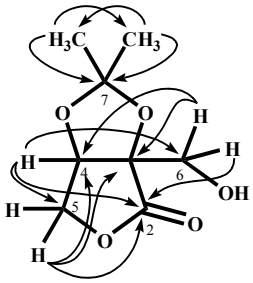

Selected HMBC correlations of **ART15**

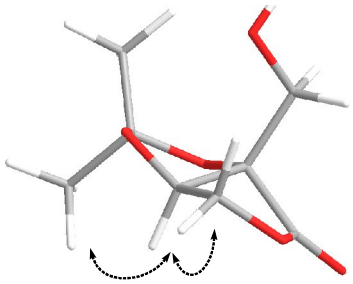

Energy-minimized (MM2) structure of **ART15**
showing selected NOESY experiment

Table 48 The NMR spectral data of **ART15**

Position	**δ_C (Type)**	**δ_H (*mult.*; J_{Hz})**	**HMBC correlations**
2	175.60 (C=O)		
3	85.53 (C)		
4	78.09 (CH)	4.83 (*d*; 3.5)	C-2, C-5, C-6
5	70.23 (CH_2)	4.45 (*d*; 11.0)	C-2, C-3, C-4
		4.39 (*dd*; 11.0, 3.5)	
6	61.41 (CH_2)	3.96 (*d*; 11.5)	C-2, C-3, C-4
		3.93 (*d*; 11.5)	C-2, C-3, C-4
7	113.51 (C)		
8	26.99 (CH_3)	1.49 (*s*)	C-7, C-9
9	26.33 (CH_3)	1.43 (*s*)	C-7, C-8

ART26: α-D-glucopyranoside penta-acetate

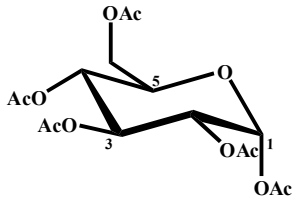

ART26 was obtained as a white solid from the acetylation of the methanolic extract of the leaves. The IR spectrum displayed absorption band for a carbonyl group at 1750 cm^{-1}. The ^{1}H NMR spectrum (**Table 49**) revealed that it was an acetyl derivative of glucose with an anomeric proton H-1 resonated at δ_H 6.32 (*d*, *J* = 3.0 Hz) while five acetyl groups resonated at δ_H 2.19, 2.10, 2.04, 2.03 and 2.02. The remaining signals corresponded to four methine protons (δ_H 5.47, *t*, *J* = 10.2 Hz, H-3; 5.14, *m*, H-4,; 5.09, *m*, H-2 and 4.13, *m*, H-5) and methylene protons at δ_H 4.27 and 4.09 (each *m*, H_2-6). The β-anomeric proton was indicated from a coupling constant value of 3.6 Hz. The ^{13}C NMR spectrum (**Table 49**) displayed the resonances of five carbonyl carbons (δ_C 170.54, 170.14, 169.58, 169.34 and 168.67), five methine carbons [δ_C 88.97, 69.78 (2xC), 69.15 and 67.85], one methylene carbon (δ_C 61.42) and five methyl carbons (δ_C 20.76, 20.58, 20.55, 20.45 and 20.34). The HMBC experiment (**Table 49**) also confirmed the structural assignment. Furthermore, **ART26** was clearly identified to be α-D-glucopyranoside penta-acetate by comparison of its ^{1}H NMR data to an authentic compound, which was prepared from acetylation of α-D-glucose.

Table 49 The NMR spectral data of **ART26**

Position	**δ_C (Type)**	**δ_H (*mult.*; J_{Hz})**	**HMBC correlations**
1	88.97 (CH)	6.32 (*d*; 3.0)	C-2, C-3, C-5, 1-C=O
2	69.15 (CH)	5.09 (*dd*; 10.2, 3.0)	C-1, C-3, 2-C=O
3	69.78 (CH)	5.47 (*t*; 10.2)	C-2, C-4, 3-C=O
4	67.85 (CH)	5.14 (*t*; 10.2)	C-3, C-5, C-6, 4-C=O
5	69.78 (CH)	4.13 (*m*)	C-1, C-4
6	61.42 (CH_2)	4.27 (*m*), 4.09 (*m*)	C-4, C-5, 6-C=O
1-OAc	168.67 (C=O)		
	20.76 (CH_3)	2.19 (*s*)	1-C=O
2-OAc	169.58 (C=O)		
	20.55 (CH_3)	2.04 (*s*)	2-C=O
3-OAc	170.14 (C=O)		
	20.34 (CH_3)	2.02 (*s*)	3-C=O
4-OAc	169.34 (C=O)		
	20.45 (CH_3)	2.03 (*s*)	4-C=O
6-OAc	170.54 (C=O)		
	20.58 (CH_3)	2.10 (*s*)	6-C=O

ART27: β-D-glucopyranoside penta-acetate

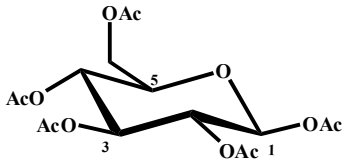

ART27, a white solid, was obtained from the acetylation of the methanolic extract of the leaves. The IR spectrum exhibited absorption at 1759 cm^{-1} for a carbonyl stretching. The ^{1}H NMR spectrum (**Table 50**) showed the resonances of an anomeric proton H-1 (δ_H 5.72, *d*, *J* = 9.3 Hz), five acetyl groups [δ_H 2.11, 2.08, 2.03 (2xCH_3) and 2.01], four methine protons (δ_H 5.23, *t*, *J* = 9.3 Hz, H-3; 5.13, *t*, *J* = 9.3 Hz, H-4; 5.11, *t*, *J* = 9.3 Hz, H-2 and 3.85, *ddd*, *J* = 9.3, 4.5 and 2.1 Hz, H-5) and methylene protons (δ_H 4.30, *dd*, *J* = 12.6 and 4.5 Hz and 4.10, *dd*, *J* = 12.6 and 2.1 Hz, H_2-6). The chemical shift and a coupling constant of *J* = 9.3 Hz of H-1 suggested that it was an α-anomeric proton. Therefore, β-D-glucopyranoside penta-acetate was assigned. The ^{13}C NMR spectrum (**Table 50**) displayed the resonances of five carbonyl carbons (δ_C 170.55, 170.04, 169.35, 169.20 and 168.91), five methine carbons (δ_C 91.65, 72.74, 72.67, 70.67 and 67.72), one methylene carbon (δ_C 61.41) and five methyl carbons [δ_C 20.76, 20.65 and 20.52 (3xC)]. The HMBC experiment (**Table 50**) completely confirmed the assigned structure. These data was in agreement with those of the authentic compound. Therefore, **ART27** was clearly identified to be β-D-glucopyranoside penta-acetate.

Table 50 The NMR spectral data of **ART27**

Position	**δ_C (Type)**	**δ_H (*mult.*; J_{Hz})**	**HMBC correlations**
1	91.65 (CH)	5.72 (*d*; 9.3)	C-3, C-5, 1-C=O
2	70.67 (CH)	5.11 (*t*; 9.3)	C-1, C-3, 2-C=O
3	72.74 (CH)	5.23 (*t*; 9.3)	C-1, C-2, C-4, 3-C=O
4	67.72 (CH)	5.13 (*t*; 9.3)	C-3, C-5, C-6, 4-C=O
5	72.67 (CH)	3.85 (*ddd*; 9.3, 4.5, 2.1)	C-1, C-3, C-4, C-6
6	61.41 (CH_2)	4.30 (*dd*, 12.6, 4.5)	C-4, C-5, 6-C=O
		4.10 (*dd*, 12.6, 2.1)	
1-OAc	168.91 (C=O)		
	20.76 (CH_3)	2.11 (*s*)	1-C=O
2-OAc	169.35 (C=O)		
	20.52 (CH_3)	2.03 (*s*)	2-C=O
3-OAc	170.04 (C=O)		
	20.52 (CH_3)	2.01 (*s*)	3-C=O
4-OAc	169.20 (C=O)		
	20.52 (CH_3)	2.03 (*s*)	4-C=O
6-OAc	170.55 (C=O)		
	20.65 (CH_3)	2.08 (*s*)	6-C=O

ART29: sucrose octa-acetate

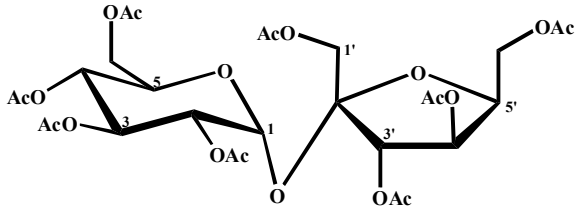

ART29 was obtained as a white solid. The IR spectrum exhibited absorptions at 1757 and 1747 cm^{-1} for a carbonyl stretching. The ^{13}C NMR spectrum (**Table 51**) displayed the resonances of twelve oxygenated carbon signals of one quaternary at δ_C 103.94, eight methine carbons at δ_C 89.87, 79.06, 75.64, 74.94, 70.21, 69.56, 68.44 and 68.15, and three methylene carbons at δ_C 63.57, 62.81 and 61.71. The spectrum further showed the presence of eight acetyl groups [δ_C 170.62, 170.42, 170.03 (2xC), 169.96, 169.83, 169.59, 169.44, and 20.61 (8xCH_3)]. These data indicated that **ART29** was a disaccharide octa-acetate. The ^1H NMR spectrum (**Table 51**) revealed the characteristic signals of α-D-glucose [δ_H 5.69 (*d*, *J* = 3.6 Hz, H-1), 5.44 (*t*, *J* = 10.5 Hz, H-3), 5.08 (*t*, *J* = 10.5 Hz, H-4), 4.87 (*dd*, *J* = 10.5 and 3.6 Hz, H-2), 4.14 (*m*, H_2-6), 4.28 (*m*, H_2-6) and 4.26 (*m*, H-5)] and fructose [δ_H 5.45 (*d*; *J* = 5.7 Hz, H-3'), 5.37 (*t*; *J* = 5.7 Hz, H-4'), 4.31 (*dd*; *J* = 11.7 and 4.5 Hz, H_2-6'), 4.24 (*m*, H_2-6'), 4.21 (*m*, H-5') and 4.18 (*s*, H_2-1')]. The resonances of eight acetyl protons [δ_H 2.18, 2.12 (2xCH_3), 2.11, 2.10 (2xCH_3), 2.05 and 2.02] were also observed. The HMBC experiment (**Table 51**) clearly confirmed the assigned structure. Its ^1H NMR data was in agreement with the data of authentic compound. **ART29** thus was confirmed as sucrose octa-acetate.

Table 51 The NMR spectral data of **ART29**

Position	δ_C (Type)	δ_H (*mult.*; J_{Hz})	HMBC correlations
1	89.87 (CH)	5.69 (*d*, 3.6)	C-3, C-5, C-2'
2	70.21 (CH)	4.87 (*dd*, 10.5, 3.6)	C-3, C-4, 2-C=O
3	69.56 (CH)	5.44 (*t*, 10.5)	C-1, C-2, C-4, 3-C=O
4	68.15 (CH)	5.08 (*t*, 10.5)	C-3, C-5, C-6, 4-C=O
5	68.44 (CH)	4.26 (*m*)	
6	61.71 (CH_2)	4.14 (*m*), 4.28 (*m*)	
2-OAc	170.03 (C=O)		
	20.61 (CH_3)	2.10 (*s*)	2-C=O
3-OAc	169.59 (C=O)		
	20.61 (CH_3)	2.02 (*s*)	3-C=O
4-OAc	169.44 (C=O)		
	20.61 (CH_3)	2.05 (*s*)	4-C=O
6-OAc	170.62 (C=O)		
	20.61 (CH_3)	2.10 (*s*)	6-C=O
1'	62.81 (CH_2)	4.18 (*s*)	C-2', C-3', 1'-C=O
2'	103.94 (C)		
3'	75.64 (CH)	5.45 (*d*; 5.7)	C-1', C-4', C-5', 3'-C=O
4'	74.94 (CH)	5.37 (*t*; 5.7)	C-3', C-5', C-6', 4'-C=O
5'	79.06 (CH)	4.21 (*m*)	
6'	63.57 (CH_2)	4.31 (*dd*; 11.7, 4.5)	C-4', C-5', 4'-C=O
		4.24 (*m*)	
1'-OAc	170.03 (C=O)		
	20.61 (CH_3)	2.12 (*s*)	1'-C=O
3'-OAc	169.83 (C=O)		
	20.61 (CH_3)	2.18 (*s*)	3'-C=O
4'-OAc	169.96 (C=O)		
	20.61 (CH_3)	2.11 (*s*)	4'-C=O

6'-OAc	170.42 (C=O) 20.61 (CH_3)	2.12 (*s*)	6'-C=O

3.2 Antibacterial activity of some of the isolated phloroglucinols

The extracts from the leaves and stems of *R. tomentosa* were tested on antibacterial activity against *S. aureus* and MRSA. The results indicated that the crude CH_2Cl_2 and Me_2CO extracts from its leaves exhibited strong activity against *S. aureus* and MRSA with MIC values of 31.25 and 62.5 μg/mL, respectively, The CH_2Cl_2 and Me_2CO extracts from its stems were found to show no activities (**Table 52**).

Some of the isolated phloroglucinols were also evaluated for their antibacterial activity against *S. aureus*, MRSA, *S. pyogenes* and *E. coli*. The results indicated that rhodomyrtosones A-G and rhodomyrtone exhibited activities against three types of Gram-positive bacteria, *S. aureus*, MRSA and *S. pyogenes* (**Table 53**). Rhodomyrtosone B (**ART9**), rhodomyrtosone D (**ART11**), rhodomyrtone (**ART6**) and rhodomyrtosone G (**ART19**) were able to inhibit the growth of *S. aureus* with MIC values of 6.25, 12.5, 0.39 and 1.56 μg/mL and MRSA with MIC values of 12.5, 25, 0.39 and 1.56 μg/mL, respectively. Rhodomyrtosone B (**ART9**), rhodomyrtosone D (**ART11**) and rhodomyrtone (**ART6**) further showed the inhibitory activity against *S. pyogenes* with MIC values of 3.125, 12.5 and 0.39 μg/mL, respectively. Compound **ART19** was not tested against *S. pyogenes* due to insufficient amount. Rhodomyrtosones A (**ART2**), C (**ART4**), E (**ART18**) and F (**ART20**) showed no activity at the concentration 100 μg/mL. Rhodomyrtone (**ART6**), which is the most active compound, provided stronger antibacterial activity than the reference antibiotic, vancomycin. No activity was observed for rhodomyrtosones A-F (**ART2**, **ART9**, **ART4**, **ART11**, **ART18** and **ART20**) and rhodomyrtone (**ART6**) against Gram-negative bacteria tested, *E. coli* ATCC 25922 and *E. coli* O157:H7 (RIMD 05091078), at the concentration 100 μg/mL.

Table 52 Antibacterial activity of the extracts from *R. tomentosa*

extract	MIC (μg/mL)	
	S. aureus	MRSA
Leaves		
CH_2Cl_2 extract	31.25	31.25
Me_2CO extract	62.5	62.5
Stems		
CH_2Cl_2 extract	NA	NA
Me_2CO extract	NA	NA
vancomycin	0.60	1.25

NA = no activity

Table 53 Antibacterial activity of acylphloroglucinols isolated from *R. tomentosa*

Compound	MIC (μg/mL)		
	S. aureus	MRSA	*S. pyogenes*
ART2	>100	>100	>100
ART4	>100	>100	>100
ART6	0.39	0.39	0.39
ART9	6.25	12.5	3.125
ART11	12.5	25	12.5
ART18	>100	>100	>100
ART19	1.56	1.56	-
ART20	>100	>100	>100
vancomycin	0.60	1.25	-
penicillin G	-	-	0.015

- = not tested

3.3 Biosynthetic proposal of some of the isolated phloroglucinols

The biosynthetic pathway of **ART2-4**, **ART9**, **ART11**, and **ART18-ART20** can now be proposed. Isovalerylphloroglucinol (**3**) was produced from condensation of isovaleryl-CoA (**1**) (Mahmud *et al.*, 2002; Bode *et al*., 2009) with three units of malonyl-CoA (**2**) by a polyketide synthase (Paniego *et al*., 1999) and was further *C*-methylated (Birch *et al.*, 1966) to give leptospermone (**4**). An intermediate **5** was then formed by condensation of **3** and **4**. This compound is not known and has not been isolated from our extract. However, it is closely related to 4-cyclohexene-1,3-dioxo-5-hydroxy-2,2,6,6-tetramethyl-4-{1-[2,6-dihydroxy-4-methoxy-3-(3-methyl-1-oxobutyl)phenyl]-3-methylbutyl}(Bloor, 1992). Cyclisation of an hydroxyl group of the isovaleryl-phloroglucinol moiety with a carbonyl group of the *β*-triketone moiety forming the hemiketal intermediate and then dehydration (Dachriyanus *et al.*, 2002) gave **ART9** (rhodomyrtosone B) and **ART6** (rhodomyrtone). The Aldol-like condensation of **ART6** (rhodomyrtone) or **ART9** (rhodomyrtosone B) with leptospermone (**4**) giving trimeric acylphloroglucinol (**3**), following by formation of benzopyran produced **ART4** (rhodomyrtosone C). Oxidation of an isobutyl group followed by formation of bisfuran via cyclisation and dehydration of **5** could give **ART2** (rhodomyrtosone A) and **ART3** (rhodomyrtosone H). Further reacted of **ART3** (rhodomyrtosone A) with **4** finally gave **ART18** (rhodomyrtosone E) and **ART20** (rhodomyrtosone F). **ART11** (rhodomyrtosone D), a symmetric molecule containing two *β*-triketone moieties, may be obtained by oxidation of an isobutyl group of the intermediate **9**, followed by formation of bisfuran. The intermediate **9** can be plausibly derived by condensation of leptospermone (**4**) and syncapic acid (**8**). The biosynthetic pathway of **ART19** (rhodomyrtosone G) would proceed in the same manner as for **ART6** (rhodomyrtone), with 2-methylbutyryl-CoA as a precursor.

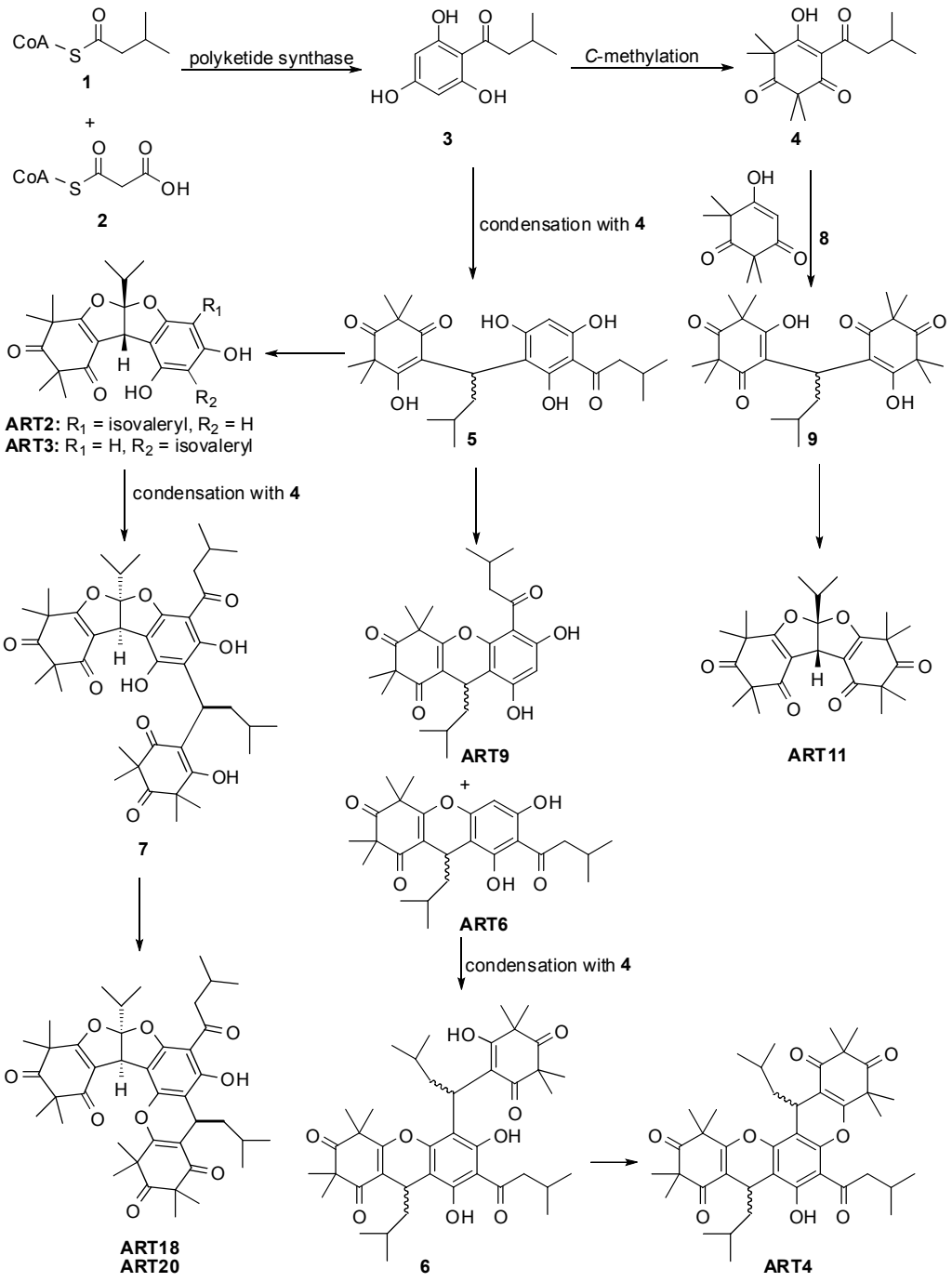

Proposed biosynthetic relationships of **ART2-4**, **ART6**, **ART9**, **ART11**, **ART18** and **ART20**

REFERENCES

Amorim, A. C. L.; Lima, C. K. F.; Hovell, A. M. C.; Miranda, A. L. P.; Rezende, C. M. **2009**. "Antinociceptive and hypothermic evaluation of the leaf essential oil and isolated terpenoids from *Eugenia uniflora* L. (Brazilian Pitanga)", *Phytomedicine*, 16, 923-928.

Anderson, N. H.; Ollis, W. D.; Underwood, J. G.; Scrowston, R. M., **1969**. "Constitution of the dibenzofuran, Ψ-rhodomyrtoxin, isolated from *Rhodomyrtus macrocarpa* Benth.", *J. Chem. Soc*., 2403-2408.

APIRS, Center for Aquatic and Invasive Plants. 2001. Invasive Non-indigenous Plants in Florida: Downy rose myrtle (*Rhodomyrtus tomentosa*). University of Florida, IFAS, Center for Aquatic and Invasive Plants, Gainesville, Florida. Available: http://aquat1.ifas.ufl.edu/rhotom.html (Accessed June 1, 2010)

Begum, S.; Hassan, S. I.; Siddiqui, B. S.; Shaheen, F.; Ghayur, M. N.; Gilani, A. H. **2002**. "Triterpenoids from the leaves of *Psidium guajava*", *Phytochemistry*, 61, 399-403.

Benyahia, S.; Benayache, S.; Benayache, F.; León, F.; Quintana, J.; López, M.; Hernández, J. C.; Estévez, F.; Bermejo, J. **2005**. "Cladocalol, a pentacyclic 28-nor-triterpene from *Eucalyptus cladocalyx* with cytotoxic activity", *Phytochemistry*, 66, 627-632.

Birch, A. J.; Willis, J. L.; Hellyer, R. O.; Salahud-Din, M. **1966**. "The biosynthesis of tasmanone", *J. Chem. Soc.*, 1337.

Bloor, S. J. **1992**. "Antiviral Phloroglucinols from New Zealand *Kunzea* Species", *J. Nat. Prod*., 55, 43-47.

Bode, H. B.; Ring, M. W.; Schwär, G.; Altmeyer, M. O.; Kegler, C.; Jose, I. R.; Singer, M.; Müller, R. **2009**. "Identification of additional players in the alternative biosynthesis pathway to isovaleryl-CoA in the Myxobacterium *Myxococcus xanthus*", *ChemBioChem*., 10, 128-140.

Bonilla, A.; Duque, C.; Garzón, C.; Takaishi, Y.; Yamaguchi, K.; Hara, N.; Fujimoto, Y. **2005**. "Champanones, yellow pigments from the seeds of Champa (*Campomanesia lineatifolia*)", *Phytochemistry*, 66, 1736-1740.

Boonyaratavej, S.; Tantayanontha, S.; Kitchanachai, P.; Chaichantipyuth, C.; Chittawong, V.; Miles, D. H. **1992**. "*Trans*-triacontyl-4-hydroxy-3-methoxy-cinnamate, a new compound from the Thai *Bridelia ovata*", *J. Nat. Prod*., *55*, 1761-1763.

Brophy, J. J.; Goldsack, R. J.; Forster, P. I., **1997**. "The essential oils of the Australian species of *Rhodomyrtus* (Myrtaceae)", *Flavour and Fragrance Journal*, 12, 103-108.

Carroll, A. R.; Lamb, J.; Moni, R.; Guymer, G. P.; Forster, P. I.; Quinn, R. J. **2008a**. "Myrtucommulones F-I, phloroglucinols with thyrotropin-releasing hormone receptor-2 binding affinity from the seeds of *Corymbia scabrida*", *J. Nat. Prod.*, 71, 1564-1568.

Carroll, A. R.; Urban, S.; Lamb, J.; Moni, R.; Guymer, G. P.; Forster, P. I.; Quinn, R. J. **2008b**. "Corymbones A and B, phloroglucinols with thyrotropin releasing hormone receptor 2 binding affinity from the flowers of *Corymbia peltata*", *J. Nat. Prod.*, 71, 881-883.

Charles, R.; Garg, S. N. ; Kumar, S. **1998**. "An orsellinic acid glucoside from *Syzygium aromatica*", *Phytochemistry*, 38, 1375-1376.

Clinical and Laboratory Standards Institute (CLSI), **2006**. "Methods for Dilution Antimicrobial Susceptibility Tests for Bacteria that Grow Aerobically; Approved Standard", 7th ed., Clinical and Laboratory Standards Institute Document M7-A7. Clinical and Laboratory Standards Institute, 900 West Valley Road, Suite 1400, Wayne, Pennsylvania 19087-1898 USA.

Consolini, A. E.; Baldini, O. A. N.; Amat, A. G. **1999**. "Pharmacological basis for the empirical use of *Eugenia uniflora* L. (Myrtaceae) as antihypertensive", *Journal of Ethnopharmacology*, 66, 33-39.

Crow, W. D.; Nicholls, W.; Sterns, M. **1971**. "Root Inhibitors in *Eucalyptus grandis*: Naturally Occurring Derivatives of the 2,3-Dioxabicyclo[4.4.0]decane System", *Tetrahedron Lett*., 18, 1353-1356.

Cutillo, F.; Dellagreca, M.; Previtera, L.; Zarrelli, A. **2005**. "C_{13} norisoprenoids from *Brassica fruticulosa*", *Nat. Prod. Res*., 19, 99-103.

D'Abrosca, B.; DellaGreca, M.; Fiorentino, A.; Monaco, P.; Oriano, P.; Temussi, F. **2004**. "Structure elucidation and phytotoxicity of C_{13} *nor*-isoprenoids from *Cestrum parqui*", *Phytochemistry*, 65, 497-505.

Dachriyanus; Fahmi, R.; Sargent, M. V.; Skelton, B. W.; White, A. W. **2004**. "5-Hydroxy-3,3',4',5',7-pentamethoxyflavone (combretol)", *Acta Cryst*., E60, o86-o88.

Dachriyanus; Salni; Sargent, M. V.; Skelton, B. W.; Soediro, I.; Sutisna, M.; White, A. H.; Yulinah, E. **2002.** "Rhodomyrtone, an antibiotic from *Rhodomyrtus tomentosa*", *Aust. J. Chem.*, 55, 229-232.

Datta, B. K.; Datta, S. K.; Rashid, M. A.; Nash, R. J.; Sarker, S. D. **2000**. "A sesquiterpene acid and flavonoids from *Polygonum viscosum*", *Phytochemistry*, 54, 201-205.

Djipa, C. D.; Delmée, M.; Quetin-Leclercq, J. **2000**. "Antimicrobial activity of bark extracts of *Syzygium jambos* (L.) Alston (Myrtaceae)", *Journal of Ethnopharmacology*, 71, 307-313.

Djoukeng, J. D.; Abou-Mansour, E.; Tabacchi, R.; Tapondjou, A. L.; Bouda, H.; Lontsi, D. **2005**. "Antibacterial triterpenes from *Syzygium guineense* (Myrtaceae)", *Journal of Ethnopharmacology*, 101, 283-286.

Elkhateeb, A.; Subeki; Takahashi, K.; Matsuura, H.; Yamasaki, M.; Yamato, O.; Maede, Y.; Katakura, K.; Yoshihara, T.; Nabeta, K. **2005**. "Anti-babesial ellagic acid rhamnosides from the bark of *Elaeocarpus parvifolius*", *Phytochemistry*, 66, 2577-2580.

El-Toumy, S. A. A.; Rauwald, H. W. **2003**. "Two new ellagic acid rhamnosides from *Pinica granatum* heartwood", *Planta Med.*, 69, 679-682.

Fernández, A.; Álvarez, A.; García, M. D.; Sáenz, M. T. **2001**. "Anti-inflammatory effect of *Pimenta racemosa* var. *ozua* and isolation of the triterpene lupeol", *Il Farmaco*, 56, 335-338.

Fuchino, H.; Satoh, T.; Tanaka, N. **1995**. "Chemical evaluation of *Betula* species in Japan. I. Constituents of *Betula ermanii*", *Chem*. *Pharm*. *Bull*., 43, 1937-1942.

Fujimoto, Y.; Usui, S.; Makino, M.; Sumatra, M. **1996**. "Phloroglucinols from *Baeckea frutescens*", *Phytochemistry*, 41, 923-925.

Fukuyama, Y.; Minami, H.; Kuwayama, A. **1998**. "Garsubellins, polyisoprenylated phloroglucinol derivatives from *Garcinia subelliptica*", *Phytochemistry*, 49, 853-857.

García, M. D.; Fernández, M. A.; Alvarez, A.; Saenz, M. T. **2004**. "Antinociceptive and anti-inflammatory effect of the aqueous extract from leaves of *Pimenta racemosa* var. *ozua* (Mirtaceae)", *Journal of Ethnopharmacology*, 91, 69-73.

Ghisalberti, E. L. **1996**. "Bioactive acyphloroglucinol derivatives from *Eucalyptus* species", *Phytochemistry*, 41, 7-22.

Goodger, J. Q. D.; Cao, B.; Jayadi, I.; Williams, S. J.; Woodrow, I. E. **2009**. "Non-volatile components of the essential oil secretory cavities of *Eucalyptus* leaves: Discovery of two glucose monoterpene esters, cuniloside B and froggattiside A", *Phytochemistry*, 70, 1187-1194.

Grangeiro, M. S.; Calheiros-Lima, A. P.; Martins, M. F.; Arruda, L. F.; Garcez-do-Carmo, L.; Santos, W. C. **2006**. "Pharmacological effects of *Eugenia punicifolia* (Myrtaceae) in cholinergic nicotinic neurotransmission", *Journal of Ethnopharmacology*, 108, 26-30.

Hasegawa, T.; Takano, F.; Takata, T.; Niiyama, M.; Ohta, T. **2008**. "Bioactive monoterpene glycosides conjugated with gallic acid from the leaves of *Eucalyptus globulus*", *Phytochemistry*, 69, 747-753.

Hattab, M. E.; Culioli, G.; Valls, R.; Richou, M.; Piovetti, L. **2008**. "Apo-fucoxanthinoids and loliolide from the brown alga *Cladostephus spongiosus* f. *verticillatus* (Heterokonta, Sphacelariales)", *Biochemical Systematics and Ecology*, 36, 447-451.

He, Limin; Lihua, Zhang; Jianbiao, Tang; Qui, Houyuan; Su, Yijuan, **1998**. "Properties and extraction of pigment from *Rhodomyrtus tomentosa* (Ait.) Hassk", *Jingxi Huagong*, 15, 27-29.

Hui, W. -H.; Li, M. -M., **1976**. "Two new triterpenoids from *Rhodomyrtus tomentosa*", *Phytochemistry*, 15, 1741-1743.

Hui, W. -H.; Li, M. -M.; Luk, K., **1975**. "Triterpenoids and steroids from *Rhodomyrtus tomentosa*", *Phytochemistry*, 14, 833-834.

Hou, A. J.; Wu, Y. J.; Liu, Y. Z., **1999**. "Flavone glycosides and an ellagitannin from Downy Rosemyrtle (*Rhodomyrtus tomentosa*)", *Zhongcaoyao*, 30, 645-648.

Igboechi, C. A.; Parfitt, R. T.; Rowan, M. G. **1984**. "Two dibenzofuran derivatives from fruits of *Rhodomyrtus macrocarpa*", *Phytochemistry*, 23, 1139-1141.

Ishikawa, T.; Donatini, R. S.; Diaz, I. E. C.; Yoshida, M.; Bacchi, E. M.; Kato, E. T. M. **2008**. "Evaluation of gastroprotective activity of *Plinia edulis* (Vell.) Sobral (Myrtaceae) leaves in rats", *Journal of Ethnopharmacology*, 118, 527-529.

Ito, H.; Iwamori, H.; Kasajima, N.; Kanedab, M.; Yoshida, T. **2004**. "Kunzeanones A, B, and C: novel alkylated phloroglucinol metabolites from *Kunzea ambigua*", *Tetrahedron*, 60, 9971-9976.

Jeong, E. -Y.; Jeon, J. -H.; Kim, H. -W.; Kim, M. -G.; Lee, H. -S. **2009**. "Antimicrobial activity of leptospermone and its derivatives against human intestinal bacteria", *Food Chemistry*, 115, 1401-1404.

Jie, C.; Craven, L. A. **2007**. "Flora of China", vol. 13, pp321-359.

Jirovetz, L.; Buchbauer, G.; Stoilova, I.; Stoyanova, A.; Krastanov, A.; Schmidt, E. **2006**. "Chemical composition and antioxidant properties of clove leaf essential oil", *J. Agric. Food Chem*., 54, 6303-6307.

Kashman, Y.; Rotstein, A; Lifshitz, A. **1974**. "The structure determination of two new acylphloroglucinols from *Myrtus communis* L.", *Tetrahedron*, 30, 991-997.

Khac, D. D.; Tran-Van, S.; Campos, A. M.; Lallemand, J.-Y.; Feizon, M. **1990**. "Ellagic compounds from *Diplopanax stachyanthus*", *Phytochemistry*, 29, 251-256.

Khambay, B. P. S.; Beddie, D. G.; Hooper, A. M.; Simmonds, M. S. J.; Green, P. W. C. **1999**. "New insecticidal tetradecahydroxanthenediones from *Callistemon viminalis*", *J. Nat. Prod.*, 62, 1666-1667.

Khambay, B. P. S.; Beddie, D. G.; Simmonds, M. S. J. **2002**. "An insecticidal mixture of tetramethylcyclohexenedione isomers from *Kunzea ambigua* and *Kunzea baxterii*", *Phytochemistry*, 59, 69-71.

Kikuzaki, H.; Miyajima, Y.; Nakatani, N. **2008**. "Phenolic glycosides from berries of *Pimenta dioica*", *J. Nat. Prod.*, 71, 861-865.

Kim, J. -P.; Lee, I. -K.; Yun, B. -S.; Chung, S. -H.; Shim, G. -S.; Koshino, H.; Yoo, I. -D. **2001**. "Ellagic acid rhamnosides from the stem bark of *Eucalyptus globulus*", *Phytochemistry*, 57, 587-591.

Kim, J. S.; Kim, J. C.; Shim, S. H.; Lee, E. J.; Jin, W. Y.; Bae, K. H.; Son, K. H.; Kim, H. P.; Kang, S. S.; Chang H. W., **2006**. "Chemical constituents of the root of *Dystaenia takeshimana* and their anti-inflammatory activity", *Arch. Pharm. Res.*, 29 (8), 617-623.

Kumari, G. N. K.; Rao, L. J. M.; Rao, N. S. P. **1985**. "Flavonol 3-*O*-methyl ethers from *Solanum pubescens*", J. *Nat. Prod.*, 48, 149-150.

Kimura, J.; Maki, N. **2002**. "New Loliolide Derivatives from the Brown Alga *Undaria pinnatifida*", *J. Nat. Prod.* 65, 57-58.

Lapčík, O.; Klejdus, B.; Kokoška, L.; Davidová, M.; Afandi, K.; Kubáň, V.; Hampl, R. **2005**. "Identification of isoflavones in *Acca sellowiana* and two *Psidium* species (Myrtaceae)", *Biochemical Systematics and Ecology*, 33, 983-992.

Lee, C. -K. **1998**. "A new norlupene from the leaves of *Melaleuca leucadendron*", *J. Nat. Prod*., 61, 375-376.

Lee, I. K.; Kim, D. H.; Lee, S. Y.; Kim, K. R.; Choi, S. U.; Hong, J. K.; Lee, J. H.; Park, Y. H.; Lee, K. R. **2008**. "Triterpenoic acids of *Prunella vulgaris* var. *lilacina* and their cytotoxic activities *in vitro*", *Arch. Pharm. Res*., 31, 1578-1583.

Lendl, A.; Werner, I.; Glasl, ; Kletter, S. C. ; Mucaji, P.; Presser, A.; Reznicek, G.; Jurenitsch, J.; Taylor, D. W. **2005**. "Phenolic and terpenoid compounds from *Chione venosa* (SW.) URBAN var. *venosa* (Bois Bandé)", *Phytochemistry*, 66, 2381-2387.

Lenherr, A.; Fang, N.; Mabry, T. J. **1986**. "Flavonols from *Gutierrezia alamanii* var. *megalocephala*", *J. Nat. Prod*., 49, 185-186.

Lounasmaa, M.; Puri, H. -S.; Widen, C. -J. **1977**. "Phloroglucinol derivatives of *Callistemon lanceolatus* leaves", *Phytochemistry*, 16, 1851-1852.

Lowry, J. B., **1976**. "Anthocyanins of the Melastomataceae, Myrtaceae and some allied families", *Phytochemistry*, 15, 513-516.

Lucas, E. J.; Belsham, S. R.; NicLughadha, E. M.; Orlovich, D. A.; Sakuragui, C. M.; Chase, M. W.; Wilson, P. G. **2005**. "Phylogenetic patterns in the fleshy-fruited Myrtaceae - preliminary molecular evidence", *Plant Syst. Evol*., 251, 35-51.

Lui, Y. Z.; Hou, A. J.; Ji, C. R.; Wu, Y. J., **1997**. "A new *C*-glycosidic hydrolysable tannin from *Rhodomyrtus tomentosa*", *Chin. Chem. Lett*., 8, 39-40.

Lui, Y. Z.; Hou, A. J.; Ji, C. R.; Wu, Y. J., **1998**. "Isolation and structure of hydrolysable tannins from *Rhodomyrtus tomentosa*", *Tianran Chanwu Yanjiu Yu Kaifa*, 10, 14-19.

Mahmud, T.; Bode, H. B.; Silakowski, B.; Kroppenstedt, R. M.; Xu, M.; Nordhoff, S.; Höfle, G.; Müller, R. **2002**. "A novel biosynthetic pathway providing precursors for fatty acid biosynthesis and secondary metabolite formation in Myxobacteria", *J. Biol. Chem.*, 277, 32768-32774.

Markman, B. E. O.; Bacchi, E. M.; Kato, E. T. M. **2004**. "Antiulcerogenic effects of *Campomanesia xanthocarpa*", *Journal of Ethnopharmacology*, 94, 55-57.

Martos, I.; Cossentini, M.; Ferreres, F.; Tomás-Barberán, F. A. **1997**. "Flavoniod composition of Tunisian honeys and propolis", *J. Agric. Food Chem*., 45, 2824-2829.

Melching, S.; Bülow, N.; Wihstutz, K.; Jung, S.; König, W. A. **1997**. "Natural occurrence of both enantiomers of cadina-3,5-diene and 6-amorphene", *Phytochemistry*, 44, 1291-1296.

Menut, C.; Molangui, T.; Lamaty, G. E. **1995**. "Aromatic plants of tropical central Africa. 23. Chemical composition of leaf essential oils of *Eucalyptus goniocalyx* F. Muell. and *Eucalyptus patens* Benth. grown in Rwanda", *J. Agric. Food Chem*., 43, 1267-1271.

Mitaine-Offer, A. -C.; Djoukeng, J. D.; Tapondjou, L. A.; Bouda, H.; Lerche, H.; Lontsi, D.; Lacaille-Dubois, M. -A. **2003**. "Constituents of the leaves of *Eucalyptus saligna*", *Biochem. Syst. Ecol*., 31, 1457-1460.

Mohamed, G. A.; Ibrahim, S. R. M. **2007**. "Eucalyptone G, a new phloroglucinol derivative and other constituents from *Eucalyptus globules* Labill", *ARKIVOC*, xv, 281-291.

Mongkolsuk, S.; Dean, F. M.; Houghton, L. E. **1966**. "Combretol from *Combretum quadrangulare*", *J. Chem. Soc*., 125.

Moon, S. -S.; Rahman, A. A.; Kim, J. -Y.; Kee, S. -H. **2008**. "Hanultarin, a cytotoxic lignan as an inhibitor of actin cytoskeleton polymerization from the seeds of *Trichosanthes kirilowii*", *Bioorg. Med. Chem*., 16, 7264-7269.

Musabayane, C. T.; Mahlalela, N.; Shode, F. O.; Ojewole, J. A. O. **2005**. "Effects of *Syzygium cordatum* (Hochst.) [Myrtaceae] leaf extract on plasma glucose and hepatic glycogen in streptozotocin-induced diabetic rats", *Journal of Ethnopharmacology*, 97, 485-490.

Mustafa, K. A.; Kjaergaard, H. G.; Perry, N. B.; Weavers, R. T. **2003**. "Hydrogen-bonded rotamers of 2',4',6'-trihydroxy-3'-formyldihydrochalcone, an intermediate in the synthesis of a dihydrochalcone from *Leptospermum recurvum*", *Tetrahedron*, 59, 6113-6120.

Nassar, M. I. **2006**. "Flavonoid triglycosides from the seeds of *Syzygium aromaticum*", *Carbohydrate Research*, 341, 160-163.

Nitta, Y.; Kikuzaki, H.; Ueno, H. **2009**. "Inhibitory activity of *Pimenta dioica* extracts and constituents on recombinant human histidine decarboxylase", *Food Chemistry*, 113, 445-449.

Nojima, J.; Murakami, T.; Kiso, A., **2007**. "Piceatannol 4'-O-*β*-D-glucopyranoside for antioxidants, antiinflammatory agents, skin-lightening agents, antiaging agents, tyrosinase inhibitors, and skin cosmetics", *Jpn. Kokai Tokkyo Koho*, JP 2007223919 A 20070906.

Nonaka, G.; Aiko, Y.; Aritake, K.; Nashioka, I. **1992**. "Tannins and related compounds. CXIX. Samarangenins A and B, novel proanthocyanidins with doubly bonded structures, from *Syzygium samarangens* and *S. aqueum*", *Chem. Pharm. Bull*., 40, 2671-2673.

Oh, W. K.; Lee, C. H.; Lee, M. S.; Bae, E. Y.; Sohn, C. B.; Oh, H.; Kim, B. Y.; Ahn, J. S. **2005**. "Antidiabetic effects of extracts from *Psidium guajava*", *Journal of Ethnopharmacology*, 96, 411-415.

Ong, H. C.; Nordiana, M. **1999**. "Malay ethno-medico botany in Machang, Kelantan, Malaysia", *Fitoterapia*, 70, 502-513.

Osawa, K.; Yasuda, H.; Morita, H.; Takeya, K.; Itokawa, H. **1995**. "Eucalyptone from *Eucalyptus globulus*", *Phytochemistry*, 40, 183-184.

Osman, H.; Rahim, A. A.; Isa, N. M.; Bakhir, N. M. **2009**. Antioxidant activity and phenolic content of *Paederia foetida* and *Syzygium aqueum*", *Molecules*, 14, 970-978.

Osorio, C.; Alarcon, M.; Moreno, C.; Bonilla, A.; Barrios, J.; Garzon, C.; Duque, C. **2006**. "Characterization of odor-active volatiles in Champa (*Campomanesia lineatifolia* R. & P.)", J. *Agric. Food Chem*., 54, 509-516.

Paniego, N. B.; Zuurbier, K. W. M.; Fung, S. -Y.; van der Heijden, R.; Scheffer, J. J. C.; Verpoorte, R. **1999**. "Phlorisovalerophenone synthase, a novel polyketide synthase from hop (*Humulus lupulus* L.) cones", *Eur. J. Biochem*., 262, 612-616.

Phan, M. G.; Tran, T. H.; Nguyen, T. H. A.; Phan, T. S., **2007**. "Contribution to the study on polar constituents from the buds of *Rhodomyrtus tomentosa* (Ait.) Hassk. (Myrtaceae)", *Tap Chi Hoa Hoc*, 45(6), 749-750.

Reynertson, K. A.; Wallace, A. M.; Adachi, S.; Gil, R. R.; Yang, H.; Basile, M. J.; D' Armiento, J.; Weinstein, I. B.; Kennelly, E. J. **2006**. "Bioactive depsides and anthocyanins from Jaboticaba (*Myrciaria cauliflora*)", *J. Nat. Prod*., 69, 1228-1230.

Reynertson, K. A.; Yang, H.; Jiang, B.; Basile, M. J.; Kennelly, E. J. **2008**. "Quantitative analysis of antiradical phenolic constituents from fourteen edible Myrtaceae fruits", *Food Chemistry*, 109, 883-890.

Rossi, A.; Rigano, D.; Pergola, C.; Formisano, C.; Basile, A.; Bramanti, P.; Senatore, F.; Sautebin, L. **2007**. "Inhibition of inducible nitric oxide synthase expression by an acetonic extract from *Feijoa sellowiana* Berg. fruits", *J. Agric. Food Chem*., 55, 5053-5061.

Ruberto, G.; Tringali, C. **2004**. "Secondary metabolites from the leaves of *Feijoa sellowiana* Berg.", *Phytochemistry*, 65, 2947-2951.

Russell, M.; Southwell, I. **2002**. "Monoterpenoid accumulation in *Melaleuca alternifolia* seedlings", *Phytochemistry*, 59, 709-716.

Shaheen, F.; Ahmad, M.; Khan, S. N.; Hussain, S. S.; Anjum, S.; Tashkhodjaev, B.; Turgunov, K.; Sultankhodzhaev, M. N.; Choudhary, M. I.; Atta-ur-Rahman. **2006**. "New α-glucosidase inhibitors and antibacterial compounds from *Myrtus communis* L.", *Eur. J. Org. Chem.*, 2371-2377.

Shao, Y.; Zhou, B. -N.; Lin, L. -Z.; Cordell,G. A. **1995**. "Triterpene saponins from *Aster yunnanensis*", *Phytochemistry*, 38, 1487-1492.

Siddiqui, B. S.; Sultana, I.; Begum, S. **2000**. "Triterpenoidal constituents from *Eucalyptus camaldulensis* var. *obtusa* leaves", *Phytochemistry*, 54, 861-865.

Singh, H. P.; Mittal, S.; Kaur, S.; Batish, D. R.; Kohli, R. K. **2009**. "Characterization and antioxidant activity of essential oils from fresh and decaying leaves of *Eucalyptus tereticornis*", *J. Agric. Food Chem*., 57, 6962-6966.

Singh, I. P.; Bharate, S. B. **2006**. "Phloroglucinol compounds of natural origin", *Nat*. *Prod*. *Rep*., 23, 558-591.

Singh, I. P.; Umehara, K.; Asai, T.; Etoh, H.; Takasaki, M.; Konoshima, T. **1998**. "Phloroglucinol-monoterpene adducts from *Eucalyptus grandis*", *Phytochemistry*, 47, l157-1159.

Smitinand, T. **2001**. "Flora of Thailand"

State of Victoria, Department of Sustainability and Environment. **2003**. "Trees and Forests Mountain Ash", pp 1-3.

Steinhaus, M.; Sinuco, D.; Polster, J.; Osorio, C.; Schieberle, P. R. **2008**. "Characterization of the aroma-active compounds in pink guava (*Psidium guajava*, L.) by application of the aroma extract dilution analysis", *J. Agric. Food Chem*., 56, 4120-4127.

Takahashi, H.; Iuchi, M.; Fujita, Y.; Minami, H.; Fukuyama, Y. **1999**. "Coumaroyl triterpenes from *Casuarina equisetifolia*", *Phytochemistry*, 51, 543-550.

Terashima, S.; Shimizu, M.; Nakayama, H.; Ishikura, M.; Ueda, Y.; Imai, K.; Suzui, A.; Morita, N. **1990**. "Studies on reductase inhibitors from medicinal plant of "Sinfito", *Potentilla candicans*, and further synthesis of their related compounds", *Chem. Pharm. Bull*., 38, 2733-2736.

Tian, L. -W.; Zhang, Y. -J.; Wang, Y. -F.; Lai, C. -C.; Yang, C. -R. **2009**. "Eucalmaidins A-E, (+)-oleuropeic acid derivatives from the fresh leaves of *Eucalyptus maideni*", *J. Nat. Prod*., 72, 1608-1611.

Tsui, W. -Y.; Brown, G. D. **1996**. "Sesquiterpenes from *Baeckea frutescens*", *J. Nat. Prod*., 59, 1084-1086.

Tuberoso, C. I. G.; Barra, A.; Angioni,A.; Sarritzu, E.; Pirisi, F. M. **2006**. "Chemical composition of volatiles in Sardinian Myrtle (*Myrtus communis* L.) alcoholic extracts and essential oils", *J. Agric. Food Chem*., 54, 1420-1426.

Tung, N. H.; Ding, Y.; Choi, E. M.; Kiem, P. V.; Minh, C. V.; Kim, Y. H. **2009**. "New anthracene glycosides from *Rhodomyrtus tomentosa* stimulate osteoblastic differentiation of MC3T3-E1 Cells", *Arch. Pharm. Res*., 32, 515-520.

Tripathi, V. K.; Pandey, V. B.; Udupa, K. N.; Rücker, G. **1992**. "Arjunolitin, a triterpene glycoside from *Terminalia arjuna*", *Phytochemistry*, 31, 349-351.

Trippett, S., **1957**. "Toxic constituents of the Australain finger cherry, *Rhodomyrtus macrocarpa* Benth.", *J. Chem. Soc*., 414-419.

Umehara, K.; Singh, I. P.; Etoh, H.; Takasaki, M. and Konoshima, T. **1998**. "Five phloroglucinol-monoterpene adducts from *Eucalyptus grandis*", *Phytochemistry*, 49, 1699-1704.

Voravuthikunchai, S. P.; Limsuwan, S.; Chusri, S. **2007**. New Perspectives on Herbal Medicines for Bacterial Infection: Natural Products II, p. 41-101. *In*: J. N. Govil, V.K. Singh, and N. T. Siddqui (eds.), Recent Progress in Medicinal Plants, Studium Press, LLC USA.

Wagner, W. L.; Herbst, D. R.; Sohmer, S. H. **1999**. Manual of the Flowering Plants of Hawai'i. 2 vols. Bishop Museum Special Publication 83, University of Hawai'i and Bishop Museum Press, Honolulu, HI.

Wandji, J.; Nkengfack, A. E.; Fomum, T.; Ubillas, R.; Killday, K. B.; Tempesta, M. S. **1990**. "A new prenylated isoflavone and long chain esters from two *Erythrina* species". *J. Nat. Prod*. 53, 1425-1429.

Wei, F. **2006**. “Manufacture of oral liquid containing traditional Chinese medicine extract for treating gynecopathy”, *Faming Zhuanli Shenqing Gongkai Shuomingshu*. China Patent No. CN1846715.

Weston, R. J. **2010**. “Bioactive products from fruit of the feijoa (*Feijoa sellowiana*, Myrtaceae): A review”, *Food Chemistry*, 121, 923-926.

Wilson, P. G.; O' Brien, M. M.; Gadek, P. A.; Quinn, C. J. **2001**. “Myrtaceae revisited: a reassessment of infrafamilial groups”, *Amer. J. Bot*., 88, 2013-2025.

Winotai, A.; Wright T.; Goolsby, J. A. **2005**. “Herbivores in Thailand on *Rhodomyrtus tomentosa* (Myrtaceae), an invasive weed in Florida”, *Florida Entomologist*, 88, 104-105.

Wolter-Filho, W.; da Rocha, A. I.; Yoshida, M.; Cottlieb, O. R. **1989**. “Chemosystematics of *Rhabdodendron*”, *Phytochemistry*, 28, 2355-2357.

Xu, R. -S.; Snyder, J. K.; Nakanishi, K. **1984**. “Robustadials A and B from *Eucalyptus obusta*”, *J. Am. Chem. Soc*., 106, 734-736.

Yagi, A.; Okamura, N.; Haraguchi, Y.; Noda, K.; Nishioka, I. **1978**. “Studies on the constituents of *Zizyphi fructus*. II. Structure of new *p*-coumaroylates of maslinic acid”, *Chem. Pharm. Bull*., 26, 3075-3079.

Yamagishi, T.; Zhang, D. -C.; Chang, J. -J.; McPhail, D. R.; McPhail, A. T.; Lee, K. -H. **1988**. “The cytotoxic principles of *Hyptis capitata* and the structures of the new triterpenes hyptatic acid-A and -B”, *Phytochemistry*, 27, 3213-3216.

Yang, G. -E.; Chen, B.; Zhang, Z.; Gong, J.; Bai, H.; Li, J.; Wang, Y.; Li, B. **2009**. “Cytotoxic activities of extracts and compounds from *Viscum coloratum* and its transformation products by *Rhodobacter sphaeroides*”, *Appl. Biochem. Biotechnol*., 152, 353-365.

APPENDIX

The NMR spectral data of known compounds from the literatures

Table 54 The NMR spectral data of **rhodomyrtone**

Position	δ_C	δ_H (***mult.***; J_{Hz})	**Position**	δ_C	δ_H (***mult.***; J_{Hz})
1	198.56		11	24.58	1.44 (*s*)
2	56.05		12	24.58	1.56 (*s*)
3	212.16		13	24.72	1.42 (*s*)
4	47.23		1'	206.75	
4a	167.65		2'	53.18	3.03 (*dd*; 15.5, 6.8) 2.97 (*dd*; 15.5, 6.8)
4b	155.63		3'	25.15	2.28 (*m*)
5	94.74	6.19 (*s*)	4'	22.81	0.98 (*d*; 6.3)
6	158.70		5'	22.74	0.98 (*d*; 6.3)
7	107.63		1"	45.82	1.48 (*m*)
8	162.84		2"	25.10	1.48 (*m*)
8a	106.30		3"	23.16	0.87 (*d*; 5.7)
9	25.19	4.30 (*t*; 5.5)	4"	22.53	0.84 (*d*; 5.7)
9a	114.26		6-OH		8.08 (*s*)
10	24.21	1.39 (*s*)	8-OH		13.39 (*s*)

Table 55 The NMR spectral data of **combretol**

Position	δ_C	δ_H (*mult.*; J_{Hz})	Position	δ_C	δ_H (*mult.*; J_{Hz})
2	155.53		1'	125.40	
3	139.34		2', 6'	106.00	7.35 (*s*)
4	178.70		3', 5'	153.06	
4a	106.00		4'	140.54	
5	161.96		3-OCH_3	60.27	3.861 (*s*)
6	97.87	6.34 (*d*; 2.2)	7-OCH_3	55.79	3.864 (*s*)
7	165.51		3', 5'-OCH_3	56.28	3.932 (*s*)
8	92.18	6.43 (*d*; 2.2)	4'-OCH_3	60.95	3.935 (*s*)
8a	156.65		5-OH		12.56 (*s*)

Table 56 The NMR spectral data of **3',5-dihydroxy-3,4',5',7-tetramethoxyflavone**

Position	δ_C	δ_H (*mult.*; J_{Hz})	Position	δ_C	δ_H (*mult.*; J_{Hz})
2	155.3		2'	108.6	7.28 (*d*; 2.0)
3	139.7		3'	149.2	
4	178.8		4'	137.8	
4a	106.1		5'	152.0	
5	162.0		6'	105.1	7.20 (*d*; 2.0)
6	98.0	6.39 (*d*; 2.0)	3-OCH_3	60.3	
7	165.6		7-OCH_3	55.8	3.87, 3.86,
8	92.2	6.75 (*d*; 2.0)	4'-OCH_3	61.1	3.82, 3.77
8a	156.8		5'-OCH_3	56.1	
1'	126.0				

Table 57 The NMR spectral data of **3,3',4-tri-*O*-methylellagic acid**

Position	δ_C	δ_H (*mult.*)	Position	δ_C	δ_H (*mult.*)
1	112.30		3'	139.90	
2	141.50		4'	152.52	
3	140.50		5'	111.58	7.51 (*s*)
4	153.70		6'	112.05	
5	107.49	7.60 (*s*)	7'	158.00	
6	114.50		3-OCH_3	61.16	4.02 (*s*)
7	157.50		4-OCH_3	56.80	3.98 (*s*)
1'	111.00		3'-OCH_3	60.89	4.04 (*s*)
2'	141.00				

Table 58 The NMR spectral data of **4-*O*-[*β*-D-glucopyranosyltetraacetate]-3,3',4'-tri-*O*-methylellagic acid**

Position	δ_C	δ_H (*mult.*)	Position	δ_C	δ_H (*mult.*)
1	114.98		3'	140.90	
2	141.30		4'	154.60	
3	141.56		5'	107.65	7.56 (*s*)
4	151.28		6'	114.98	
5	113.34	8.00 (*s*)	7'	158.10	
6	112.36		3-OCH_3	62.06	4.02 (*s*)
7	158.10		3'-OCH_3	61.80	3.96 (*s*)
1'	112.17		4'-OCH_3	56.64	3.36 (*s*)
2'	141.23				

recorded in C_6D_6 for ^1H and $CDCl_3$ for ^{13}C

Table 59 The ^{1}H NMR spectral data of **4-*O*-methylellagic acid 3'-α-rhamnoside** (A), **3-*O*-methylellagic acid 3'-*O*-α-rhamnopyranoside** (B) and **3-*O*-methyl ellagic acid 4-*O*-α-rhamnopyranoside** (C)

Position	A[b]	B[b]	C[c]
	δ_H (*mult.*; J_{Hz})	δ_H (*mult.*; J_{Hz})	δ_H (*mult.*; J_{Hz})
5	7.20 (*s*)	7.46 (*s*)	7.54 (*s*)
5'	7.30 (*s*)	7.47 (*s*)	7.71 (*s*)
1"	5.52 (*br s*)	5.73 (*d*, 1.6)	5.49 (*d*, 1.2)
2"	4.20 (*br s*)	4.34 (*dd*, 1.6, 3.4)	4.02 (*br*)
3"	3.96 (*dd*, 2.5, 9.8)	4.05 (*dd*, 3.4,9.6)	3.84 (*dd*, 9.4, 3.0)
4"	3.41 (*t*, 9.8)	3.46 (*t*, 9.6)	3.34 (*t*, 9.4)
5"	4.25 (*dd*, 6.1, 9.8)	4.46 (*dq*, 9.6, 6.2)	3.56 (*m*)
6"	1.14 (*d*, 6.1)	1.21 (*d*, 6.2)	1.15 (*d*, 6.0)
OCH_3	3.85 (*s*)	4.12 (*s*)	4.05 (*s*)

[a]recorded in $CDCl_3$+DMSO-d_6; [b]recorded in CD_3OD; [c]recorded in DMSO-d_6

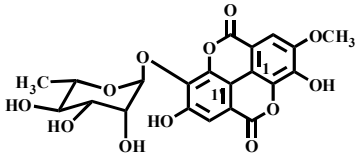

A

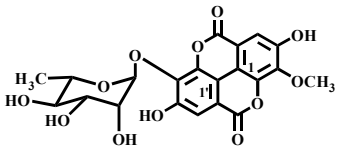

B

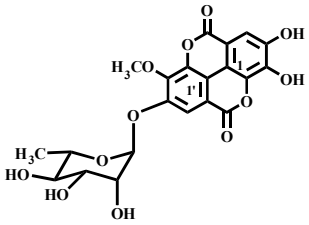

C

Table 60 The ^{13}C NMR spectral data of 4-***O*-methylellagic acid 3'-α-rhamnoside** (A), **3-*O*-methylellagic acid 3'-*O*-α-rhamnopyranoside** (B) and **3-*O*-methylellagic acid 4-*O*-α-rhamnopyranoside** (C)

Position	A[b]	B[b]	C[c]
	δ_C	δ_C	δ_C
1	113.1	112.3	115.12
2	138.2	142.3	137.07
3	152.0	143.5	140.74
4	154.0	154.4	153.31
5	107.6	114.0	112.23
6	115.2	113.3	113.84
7	161.0	161.8	159.52
1'	113.1	110.6	111.99
2'	143.8	143.6	137.07
3'	138.2	140.3	142.63
4'	154.0	153.7	147.51
5'	112.6	115.2	112.83
6'	115.2	114.6	108.14
7'	160.8	161.8	159.60
1"	103.7	102.9	100.66
2"	71.9	72.0	70.61
3"	72.1	72.2	70.80
4"	73.6	73.9	72.53
5"	71.9	71.7	70.83
6"	17.9	17.9	18.60
OCH_3	57.1	61.6	61.62

[a]recorded in $CDCl_3$+DMSO-d_6; [b]recorded in CD_3OD; [c]recorded in DMSO-d_6

Table 61 The NMR spectral data of **(6*R*,7*E*,9*R*)-9-hydroxy-4,7-megastigmadien -3-one** (A) and **(6*R*,7*E*,9*S*)-9-hydroxy-4,7-megastigmadien-3-one** (B)

Position	A		B	
	δ_C	δ_H (*mult.*; J_{Hz})	δ_C	δ_H (*mult.*; J_{Hz})
1	36.0		36.0	
2	47.4	2.32 (*d*; 16.8)	47.4	2.34 (*d*; 17.0)
		2.06 (*d*; 16.8)		2.08 (*d*; 17.0)
3	199.0		199.0	
4	125.7	5.89 (*s*)	125.7	5.89 (*s*)
5	161.7		161.7	
6	55.3	2.54 (*d*; 8.2)	55.3	2.52 (*d*; 8.6)
7	126.6	5.54 (*dd*; 15.5, 8.2)	126.6	5.53 (*dd*; 16.0, 8.8)
8	138.5	5.56 (*dd*; 15.5, 5.6)	138.5	5.67 (*dd*; 16.0, 6.0)
9	68.2	4.34 (*m*)	68.2	4.35 (*m*)
10	23.5	1.28 (*d*; 6.6)	23.5	1.30 (*d*; 6.4)
11	27.8	1.03 (*s*)	27.7	1.03 (*s*)
12	27.0	0.97 (*s*)	26.9	0.97 (*s*)
13	23.4	1.88 (*d*; 1.2)	23.4	1.90 (*s*)

Table 62 The NMR spectral data of **loliolide** and **isololiolide**

Position	Loliolide		Isololiolide
	δ_C	δ_H (*mult.*; J_{Hz})	δ_H (*mult.*; J_{Hz})
1	36.3		
2	47.7	1.97 (*ddd*; 14.5, 3.0, 2.3)	2.03 (*ddd*; 12.9, 4.4, 2.2)
		1.53 (*dd*; 14.7, 3.7)	1.33 (*dd*; 12.1,12.1)
3	67.2	4.33 (*quin*; 3.4)	4.13 (*tt*; 11.6, 4.5)
4	46.0	2.46 (*ddd*; 14.0, 3.2, 2.3)	2.53 (*ddd*; 11.5, 4.0, 2.2)
		1.78 (*dd*; 13.5, 3.7)	1.51 (*dd*; 11.7, 11.5)
5	87.1		
6	182.8		
7	113.3	5.69 (*s*)	5.71 (*s*)
8	172.3		
9	26.9	1.47 (*s*)	1.26 (*s*)
10	31.1	1.27 (*s*)	1.31 (*s*)
11	27.4	1.78 (*s*)	1.58 (*s*)

Table 63 The NMR spectral data of **3*β*-*O*-*E*-coumaroylmaslinic acid**

Position	δ_H (*mult.*; J_{Hz})	Position	δ_H (*mult.*; J_{Hz})
2	3.98 (*sext*; 10.0, 10.0, 4.0)	27	1.20 (*s*)
3	4.70 (*d*; 10.0)	29	0.96 (*s*)
12	5.36 (*t*; 4.0)	30	0.96 (*s*)
18	2.97 (*dd*; 14.0, 4.0)	2'	6.29 (*d*; 16.0)
23	0.96 (*s*)	3'	7.63 (*d*; 16.0)
24	0.96 (*s*)	5', 9'	7.38 (*d*; 8.0)
25	1.03 (*s*)	6', 8'	6.88 (*d*; 8.0)
26	0.84 (*s*)		

Table 64 The NMR spectral data of **3*β*-O-*Z*-coumaroylmaslinic acid**

Position	δ_H (*mult.*; J_{Hz})	Position	δ_H (*mult.*; J_{Hz})
2	3.84 (*sext*; 10, 10, 4.0)	27	1.17 (*s*)
3	4.61 (*d*; 10.0)	29	0.93 (*s*)
12	5.32 (*t*; 4.0)	30	0.98 (*s*)
18	2.95 (*dd*; 14.0, 4.0)	2'	5.82 (*d*; 12.0)
23	0.98 (*s*)	3'	6.82 (*d*; 12.0)
24	0.98 (*s*)	5', 9'	7.66 (*d*; 8.0)
25	0.93 (*s*)	6', 8'	6.83 (*d*; 8.0)
26	0.84 (*s*)		

recorded in $CDCl_3$+pyridine-d_5 (10:1)

Table 65 The NMR spectral data of **3*β*-*O*-*E*-coumaroyloleanolic acid**

Position	δ_C	δ_H (*mult.*; J_{Hz})	Position	δ_C	δ_H (*mult.*; J_{Hz})
1	37.4		20	30.3	
2	23.1		21	36.5	
3	79.8	4.90 (*dd*; 11.4, 5.5)	22	32.3	
4	37.5		23	27.6	7 quaternary Me (23-27, 29 and 30)
5	54.9		24	14.7	0.86 (*s*), 0.96 (*s*),
6	17.8		25	16.5	0.98 (*s*, 2xCH_3),
7	32.5		26	16.7	1.01 (*s*), 1.02 (*s*),
8	39.0		27	25.5	1.30 (*s*)
9	47.2		28	179.3	
10	37.5		29	33.5	
11	23.4		30	23.1	
12	121.6	5.49 (*br s*)	1'	166.4	
13	144.1		2'	115.0	6.71 (*d*; 16.1)
14	41.4		3'	144.0	8.04 (*d*; 16.1)
15	27.6		4'	125.4	
16	23.0		5', 8'	129.9	7.67 (*d*; 8.4)
17	45.9		6', 9'	116.0	7.18 (*d*; 8.4)
18	41.3		7'	160.6	
19	45.7				

recorded in pyridine-d_5

Table 66 The NMR spectral data of **arjunolic acid** and **hyptatic acid-A**

Position	arjunolic acia[a]		hyptatic acid-A[b]	
	δ_C	δ_H (*mult.*; J_{Hz})	δ_C	δ_H (*mult.*; J_{Hz})
1	47.3		46.7	
2	68.7	4.21 (overlap)	68.1	3.79 (*ddd*; 12.0, 10.0, 5.0)
3	78.1	4.20 (overlap)	84.5	3.39 (*d*; 10.0)
4	43.5		39.1	
5	48.3		55.7	
6	18.6		18.4	
7	33.6		32.2	
8	40.0		48.1	
9	47.7		47.3	
10	38.4		37.7	
11	24.2		22.6	
12	123.2	4.23 (overlap)	121.6	5.25 (*br s*)
13	144.5		144.2	
14	42.1		46.0	
15	28.3		24.9	
16	24.8		22.3	
17	47.9		46.4	
18	41.2	3.26 (*dd*; 10.5, 4.0)	41.4	2.88 (*dd*; 12.0, 5.0)
19	45.9		42.9	
20	29.1		30.2	
21	35.6		33.6	
22	32.9		32.8	
23	66.3	a: 4.19 (*d*, 10.4) b: 3.71 (*d*, 10.4)	27.4	a: 4.04 (*d*; 11.0) b: 3.06 (*d*; 11.0)

[a]recorded in pyridine-d_5; [b]recorded in CD_3OD

Table 66 (Continued)

Position	arjunolic acia[a]		hyptatic acid-A[b]	
	δ_C	δ_H (*mult.*; J_{Hz})	δ_C	δ_H (*mult.*; J_{Hz})
24	14.2		64.7	1.24 (*s*)
25	17.6		16.0	0.82 (*s*)
26	17.2		16.3	1.00 (*s*)
27	28.8		23.4	1.17 (*s*)
28	180.5		180.2	
29	34.6		32.5	0.95 (*s*)
30	24.8		22.7	0.91 (*s*)

[a]recorded in pyridine-d_5; [b]recorded in CD_3OD

Table 67 The NMR spectral data of **oleanolic acid**

Position	δ_C	δ_H (***mult.***; J_{Hz})	**Position**	δ_C	δ_H (***mult.***; J_{Hz})
1	38.5		16	23.4	
2	27.1		17	46.6	
3	79.0	3.21 (*m*)	18	41.0	
4	38.7		19	45.8	
5	55.2		20	30.7	
6	18.3		21	33.8	
7	32.6		22	32.4	
8	38.9		23	28.1	0.98 (*s*)
9	47.6		24	15.5	0.75 (*s*)
10	37.0		25	15.3	0.89 (*s*)
11	22.9		26	16.8	0.74 (*s*)
12	122.6	5.26 (*t*; 3.0)	27	26.0	1.11 (*s*)
13	143.5		28	179.1	
14	41.6		29	33.0	0.91 (*s*)
15	27.6		30	23.6	0.96 (*s*)

recoded in $CDCl_3$

Table 68 The NMR spectral data of ***β*-sitosterol**

Position	δ_C	δ_H (***mult.***; J_{Hz})	**Position**	δ_C	δ_H (***mult.***; J_{Hz})
1	37.2		16	28.2	
2	31.9		17	56.0	
3	71.8	3.53 (*m*)	18	12.0	0.69 (*s*)
4	42.3		19	19.0	1.01 (*m*)
5	140.7		20	36.1	
6	121.7	5.35 (*d*, 5.2)	21	18.8	0.97 (*d*, 6.5)
7	31.9		22	33.9	
8	31.7		23	26.1	
9	50.1		24	45.8	
10	36.5		25	29.1	
11	21.1		26	19.4	0.92 (*d*, 6.5)
12	39.8		27	19.8	0.81 (*d*, 6.6)
13	42.3		28	23.1	
14	56.7		29	11.9	0.84 (*t*, 7.5)
15	24.3				

recorded in $CDCl_3$

Table 69 The NMR spectral data of ***β*-sitosterol glucopyranoside** (**daucosterol**)

Position	δ_C	δ_H (*mult.*; J_{Hz})	Position	δ_C	δ_H (*mult.*; J_{Hz})
1	36.8	*α*: 1.09 (*t*; 13)	17	55.5	1.07-1.17 (*m*)
		β: 1.88 (*d*; 13)	18	11.1	0.70 (*s*)
2	29.0	a: 1.57-1.66 (*m*)	19	18.5	1.03 (*s*)
		b: 1.90-1.97 (*m*)	20	35.6	1.34-1.42 (*m*)
3	78.4	3.57-3.65 (*m*)	21	18.0	0.94 (*d*; 6.4)
4	38.1	a: 2.24-2.32 (*m*)	22	33.4	a: 1.00-1.07 (*m*)
		b: 2.39-2.45 (*m*)			b: 1.32-1.39 (*m*)
5	139.9		23	25.4	1.15-1.22 (*m*)
6	121.4	5.36-5.39 (*m*)	24	45.4	0.91-0.98 (*m*)
7	31.4	a: 1.53-1.59 (*m*)	25	28.6	1.64-1.72 (*m*)
		b: 1.95-2.03 (*m*)	26	18.1	0.83 (*d*; 6.5)
8	31.4	1.43-1.50 (*m*)	27	18.9	0.85 (*d*; 6.5)
9	49.7	0.90-0.99 (*m*)	28	22.5	1.21-1.32 (*m*)
10	36.2		29	11.1	0.86 (*t*; 8.3)
11	20.5	1.45-1.55 (*m*)	1′	100.6	4.41 (*d*; 7.8)
12	39.3	*α*: 1.19 (*t*; 11.5)	2′	73.1	3.22 (*t*; 8.3)
		β: 2.00-2.06 (*m*)	3′	76.1	3.38-3.44 (*m*)
13	41.8		4′	69.7	3.35-3.42 (*m*)
14	56.3	0.97-1.07 (*m*)	5′	75.6	3.27-3.31 (*m*)
15	23.7	a: 1.04-1.13 (*m*)	6′	61.1	a: 3.73 (*dd*; 12.0,
		b: 1.57-1.64 (*m*)			5.1)
					b: 3.86 (*dd*; 12.0,
					2.6)
16	27.7	a: 1.24-1.32 (*m*)			
		b: 1.83-1.92 (*m*)			

Table 70 The NMR spectral data of **stimast-4-en-3-one**

Position	δ_C	δ_H (***mult.***; J_{Hz})	**Position**	δ_C	δ_H (***mult.***; J_{Hz})
1	35.7		16	28.1	
2	33.9		17	56.1	
3	198.9		18	12.0	0.72 (*s*)
4	123.6	5.74 (*d*; 2.2)	19	17.4	1.19 (*s*)
5	171.0		20	36.1	
6	32.9		21	18.7	0.93 (*d*; 6.6)
7	32.1		22	34.0	
8	35.7		23	26.0	
9	53.8		24	45.8	
10	38.6		25	29.1	
11	21.0		26	19.8	0.84 (*d*; 6.8)
12	39.5		27	19.2	0.82 (*d*; 6.8)
13	42.4		28	23.1	
14	55.9		29	11.4	0.85 (*t*; 7.2)
15	24.1				

Table 71 The NMR spectral data of ***trans*-triacontyl-4-hydroxy-3-methoxy-cinnamate**

Position	δ_C	δ_H (*mult.*; J_{Hz})	Position	δ_C	δ_H (*mult.*; J_{Hz})
1	167.39		1'	64.59	4.12 (*t*)
2	114.65	6.23 (*d*; 15.8)	2'	31.94	
3	146.71	7.61 (*d*; 15.8)	3'-29'	29.68,	1.26 (27xCH_2)
4	127.11			25.98,	
5	109.35	6.94 (*s*)		22.70	
6	147.84		30'	14.12	0.89 (*t*)
7	144.67		7-OH		5.84 (*s*)
8	122.99	7.15 (*d*)	6-OCH_3	55.94	3.93 (*s*)
9	115.72	7.15 (*d*)			

Table 72 The NMR spectral data of ***trans*-triacontyl-4-hydroxycinnamate**

Position	δ_C	δ_H (*mult.*; J_{Hz})	Position	δ_C	δ_H (*mult.*; J_{Hz})
1	169.3	-	2'	26.1	
2	110.5	6.29 (*d*; 16.0)	3'-29'	31.9,	1.25 (*br*)
3	144.4	7.63 (*d*; 16.0)		30.8,	
4	127.5			29.6,	
5, 9	129.9	7.43 (*d*; 8.0)		29.4,	
6, 8	115.9	6.85 (*d*; 8.0)		29.3,	
7	152.3			22.6	
1'	64.6	4.19 (*t*; 7.5)	30′	14.0	0.93 (*t*; 6.7)

Table 73 The NMR spectral data of **9,9′-*O*-diferuloyl-(-)-secoisolariciresinol**

Position	δ_C	δ_H (***mult.***; J_{Hz})
1,1′	131.7	
2,2′	111.3	6.53 (*d*, 1.8)
3,3′	146.5	
4,4′	144.0	
5,5′	114.2	6.81 (*d*, 8.1)
6,6′	121.8	6.61 (*dd*, 8.1, 1.8)
7,7′	35.3	2.75 (*dd*, 14.1, 7.5)
		2.70 (*dd*, 14.1, 7.5)
8,8′	40.2	2.22 (*m*)
9,9′	64.5	4.39 (*dd*, 11.4, 5.7)
		4.22 (*dd*, 11.4, 5.5)
3,3′-OCH_3	55.8	3.77 (*s*)
1″,1‴	126.9	
2″,2‴	109.5	7.01 (*d*, 1.8)
3″,3‴	146.8	
4″,4‴	148.1	
5″,5‴	115.2	6.91 (*d*, 8.2)
6″,6‴	123.1	7.06 (*dd*, 8.2, 1.8)
7″,7‴	145.2	7.59 (*d*, 15.9)
8″,8‴	114.8	6.28 (*d*, 15.9)
9″,9‴	167.3	
3″,3‴-OCH_3	56.0	3.92 (*s*)

VITAE

Name Mr. Asadhawut Hiranrat

Student ID 4910230011

Education Attainment

Degree	Name of Institution	Year of Graduation
B.Sc.(Chemistry)	Prince of Songkla University	1998
M.Sc.(Organic Chemistry)	Prince of Songkla University	2001

Scholarship Awards during Enrolement

1. Thailand Research Fund through the Royal Golden Jubilee Ph.D. Program (Grant No. PHD0206/2549)
2. Center for Innovation in Chemistry (PERCH-CIC), Office of the Higher Education Commission, Ministry of Education
3. Prince of Songkla University Graduate Studies Grant
4. CHE-RES-RG, Office of the Higher Education Commission, Ministry of Education

List of Publication and Proceeding

Publications

1. **Asadhawut Hiranrat**, Wilawan Mahabusarakam. **2008**. "New acylphloroglucinols from the leaves of *Rhodomyrtus tomentosa*" *Tetrahedron*, 64 (9), 11193-11197.

2. Jongkon Saising, **Asadhawut Hiranrat**, Wilawan Mahabusarakam, Metta Ongsakul, Supayang Piyawan Voravuthikunchai. **2008**. "Rhodomyrtone from *Rhodomyrtus tomentosa* (Aiton) Hassk. as a Natural Antibiotic for Staphylococcal Cutaneous Infections" *Journal of Health Science*, 54 (5), 589-595.

3. Surasak Limsuwan, Erik N. Trip, Thijs R. H. M. Kouwen, Sjouke Piersma, **Asadhawut Hiranrat**, Wilawan Mahabusarakam, Supayang Piyawan Voravuthikunchai, Maarten van Dijl Jan, Oliver Kayser. **2009**. "Rhodomyrtone: a new candidate as natural antibacterial drug from *Rhodomyrtus tomentosa*", *Phytomedicine*, 16 (6-7), 645-651.

Proceedings

1. **Asadhawut Hiranrat**, Wilawan Mahabusarakam, Supayang Voravuthikunchai and Surasak Limsuwan. "Two new acylphloroglucinols from the leaves of Downy Rose Myrtle (*Rhodomyrtus tomentosa*)" The Sixth Princess Chulabhorn International Science Congress, Shangri-La Hotel, Bangkok, Thailand, November 25-29, 2007. (international; poster presentation)

2. **Asadhawut Hiranrat** and Wilawan Mahabusarakam. "Chemical Constituents of *Rhodomyrtus tomentosa* (Aiton) Hassk." The Sixth Regional IMT-GT Uninet Conference 2008, The Gurney Resort Hotel & Residences, Penang, Malaysia, August 28-30, 2008. (international; poster presentation)

3. **Asadhawut Hiranrat** and Wilawan Mahabusarakam. "New Acylphloroglucinols from the Leaves of *Rhodomyrtus tomentosa*" RGJ-Ph.D. Congress X, Jomtien Palm Beach Resort, Pattaya, Chonburi, Thailand, April 3-5, 2009. (international; oral presentation)

4. **Asadhawut Hiranrat** and Wilawan Mahabusarakam. "New Acylphloroglucinols from the Leaves of *Rhodomyrtus tomentosa*" PERCH-CIC Congress VI, Jomtien Palm Beach Resort, Pattaya, Chonburi, Thailand, May 3-6, 2009. (international; oral presentation)

5. **Asadhawut Hiranrat**, Wilawan Mahabusarakam, Surasak Limsuwan and Supayang Piyawan Voravuthikunchai. "Chemical Constituents from the Leaves of *Rhodomyrtus tomentosa*" การสัมมนาวิชาการ "วิทยาศาสตร์ชีวภาพโมเลกุล-ปัจจุบันและอนาคต", Faculty of Science, Mahidol University, Bangkok, Thailand, August 26, 2009. (meeting; poster presentation)

6. **Asadhawut Hiranrat**, Wilawan Mahabusarakam, Surasak Limsuwan and Supayang Piyawan Voravuthikunchai. “Antibacterial Acylphloroglucinols from *Rhodomyrtus tomentosa*” RGJ Seminar Series LXIV: Science and Technology for the Sustainable Development, Faculty of Science, Prince of Songkla University, Songkhla, Thailand, September 4, 2009. (national; poster presentation)